



UNIVERSITAT DE
BARCELONA

Molecular and cellular mechanisms of fertilization failure after ICSI

Marc Torra Massana

ADVERTIMENT. La consulta d'aquesta tesi queda condicionada a l'acceptació de les següents condicions d'ús: La difusió d'aquesta tesi per mitjà del servei TDX (www.tdx.cat) i a través del Dipòsit Digital de la UB (diposit.ub.edu) ha estat autoritzada pels titulars dels drets de propietat intel·lectual únicament per a usos privats emmarcats en activitats d'investigació i docència. No s'autoritza la seva reproducció amb finalitats de lucre ni la seva difusió i posada a disposició des d'un lloc aliè al servei TDX ni al Dipòsit Digital de la UB. No s'autoritza la presentació del seu contingut en una finestra o marc aliè a TDX o al Dipòsit Digital de la UB (framing). Aquesta reserva de drets afecta tant al resum de presentació de la tesi com als seus continguts. En la utilització o cita de parts de la tesi és obligat indicar el nom de la persona autora.

ADVERTENCIA. La consulta de esta tesis queda condicionada a la aceptación de las siguientes condiciones de uso: La difusión de esta tesis por medio del servicio TDR (www.tdx.cat) y a través del Repositorio Digital de la UB (diposit.ub.edu) ha sido autorizada por los titulares de los derechos de propiedad intelectual únicamente para usos privados enmarcados en actividades de investigación y docencia. No se autoriza su reproducción con finalidades de lucro ni su difusión y puesta a disposición desde un sitio ajeno al servicio TDR o al Repositorio Digital de la UB. No se autoriza la presentación de su contenido en una ventana o marco ajeno a TDR o al Repositorio Digital de la UB (framing). Esta reserva de derechos afecta tanto al resumen de presentación de la tesis como a sus contenidos. En la utilización o cita de partes de la tesis es obligado indicar el nombre de la persona autora.

WARNING. On having consulted this thesis you're accepting the following use conditions: Spreading this thesis by the TDX (www.tdx.cat) service and by the UB Digital Repository (diposit.ub.edu) has been authorized by the titular of the intellectual property rights only for private uses placed in investigation and teaching activities. Reproduction with lucrative aims is not authorized nor its spreading and availability from a site foreign to the TDX service or to the UB Digital Repository. Introducing its content in a window or frame foreign to the TDX service or to the UB Digital Repository is not authorized (framing). Those rights affect to the presentation summary of the thesis as well as to its contents. In the using or citation of parts of the thesis it's obliged to indicate the name of the author.

MOLECULAR AND CELLULAR MECHANISMS OF FERTILIZATION FAILURE AFTER ICSI

Marc Torra Massana

Thesis supervisors:

Dr. Rita Vassena (director)

Prof. Rafael Oliva Virgili (director and tutor)

Clínica Eugin and Molecular Biology of Reproduction and Development Group
(University of Barcelona)

Faculty of Medicine, University of Barcelona, Doctoral program in Medicine and
Translational Research

With the support of the Secretary for Universities and Research of the Ministry of
Economy and Knowledge of the Government of Catalonia



Al meu pare

ACKNOWLEDGMENTS

Més de tres anys després de començar, només puc dir que em sento feliç i afortunat d'haver pogut fer el meu doctorat en un lloc tan privilegiat i amb gent tan maca al meu voltant. Si abans de començar la tesi m'haguessin demanat com voldria que fos, hagués volgut uns tres anys molt similars als que he tingut!

Abans de res, vull donar les gràcies als meus directors de tesi. Rita, muchas gracias por todo, no solo por darme la oportunidad de realizar esta tesis y dirigir mi trabajo, también por transmitirme la importancia de la investigación en un campo como el de la reproducción asistida, por apostar por nuestra formación continuamente y por ayudarnos en nuestro futuro y carrera profesional. Rafael, gràcies per donar-me l'oportunitat de realitzar aquesta tesi i pel teu ajut al llarg del projecte.

Montse, gràcies per ensenyar-me tantes coses que m'han fet un millor científic, no només a nivell experimental, sinó també a raonar i a tenir pensament crític. Gràcies per cuidar-nos tan bé, per insistir-nos, per aconsellar-nos, per ajudar-nos, i per aguantar-me els dies que estava més pesat ☺. Gustavo, gracias por tu ayuda, y por esos excelentes asados que nos preparaste, ¡quiero repetir!

Paula i David, amb vosaltres vaig començar i acabar aquest camí, des del nostre primer cafè el dia que vam firmar el contracte, fins avui! Gràcies per tot els moments que hem compartit, converses, festes, cerveses, cursos i congressos, hores i hores al lab... no cal que us digui que sou molt més que companys de laboratori!

Agus, ets un exemple de superació i optimisme. Trobo a faltar les estones que passavem al lab, les discussions sobre projectes esbojarrats que es podrien fer amb les vesícules extracel·lulars, els conflictes per dinar al sol i no "achicharrarse", les teves històries sobre el Camino de Santiago... D'aquí poc passarà tot, segueix així!

Evi, voy a echar de menos que me llames "Marculito" y todos los momentos que hemos pasado!
Anna, gràcies per tot, matinades a les 7h per desvitri i "bailoteos" pel sopar de Nadal inclosos!
Farners, espero que no miris gaires vegades el video que et vam fer per la tesi (¿y el spindle???)... estic content que et vagi tot bé pels USA, i espero que ens veiem aviat! Filippo, gracias por tus mitoprimeros y todos los momentos dentro y fuera del lab! "Apreciada" Désirée, hoy no te mando saludos, sinó que te doy las gracias por todo ☺.
Sarai, gracias por tu ayuda con esas interminables bases de datos. Emanuela, Aina, Judit, guardo muy buenos recuerdos de vuestro paso por el PCB, espero que os vaya muy bien a todas! Sandra i Raquel, espero que sigamos perfeccionando la técnica en la bolera! A todos, espero iros viendo a menudo y visitar el PCB cuando pueda, que no me entere que quitáis las tonterías que dejé colgadas por el lab!

Vull donar també mil gràcies a la Mercè per la seva implicació i ajut amb la meva tesi, a l'Andreu pel seu ajut amb SPETI (ho faràs de conya a Viena!). I, sens dubte, gràcies, a tots els membres del laboratori d'embriologia, aquesta tesi no hagués sigut possible sense vosaltres, que recolliu les mostres que necessitem, que m'heu agafat mil trucades desde el PCB, que m'expliqueu superbé tots els protocols del lab... Estic segur que aquesta nova etapa amb vosaltres anirà de perles!

Ada i Ferran, ha estat un plaer tornar-vos a veure després del màster i treballar amb vosaltres, encara que fos una temporada molt curteta! Sort amb la última etapa de la tesi, i no dubteu que us tornaré a visitar! Gràcies també a la Meri, la Judit i el David per la seva gran ajuda amb el meu projecte.

Arnau, Gerard, Sergi, Xavi, Uri, Joan, Marc, Nil, gràcies per ser-hi. No sé si mai us llegireu aquesta tesi, però us convido a fer-ho i veureu que no només “jugo amb semen”! 😊

Emma, simplement gràcies per estimar-me i deixar-te estimar. Espero seguir compartint la vida al teu costat durant molt de temps!

Roc, Jana – que m'alegreu els dinars de diumenge-, Alba, Pep, gràcies per ser-hi. Mama, gràcies per estimar-me tant i donar-me sempre el teu suport.

Papa, intento fer sempre el que em vas transmetre: prendre'm la vida amb un somriure. Des del dia que vas marxar, em vaig prometre que et dedicaria tots els èxits i coses bones que tingués a la vida. Aquesta tesi va per tu.

PREFACE

The work presented here is the result of an Industrial Doctorate collaboration between Clínica Eugin and the Molecular Biology of Reproduction and Development Group at the University of Barcelona. This thesis has been supervised by the two codirectors: Dr. Rita Vassena (Clínica Eugin) and Prof. Rafael Oliva (University of Barcelona).

Fertilization is defined as the process by which the sperm and the oocyte fuse to form an embryo. This process involves two of the most specialized cells in human (the sperm and the oocyte), a transition from meiosis to mitosis, establishment of diploidy and global epigenetic reprogramming, all of which results in the generation of a totipotent cell. Fertilization is one of the most complex and impressive biological phenomena in nature.

In the context of assisted reproduction, fertilization failure (FF) results in absence of embryos to transfer and is one of the most frustrating events for patients and doctors. The high impact of FF in both patients and clinicians, the lack of tools to manage FF (in terms of diagnosis, prognosis and treatment), and the high molecular and cellular complexity of the fertilization justifies the need for a wide and comprehensive approach: from the characterization of the basic biology of the gametes to the analysis of reproductive outcomes of the infertile patients undergoing an ICSI treatment.

TABLE OF CONTENTS

ACKNOWLEDGMENTS	5
PREFACE	7
ABBREVIATIONS LIST	9
INTRODUCTION	11
1. A LOOK INTO MALE INFERTILITY: A PROBLEM STILL UNKNOWN	13
1.1. MALE INFERTILITY: DEFINITION AND ORIGIN	13
1.2. CURRENT TECHNIQUES AND PARAMETERS TO DIAGNOSE MALE INFERTILITY	13
2. THE THREE PLAYERS IN FERTILIZATION	15
2.1. THE SPERM	15
2.2. THE OOCYTE	17
2.3. THE PREIMPLANTATION EMBRYO	19
3. A LONG JOURNEY: FROM THE TESTIS TO THE OOCYTE	22
3.1. SPERMATOGENESIS	22
3.2. SPERM MATURATION, CAPACITATION AND OOCYTE FERTILIZATION	25
4. FERTILIZATION EVENTS AFTER SPERM ENTRY INTO THE OOCYTE	26
4.1. OOCYTE ACTIVATION	26
4.2. THE IMPORTANCE OF OOCYTE CALCIUM SIGNALLING AND ITS REGULATION	26
4.3. A COMPLEX DOWNSTREAM SIGNALING	28
4.4. THE SPERM INSIDE THE OOCYTE	31
5. FERTILIZATION THROUGH ASSISTED REPRODUCTION TECHNIQUES	33
5.1. MAIN ART TECHNIQUES: IUI, IVF, ICSI	33
5.2. SPERM PROCESSING AND SELECTION IN THE IVF LABORATORY	35
6. FERTILIZATION FAILURE AFTER ICSI	36
6.1. CHARACTERIZATION OF ICSI FERTILIZATION FAILURE AND ITS CLINICAL IMPACT	36
6.2. AOA FOR FERTILIZATION FAILURE AFTER ICSI	38
7. CAUSES AND MECHANISMS OF FF AFTER ICSI	40
7.1. TECHNICAL CAUSES OF FERTILIZATION FAILURE	40
7.2. OOCYTE-RELATED FERTILIZATION FAILURE	41
7.3. SPERM-RELATED FERTILIZATION FAILURE	43
7.3.1. SPERM-BORNE OOCYTE ACTIVATION FACTORS (SOAF): A BRIEF REVIEW	43

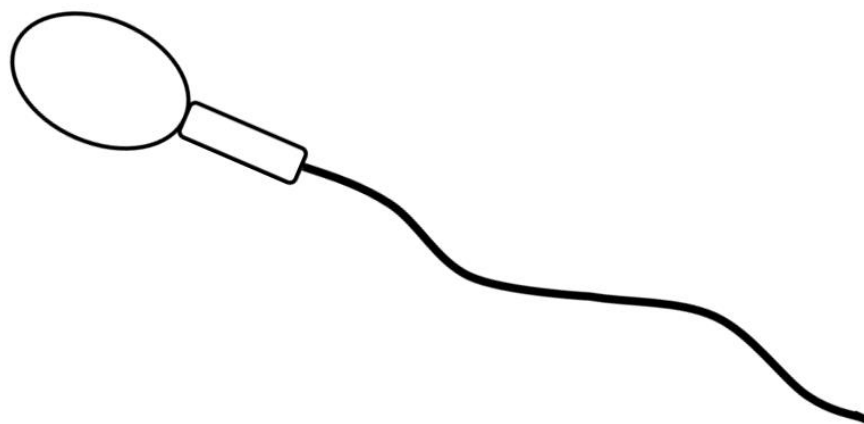
7.3.2. PLC ζ	44
7.3.3. PAWP AND WBP2	46
7.3.4. SPERM DNA AND FERTILIZATION FAILURE	47
8. RESEARCH ON FERTILIZATION FAILURE AFTER ICSI: STILL MUCH TO DO	49
8.1. WHY IS MORE RESEARCH ON FERTILIZATION FAILURE NEEDED?	49
8.2. MAIN APPROACHES TO STUDY SPERM-RELATED FERTILIZATION FAILURE	49
OBJECTIVES	53
RESULTS	57
CHAPTER 1. Is there an association between PAWP/WBP2NL sequence, expression, and distribution in sperm cells and fertilization failures in ICSI cycles?	59
CHAPTER 2. Novel phospholipase C zeta 1 mutations associated with fertilization failures after ICSI	79
CHAPTER 3. Sperm telomere length in donor samples is not related to ICSI outcome	119
CHAPTER 4. Prediction of sperm markers for oocyte activation failure by in silico analysis of protein-protein interactions	141
CHAPTER 5. Comparative proteomics uncovers differentially expressed proteins related to mitochondrial and proteasomal function in sperm samples producing fertilization failure after ICSI	157
CHAPTER 6. Use of assisted oocyte activation (AOA) after a failed fertilization cycle: where is the evidence?	193
DISCUSSION	201
CONCLUSIONS	211
BIBLIOGRAPHY	215
RESUM	231
ANNEX	241
ANNEX 1. How long can the sperm wait? Effect of sperm processing time on reproductive outcomes after ICSI	243

ABBREVIATIONS LIST

AOA	Assisted oocyte activation
AMH	Anti-Müllerian hormone
ART	Assisted reproduction technologies
AU	Arbitrary unit
BMI	Body mass index
EGA	Embryonic genome activation
ER	Endoplasmic reticulum
ET	Embryo transfer
FDR	False discovery rate
FF	Fertilization failure
ICM	Inner cell mass
ICSI	Intracytoplasmic sperm injection
IUI	Intrauterine insemination
IVF	<i>In vitro</i> fertilization
IVM	<i>In vitro</i> maturation
LB	Live birth
LC	Liquid chromatography
LH	Luteinizing hormone
mtDNA	Mitochondrial DNA
MMP	Mitochondrial membrane potential
MPF	Maturation-promoting factor
MS	Mass spectrometry
OAF	Oocyte activation failure
PAWP	Postacrosomal sheath WW domain-binding protein
PB	Polar body
PLCZ1/PLC ζ	Phospholipase C Zeta 1
PN	Pronucleus / pronuclei
PPI	Protein-protein interaction
PSM	Peptide spectrum match
qPCR	Real-time quantitative PCR
RU	Relative unit
SOAF	Sperm-borne oocyte activation factor(s)
SOCE	Store-operated calcium entry

STL	Sperm telomere length
WHO	World Health Organization
ZP	Zona pellucida

INTRODUCTION



1. A LOOK INTO MALE INFERTILITY: A PROBLEM STILL UNKNOWN

1.1. MALE INFERTILITY: DEFINITION AND ORIGIN

Infertility is defined as the inability of a sexually active couple to get pregnant after one year of unprotected sexual intercourse. In the global population, 15% of couples and 7% of men are estimated to be affected by infertility, but it is very difficult to assess this percentage with precision (Inhorn and Patrizio, 2014; Barratt et al., 2017).

Currently, it is estimated that male factor explains 20–30% of infertility problems, while 25–40% of infertility cases are associated with both male and female factors (Yeste et al., 2016). Male infertility may be caused by various combinations of genetic, epigenetic, systemic and environmental factors. The main cause of male infertility are defects in spermatogenesis (see section 3.1), a process which can be affected by obesity, diabetes, environmental chemicals, varicocele, transcriptomic profile, genetic and chromosomic alterations (such as Klinefelter syndrome and Y chromosome microdeletions), or high scrotal temperature, among other factors (Neto et al., 2016). It is important to mention that chemotherapy and radiotherapy, treatments used for oncological treatment, cause devastating effects on spermatogenesis.

However, around 50% of male factor infertility cases remain unexplained (Hotaling, 2014), in part due to incomplete knowledge about spermatogenesis and sperm function and biology, and a lack of diagnostic tools. This supposes a major concern as, according to a recent meta-regression analysis, a considerable decline in male fertility has occurred in the last 40 years worldwide (Levine et al., 2017).

1.2. CURRENT TECHNIQUES AND PARAMETERS TO DIAGNOSE MALE INFERTILITY

In most fertility clinics, the study of the male patient includes a review of the reproductive history (coitus frequency, previous offspring, previous infertility problems in the couple or in the family, etc.), medical history and diseases relevant for fertility (cryptorchidism, testis tumours, infections, varicocele, chronic diseases, abnormal hormonal levels, etc.), and exposure to factors which may reduce fertility (such as alcohol, drugs and smoking). This analysis allows identification of significant diseases in 1.1 - 6% of infertile men, some of them associated with abnormal semen parameters (Barratt et al., 2017). In men with risk factors in their reproductive history, physical examination is usually recommended.

Evaluation of the semen sample by routine spermiogram is the most common male infertility diagnostic performed. Sample volume, pH, viscosity, vitality and assessment of the percentage of round cells (immature germ cells, epithelial cells, leukocytes, etc.) are some of the parameters usually evaluated in the semen sample. Main informative parameters are sperm concentration (expressed as million sperm per ml), motility and morphology. Three categories are considered when evaluating sperm motility: progressive motility, non-progressive motility, and immotile. Correct sperm morphology is characterized by a smooth and oval head with few or no vacuoles, a regular and properly aligned midpiece, and a thin and uniform tail; any cell not following this general pattern is classified as abnormal (World Health Organization, 2010).

Semen sample evaluation is based on the guidelines published by World Health organization (WHO 2010), which defines reference values for the diagnostic of male infertility (**Table I**). All these definitions may go together; for example, a patient with low levels of both sperm concentration and motility presents oligoasthenozoospermia.

Table I. Main criteria and nomenclature used for semen sample evaluation and male infertility classification, established by World Health Organization (WHO 2010).

Definition	Affected semen parameter	Threshold
Normozoospermia	None	-
Oligozoospermia	Concentration	< 15 million / ml
Cryptozoospermia	Concentration	< 0.1 million in total ejaculate
Azoospermia	Concentration	0 million / ml (absence of sperm)
Asthenozoospermia	Motility	< 32 % a + b (progressive motility)
Teratozoospermia	Morphology	< 4% normal forms
Hypospermia	Volume	< 1.5 ml ejaculate
Necrozoospermia	Vitality	< 58% live sperm (Cooper et al., 2010)
Leukospermia	Leukocyte concentration	> 1 million leukocytes / ml

Around 40-60% of infertile men show some alterations in at least one of these sperm parameters (concentration, motility, or morphology) (Dohle et al., 2005). In some cases, additional sperm characterization include evaluation of sperm DNA fragmentation (associated with poor embryo quality and pregnancy rates), presence of antisperm antibodies, cytogenetic evaluation of specific Y chromosome microdeletion (indicative of azoospermia), or evaluation of the karyotype to search

for chromosomal alterations (i.e. translocations, more common in infertile men) (O'Flynn et al., 2010).

However, despite being informative in many cases, these parameters and diagnostic tools usually provide little or no information about sperm health, function, fertilizing ability and reproductive potential after ICSI or other IVF techniques. Infertile patients can experience sperm-related fertilization failure after ICSI despite being normozoospermic, as well as many other infertility problems such as poor embryo development, repetitive implantation failure or miscarriage. For this reason, additional tests for male infertility diagnosis and sperm quality assessment are needed in fertility clinics.

2. THE THREE PLAYERS IN FERTILIZATION

In sexual reproduction, fertilization is the biological process by which male and female gametes, the sperm and the oocyte, fuse together to form an embryo and to initiate the development of a new organism.

Before explaining the biological mechanisms involved in fertilization, how fertilization through assisted reproduction techniques works, and why fertilization sometimes fails, it is essential to understand the basics of the three key players in fertilization: the sperm, the oocyte, and the resulting embryo.

2.1. THE SPERM

Sperm is the smallest cell in the human body (~ 50 μm). Sperm acquires unique morphological features such as flagellum, acrosome, and highly condensed chromatin. In general, three main regions can be identified in sperm: the sperm head, the midpiece, and the tail (**Figure 1**).

Sperm head contains the nucleus, which has a highly compacted DNA. This high level of DNA packaging is acquired during spermatogenesis, where histones are replaced by protamines (protamine 1 and protamine 2). DNA compaction allows the sperm head to be smaller, thus favouring sperm motility and passage through female reproductive tract, offers protection of genomic DNA, and contributes to sperm transcriptional silencing.

The sperm head also contains the acrosome, a membrane-surrounded vesicle derived from the Golgi apparatus during spermatogenesis. Acrosome is essential for fertilization, as it contains lytic enzymes required for the sperm to digest the oocyte zona pellucida (ZP) and reach the oocyte

membrane. These enzymes are released during acrosome reaction, an exocytosis-dependent mechanism. A population of proteasomes are associated with the inner and outer acrosomal membranes, whose function is essential for successful fertilization (Sutovsky et al., 2004).

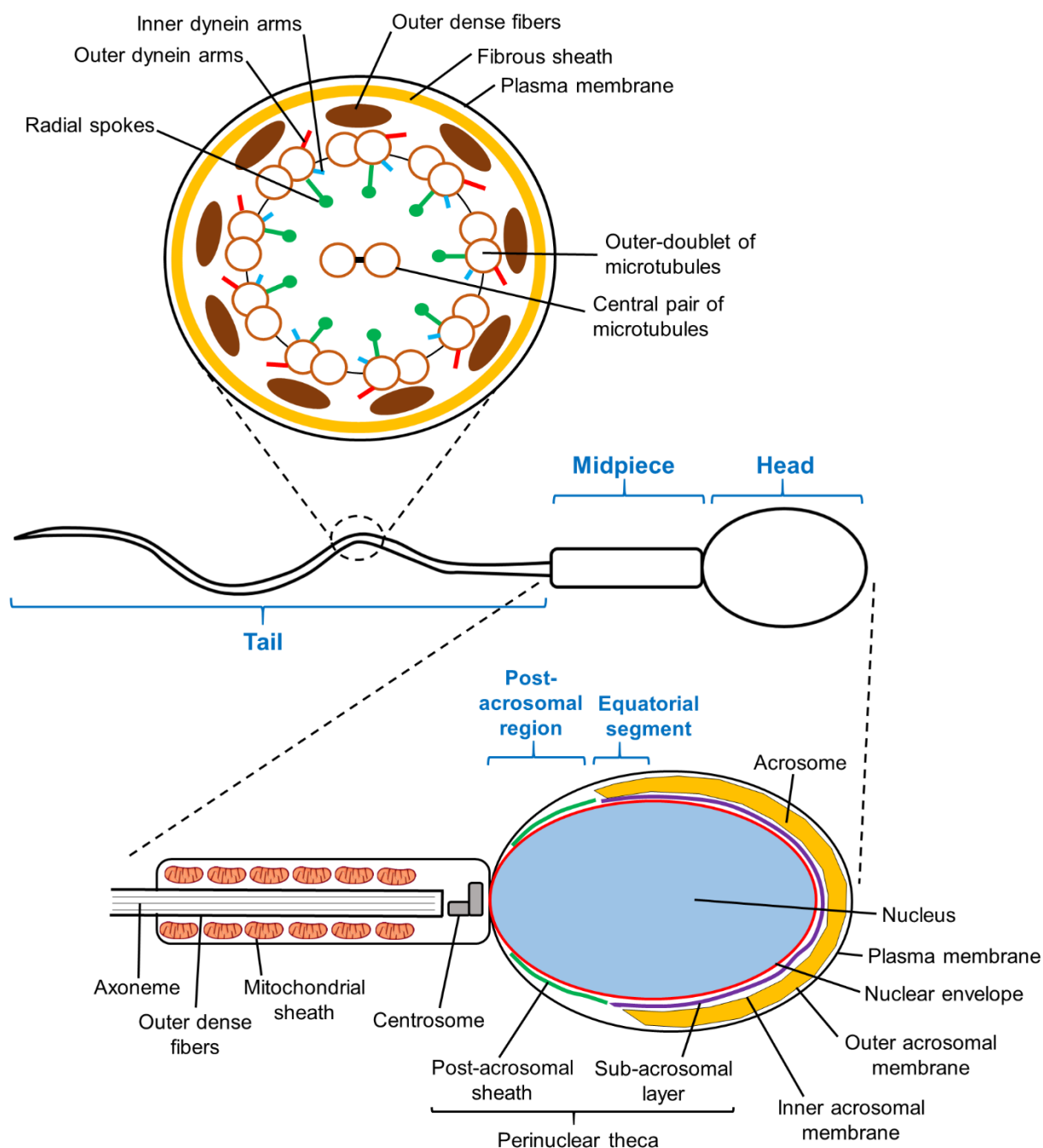


Figure 1. Diagram of the main human sperm regions (indicated in blue) and subcellular structures (indicated in black), including a detailed representation of the internal part of the sperm tail and axoneme, the sperm head and the midpiece. Source: own elaboration.

The sperm perinuclear theca, which surrounds the nucleus (except in the caudal region), is a region in the sperm head with special relevance for triggering oocyte activation (**Figure 1**). This structure

is a condensed cytosolic fraction containing different proteins and is made up of two different regions: the sub-acrosomal layer and the post-acrosomal sheath (Oko and Sutovsky, 2009). The post-acrosomal sheath has been reported to be required for oocyte interaction and successful oocyte activation (Sutovsky et al., 2003; Ito et al., 2009). As most soluble proteins are lost during acrosome reaction, any factor involved in oocyte activation must reside in the region which first contacts with the oocyte cytoplasm: the perinuclear theca (Fujimoto et al., 2004).

Another sperm region of vital importance for fertilization is the midpiece, located between the head and the tail (**Figure 1**). The midpiece contains the centrosome, a structure essential to support the first mitotic division and early development of the embryo, by microtubule enucleation and formation of the mitotic spindle in the zygote (Amargant et al., 2018). The centrosome, which consists of two centrioles (barrel-shaped microtubule structures) and pericentriolar material, also acts as a basal body for flagellum anchoring and axoneme regulation. The midpiece also contains sperm mitochondria, forming a structure called the mitochondrial sheath. This region is considered the powerhouse of the sperm, where metabolism takes place and energy in form of ATP is produced. Inside the oocyte, the mitochondrial sheath needs to be disrupted by the sperm own proteasomes to release the mitotic spindle, allow proper mitophagy of sperm mitochondria and to ensure correct formation of the sperm aster (Rawe et al., 2008).

The tail or flagellum is essential for sperm motility. The flagellum is formed by the axoneme (a pair of microtubules surrounded by 9 microtubule doublets (9+2 structure)) and outer dense fibers, both surrounded by a cytoskeletal structure called the fibrous sheath (Eddy et al., 2003).

Overall, this highly specialized structure allows the sperm to fulfil its main task: to transport the paternal genetic material (DNA) to the oocyte. Nevertheless, sperm is no longer believed to be a mere DNA-carrier, as different sperm contributions to the future embryo have been pointed out. For example, sperm provides the oocyte with important RNA elements (Jodar et al., 2015), an epigenetics code (Siklenka et al., 2015), a functional centriole (Sathananthan et al., 1996) and a complex set of proteins with potential involvement in fertilization and early development (Castillo et al., 2018). Some of these factors will be depicted along the present thesis.

2.2. THE OOCYTE

The oocyte is the biggest cell in the human body (~ 100 µm). What we understand as a “mature oocyte” is an ovulated oocyte which has already completed the first meiotic division (and extruded the first polar body), is ready to be fertilized and is competent to support embryo development.

The oocyte is composed by a cytoplasm and the genetic material, and it is surrounded by a plasma membrane (called oolema). It contains a rich population of RNAs and proteins, as well as organelles such as mitochondria, the endoplasmic reticulum, or proteasomes. The oocyte is surrounded by a layer of glycoproteins called zona pellucida (ZP), important for species-specific monospermic fertilization. In addition, layers of somatic cellular layers, called cumulus cells or *cumulus oophorus*, surround the oocyte during ovarian maturation and sperm fertilization. The physiological unit formed by the oocyte and the cumulus cells is commonly referred to as the oocyte-cumulus complex. Cumulus cells are in close contact with the oocyte by gap junctions, and are essential for oocyte maturation and regulation, as they provide nutrients and regulatory factors.

Oocytes are formed in the ovary through a process called oogenesis. In the human fetus, oocytes originate from primordial germ cells (PGCs), proliferate by mitosis and start meiosis at 12-16 weeks post-coitum, but they arrest at meiotic prophase I (germinal vesicle (GV) stage). Oocyte remain arrested in primordial follicles (oocyte + layer of granulosa cells) until puberty when, periodically, oocytes start the process of oocyte growth or folliculogenesis (110-120 days), in which granulosa cells divide, the oocyte accumulates RNAs and proteins and increases in size, and the ZP is formed. At this point, the monthly surge of luteinizing hormone (LH) triggers oocyte maturation. This is characterized by follicular growth, germinal vesicle breakdown (dissolution of the nucleus of the oocyte arrested at prophase I), resumption of meiosis, assembly of first meiotic spindle and translocation of chromosomes close to the oolema, where the first polar body will be extruded. In summary, oocyte maturation involves the transition from germinal vesicle (GV) to a mature oocyte (**Figure 2**); in fertility clinics, this maturation can be performed by *in vitro* culture.

At the end of maturation, the mature oocyte is transcriptionally silent and is arrested at metaphase II (MII oocyte), as it contains high levels of maturation promoting factor (MPF) activity. The mature oocyte is extruded from the ovary (ovulation), released into the Fallopian tubes, and is ready to be fertilized by sperm. The oocyte will not be released from its meiotic arrest until oocyte activation is triggered by contact with the sperm, at which point meiosis is completed and the 2nd polar body (containing half of the sister chromatids) is extruded. If fertilization does not occur, the oocyte will undergo apoptosis approximately 16h after ovulation.

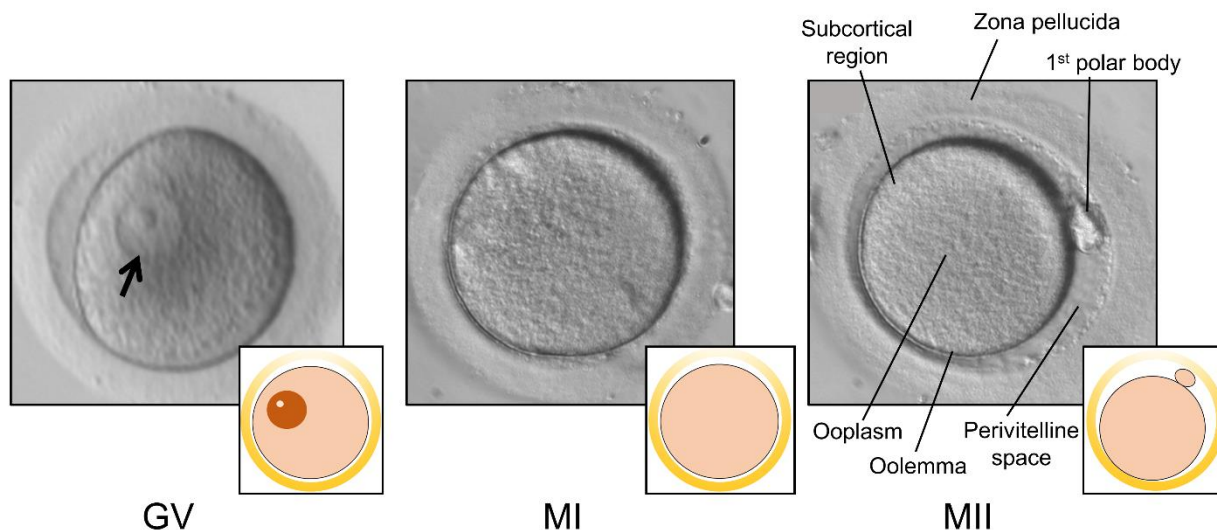


Figure 2. Different stages of oocyte *in vitro* maturation. During meiotic maturation, the oocyte is released from their primary arrest, and enter a second arrest at metaphase II (MII). Fertilization triggers the release from the second arrest and the completion of meiosis. The germinal vesicle is indicated with a black arrow. The main structures of a mature oocyte are indicated. Source: own elaboration.

The quality of a mature oocyte, understood as its ability to be fertilized and undergo a correct embryo development (developmental competence) depends on a wide variety of molecular and cellular factors, including cytoplasmic and nuclear maturation status. Poor quality can be assessed by different prognostic morphological parameters (excessive vacuolization, giant polar body, presence of endoplasmic reticulum aggregates, etc.) (ASEBIR, 2015). Recently, the transcriptomic and proteomic profile of the oocyte offered a powerful approach to search new markers of oocyte quality (Virant-Klun et al., 2016; Barragán et al., 2017).

2.3. THE PREIMPLANTATION EMBRYO

Successful monospermic fertilization results in a zygote with 2 pronuclei, which will resume mitosis and divide in two cells, thus becoming a preimplantational embryo. “Preimplantation” is the period between fertilization and embryo implantation in the uterus which lasts 5 to 6 days in humans and during which the embryo attaches and invades the maternal endometrium.

In the embryology lab, the day of insemination is considered D+0. During the first hours, oocyte activation is triggered by sperm, which will lead to meiotic resumption, genetic and epigenetic reprogramming, and first mitotic division. Recently, time-lapse technology has allowed precise description of the timing of fertilization events (Coticchio et al., 2018). For example, in correctly developing human embryos, the 2nd polar body is extruded after 3.3 hours, and pronuclei appear

after 6.2 hours. During this period, at 5.5h post-insemination, a characteristic cytoplasmic movement occurs, called “cytoplasmic wave”.

At D+1, embryos should be evaluated between 16-18h post-insemination, by checking pronuclei formation and 2nd polar body extrusion (**Figure 3**). Any cell in which 2PN and 2PB are not observed (i.e. absence of pronuclei and PB, 3 PN, etc.) is considered as an oocyte which failed to fertilize and is discarded for reproductive purposes. PN breakdown occurs after 24.5 hours, and cell division occurs after 27.7 hours, generating two symmetric daughter cells. In some cases, direct cleavage (zygote divides in 3 cells directly) occurs, a fact that is associated with bad prognosis in terms of aneuploidy and implantation rate of the embryo.

At D+2, embryos are evaluated at 43-45h post-insemination, at which time they usually have 4 symmetric cells (blastomeres). The first wave of embryonic genome activation (EGA) occurs at this time (Vassena et al., 2011).

At D+3, the third division occurs 67-69h after insemination, generating embryos with 7-8 cells. At this stage, the major wave of EGA occurs; before this time, development is mainly supported by maternal-stored mRNA, which undergoes gradual turnover (Vassena et al., 2011).

At D+4, embryo evaluation should be performed at 90-94h post-insemination, at which time the embryo has already started the 4th round of mitotic division (resulting in > 8 cells). This cell division is accompanied by compaction, the process by which the different blastomeres generate tight intercellular junctions, generating a morula. Compaction supposes the end of the “cleavage” stage and determines cell polarity, a prerequisite for embryonic cell fate acquisition. A fully compacted morula is a cellular mass in which individual blastomeres can no longer be distinguished under the optic microscope (**Figure 3**). In some cases, compaction may be incomplete: some cells may be excluded from the morula and the future blastocyst. This is considered a bad prognosis only when compaction comprises less than 50% of cells in the embryo (ASEBIR, 2015).

At D+5, evaluation is performed 114-118h post-insemination. Cell division continues, and morula becomes a blastocyst. Only 40-60% of fertilized oocytes reach the blastocyst stage (Gardner and Lane, 1998). During cavitation, a fluid filled cavity (the blastocoel) is formed and the embryo forms a blastocyst, in which two different structures can be differentiated: the trophoectoderm (which will form the placenta and extraembryonic tissues) and the inner cell mass (ICM, will form the future embryo) (**Figure 3**). The morphology of both structures determines the probability of the embryo to implant (ASEBIR, 2015). In some cases, embryo can reach the D+6 or D+7 in culture.

Nevertheless, embryos reaching the blastocyst stage later than D+5 present lower implantation rates (Shapiro et al., 2008). Before implantation, the blastocyst hatches from the protective ZP.

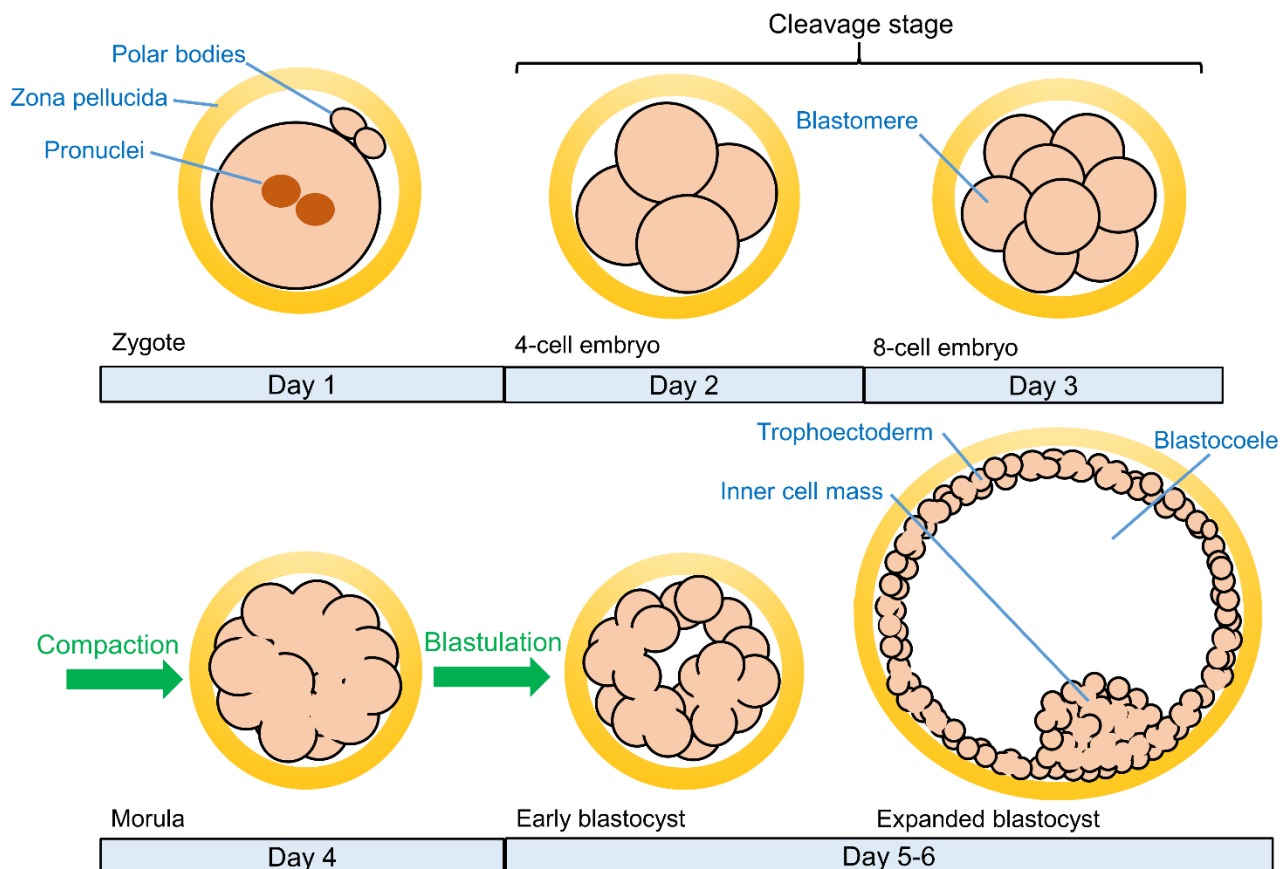


Figure 3. Representation of human preimplantational development. The fertilized oocyte (zygote) will undergo different mitotic divisions during the cleavage stage. Compaction is the process by which the morula is generated, after which blastulation will start. The main structures of the zygote and the blastocyst are indicated in blue. Source: own elaboration.

The quality of the transferred embryo and its probability to implant can be affected by a number of factors reviewed in the ASEBIR guidelines (ASEBIR 2015), including: stimulation protocol and hormonal levels, maternal or parental age, laboratory conditions, oocyte parameters (such as diffused cytoplasmic granularity, aggregation of endoplasmic reticulum, presence of cytoplasmic vacuoles, or presence of a big 1st polar body (Ebner et al., 2006; Rienzi et al., 2008)); zygote parameters such as PN and nucleolar precursor bodies (NPB) symmetry and position (Tesarik and Greco, 1999), presence of cytoplasmic halo (Salumets et al., 2001), cleavage stage (D+2 and D+3) parameters (such as presence of cellular fragments, multinucleation, presence of cytoplasmic vacuoles, abnormal ZP, or the number and stage-specific size of the blastomeres constituting the embryo (D3 embryos with ≤ 6 or ≥ 9 cells present higher aneuploidy rates)), or blastocyst parameters (such as grade of expansion, and number of cells and morphology of trophoectoderm

and ICM). In addition, time-lapse technologies currently applied in fertility clinics allow the introduction of morphokinetic parameters for embryo quality evaluation and selection.

In most cases, the best embryo is transferred at the cleavage stage (D+2 or D+3), at the blastocyst stage (D+5) and, less frequently, at the morula stage. The transfer at blastocyst stage resembles more what happens in an *in vivo* situation, allows better embryo selection, and offers better reproductive results when compared to transfer at D+2 or D+3 (Papanikolaou et al., 2006). In Spain, a maximum of three embryos can legally be transferred into the uterus; however, reproductive health professionals recommend a maximum of two transferred embryos per cycle.

In fertility clinics, preimplantational embryos are usually cryopreserved by vitrification, either at cleavage or blastocyst stage. The transfer of frozen-thawed embryos offers good results, with outcomes similar to those obtained in fresh embryo transfers.

3. A LONG JOURNEY: FROM THE TESTIS TO THE OOCYTE

The present thesis focuses on fertilization failure after ICSI, in which only the final mechanisms of human fertilization (i.e. oocyte activation) are involved. Nevertheless, understanding how sperm are formed in the testis (spermatogenesis), and the main events occurring in an *in vivo* situation prior to oocyte penetration is of critical importance to understand sperm biology, fertilization through ICSI, and the alterations that may lead to problems in oocyte activation and early development events.

3.1. SPERMATOGENESIS

Spermatogenesis is the process by which spermatogonia, diploid male germ cells, undergo meiosis and become mature haploid spermatozoa with fertilization potential. Spermatogenesis takes place in the seminiferous tubules of the testis. Spermatogenesis is supported by different somatic cells such as Leydig cells, which produce testosterone when stimulated by LH, and Sertoli cells, which constitute the blood-testis barrier, secrete endocrine factors (AMH, estradiol, inhibin B, androgen-binding protein, etc.), maintain the spermatogonial stem cell niche, and phagocyte degenerating germ cells and residual bodies from spermatids (Neto et al., 2016).

In humans, the spermatogenesis takes 42 to 76 days, and a man can produce 150 to 275 million spermatozoa per day (Misell et al., 2006). Spermatogenesis involves the following processes:

spermatogonia proliferation; differentiation of spermatogonia into spermatocytes; meiotic division of spermatocytes producing round spermatids; and spermiogenesis.

Spermatogonia, the diploid progenitors of the male germ line, are formed between birth and 6 months. They stay quiescent until the age of 5-7 years old, when they start proliferating via mitosis, and in puberty (and throughout the entire life of the man) they start the differentiation process toward spermatozoa. Three different spermatogonia have been described: “type A dark”, which are stem germ cells that rarely divide; “type A pale”, which proliferate actively via mitosis and produce the “type B” spermatogonia, the ones that will undergo meiosis and initiate the differentiation process (de Rooij and Russell, 2000). When the spermatogonium initiates the differentiation process, DNA replication occurs, generating the primary spermatocyte, a 4n cell (for each spermatogonium, 4 mature haploid spermatozoa will be formed) (**Figure 4**). Primary spermatocyte, which start the process of meiosis, can be classified according to the different stages of prophase 1: preleptotene, leptotene, zygotene, and pachytene, where DNA recombination occurs. The transition from metaphase I to anaphase I is critical, and problems in this process can lead to recombination failure, aneuploidy and idiopathic infertility. The first meiotic division generates secondary spermatocytes, followed by the second meiotic division, which generates haploid round spermatids.

Once meiosis is completed, spermatogenesis continues with spermiogenesis, the series of cellular and molecular events occurring to transform round spermatids into elongated spermatids and, eventually, spermatozoa (**Figure 4**). In spermatogenesis there are no cellular division events, and the process of sperm DNA condensation occurs, in which histones are replaced by more basic and positively charged nuclear proteins, the protamines (Oliva and Dixon, 1991). First, histones are replaced by transition nuclear proteins (TPs). Secondly, TPs are replaced by protamines; DNA is packed around them in supercoiled structures named toroids. Of note, this replacement is not global, as histones will remain in around 15% of the chromatin in mature sperm.

As detailed in **Figure 4**, during spermiogenesis the tail is formed from the centriole, and the spermatid gradually elongates. The axoneme (formed by microtubules disposed in 9+2 formation) is assembled, together with two additional sperm tail structures: the fibrous sheath and the outer dense fibers. Mitochondria increase in number and cluster around the tail basis, forming the midpiece. The acrosome, a large vesicle derived from the Golgi apparatus (Oko and Sutovsky, 2009), is also formed during spermiogenesis. In addition, most of the cytoplasm is lost in residual bodies, forming the “cytoplasmic droplet”, which will be eliminated during sperm maturation.

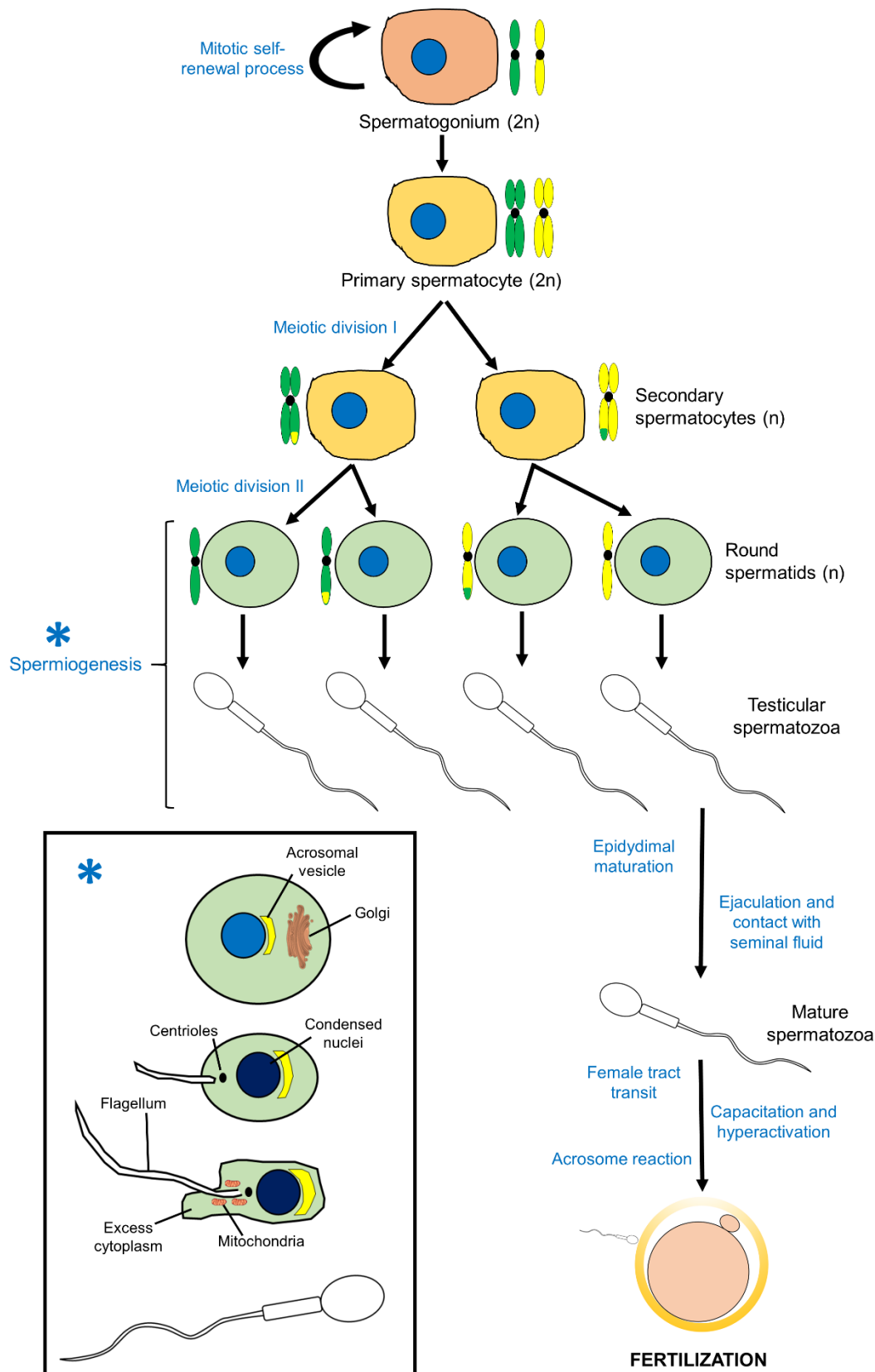


Figure 4. Representation of the main stages and events occurring in spermatogenesis and sperm maturation. Meiosis completion results in the production of haploid round spermatids, which undergo spermiogenesis, an essential process to generate all the specific structures and characteristics of the mature spermatozoa. Once spermatogenesis is completed, important changes are required for sperm to acquire motility and fertilizing ability, driven by epididymal maturation, contact with seminal fluid and capacitation. Source: own elaboration.

3.2. SPERM MATURATION, CAPACITATION AND OOCYTE FERTILIZATION

Once spermiogenesis is complete, spermatozoa are still “immature”, and are stored in the epididymis. At this point, epididymal maturation occurs, a series of biochemical changes essential for sperm to acquire its capacity to move and fertilizing ability. These changes are regulated by the epididymosomes, secreted extracellular vesicles (50–250 nm) containing RNA and proteins which are incorporated in sperm (Sullivan et al., 2005).

During ejaculation, sperm exit the testis through the vas deferens and the urethra. Ejaculated semen contains mature spermatozoa (5% of the semen volume), and seminal fluid, composed by the secretions of the seminal vesicles and prostate. These secretions contain sugars, lipids, steroids, polyamines, nitrogenous bases, proteins (needed for coagulation and liquefaction of semen), and immune factors. The prostate gland secretes extracellular vesicles named prostasomes (containing different lipids, RNA and proteins), which stimulate sperm motility and protect the sperm from the immune response in the female tract, among other functions (Aalberts et al., 2014).

During passage along the female reproductive tract, sperm face several obstacles and strict selection barriers (Sakkas et al., 2015). In human natural conception, of the million sperm present in a normal ejaculate, only some hundreds reach the Fallopian tube, and few reach the oviduct, a region that can act as a sperm reservoir and where oocyte fertilization takes place (Williams et al., 1992). In numbers, this means only one in 14 million ejaculated sperm reach the oviduct (Publicover et al., 2007).

In humans, semen is ejaculated in the anterior vagina, near the cervical opening, where sperm faces a low pH and immune response, and there is substantial sperm loss. Once ejaculated, semen forms a coagulate which is rapidly enzymatically degraded by prostatic proteases, so the motile sperm fraction can pass through the cervical mucus and enter the uterus within few minutes (Sakkas et al., 2015). Motile sperm progress through the uterus in less than 10 minutes, aided by peristaltic contractions of the myometrium (Kunz et al., 1996). Then, sperm must find the uterotubal junction, a narrow entrance to Fallopian tubes filled with mucus. Sperm motility, morphology and ability to interact with the epithelium in the Fallopian tube are essential for sperm progression along the tract.

The contact with the female reproductive tract triggers sperm capacitation (Austin 1951). Sperm capacitation involves a group of cellular processes which include the activation of cAMP production and PKA activity, sperm motility hyperactivation, increase in phosphorylation levels of several proteins, and changes in calcium intracellular levels and pH (Kwon et al., 2014). Sperm

capacitation involves a reduction of sperm cholesterol levels in the plasma membrane, increasing the permeabilization of the sperm and promoting hyperactivation and acrosome reaction.

Upon reaching the oocyte, sperm needs to penetrate through a thick layer of cumulus cells, digest the 10-30 μm of ZP, and fuse with oocyte membrane. Acrosome reaction and acrosomal proteases (such as acrosin and hyaluronidase), propulsive force produced by sperm flagellum and hyperactivation, and specific receptor and binding proteins play essential roles in these steps of fertilization. Finally, membrane fusion between gametes occurs, in which the JUNO receptor (in the oolema) and the IZUMO1 protein (in sperm) interaction is essential for human fertilization to occur (Jean et al., 2019).

4. FERTILIZATION EVENTS AFTER SPERM ENTRY INTO THE OOCYTE

4.1. OOCYTE ACTIVATION

The metaphase II arrested oocyte, upon contact with the sperm, undergoes several essential cellular and molecular processes. Oocyte activation and “oocyte to embryo transition” comprise several processes including cortical reaction (extrusion of cortical granules), zona pellucida remodelling to prevent polyspermy, exit from meiotic arrest, 2nd polar body extrusion and cell cycle progression to first mitotic division, decondensation of the sperm DNA, DNA replication and pronuclear (male and female) formation and migration, epigenetics reprogramming, changes and recruitment of maternal mRNA and proteins, regulation of gene expression and cytoskeletal rearrangements (Ducibella and Fissore, 2008; Swann and Yu, 2008).

Oocyte activation and early fertilization events can also affect later stages of preimplantational development (Ajduk et al., 2011). All these events occur in oocyte interphase, a period between meiotic resumption and first mitotic division, which in humans lasts around 16 hours.

4.2. THE IMPORTANCE OF OOCYTE CALCIUM SIGNALLING AND ITS REGULATION

Oocyte activation is induced and tightly regulated by a series of repetitive intracellular calcium (Ca^{2+}) rises (usually called calcium oscillations) which are propagated through the whole ooplasm after sperm entry (Tesarik et al., 1994). The sperm triggers this signalling process by introducing a soluble factor into the oocyte cytoplasm.

In humans, calcium oscillations occur at time intervals of 10-30 minutes, and each one lasts for about one minute (Taylor et al., 1993). Their specific number, frequency, amplitude, and duration are involved in early fertilization events, control of gene expression and preimplantational embryo development (Yamaguchi et al., 2017). These calcium oscillations can be monitored in the oocyte by using different imaging systems (**Figure 5**).

Intracellular calcium rises upon fertilization is a conserved signalling mechanism, but the specific signalling pattern and oscillations differ between species (Stricker 1999). Calcium oscillations, which can continue for several hours, stop after pronuclei formation in mice (Marangos et al., 2003), but continue far beyond this point in humans (Yeste et al., 2016).

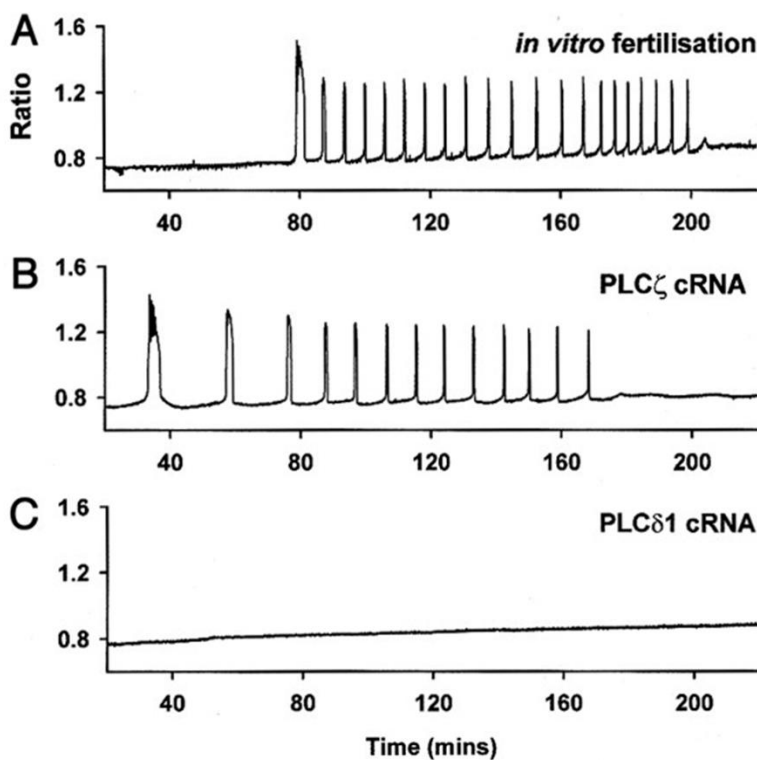


Figure 5. Calcium oscillations measured in mouse oocytes loaded with fura-red after sperm in vitro fertilization (A), injection of *PLCZ1* cRNA (B), and injection of cRNA from another phospholipase (*PLCD1*), which fails to generate this specific calcium signalling in the oocyte (C). This figure has been modified from Saunders et al., 2002.

Upon sperm contact, acrosomal phospholipase C zeta ($PLC\zeta$) hydrolyses its substrate phosphatidylinositol 4,5-bisphosphate (PIP_2) from intracellular vesicles distributed across the oocyte cytoplasm (Sanders et al., 2018), generates 1,4,5-trisphosphate (IP_3) and diacylglycerol (DAG). IP_3 binds to its receptor (IP_3R), a ligand-gated channel, located in the endoplasmic reticulum (ER) membrane (**Figure 6**). After this interaction, the channel opens and calcium ions stored in the ER move to the cytoplasm (Taylor et al., 2014), causing the specific calcium rise observed in oocyte activation. High levels of Ca^{2+} and IP_3 in the cytoplasm sensitize and

downregulate the IP₃Rs, causing a reduction in the frequency of calcium oscillations with time (Jellerette et al., 2000; Lee et al., 2010).

In addition to intracellular calcium stores, extracellular calcium levels are essential for oocyte activation, as the process fails when membrane calcium channels are inhibited. “Store-operated calcium entry” (SOCE) is a transport channel system which regulate Ca²⁺ entry / refill into intracellular stores. When intra-ER Ca²⁺ levels are reduced, this mechanism is activated and provides Ca²⁺ influx from the extracellular space. The components of this system are stromal interaction molecule 1 (STIM1), calcium release-activated calcium channel protein 1 (ORAI1), and sarco/endoplasmic reticulum calcium ATPase (SERCA) (Wang and Machaty, 2013). STIM1, a transmembrane protein in the ER, has a luminal region (containing EF-hand and sterile alpha motif domains) which acts as a calcium sensor (Liou et al., 2007). Sperm-derived calcium efflux from the ER is detected by STIM1, which translocates to the plasma membrane and produces a conformational change in ORAI1 channels, allowing calcium entry into the oocyte (Park et al., 2009) (**Figure 6**). SERCA are ion pumps that transport calcium ions from cytosol to the ER lumen, refilling the intracellular calcium stores of the oocyte, a process needed to generate new calcium oscillations. Additional calcium channels in the oocyte membrane (PMCA, TRPM7, TRPV3, Cav3.2) have been reported to participate in the regulation of calcium homeostasis during fertilization (Xu and Yang, 2017).

Other characteristic features of fertilization are the hyperpolarization of membrane potential across the plasma membrane, and the “zinc spark”, which consists of a fast release of zinc from the oocyte cytoplasm to the extracellular space (within minutes of fertilization) (Kim et al., 2011). Previous studies determined that this phenomenon is necessary for cell cycle resumption, and that zinc chelation may be enough to trigger oocyte activation in humans (Duncan et al., 2016). In addition, the intracellular levels of zinc have been associated with the regulation of PKC, MAPK and Emi2 activity (Krauchunas and Wolfner, 2013; Zhao et al., 2014).

4.3. A COMPLEX DOWNSTREAM SIGNALING

The process of calcium signalling activates different kinases through which downstream events are triggered. During oocyte activation, protein kinase C (PKC), a Ser/Thr-protein kinase, is activated (by DAG and calcium) and is rapidly translocated from the cytoplasm to the oocyte membrane just after the first calcium rise (Nishizuka, 1992). This translocation allows PKC to phosphorylate a myristoylated alanine-rich C-kinase substrate (MARCKS) protein, causing disassembly of the cortical actin network and extrusion of cortical granules to prevent polyspermy (Tsaadon et al.,

2008) (**Figure 6**). PKC is associated to the oocyte meiotic spindle and regulates the second meiotic division (Baluch et al., 2004). At the same time, PKC activity seems to be involved in a positive feedback, helping to generate new calcium transients (calcium oscillations stop when inhibiting PKC), by phosphorylating calcium channels in the oolema (Rajagopal et al., 2014; Yeste et al., 2016).

Calcium/calmodulin-dependent protein kinase type II (CAMKII), another kinase fundamental to the process, is activated by calcium and calmodulin (CaM), essential for meiotic exit and entry into the first mitotic cell cycle (Markoulaki et al., 2004). CAMKII activity oscillates with calcium during oocyte activation (Markoulaki et al., 2004). In fertilization, CAMKII phosphorylates early mitotic inhibitor 2 (Emi2, also called F-box only protein 43). The function of Emi2, an oocyte-specific protein, is to maintain meiotic arrest by blocking cyclin B1 proteasomal degradation via inhibition of the anaphase-promoting complex (APC/C, an E3 ubiquitin ligase). Cyclin B1 and cyclin-dependent kinase 1 (CDK1 / Cdc2) are components of the M phase/maturation-promoting factor (MPF) (Ducibella and Fissore, 2008). Emi2 is degraded after being phosphorylated by CAMKII and PLK1 (which generates a second phosphorylation site at Emi2), so Cyclin B1 is ubiquitinated by APC and degraded by the proteasome (Jia et al., 2015) (**Figure 6**). This inactivates MPF, causing release of metaphase II arrest and completion of meiosis (extrusion of 2nd polar body and formation of female PN) (Nixon et al., 2002; Marangos and Carroll, 2004).

Other factors and mechanisms participate in the regulation of these signalling events. For instance, the components of the spindle assembly checkpoint (SAC) are involved in APC/C inhibition until the establishment of stable bipolar microtubule attachments (Nabti et al., 2014). Myosin light chain kinase (MLCK) is a Ca²⁺/CaM-dependent kinase, involved in cortical cytoskeletal remodelling, CG exocytosis, and polar body extrusion by regulating myosin II (Ducibella and Fissore, 2008). Wee2 is another example of an oocyte kinase involved in oocyte activation. Phosphorylated and activated by CAMKII, Wee2 activity is necessary for MPF inactivation and meiotic resumption (Oh et al., 2011) (**Figure 6**). Considering the relevant role of all these kinases in oocyte activation, it is not surprising that disrupting phosphorylation during fertilization causes failure to form and extrude the second polar body, aberrant cytoskeletal reorganization and abnormal early preimplantational development (Tatone et al., 2002).

Finally, another essential kinase-dependent signalling is involved in oocyte activation: the MAPK pathway. MAPK activity (regulated by Mos kinase, among other factors) is required to maintain meiotic arrest in the mature oocyte, a function conserved between different species (Madgwick and Jones, 2007). Sperm-entry inactivates MAPK activity allowing the oocyte to complete meiosis.

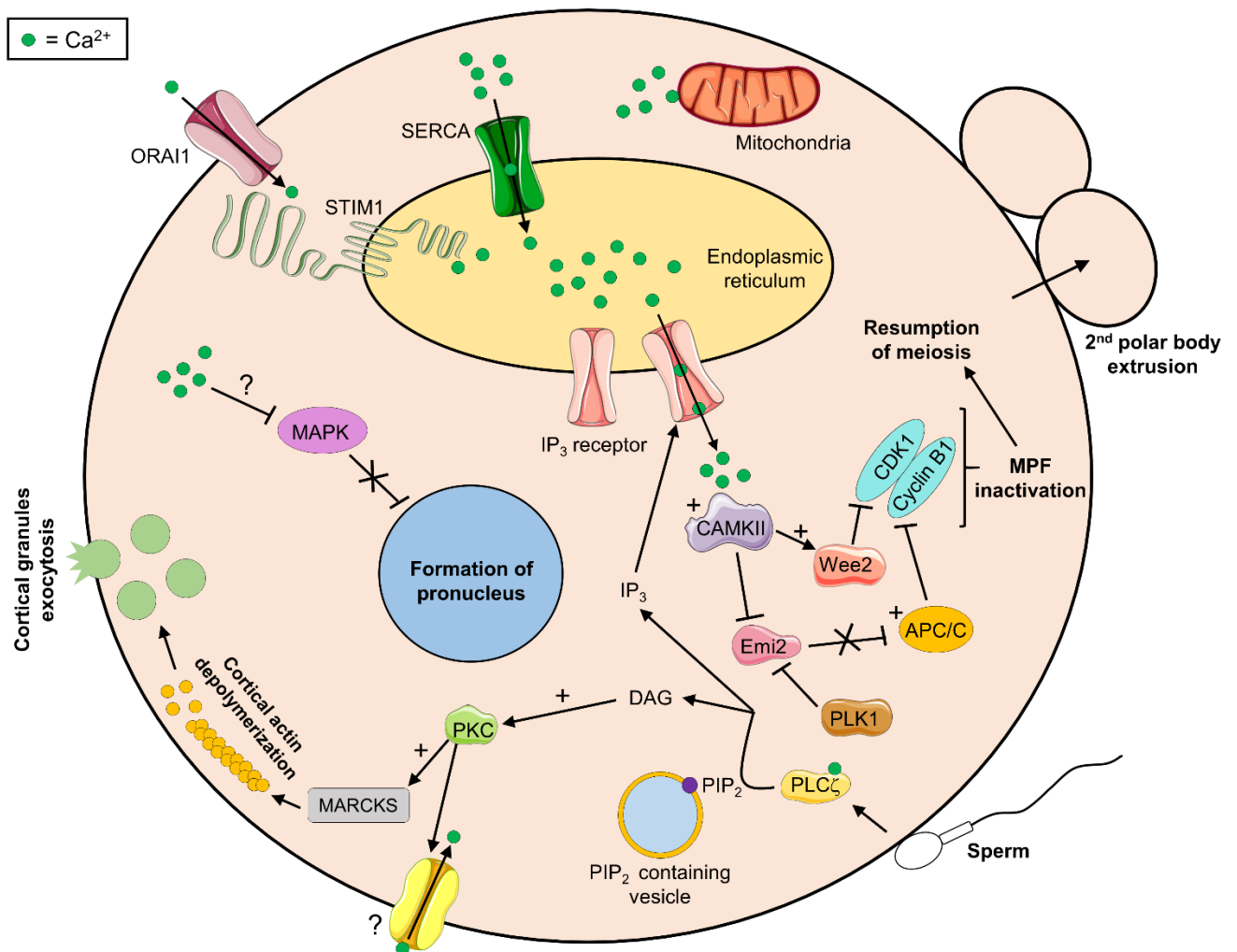


Figure 6. Molecular signalling and main cellular events during oocyte activation. Sperm triggers calcium oscillations via PLC ζ , causing the release of cortical granules and CAMKII activation. Emi2 is inhibited and APC/C liberated; which subsequently reduces the levels of cyclin B1, a phenomenon that causes MPF inactivation and release of meiotic (metaphase II) arrest. Calcium signalling also regulates MAPK activity, with MAPK decreased activity required for pronuclei formation. The SOCE system (STIM1, ORAI1 and SERCA) guarantees the homeostasis of calcium signalling and the refilling of endoplasmic reticulum calcium stores. Oocyte mitochondria participate in the regulation of intracellular calcium levels, and become more active during oocyte activation. APC/C: anaphase-promoting complex/cyclosome; CAMKII: calcium/calmodulin-dependent protein kinase II; CDK1: cyclin-dependent kinase 1; DAG: diacylglycerol; Emi2: early mitotic inhibitor 2; IP₃: inositol 1,4,5-trisphosphate; MAPK: mitogen-activated protein kinase; ORAI1: calcium release-activated calcium channel protein 1; PIP₂: phosphatidylinositol 4,5-bisphosphate; PKC: protein kinase C; PLC ζ : phospholipase C zeta 1; PLK1: serine/threonine-protein kinase PLK1; SERCA: sarco/endoplasmic reticulum calcium ATPase; STIM1: stromal interaction molecule-1; Wee2: Wee1-like protein kinase 2. Source: own elaboration based on Yeste et al., 2016.

Other events like calcium release and PN formation seem to be under MAPK control also, as the inactivation of MAPK activity (by a mechanism still unknown in mammals) is required for PN formation (Moos et al., 1995) (**Figure 6**). In mouse, constitutive expression of active MEK kinase, responsible for activating MAPK, prevent PN formation (Moos et al., 1996); while DMAP (a

kinase inhibitor) inactivates MAPK activity and accelerates PN formation (Liu and Yang, 1999). Once PN are formed, a later MAPK activity increase will cause nuclear envelope breakdown and PN fusion. Finally, ERK, member of the MAPK family, seems to interact with IP₃Rs (Bai et al., 2006); but if ERK can participate in the regulation of IP₃Rs and calcium oscillation in human oocytes remains to be demonstrated.

Calcium transients also stimulate oocyte mitochondrial activity, activating the Krebs cycle and increasing the levels of NADH and ATP, which support all the events occurring during oocyte activation (cell cycle progression, calcium channels, exocytosis, cytoskeleton rearrangement, etc.). At the same time, maternal mitochondria contain important stores of Ca²⁺ and they are in close association with the endoplasmic reticulum, so they could play a crucial role in sustaining sperm triggered calcium oscillations and intracellular calcium homeostasis (Dumollard et al., 2004).

4.4. THE SPERM INSIDE THE OOCYTE

Once inside the oocyte, sperm function is not limited to PLC ζ provision. In addition to supplying different molecular factors (see section 2.1), some important processes related to the male gamete occur in parallel to oocyte activation and are needed to complete the fertilization process and start embryo development.

Soon after incorporation into the oocyte, the sperm is gradually demembrated, and the nuclear envelope and the tail fibrous sheath are quickly dissolved (Sutovsky et al., 1997). The striated columns surrounding the centriole disassemble, a process required for the formation of the zygotic centrosome and microtubule enucleation (Sutovsky et al., 1996). Sperm proteasomes, present in the midpiece, seem to be involved in this degradation mechanism of the sperm connecting piece and structures surrounding the proximal centriole, and are essential for correct sperm aster formation (Rawe et al., 2008) (**Figure 7**). Concomitantly, the first enucleated microtubules may help recruiting and directing factors needed for degradation of the mitochondrial sheath and other sperm structures (Song et al., 2016).

Sperm mitochondria become ubiquitinated inside the oocyte and targeted for degradation by oocyte proteasomal proteolysis and autophagic machinery (Song et al., 2016). This process, which is required for normal proper preimplantational development, explains why mtDNA inheritance is maternal and does not follow Mendelian rules. Surprisingly, biparental mitochondrial DNA inheritance was recently documented in some isolated family cases (Luo et al., 2018).

In parallel, also soon after sperm entry, sperm DNA decondensation is needed for fertilization to progress, a process dependent on oocyte cytoplasmic factors. Protamines in the highly condensed chromatin are rapidly exchanged by histones, mostly of maternal origin, implying a reduction of sperm chromatin sulphide bonds (**Figure 7**). Sperm decondensation is required for proper formation of the male pronucleus, and to initiate the paternal epigenetic reprogramming. This reprogramming is characterized by a global and active demethylation of the paternal genome by maternal TET3 demethylase, but some regions remain methylated (called “imprinting control regions”) (Shen et al., 2014). Interestingly, protamine-containing sperm are more capable of being reprogrammed after fertilization (Okada and Yamaguchi, 2017). All these events trigger what is called the minor zygotic gene activation (ZGA), a transcription wave starting at the S-phase of the 1-cell stage which is critical for preimplantational development (Abe et al., 2018).

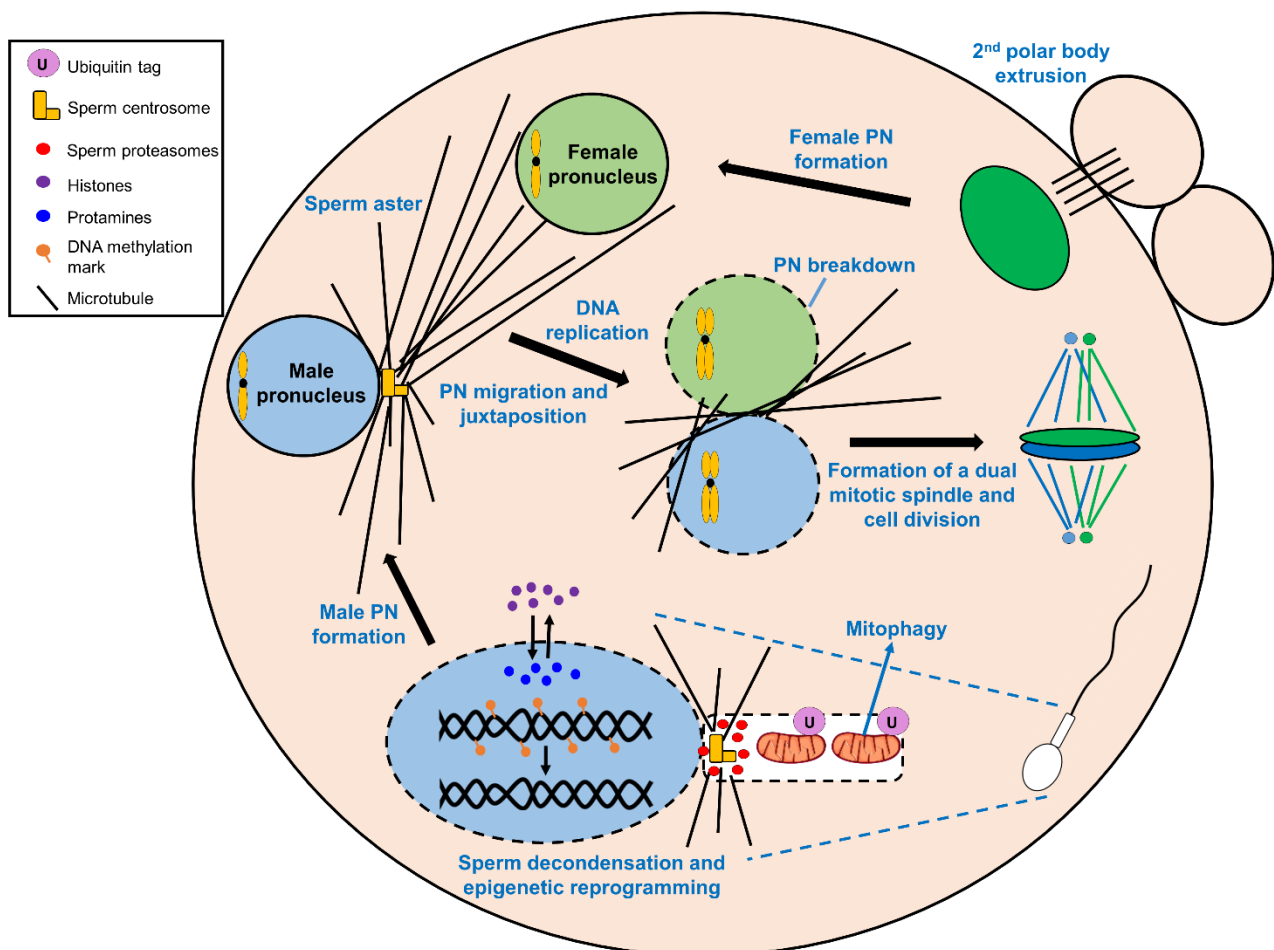


Figure 7. Main cellular events occurring in the male gamete and paternal genome after oocyte fusion and penetration. Most subcellular sperm structures are lost or dissolved; mitochondria are eliminated by mitophagy. Sperm nucleus undergoes decondensation by protamine-histone exchange followed by epigenetic reprogramming involving active DNA demethylation. Sperm proteasomes participate in the degradation of the midpiece. Liberation of the sperm centrosome, required for aster formation, is in turn needed for PN migration and juxtaposition. Zygotic pronuclei fade after nuclear envelope breakdown, and the first mitotic division, driven by two spindles enucleated by maternal and paternal own chromosomes, occurs shortly after. Source: own elaboration.

The sperm centrosome is required to enucleate a radial array of microtubules (acting as a microtubule organizing center, MTOC), forming the sperm aster. The sperm aster arises from the sperm midpiece and is needed for pronuclei migration and apposition (regulated by dynein and dynactin proteins) (**Figure 7**) (Payne et al., 2003; Tremoleda et al., 2003). The sperm centrosome is essential, as the oocyte loses its centrosome at early stages of gametogenesis (oocytes retain pericentriolar material, but lack centrioles).

Aproximately 6 hours after fertilization, both pronuclei are formed by reconstitution of the nuclear envelope by membrane vesicle fusion and nuclear lamina formation, and both PN will fuse after 8-9 hours (juxtaposition), aided by the sperm aster cytoskeletal structure (Coticchio et al., 2018). In humans, DNA synthesis / replication in the male pronucleus, dependent on oocyte machinery, starts around 12 hours after gamete fusion, and is usually completed between 14 and 22 hours (Capmany et al., 1996). Aproximately 24 hours after fertilization, nuclear envelope breakdown (pronuclei fade and cannot be visible anymore) occurs, the mitotic spindle forms, and the first cell division occurs (**Figure 7**). As recently described, the first mitotic division is dependent on the formation of a dual mitotic spindle (or two zygotic spindles) that keep both genomes (paternal and maternal) apart along the 1-cell stage (Reichmann et al., 2018).

As it will be discussed in the present thesis, different biological processes occurring before sperm entry (spermiogenesis, nuclear condensation, sperm capacitation and metabolism, etc.) can affect the occurrence and normal sequence of these events, affecting or preventing normal fertilization.

5. FERTILIZATION THROUGH ASSISTED REPRODUCTION TECHNIQUES

5.1. MAIN ART TECHNIQUES: IUI, IVF, ICSI

In fertility clinics, assisted reproduction techniques (ART) are used to treat infertility, a problem with a high prevalence in the general population. The main techniques used in ART include intrauterine insemination (IUI) and, most commonly, one of the following fertilization techniques: *in vitro* fertilization (IVF) and intracytoplasmic sperm injection (ICSI). In 2016, 138,553 IVF cycles (IVF + ICSI) and 36,463 IUI cycles were performed in Spain (Registro SEF 2016). The first live birth through IVF was achieved in 1978 (Stepoe and Edwards, 1978), and the first live birth through ICSI was achieved in 1992 (Palermo et al., 1992). To date, over 6 million children have been born worldwide through ART.

In IVF treatments, it is usual to use hormonal ovarian stimulation protocols to increase the number of mature oocytes produced, in order to generate more embryos and optimize reproductive success. These oocytes are surgically retrieved from the ovary once follicular growth is complete. The specific protocol for ovarian stimulation depends on the ovarian reserve, treatment of choice and patient characteristics, among other factors (La Marca and Sunkara, 2014).

IUI is an inexpensive and non-invasive ART technique that involves placing the sperm inside the woman's uterine cavity. In IVF, fertilization is facilitated by *in vitro* culture of mature oocytes together with selected motile sperm (**Figure 8**); however, FF occurs in 5-15% of cycles when using this technique (Combelles et al., 2010). Failure in these techniques may be caused by problems in female reproductive tract transit (for IUI only), deficient sperm motility (the main cause in both techniques), abnormal capacitation and acrosome reaction, or failure of sperm to penetrate the layers surrounding the oocyte (cumulus cells and zona pellucida) or to undergo membrane fusion. In IVF, total fertilization failure occurs in 5-16 % of cycles, explained by problems in sperm penetration in 60% of cases.

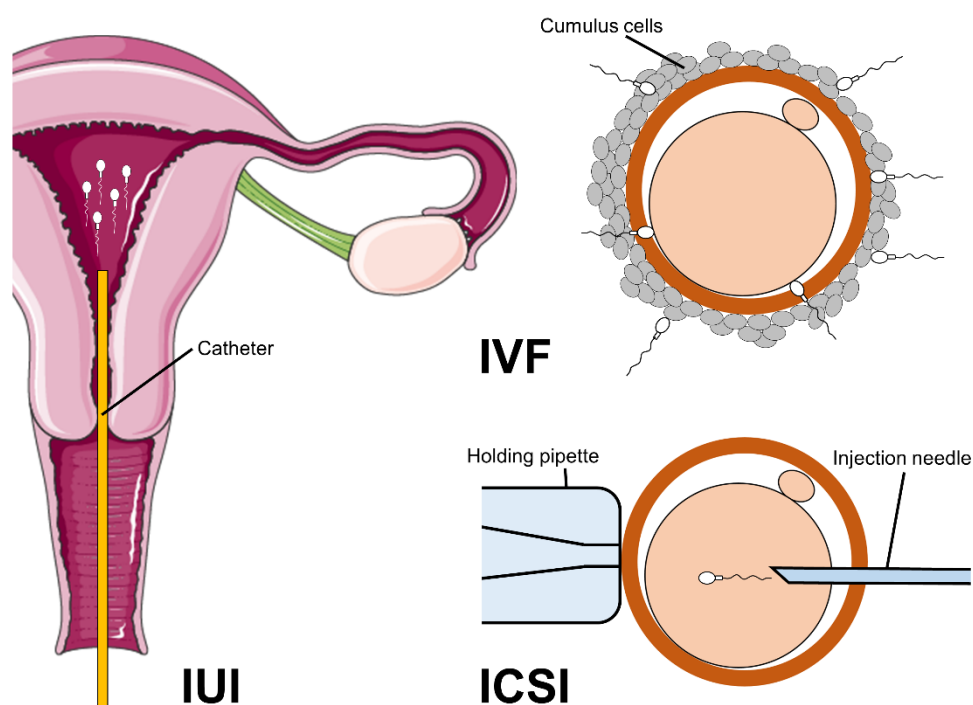


Figure 8. Main techniques applied in assisted reproduction technology (ART): intrauterine insemination (IUI), in vitro fertilization (IVF), and intracytoplasmic sperm injection (ICSI). Source: own elaboration.

By contrast, these problems are by-passed by intracytoplasmic sperm injection (ICSI), which consists of the direct introduction of a single spermatozoon into the cytoplasm of a mature oocyte (**Figure 8**). ICSI is a very efficient technique, having an average fertilization rate of 70-80% (Neri

et al., 2014). The original indication for ICSI use was a male factor (mainly low sperm concentration and / or motility), but currently ICSI is being used for all cases of infertility and is globally accepted as a technique leading to successful pregnancy and healthy offspring. In Spain, ICSI is applied in the 89.6% of all IVF cycles (Registro SEF 2016).

When using ICSI, sperm does not need to penetrate the ZP and fuse to the oocyte membrane, so the calcium oscillations occur immediately after injection of the single sperm. In conventional IVF, the calcium intracellular increase starts a few minutes after sperm-oocyte fusion (Lawrence et al., 1997).

5.2. SPERM PROCESSING AND SELECTION IN THE IVF LABORATORY

Semen processing is a necessary practice in all fertility clinics. This processing is needed for all ART techniques, but selection of the optimal sperm population is especially desirable for ICSI, in which a single spermatozoon is used for insemination. Sperm within the same ejaculate are highly heterogeneous in terms of morphology, biochemical and physiological characteristics (Wang et al., 2012).

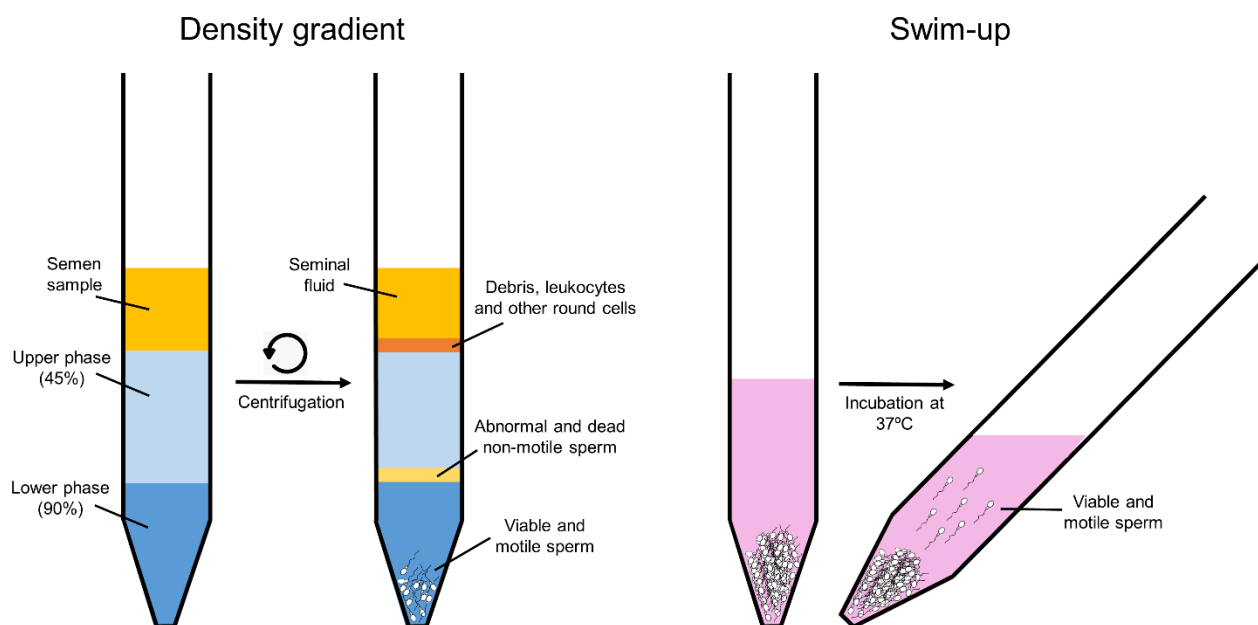


Figure 9. Main techniques used for sperm processing and selection in IVF laboratories. Different layers at different density constitute the density gradient column, which after centrifugation will be useful to select the highly motile and viable population of spermatozoa. Swim-up relies on selecting the sperm with better quality based on its own ability to swim in the culture medium. Source: own elaboration.

Different protocols and techniques have been described to process sperm, including swim-up and density gradient processing, able to select a population of motile and morphologically normal

sperm (Sakkas et al., 2015) (**Figure 9**). These protocols, while failing to mimick the selection occurring *in vivo*, have been described to improve fertilization rates and reproductive outcomes while also minimizing the risk of fertilization failure. The specific protocol and time of incubation can vary depending on the ART procedure used (IUI, IVF or ICSI), and the semen parameters (mainly concentration and motility).

In addition, complementary sperm selection methods are starting to be introduced in fertility clinics, but in many acses their efficiency has not been yet confirmed. As, hyaluronic acid (HA) is an abundant component of the oocyte-cumulus complex, testing of sperm ability to bind to HA (PICSI) has been proposed as a useful selection technique in ART. Although some studies found that HA-bound sperm presented higher fertilization rates or embryo quality (Nasr-Esfahani et al., 2008; Parmegiani et al., 2010), it seems that this technique does not improve ICSI outcomes (Beck-Fruchter et al., 2016; Kirkman-Brown et al., 2019). Another example of sperm selection is intracytoplasmic morphologically selected sperm injection (IMSI), using interference contrast microscopy at high magnification (at least $\times 6000$) that allows visualization of sperm organelles and vacuoles, but results from different studies and RCTs do not support its clinical use (Teixeira et al., 2013; McDowell et al., 2014). Magnetic activated cell sorting (MACS) use columns and annexin-V magnetic beads to deselect dead and apoptotic sperm within a sample, and some studies using this technique report improved pregnancy rates after ICSI (Dirican et al., 2008).

Finally, novel and promising technologies are making their way into clinical practice; for example, microfluidics systems (Vaughan and Sakkas, 2019) aiming at mimiking the viscoelastic environment found by sperm when passing though female reproductive tract and mucus in an *in vivo* situation.

6. FERTILIZATION FAILURE AFTER ICSI

6.1. CHARACTERIZATION OF ICSI FERTILIZATION FAILURE AND ITS CLINICAL IMPACT

Despite the high fertilization rates achieved by ICSI, total fertilization failure (FF) is still an important concern in fertility clinics, as it occurs in 1-5 % of all cycles (Combelles et al., 2010; Shinar et al., 2014). In addition, poor fertilization rates (<50%) are common (Flaherty et al., 1995), and diminish the chances for successful pregnancy and live birth. Overall, when using ICSI, around 25% of the inseminated oocytes present fertilization errors and arrest their development at day 1 (Joergensen et al., 2014).

The main cause of fertilization failure is oocyte activation deficiency (OAF, in 40% of cases), in which oocytes remain arrested at metaphase II, without the 2nd polar body and pronuclei (Asch et al., 1995; Flaherty et al., 1998) (**Figure 10**). Nevertheless, other situations can be observed in fertilization failure, such as abnormal fertilization, characterized by an abnormal number of formed pronuclei, usually classified as 1 PN, 3 PN, or > 3 PN (**Figure 10**).

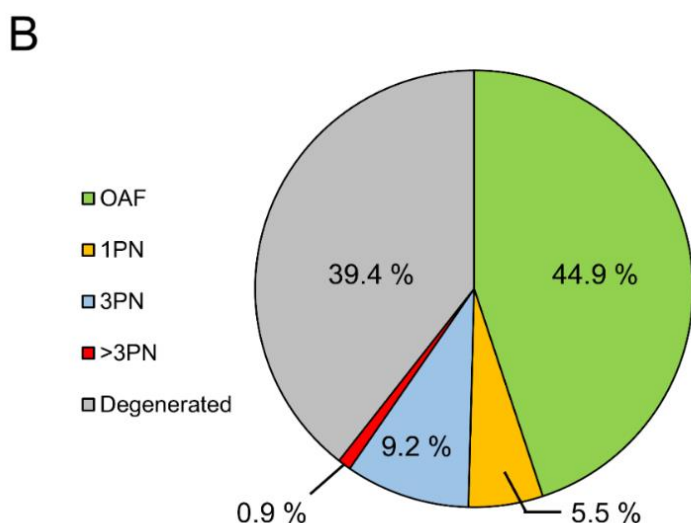
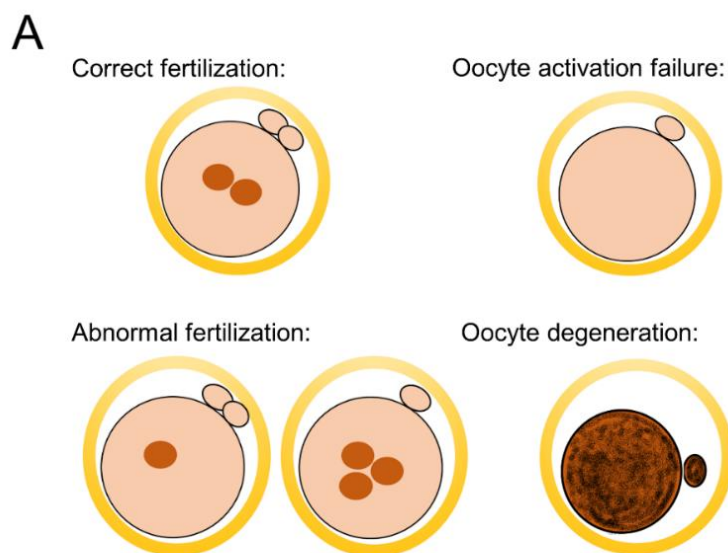


Figure 10. A. Main outcomes after fertilization through ICSI. Dark circles indicate the pronucleus / pronuclei. **B.** Analysis of fertilization outcome in 122 ICSI cycles with fertilization failure, either total or partial (0% or $\leq 20\%$ fertilization rate, respectively), comprising a total of 728 oocytes which failed to fertilize. A minimum of 5 mature oocytes from donors between 18 and 35 years old were used in each cycle.

In any of these situations, fertilization failure is characterized by developmental arrest at the one cell stage (within the first day after insemination). When evaluating non-fertilized oocytes, it is difficult to determine where this arrest exactly takes place along the timeline between oocyte activation and entry into interphase and first mitotic division (Combelles et al., 2010). For example, in the case of oocytes with absence of pronuclei, it is likely that the arrest occurred before the interphase stage, but it is difficult to determine if specific steps of fertilization like calcium

oscillations (normal or partial / altered), sperm decondensation or sperm aster formation occurred or not. According to previous reports, almost one half of non-fertilized oocytes had initiated aspects of the fertilization process after the successful incorporation of the spermatozoon (Asch et al., 1995).

In addition, the occurrence of cell death leading to oocyte degenerating during or shortly after insemination is a common phenomenon in ICSI, reaching 30%–50% of inseminated oocytes in most severe cases (Rosen et al., 2006). At day 1 after ICSI, oocyte degeneration is characterized by a retracted or darkened cytoplasm. Levels of FSH at day 3, number of mature oocytes retrieved, and E2 levels seem to be independent predictors of degeneration rate (Rosen et al., 2006).

Finally, in addition to pronuclei number, the number of polar bodies are also evaluated; a fertilized oocyte with 1 or 3 polar bodies is considered as abnormal fertilization (even if 2 pronuclei are present) and should be discarded. Nevertheless, evaluation of the number of polar bodies is not always performed, as they can be difficult to visualize; it is difficult to determine if the number of polar bodies observed is indeed the total number that were produced, as they can fragment and disappear.

From a clinical point view, fertilization failure is difficult to predict. Despite being rare, each specific case of FF deserves a comprehensive management due to its impact. FF can be either sporadic or recurrent / repetitive (≥ 2 cycles); recurrent FF presents a high degree of difficulty in terms of treatment and clinical management.

FF results in a high economic and psychological impact for patients and present a difficult clinical management. Currently, treatment options for FF patients are limited to use of donor gametes, ICSI combined with assisted oocyte activation (AOA), or repetition of the cycle using the same gametes.

6.2. AOA FOR FERTILIZATION FAILURE AFTER ICSI

Assisted oocyte activation (AOA) aims to induce artificial calcium rises in order to overcome OAF in ART, by increasing the intracellular calcium levels in the oocyte, required for proper fertilization and preimplantational development initiation.

AOA should be applied in ICSI after a previous cycle with total or partial FF (Vanden Meerschaut et al., 2012). In some cases, AOA is performed one day after ICSI in the unfertilized oocytes in an attempt to overcome FF in the present cycle, a procedure called “rescue-ICSI” (Zhang et al., 1999;

Huang et al., 2015). In this approach, which presents less efficiency than a regular ICSI-AOA, negative effects caused by *in vitro* oocyte aging cannot be discarded (Miao et al., 2009).

These methods are based on applying mechanical (Tesarik et al., 2002), electrical (Yanagida et al., 1999) or chemical stimuli (Heindryckx et al., 2008; Borges et al., 2009) (**Table II**). The most commonly used chemical reagents are calcium ionophores such as ionomycin and calcimycin (A23187). These reagents are lipid-soluble and can transport calcium ions across the membrane of the main reservoirs within the oocyte.

Table II. Main AOA approaches used in ICSI treatments in patients with previous fertilization failure.

Method	Description
Mechanical	Modified ICSI procedure: aspiration of peripheral cytoplasm, followed by deposition of the aspirated cytoplasm in the centre of the oocyte.
Electrical	Use of direct current voltage which causes rearrangement of the proteins of the cell membrane, leading to the formation of pores that allow the influx of extracellular calcium.
Chemical	Incubation with calcium ionophores which allow transport of calcium ions across oocyte membrane.

Studies in animal models indicate that the pattern of calcium signalling during fertilization can have long-term effects on gene expression, epigenetics and development to term (Ducibella et al., 2002). The different AOA methods described above induce aberrant calcium patterns in the oocyte, and the potential effects of this phenomenon in the offspring are unknown (Yamaguchi et al., 2017). For example, chemical AOA, the most used strategy in ART, generally induces a single calcium rise without subsequent oscillations (Swann and Ozil, 1994). Even in those approaches trying to “mimic” the natural calcium oscillations, for example by combining calcium ionophores with injection of CaCl₂, present notable differences in the signalling obtained.

For the aforementioned reasons AOA is still considered an experimental technique. Concerns regarding its safety include the possibility that these approaches could cause alterations in embryo development and the health of the future offspring. Nevertheless, recently, normal health in children born after AOA was reported by several long-term follow-up studies (D'haeseleer et al., 2014; Vanden Meerschaut et al., 2014; Deemeh et al., 2015).

AOA efficiency is still under debate. ICSI followed by AOA is primarily intended for patients with male-related OAF, but this technique have been also used for all kinds of fertilization failure. The usefulness of AOA for couples experiencing FF and if fertilization and pregnancy rates are equivalent or improved after ICSI-AOA compared with conventional ICSI are still uncertain, explained by the heterogeneity of AOA methods and groups of patients included. Some systematic reviews and meta-analysis report better fertilization rates and reproductive outcomes (Murugesu et al., 2017; Fawzy et al., 2018), while other authors do not find this association (Sfontouris et al., 2015).

Some authors found that AOA is not beneficial for all FF patients (Vanden Meerschaut et al., 2012). Our hypothesis is that AOA should be limited to cases with a clear sperm defect to trigger oocyte activation and would result in no benefit in cases where sperm defects are not identified. A specific chapter in this thesis will be focused on AOA treatment in FF after ICSI (Chapter 6).

7. CAUSES AND MECHANISMS OF FERTILIZATION FAILURE AFTER ICSI

The problem of fertilization failure after ICSI is not completely understood. However, different causes have been described, which can be divided in three main groups: technical and protocol, oocyte-related and sperm-related, with the latter accounting for more than a half (50-75%) of total fertilization failure cases after ICSI (Shinar et al., 2014; Yeste et al., 2016). We will analyse the main causes of FF after ICSI, with focus on the main topic of this thesis: causes on sperm-related OAF.

7.1. TECHNICAL CAUSES OF FERTILIZATION FAILURE

Incorrect sperm injection or sperm expulsion during injection account for ICSI technical errors, but in only 10-12 % of unfertilized oocytes after ICSI the sperm DNA is outside the oocyte (Swain and Pool, 2008; Hojnik and Kovacic, 2019).

ICSI is an invasive technique. During sperm injection, the procedure may cause subtle damage in oocyte structures like microtubules and meiotic spindle. However, in a properly set up laboratory with well-trained professionals, FF due to technical errors is very low.

In addition, use of reagents in poor conditions or the use of suboptimal protocols for sperm processing or cryopreservation may reduce the fertilization rates. Nevertheless, the quality controls

applied in fertility clinics minimize the risk of FF due to these causes. In addition, the correct timing in the IVF protocols and the time of incubation of gametes are reported to affect reproductive outcomes (Pujol et al., 2018). However, it is not known if the sperm incubation time before ICSI can affect fertilization rates, something which is addressed in the annex of the present thesis.

7.2. OOCYTE-RELATED FERTILIZATION FAILURE

Although this thesis will be focused on sperm-related fertilization failure mechanisms, it is important to remember the role of its counterpart, the oocyte. Obviously, OAF is not only restricted to sperm alterations, and the female factor may also contribute to a considerable proportion of FF cases after ICSI. As previously explained, oocyte-borne factors are responsible of several signalling events downstream of sperm entry.

The use of a low number of oocytes (< 3) to perform ICSI increases the possibility of total FF (Flaherty et al., 1998). This is common in cycles involving women with advanced reproductive age, in which the ovarian reserve is low. In these cases, FF occurs not only because of the stochastic effect of inseminating few oocytes (1 or 2 in most cases), but also because of lower oocyte developmental competence due to age. The following data highlights the impact of inseminating few oocytes: total FF occurs in 1-3 % of cycles with ≥ 3 oocytes available, in ~ 17 % of cycles with < 3 oocytes, and in ~ 31 % of cycles when only one mature oocyte is available (Hojnik and Kovacic, 2019).

A number of events during oogenesis and maturation are required for proper oocyte fertilization, including a calcium signalling response machinery (including a coordinated mobilization of intracellular calcium stores), spindle and chromosome organization, organization of organelles involved in fertilization process (ER, mitochondria and cortical granules), antioxidant system, membrane and zona pellucida modifications (i.e. JUNO) or maternal proteins and RNA, among others. In this sense, deficient oocyte maturation (either nuclear or cytoplasmic) could inhibit the response to sperm PLC ζ (Swain and Pool, 2008). Oocyte cytoplasmic maturation is important for ER reorganization (ER need to be reorganized in cortical clusters prior to sperm entry), increase in IP₃ receptors abundance, and increased Ca²⁺ ions concentration in the ER (Kline et al., 1999; Swain and Pool, 2008). Oocyte immaturity is also associated with premature sperm chromosomal condensation (PCC), a problem that that can explain part of the FF cases (Calafell et al., 1991; Rosenbusch, 2000). Following extrusion of the first polar body, oocyte activation ability progressively increases from time of metaphase II arrest (Balakier et al., 2004; Pujol et al., 2018).

This explains why most of the oocytes inseminated by ICSI soon after PB extrusion remain unfertilized (more than 60%), while the proportion of normally activated oocytes (containing two pronuclei and two polar bodies) increases after incubation for some hours (Balakier et al., 2004). Cytoplasmic maturation can also explain why fertilization rates are lower when using *in vitro* matured oocytes, and why these oocytes present calcium oscillations of lower frequency and duration when compared to *in vivo* matured oocytes (Nikiforaki et al., 2014). Hence, assuming that oocytes are competent to fertilize should not be based upon presence of the first polar body only, as cytoplasmic maturation could not be complete.

Oocyte spindle formation or function defects can also explain fertilization failure and OAF (Asch et al., 1995; Rawe et al., 2000). Defects in microtubule assembly can result in oocytes displaying absence or abnormal sperm asters (Asch et al., 1995). In relation to this, female severe obesity can increase the percentage of oocytes with aberrant spindles, thus causes a higher proportion of low fertilization or FF after ICSI (Machtinger et al., 2011).

In addition, alterations in different factors involved in the oocyte activation cascade (i.e. CAMKII, MAPK, etc.) and downstream events could explain oocyte-related fertilization failure (Yeste et al., 2016). For example, specific genetic mutations in *TLE6* (member of the subcortical maternal complex needed for first mitotic division) or, more recently, in *WEE2* (oocyte-specific kinase required for metaphase II exit during oocyte activation), have been associated to fertilization failure after ICSI (Alazami et al., 2015; Sang et al., 2018). Oocyte which failed to fertilize after ICSI showed an altered transcriptional profile, with underexpression of genes related to meiosis, cell growth and apoptosis (Gasca et al., 2008).

Regarding specific organelles and oocyte subcellular structures, mitochondrial alterations could underlie some cases of oocyte-related OAF (Van Blerkom, 2011). Cytoplasmic vacuoles have also been associated with lower fertilization rates after ICSI (Ebner et al., 2005).

Finally, reduced ability of the oocyte to generate sperm decondensation accounts for up to 10% of FF after ICSI (Flaherty et al., 1995). In the pig, oocyte protein PDIA3, a disulfide isomerase, is reported to be essential for sperm head decondensation and proper fertilization (Li et al., 2014). If the sperm chromatin remains condensed, there is limited accessibility of other oocyte factors responsible for male pronucleus formation (Tesarik and Kopecny, 1989).

7.3. SPERM-RELATED FERTILIZATION FAILURE

In this section, the male contribution to unsuccessful fertilization after ICSI will be depicted. For example, FF after ICSI is more prone to occur in patients with severe male infertility (~ 23 %), characterized by cryptozoospermia or azospermia, in which testicular spermatozoa are used (Hojnik and Kovacic, 2019). However, different molecular alterations have been reported to be potential causes of FF.

7.3.1. SPERM-BORNE OOCYTE ACTIVATION FACTORS (SOAF): A BRIEF REVIEW

The fact that sperm triggers oocyte activation by introducing soluble factors in the oocyte cytoplasm has been known since the early 90s. The injection of boar and hamster sperm cytoplasmic extracts into oocytes could elicit calcium oscillations similar to those observed when doing IVF (Swann, 1990; Jones et al., 1998).

Since then, research has focused on finding the sperm-borne oocyte activation factor (SOAF), by trying to identify and characterize different sperm proteins. The first proposed protein to trigger calcium oscillations was oscillin (Parrington et al., 1996), but later reports demonstrated it was not involved (Wolny et al., 1999).

A truncated form of c-kit tyrosine kinase receptor (tr-kit) was also proposed as a SOAF candidate and proposed to release mouse oocytes from meiotic arrest and pronuclei formation. Tr-kit appeared to be located in the equatorial and sub-acrosomal region of the sperm head (Sette et al., 1997; Muciaccia et al., 2010). Tr-kit was proposed to interact with an oocyte tyrosine kinase (Fyn), forming a complex able to interact with PLC γ and trigger oocyte activation via this phospholipase (Sette et al., 2002). However, the role of PLC γ in triggering calcium oscillations in oocytes has been studied in non-mammalian species, such as *Xenopus* (Sato et al., 2006), but sperm does not stimulate calcium via Src-like kinases in mammals. Similarly, a role in oocyte activation was proposed for citrate synthase in amphibians (Harada et al., 2007), but it has been discarded as a potential SOAF in mammals.

Finally, two sperm-specific proteins have gained more attention as SOAFs: phospholipase C zeta (PLC ζ) and postacrosomal sheath WW domain-binding protein (PAWP). In the present thesis, both factors will be characterized and studied from a genetic, cellular and functional point of view in FF samples.

7.3.2. PLC ζ

Phospholipase C-zeta (PLC ζ) is a sperm-specific soluble enzyme responsible to trigger oocyte activation via inducing intracellular calcium oscillations. As described above, PLC ζ hydrolyses its substrate, PIP₂, producing IP₃ (Sanders et al., 2018), a messenger that activates the downstream signalling. The fact that PLC ζ substrate is present in intracellular cytoplasmic vesicles explains why PLC ζ -dependent calcium oscillations are oocyte-specific, and these oscillations cannot be observed when expressing PLC ζ in somatic cells (Phillips et al., 2011).

PLC ζ is conserved throughout many taxonomic groups, in both mammal and non-mammalian species (Coward et al., 2005). However, there are some differences in its function and mechanisms between humans and other species. For example, in mouse, calcium oscillations stop after zygotic pronuclear formation, as PLC ζ is sequestered by the forming pronuclei through a nuclear localization signal (NLS) (Larman et al., 2004). But in human, calcium oscillations continue after PN formation, and the occurrence of PLC ζ nuclear translocation has not been documented (Cooney et al., 2010). Another difference can be found in PLC ζ ability to trigger calcium oscillation; for example, human PLC ζ injected into mouse oocytes shows higher potency than monkey or mouse PLC ζ (Cox et al., 2002).

PLC ζ is the smallest PLC (~ 70 kDa in humans) and is the only one that does not reside in the plasma membrane, as it lacks the pleckstrin homology (PH) domain. PLC ζ contains different domains which are essential for its function and regulation: four EF hand domains, conferring calcium sensitivity to the enzyme; catalytic X and Y core domains, required for enzymatic catalytic activity; C2 domain, which binds to PI(3)P and PI(5)P-containing liposomes and allows substrate (PIP₂) accessibility for PLC ζ ; and the XY linker region, essential for enzymatic function and regulation (Saunders et al., 2002; Kouchi et al., 2005) (**Figure 11**).

Several lines of evidence support the role of PLC ζ as an essential SOAF in both animal models and human (Saunders et al., 2002; Yeste et al., 2016). Use of specific antibodies to deplete PLC ζ from sperm extracts abolishes the induction of Ca²⁺ oscillations in the oocyte (Saunders et al., 2002). Microinjection of human *PLCZI* cRNA or recombinant PLC ζ protein into human oocytes can cause parthenogenetic oocyte activation and development to the blastocyst stage, releasing calcium oscillations which are very similar to those observed after sperm fertilization in both human and animal models (Rogers et al., 2004; Yoon et al., 2012). In addition, sperm from PLC ζ -KO mice are unable to trigger oocyte activation after ICSI (Hachem et al., 2017; Nozawa et al., 2018), leading to FF.

Considering the key role of PLC ζ , sperm-related abnormalities or deficiencies in PLC ζ are usually suspect in cases of OAF (Nomikos et al., 2013). For example, efforts have been made to characterize the subcellular localization patterns of PLC ζ within the sperm. In fertile men, mature sperm contain PLC ζ in the acrosome, equatorial region and post-acrosomal sheath, in the perinuclear theca (**Figure 11A**). Some studies report that abnormal protein localization and levels could explain FF after ICSI in some cases (Yoon et al., 2008; Yelumalai et al., 2015), but other studies including groups of patients with FF report that these parameters are not altered in FF samples (Ferrer-Vaquero et al., 2016; Kashir et al., 2017).

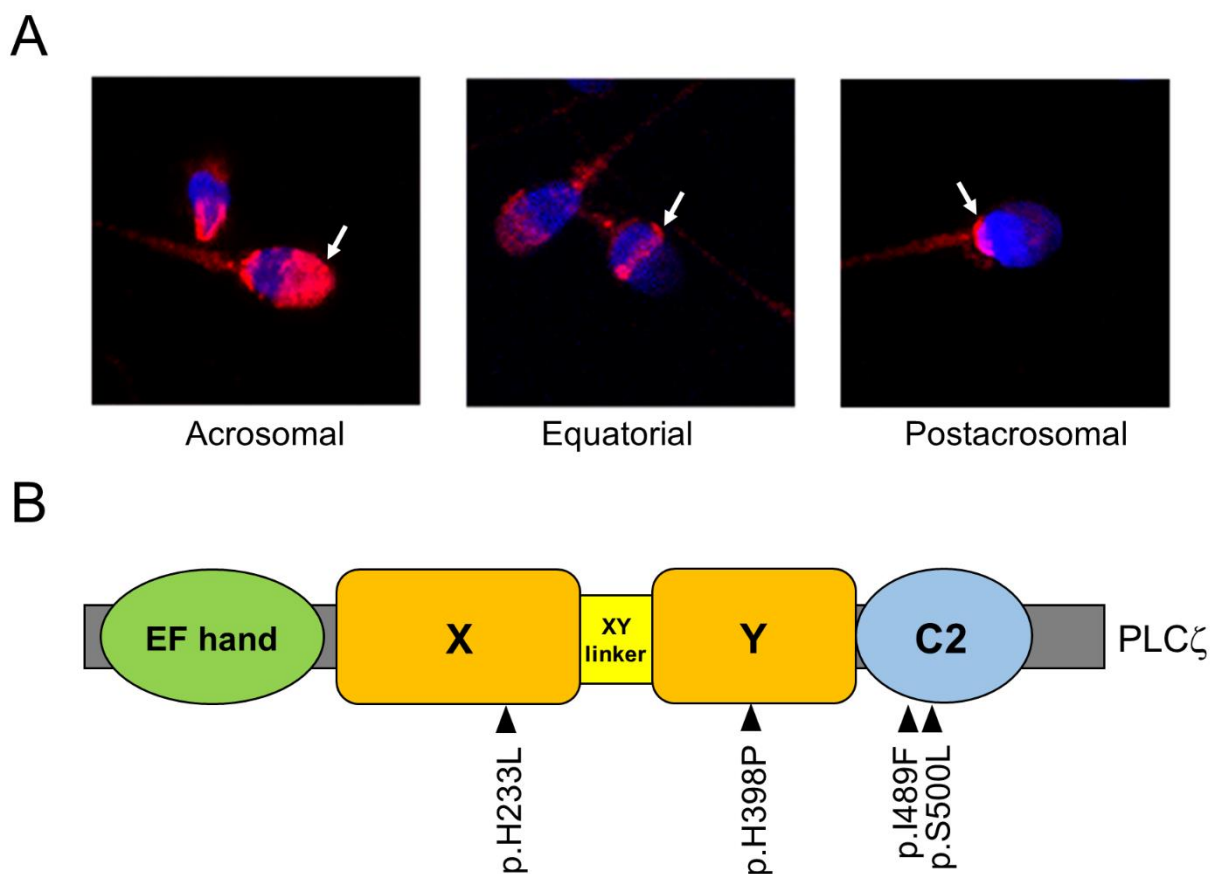


Figure 11. **A.** Main subcellular localizations of PLC ζ (red staining) in human sperm, indicated by white arrows and in relation to the nucleus (stained in blue): acrosomal, equatorial and postacrosomal. Figure modified from Ferrer-Vaquero et al., 2016. **B.** Representation of the main protein domains of human PLC ζ protein. The PLC ζ genetic mutations previously described in the literature and their position are indicated.

In addition, there is more consensus on the detrimental effect that specific deleterious mutations described in *PLCZ1* seem to have in OAF. *PLCZ1* mutations impair protein function, lead to absence or altered calcium oscillations, and causes failure to orchestrate and synchronize all downstream oocyte activation events. So far, 4 deleterious point mutations have been described in

different protein domains: p.H233L, p.H398P, p.I489F and p.S500L (Heytens et al., 2009; Kashir et al., 2012; Escoffier et al., 2016) (**Figure 11B**). Nevertheless, there are few papers addressing PLC ζ from a genetic point of view, and these mutations have been described in punctual cases of FF. Studies using a large cohort of FF cases are needed to set the frequency of *PLCZ1* mutations in ICSI FF patients, as well as to set up the potential benefit of *PLCZ1* gene sequencing in a clinical setting. This thesis includes such a study (see Chapter 2).

7.3.3. PAWP AND WBP2

The post-acrosomal WW domain-binding Protein, PAWP (also known as WBP2NL), is a sperm-specific protein expressed in elongated spermatids located in the post-acrosomal sheath of mature sperm (Wu et al., 2007). This protein contains a C-terminal region rich in proline, with a PPXY consensus sequence which can interact with WW- group I domain-containing proteins, as well as a repeated motif (YGXPPXG), and a GRAM domain in the N-terminus (Wu et al., 2007).

Wu and colleagues originally described that PAWP could promote meiotic resumption and pronuclear formation when injected in porcine, bovine, macaque, and *Xenopus* oocytes (Wu et al., 2007). The PPXY-WW1 domain interaction seems to be essential for this function, as oocyte activation is blocked when injecting a synthetic peptide derived from the PPXY motif of PAWP (Wu et al., 2007; Aarabi et al., 2014). It was suggested that PPXY motifs could interact with the WW domain present in PLC γ , which in turn would hydrolyse PIP $_2$ and trigger oocyte activation following a non-canonical pathway (Aarabi et al., 2014). Moreover, higher levels of PAWP were associated with higher sperm quality and fertility in bulls (Kennedy et al., 2014).

However, PAWP role in oocyte activation needs further revision, as it is not clear if PLC γ is able to generate calcium oscillations in the human oocyte (Mehlmann et al., 1998). While some reports proposed that PAWP (either cRNA or recombinant protein) can trigger calcium oscillations and oocyte activation (Aarabi et al., 2014), other authors did not find any of these events when studying this potential SOAF (Nomikos et al., 2014). Additional data reported normal fertility in *Pawp/Wbp2nl*^{-/-} mice (Satouh et al., 2015), and PAWP does not seem to rescue the FF phenotype observed in patients presenting non-functional PLC ζ (Escoffier et al., 2016). For all these reasons, some controversy and debate still exists on the potential role of PAWP in oocyte activation.

According to a recent report using the mouse model, WBP2, the close ortholog of PAWP (a gene that arose from a duplication of WBP2NL gene), contains the same domains associated with PAWP function, shares the same subcellular localization (in the perinuclear theca), is able to trigger oocyte

activation when being injected into mouse oocytes, and could compensate for defects in PAWP (Hamilton et al., 2018).

7.3.4. SPERM DNA AND FERTILIZATION FAILURE

Sperm brings the paternal genetic content needed to generate a new organism. This DNA needs to be in good conditions to guarantee the different processes occurring in fertilization and early development steps. In general, sperm DNA damage is associated with abnormal spermatogenesis and male infertility. Moreover, different parameters in sperm DNA have been somehow related to the fertilization process and will be discussed: sperm DNA condensation, sperm DNA fragmentation, and sperm telomere length. Telomere length will be analysed in the present thesis in relation to fertilization rates and reproductive outcomes after ICSI.

SPERM DNA CONDENSATION

As commented above, spermiogenesis results in a unique feature of sperm: a highly condensed chromatin. Poor sperm DNA condensation has been reported to increase sperm DNA fragmentation levels and is associated with fertilization failure after ICSI. Sperm protamine mRNA ratio has been used as an indirect measurement of sperm condensation status and has been reported to correlate with fertilization rates in ART (Rogenhofer et al., 2013). Different studies, which use different methods to evaluate sperm chromatin condensation (such as chromomycin CMA3) indicate that lower levels of condensation (or protamine deficiency) are associated with lower fertilization rates after ICSI (Nasr-Esfahani et al., 2004; Lazaros et al., 2011). PCC, which can explain part of the FF cases in humans (Schmiady and Kentenich, 1989), is associated with deficient sperm condensation, low protamine / histone ratio (Nasr-Esfahani et al., 2006). Absence or incomplete oocyte activation is associated with higher levels of condensing factors in the oocyte cytoplasm (e.g. MPF), which impairs sperm chromatin decondensation and causes failure to form male pronucleus (Zenses and Casper, 1992).

SPERM DNA FRAGMENTATION

Sperm DNA fragmentation consists of either single DNA strand breaks (SSB) or double strand breaks (DSB). Four main techniques are used to measure DNA fragmentation in sperm: Sperm Chromatin Dispersion test (SCD), Terminal deoxynucleotidyl transferase dUTP nick-end labelling (TUNEL), Sperm Chromatin Structure Assay (SCSA), and alkaline or neutral comet assay (Ribas-Maynou et al., 2012). High levels of sperm DNA fragmentation have been associated with poor embryo development and higher risk of miscarriage (Fatehi et al., 2006; Robinson et al., 2012).

However, recent meta-analysis does not support sperm DNA fragmentation assessment in ART, based on its lack of predictive value for pregnancy and live birth rates (Cissen et al., 2016). Moreover, sperm DNA damage *per se* seems not to affect the fertilization process. Supplemental antioxidant therapies have been suggested to be beneficial for patients presenting high sperm DNA fragmentation; but, to date, there is insufficient data to recommend their use for male infertility treatment (Barrat et al., 2017).

SPERM TELOMERE LENGTH

Telomeres are repetitive hexamers of non-coding DNA (5'-TTAGGG-3') located at the ends of eukaryotic chromosomes. They protect the chromosomes by maintaining genome integrity, prevent chromosome end joining, and facilitate homologue pairing during meiosis (O'Sullivan et al., 2010). In most cell types, telomere length decreases with each cell division, and when telomeres reach a critical length, apoptosis and cell cycle arrest can occur. However, specific mechanisms in spermatogenesis cause a progressive increase in telomere length in male germ cells (Ozturk, 2015).

Telomere length in mature sperm (STL) is very heterogeneous between individuals and within sperm in the same ejaculate, and can be affected by different factors (oxidative stress, environmental factors, diet, age, etc.) (Antunes et al., 2015). Shorter STL has been associated with sperm motility, vitality, condensation or DNA fragmentation, but other studies have not found these associations (Turner and Hartshorne, 2013; Rocca et al., 2016; Cariati et al., 2018).

Telomeres participate in chromosomal orientation, synapsis, and segregation. Sperm telomeres are the first region in the sperm genome to respond to oocyte signals for pronucleus formation (Thilagavathi et al., 2013), and oocytes fertilized with sperm from telomerase-null ($TR^{-/-}$) mice exhibit high rates of abnormally fertilized oocytes, with increasing percentages of oocytes with one pronucleus (Liu et al., 2002). For these reasons, STL could affect the fertilization process and the first mitotic division. However, the potential effect of STL on fertilization rates or FF after ICSI is unknown, and there is a lack of studies addressing STL and fertilization in human samples.

8. RESEARCH ON FERTILIZATION FAILURE AFTER ICSI: STILL MUCH TO DO

8.1. WHY IS MORE RESEARCH ON FERTILIZATION FAILURE NEEDED?

Fertilization through assisted reproduction can still be optimized further. Apart from all the mechanisms of ICSI FF previously detailed, other sperm mechanisms and alterations are expected to be involved in this infertility problem. Currently, in the routine practice of ART, there are no established methods to diagnose or predict fertilization failure. Unless there is a clear male factor (severe asthenozoospermia, use of sperm from testicular biopsy, etc.), injection of *in vitro* matured oocytes or very few mature oocytes (< 3 oocytes), or a previous evidence of fertilization failure using the same gametes, FF after ICSI is a rare occurrence. For this reason, fertilization failure is of special concern in the clinic, but it has been poorly addressed by basic researchers and scientific community.

Heterologous ICSI models, using mouse or hamster oocytes in most cases, have been proposed as a diagnostic tool for sperm-related fertilization failure (Heindryckx et al., 2005). These systems include MOAT (mouse oocyte activation test) and MOCA (mouse oocyte calcium analysis); as well as its variant in human gametes, HOCA. Similarly, heterologous models using bovine, rabbit or *Xenopus* oocytes can be applied to test sperm aster formation and / or microtubule enucleation (Tachibana et al., 2009; Amargant et al., 2018). However, these methods cannot easily be introduced in the routine fertility clinic practice due to technical or cost-effectiveness limitations.

In addition, the tests currently applied to assess sperm quality in fertility clinics do not cover all sperm function alterations and potential events of fertilization that may go wrong. There is need of specific biomarkers and procedures for prediction of FF applied in the clinical setting. In this thesis, we propose *PLCZI* gene sequencing as a useful and fast method to diagnose a high percentage of cases with OAF after ICSI.

8.2. MAIN APPROACHES TO STUDY SPERM-RELATED FERTILIZATION FAILURE

Research on human fertilization suffers from intrinsic legal, ethical and technical limitations. Many countries do not allow research on fertilized material, nor use of fertilization for research purpose. However, a wide range of approaches have been used to study human fertilization from a molecular

and cellular point of view. Different techniques have been used to study sperm fertilization ability, including sperm transcriptomics, morphological evaluation of sperm ultrastructure, measurement of sperm metabolism and fertilization associated processes (such as capacitation and acrosome reaction). In this section three of these main approaches (all of them included in the present thesis) will be described: gene sequencing, proteomics and *in silico* techniques.

GENE SEQUENCING

Gene sequencing techniques are useful to identify mutations in the genes that code for specific factors in biological phenomena. Gene sequencing techniques are fast, cheap, and can be performed on very small amounts of sample (i.e. single oocytes) or even in tissues different from gametes (i.e. blood or saliva). Despite being an indirect analysis, missense variants in the coding region (exons), which can produce aminoacid changes in the resulting protein and have potential to affect protein function. Variants in intronic regions or SNPs may not have such a clear effect but could potentially affect regulatory regions.

For example, gene sequencing could identify specific mutations in *DPY19L2* gene as the cause of globozoospermia, a rare and severe form of teratozoospermia, characterized by presence of sperm with a big and round head unable to fertilize due to problems in oocyte penetration and activation (Koscinski et al., 2011). In addition, as explained above, different deleterious mutations have been found in sperm *PLCZI* and the oocyte *WEE2* kinase, all of them causing a phenotype of OAF.

SPERM PROTEOMICS

Sperm specialized function and morphology is reflected in its peculiar protein composition. Proteins are the major drivers of all processes related to sperm function, fertilization and oocyte activation, as there is little or no transcription in the mature sperm nor during the oocyte-to-embryo transition. The study of sperm protein roles and anomalies is crucial to understand fertilization mechanisms, identify new FF biomarkers, as well as to improve the diagnosis and treatment of male infertility.

During recent years, the use of mass spectrometry and proteomics technologies on sperm samples has increased the general knowledge about male infertility. To date, around 7000 different proteins have been described in human sperm (Castillo et al., 2018). These approaches are very useful not only to understand the molecular mechanisms behind infertility and abnormal sperm function, but also to identify specific proteins or biomarkers with potential to diagnose, predict or treat specific problems.

Sperm is a suitable model to be subjected to proteomics: obtaining a semen sample is fast and easy, usually millions of cells are present in a single ejaculate, sperm can be easily isolated from seminal fluid, and sperm does not generate new proteins, as it is transcriptionally and translationally inactive.

Descriptive proteomics has been used on either whole human sperm, or subcellular sperm fractions: tail (Amaral et al., 2013), nucleus (de Mateo et al., 2011), membrane (Nixon et al., 2011), etc, in order to better understand sperm biology and molecular mechanisms underlying its function. In addition, differential proteomics has been used to identify new biomarkers and understand the mechanisms behind different groups of male infertility:

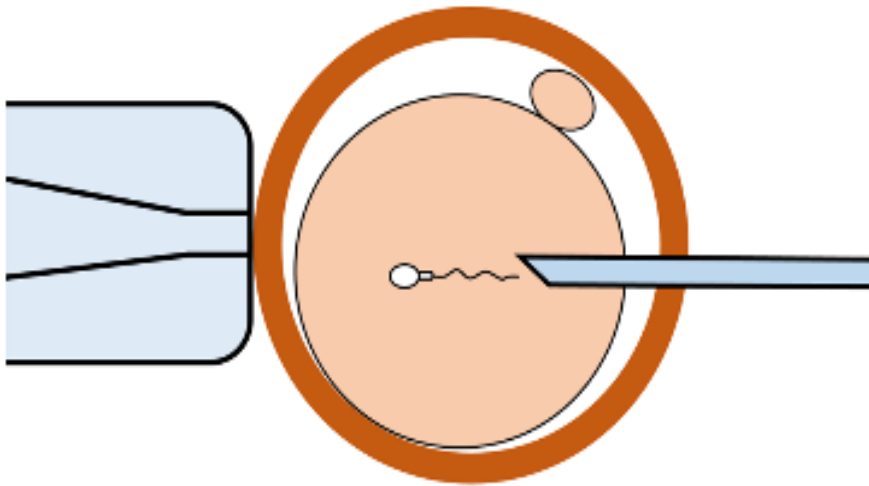
To our knowledge, four studies used proteomics to study fertilization failure after IVF (Pixton et al., 2004; Frapsauce et al., 2014; Légaré et al., 2014; Liu et al., 2018). However, there is no study using proteomics to study fertilization failure after ICSI.

IN SILICO TECHNIQUES TO STUDY FERTILIZATION

As commented above, research on human fertilization is a process with intrinsic ethical and legal restrictions, and human oocytes are samples difficult to obtain in most cases. For this reason, *in silico* analysis are useful tools to understand the fertilization process, as demonstrated by different authors (Sabetian et al., 2014; Ntostis et al., 2017). For example, prediction of protein-protein interactions could be an alternative to infer new sperm roles in the oocyte, probably some of them not observed by conventional functional association methods or gene ontology analysis.

Recently, a comprehensive analysis of sperm proteomics and transcriptomics data by gene ontology analysis, could predict *in silico* not only a list of protein involved in the fertilization process, but also sperm contribution to primplantational development (i.e. sperm factors may participate in gene expression regulation in the embryo) (Castillo et al., 2018).

OBJECTIVES



The main objective of the present thesis is **to identify and characterize the molecular and cellular alterations in sperm which are responsible for fertilization failure after ICSI**, with a special emphasis in sperm protein factors and mechanisms involved in oocyte activation.

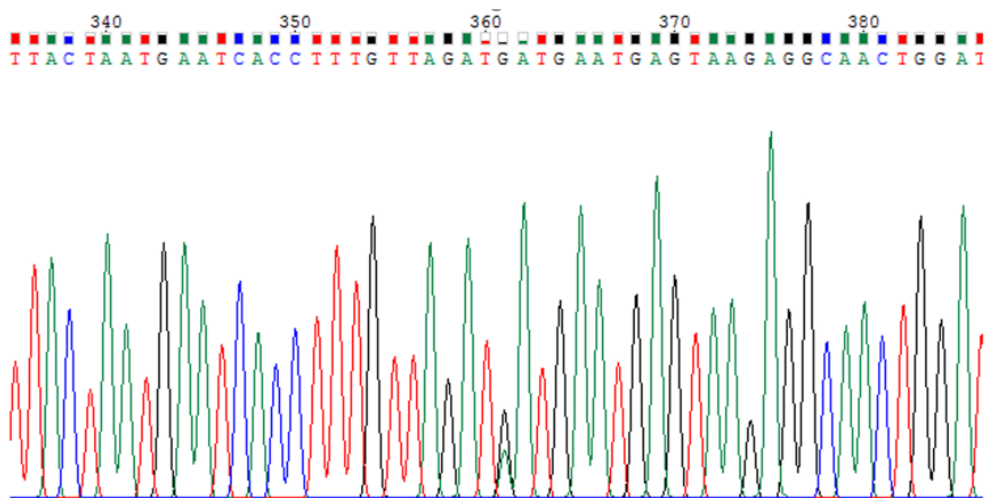
The specific objectives are:

1. To characterize the two main sperm factors described as potential markers of ICSI fertilization failure, PAWP and PLC ζ , especially from a genetic point of view.
2. To identify and characterize novel sperm factors and mechanisms involved in FF after ICSI, by using comparative proteomics techniques and *in silico* approaches.

Three secondary objectives are included in this thesis:

3. To study the effect of a sperm genomic parameter (telomere length) on fertilization rates and reproductive outcomes.
4. To determine if one instance of fertilization failure is enough indication for AOA use, in order to provide a better characterization of FF and its management from a clinical point of view.
5. To evaluate the effect of sperm incubation time before ICSI on fertilization rates and reproductive outcomes up to live birth

RESULTS



CHAPTER 1: Is there an association between PAWP/WBP2NL sequence, expression, and distribution in sperm cells and fertilization failures in ICSI cycles?

PUBLISHED AS:

Freour T, Barragan M, Torra-Massana M, Ferrer-Vaquer A, Vassena R. **Is there an association between PAWP/WBP2NL sequence, expression, and distribution in sperm cells and fertilization failures in ICSI cycles?** *Mol Reprod Dev* 2018; 85:163-170.

TITLE PAGE

TITLE

Is there an association between PAWP/WBP2NL sequence, expression and distribution in sperm cells and fertilization failures in ICSI cycles?

SHORT TITLE: PAWP/WBP2NL and fertilization failure

AUTHORS

Freour T^{1,2,3,4}, Barragan M¹, Torra-Massana M¹, Ferrer-Vaquer A¹, Vassena R^{1,*}

¹Clínica Eugin, Barcelona 08029, Spain

²Service de médecine de la reproduction, CHU de Nantes, 44093 Nantes, France

³Inserm UMR1064 – ITUN, 44000 Nantes, France

⁴Faculté de médecine, Université de Nantes, 44000 Nantes, France

*Corresponding author: Dr Rita Vassena, Clínica Eugin, Traversera de les Corts, 322 – 08029 BARCELONA, Spain. Tel: (+34) 933 221 122 - Email: rvassena@eugin.es

KEY WORDS:

Idiopathic infertility, fertilization failure, PAWP, WBP2NL, oocyte activation, SOAF.

Disclosures

All the authors affirm that they have no conflict of interest related to this work.

Funding Information

This work was supported by intramural funding of Clinica EUGIN. MTM is partially supported by the Secretary for Universities and Research of the Ministry of Economy and Knowledge of the Government of Catalonia (2015 DI 049).

ABSTRACT

Successful fertilization in mammals depends on the sperm ability to initiate intracellular Ca^{2+} oscillations in the oocyte. This phenomenon is elicited by Sperm Oocyte Activating Factors (SOAFs), whose quantitative and/or qualitative defect might result in fertilization failure. Post-Acrosomal WW domain-binding Protein (PAWP/WBP2NL) has been proposed as a putative SOAF, but its ability to activate human oocytes has been questioned in the recent literature, and its implication in human fertilization failure remains unknown. We sought to determine whether PAWP/WBP2NL protein expression and distribution in sperm cells was associated with low/complete fertilization failure in ICSI cycles. This prospective study was conducted on 8 couples referred for elective ICSI with either the woman's own (n=4) or donor oocytes (n=4). In parallel, 8 sperm donor samples used in ICSI and leading to normal fertilization rates were used as control. For each male patient and donor sperm, *PAWP/WBP2NL* sequence, protein expression, and cellular distribution were analyzed by PCR amplification-sequencing, western blot and immunofluorescence, respectively. PAWP/WBP2NL was present in all samples. No significant differences were detected between patients with fertilization failure and donors in sequence variants or mean protein expression, or in the proportion of PAWP/WBP2NL positive sperm. In conclusion, we could not find a clear association between PAWP/WBP2NL protein expression in sperm and fertilization outcome in ICSI.

INTRODUCTION

Human infertility treatment has been revolutionized in the 1990's, thanks to the development of intracytoplasmic sperm injection (ICSI), yet approximately two thirds of all in vitro fertilization (IVF)/ICSI cycles do not result in pregnancy (Calhaz-Jorge et al., 2016). Among the causes of ICSI failure, low fertilization or total fertilization failure, resulting in no fertilized eggs, is reported for a sizeable proportion of ICSI cycles (Esfandiari et al., 2005; Flaherty et al., 1998; Shinar et al., 2014; Pabuccu et al., 2016).

Successful mammalian fertilization is highly reliant on a sperm's ability to initiate intracellular Ca^{2+} oscillations, leading to egg activation and subsequent meiotic resumption, cortical granules extrusion, and pronuclei formation (Kline & Kline, 1992; Rawe et al., 2000). This intracellular release of Ca^{2+} is elicited by Sperm-egg activating factors (SOAFs), a defect in which causes low fertilization success or fertilization failure, regardless of the outcome of other conventional semen analysis parameters (Yeste et al., 2016). The identity and mechanisms of SOAF candidates are still

debated (Amdani et al., 2015). One candidate is the soluble, testis-specific isoform of PLC (PLC-zeta [PLC ζ]), which was shown to initiate calcium oscillations in mice (Saunders et al., 2002) and other mammalian and non-mammalian species (Amdani et al., 2013; Kashir et al., 2013). Point mutations have also been described in the gene that encodes PLC ζ that affect its ability to promote Ca²⁺ oscillations after fertilization-including in clinical evidence supporting its role in human egg activation (Escoffier et al., 2016; Heytens et al., 2009; Kashir et al., 2011, 2012; Nomikos et al., 2011; Yeste et al., 2016). Yet, the central role of PLC ζ in egg activation is still debated (Aarabi et al., 2015; Aarabi et al., 2014a; Amdani et al., 2015; Hachem et al., 2017), when levels and distribution of PLC ζ protein in sperm cells are within normal range (Ferrer-Vaquer et al., 2016).

Post-Acrosomal WW domain-binding Protein (PAWP/WBP2NL), a protein located in the post-acrosomal sheath region of the perinuclear theca, was recently reported to promote meiotic resumption and pronucleus formation (Wu et al., 2007) and to induce Ca²⁺ oscillations (Aarabi et al., 2014a) - functions that nominate this protein to the list of SOAFs, although independent confirmation of these results is still lacking (Nomikos et al., 2014, 2015).

No clear enzymatic function has been associated to PAWP/WBP2NL. The high homology of its amino terminus, containing a GRAM domain, to WW domain-binding protein 2 (WBP2), and two extra motifs in its carboxyl terminus, one PPXY motif (known to interact with WW domain) and an unidentified repeated motif (YGXPPXG), pose the question of how these domains engage the signaling machinery following fertilization (Wu et al., 2007). The conserved GRAM domain at the amino terminus was suggested to determine PAWP/WBP2NL function, while the carboxyl terminus could drive protein-protein interactions through the PPGY motif, given that this region could block sperm-induced porcine egg activation (Wu et al., 2007). Yet, no mutational analysis has been performed that would provide any insight to how the PPXY and YGXPPXG motifs might promote meiotic resumption and pronucleus formation during fertilization.

Additional concerns regarding the role of PAWP/WBP2NL as a sperm-egg activating factor come from recent studies demonstrating that PAWP/WBP2NL is not required for mouse egg activation (Satouh et al., 2015), and that defective human egg activation induced by mutated PLC ζ was not rescued by PAWP/WBP2NL (Escoffier et al., 2016). Few studies to date have investigated the association between PAWP/WBP2NL abundance in sperm versus reproductive outcome in humans; results from such research are conflicting (Aarabi et al., 2014b; Freour et al., 2017; Tavalae & Nasr-Esfahani, 2016). Therefore, we asked if fertilization failure during ICSI can be associated with genetic mutations or polymorphisms, altered protein abundance, and/or abnormal localization of PAWP/WBP2NL.

Table I: Demographic of male patients and donors. Values are presented as % or mean \pm standard deviation [range] when appropriate.

	Patients (n=8)	Donors (n=8)
Male age (years)	45.1 \pm 7.9 [31-55]	26.8 \pm 5.7 [19-34]
Male BMI (kg/m ²)	26.3 \pm 2.8 [23.7-30.5]	23.4 \pm 1.9 [21.2-26.3]
Female age (years)	33.9 \pm 5.6 [26-44]	34.6 \pm 6.5 [21-42]
Partner	37.3 \pm 5.7 [30-44] (n=4)	37.0 \pm 3.8 [31-42] (n=6)
Donor	30.5 \pm 3.1 [26-33] (n=4)	27.5 \pm 9.2 [21-34] (n=2)
Female BMI (kg/m ²)	23.9 \pm 3.8 [18.7-31.5]	25.2 \pm 4.2 [19.0-30.4]
Partner	25.8 \pm 4.1 [21.8-31.5]	25.9 \pm 3.8 [19.4-30.4]
Donor	22.1 \pm 2.7 [18.7-25.2]	23.3 \pm 6.1 [19.0-27.6]
Fertilization rate (%)	5.4 \pm 7.4 [0-15]	74.4 \pm 21.3 [44-100]
Total Fertilization Failure	5 out of 8	0 out of 8

RESULTS

Study cohort

Eight patients presenting with clinically defined fertilization failure consented to participate in this prospective study after a referred cycle with elective ICSI presenting either low fertilization (n = 3) or total fertilization failure (n = 5). Half of the cycles were performed with the partner's own eggs and half with donor eggs. The controls consisted of eight sperm donor samples, three of whom used donor eggs that resulted in normal fertilization (74% average). Patients' and donors' characteristics are presented in **Table I** and **Supplementary Table I**.

Table II. PAWP/WBP2NL allele variants found in genomic DNA from sperm. Het, heterozygous; Hom, homozygous; MAF; Minor Allele Frequency; NA, not applicable.

Genome coordinates (22q13.2) (GRCh38)	Genomic location	Protein Sequence variant	Allele variant (SNP)	5' and 3' surrounding sequence (8 bp) (clone CTA-250D10)	dbSNP	MAF frequency (1000 genomes)	Presence of Minor Allele in Patients	Presence of Minor Allele in Donors
41998608	Promoter	NA	c.-211G>C	TTCTCAGGGCCCGCTC	rs4822079	C=0.2810/1407	Het. 2/7	Het. 1/6
41998831	Exon 1	p.Gln5Glu	c.+13C>G	CGGTGAATCAGAGCCAC	rs17002790	G=0.0310/155	Hom. 1/7	0/6
42020052	Exon 4	p.Asp121Gly	c.+362A>G	AAATGGAGATGCCATTG	rs133335	A=0.4539/2273	Het. 2/7 Hom. 2/7	Het. 1/6 Hom. 3/6
42022106	Intron4-5	NA	c.407-143T>A	CCCATGTTTCTTTTTTA	rs9607869	A=0.2642/1323	0/8	Hom. 1/6
42022181	Intron4-5	NA	c.407-68C>T	TAATTGTTT T AGTTGATA	rs133341	T=0.1915/959	Het. 1/8 Hom. 2/8	Het. 1/6 Hom. 2/6
42022351	Exon 5	p.Cys170Phe	c.409G>T	GATGCCCTTGTTCAGGTA	rs17002802	T=0.0337/169	Hom. 1/8	0/6
42027106	Exon 6	p.Gln285His	c.855G>C	AGGCTCAGGAATCTAC	rs2301521	G=0.2222/1113	Hom. 2/8	Het. 1/6 Hom. 2/6

Semen parameters and ICSI cycles

Individualized semen characteristics of all patients and donors are presented in Supplementary **Table I**. Five patients and all eight donors presented with normozoospermia. Mean fertilization rate of the cycle performed with the ejaculate included in the study was 5.4% (range, 0–15%) in patients and 74.4% in donors (range, 44–100%).

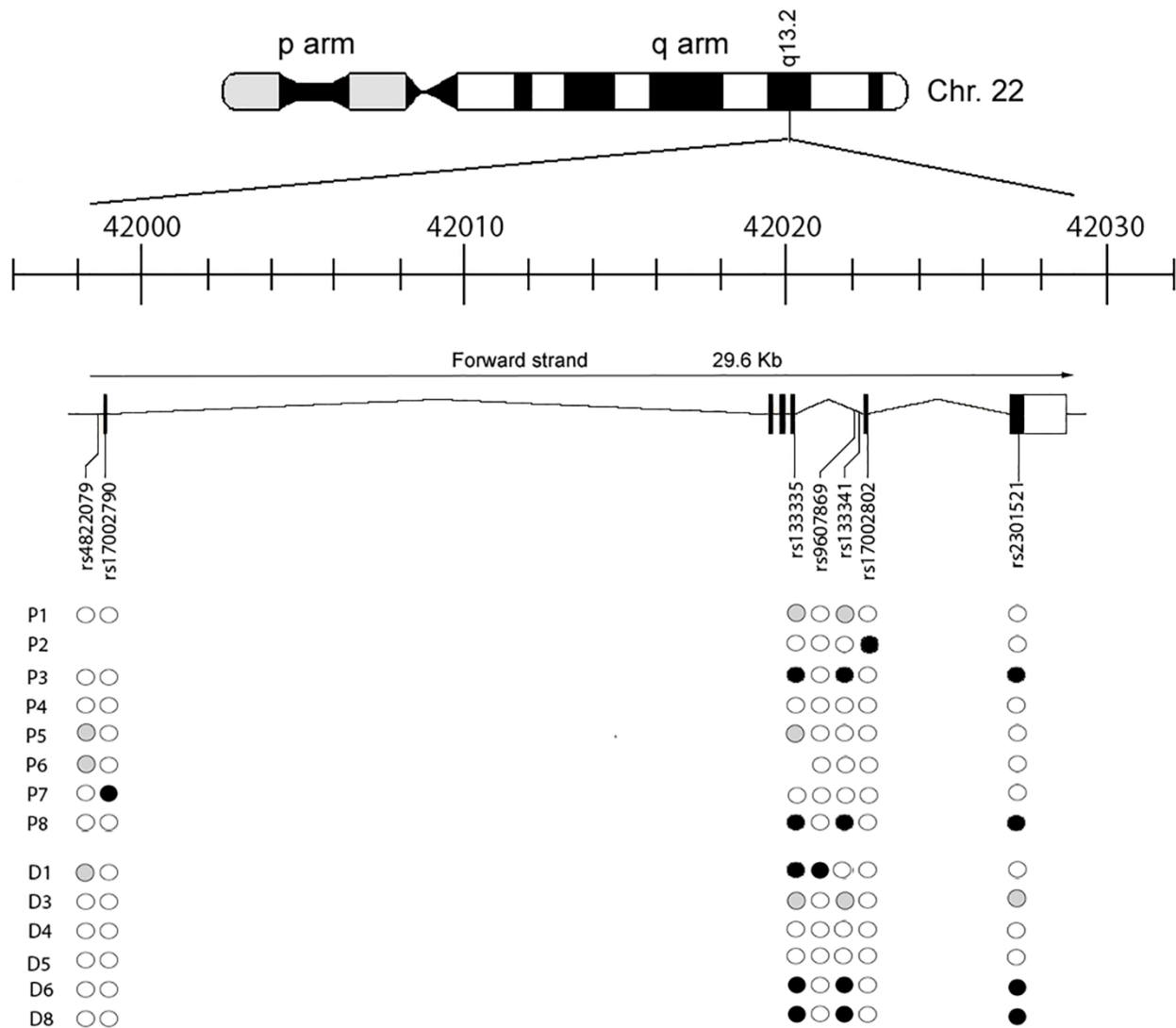


Figure 1. The human genomic locus containing *PAWP/WBP2NL* on chromosome 22 (22q13.2). Schematic of *PAWP/WBP2NL*, on the forward strand, shows allelic variants (circles) found in patient (P) and donor (D) sperm samples. Locations of allelic variants for seven different haplotype-tagging single nucleotide polymorphisms are indicated. White circles represent the presence of major allele in homozygosis compared to a reference sequence (Human DNA sequence CTA-250D10, CalTech human BAC library A); gray circles represent the presence of a major and minor allele (heterozygous); and black circles represent presence of minor allele (homozygous).

***PAWP/WBP2NL* gene sequence**

The *PAWP/WBP2NL* gene is located at the long arm of chromosome 22, forward strand (22q13.2), and consists of six exons (**Figure 1**). Seven allelic variants were detected, all of which were already reported in the public single nucleotide polymorphism database (**Figure 1, Table II**). Two different missense variants were detected in the coding region of *PAWP/WBP2NL* in two patients: at exon 1 (p. Gln5Glu) for Patient 7 and at exon 5 (p. Cys170Phe) for Patient 2. Additionally, five sequence variants were detected at similar proportions in both patients and donors (**Table II**). With the exception of Patient 4, all other patients with fertilization failure presented at least one SNP variant in either the coding or intronic region. Two additional missense variants rs133335 (p. Asp121Gly, exon 4) and rs2301521 (p. Gln285His, exon 6) were found in similar proportion in patients and donors, indicating that these missense variants likely do not affect fertilization ability.

***PAWP/WBP2NL* protein levels and cellular distribution**

PAWP/WBP2NL was present in all sperm samples, but at heterogeneous abundance relative to α -tubulin (**Figures 2a and 2b**). Mean relative expression for *PAWP/WBP2NL* isoform 1 (~35 kDa) was not significantly different between patients with fertilization failure (mean 4.0 ± 3.2 arbitrary units; range, 1.42–11.61) versus fertile donors (mean 1.6 ± 1.1 arbitrary units; range, 0.30–3.64) ($p > .05$) (**Figure 2c**). According to Grubbs' test, Patient 1 was detected as outlier (**Figure 2c**) ($p < 0.05$, two-sided; critical value of $Z = 2.13$); his removal revealed significant differences ($p < 0.05$) between patients with fertilization failure (mean 2.9 ± 1.1 arbitrary units; range, 1.42–4.26) and donors (mean 1.6 ± 1.1 arbitrary units; range, 0.30–3.64). Conversely, no statistically significant differences were observed between patients and donors for *PAWP/WBP2NL* isoform 2 (~28 kDa) (patient mean 0.4 ± 0.4 arbitrary units; range, 0.0–1.1 vs. donor mean 0.3 ± 0.3 arbitrary units; range, 0.1–0.9), either including or excluding the outlier (Donor 3) ($p > 0.05$) (**Figure 2d**). Also, no differences were detected in *WBP2* protein abundance (**Supplementary Figure 1**).

Sperm presented unspecific *PAWP/WBP2NL*-positive tail staining, as previously described (Freour et al., 2017), so analysis of sperm by immunofluorescence was limited to staining in the head (acrosomal and equatorial staining) and was presented as the proportion of sperm positive for *PAWP/WBP2NL* over the total number of cells counted (**Figure 3a**). On average, the proportion of *PAWP/WBP2NL*-positive sperm was not different between patients ($53.6\% \pm 24.1$; range, 26–90) and donors ($65.7\% \pm 12.9$; range, 50–74) ($p > .05$) (**Figure 3b**). The same was true when only

sperm with a visible acrosome were considered for PAWP/WBP2NL staining ($55.5\% \pm 25.2$ vs. $66.2\% \pm 12.6$ in patients and donors, respectively, $p > 0.05$) (**Supplementary Figure 2**).

DISCUSSION

More than 30 years after its implementation, ICSI still does not provide 100% fertilization rates because fertilization failure occurs in a sizeable proportion of cycles—the exact molecular factors responsible of which are not completely understood. We previously reported significant variability in the protein abundance and localization of PAWP/WBP2NL across ranges of percentage fertilization outcomes (Freour et al., 2017); here, we aimed to determine if any aspect of this Protein PAWP/WBP2NL correlates with cases of failed fertilization after ICSI, including abnormal fertilization (1 or 3 pronuclei). Our results are consistent with the increasing literature questioning the role of PAWP/WBP2NL as a SOAF in mammals (Escoffier et al., 2016; Freour et al., 2017; Satouh et al., 2015). Indeed, since the initial hypothesis that PAWP/WBP2NL participates in egg activation and fertilization, in 2007 (Wu et al., 2007), a firm case in its favor has not yet been established (Aarabi et al., 2015; Amdani et al., 2015; Nomikos et al., 2015). Although sperm-derived PAWP/WBP2NL is released into the ooplasm at the time of gamete fusion (Wu et al., 2007) and microinjection of recombinant PAWP/WBP2NL protein or *PAWP/WBP2NL* cRNA into eggs triggered activation (Aarabi et al., 2014a), recent data reported normal fertility in *Pawp/Wbp2nl*^{-/-} mice (Satouh et al., 2015) and no fertilization rescue by PAWP/WBP2NL in human patients with defective egg activation due to an inactive PLC ζ (Escoffier et al., 2016; Nomikos et al., 2017). Most mechanistic studies have focused on the role of PAWP/WBP2NL on egg activation and the subsequent Ca²⁺ spikes, although additional roles for this protein downstream of Ca²⁺ oscillations cannot be ruled out (Wu et al., 2007).

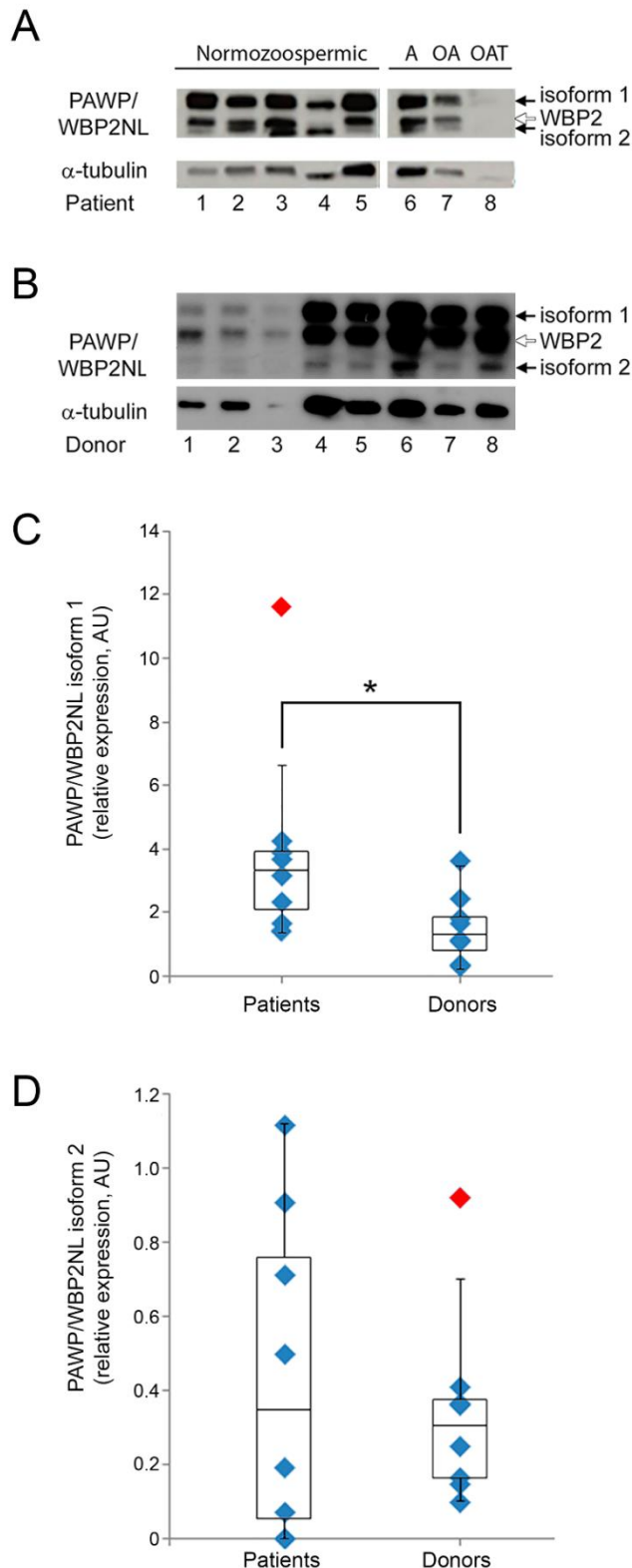


Figure 2. PAWP/WBP2NL protein abundance in sperm samples. (a and b) Western blots probed for PAWP/WBP2NL and α -tubulin in total protein lysates of (a) patient and (b) donor samples. Blots were run on different days and sequentially hybridized for PAWP/WBP2NL followed by α -tubulin. Asthenozoospermic (A), oligoasthenozoospermic (OA), and oligoasthenoteratozoospermic (OAT) samples were included for comparison of abundance. (c-d) Quantified relative expression of PAWP/WBP2NL ~35 kDa isoform 1 (c) and ~28 kDa isoform 2 (d), normalized to α -tubulin in patients and donors. Results are presented as individual values (blue diamond) and box-plot distribution. Red diamond indicates an outlier, based on the Grubb's test. * $p < 0.05$, Students t -test.

Little is published regarding the expression of PAWP/WBP2NL in human sperm. One recent study reported significant correlations between sperm PAWP/WBP2NL levels versus fertilization rates and normal embryonic development after ICSI in infertile couples (Aarabi et al., 2014b). Although interesting, important details on the patients' sperm parameters and female characteristics were

absent, making the infertility phenotype difficult to assign as a male or female factor. We recently reported that neither *PAWP/WBP2NL* sequence nor protein abundance/distribution were associated with fertilization rates in couples referred for egg donation (Freour et al., 2017). Another recent study asked if a correlation existed between *PAWP/WBP2NL*, *PLCζ*, or *TR-KIT* expression in sperm cells and fertilization in ICSI cycles performed in globozoospermic patients (Tavalaee & Nasr-Esfahani, 2016). The authors of this globozoospermia study reported that none of these putative sperm-egg activating factors predicted fertilization rate among their enrolled couples — a finding that is not generalizable to infertile men, given that globozoospermia represents a very rare and specific male infertility pattern (Chansel-Debordeaux et al., 2015; Escoffier et al., 2015). In addition, none of these three studies performed a specific subgroup analysis in patients with failed fertilization.

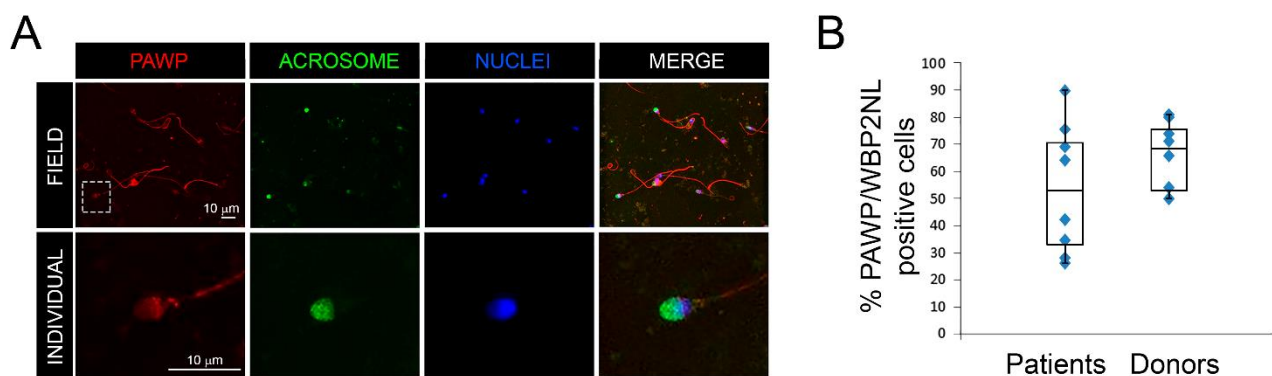


Figure 3. Localization of PAWP/WBP2NL in human sperm. (a) Sperm stained for PAWP/WBP2NL (red), the acrosome (green, using peanut agglutinin), and nuclei (blue, using Hoechst 33342). Upper panels show a representative field; lower panels show a magnified view of an individual sperm. Scale bar, 10 μ m. (b) Proportion of PAWP/WBP2NL-positive sperm versus all sperm cells in patients and donors samples. Individual values (blue diamonds) and box-plot distribution are presented

The present study included eggs from donation cycles in order to limit, as much as possible, any confounding factors related to female infertility or egg quality. We also focused on failed fertilization cases since it could be postulated, based on the required characteristics of a SOAF, that PAWP/WBP2NL expression in sperm cells would be clearly modified in these cases compared to cycles using sperm donor samples. In addition, we sequenced the *PAWP/WBP2NL* gene to look for sequence variants that might segregate with cases of failed fertilization. We detected seven allelic variants that were evenly distributed between patients and donors, which is similar to the minor allele frequency data recorded in populational studies (1000 Genomes Browser Phase 3; <https://www.ncbi.nlm.nih.gov/variation/tools/1000genomes/>). Four of the identified allelic variants were located in the coding region of *PAWP/WBP2NL*, and represented missense variants of the protein; none associated with clinical outcomes, including male infertility. Two of the

missense variants (p.Asp121Gly and p.Gln285His) were found in both patients and donors, whereas the other two variants (p. Gln5Glu and p.Cys170Phe) were homozygous in two patients presenting total fertilization failure due to 50% of the zygotes possessing one or three pronuclei.

In conclusion, our results indicate that the quantity and distribution of PAWP/WBP2NL do not differ significantly in patients with failed fertilization after ICSI compared to fertile donors. Although we set out to isolate male-factor fertilization failure cases, we cannot exclude an unpredicted egg effect on the observed outcomes. Furthermore, reassessment of these questions in a larger cohort, particularly one associated with egg donation programs, would be beneficial to provide more definitive results. Large studies would also be valuable for investigating if missense sequence variants affect the function of PAWP/WBP2NL, and may provide the needed insight to define its function following fertilization - whether this is directly related to egg activation or occurs down-stream of Ca²⁺ oscillations.

MATERIALS AND METHODS

Study cohort

This study was conducted in accordance with the guidance on Good Clinical Practice (CPMP/ICH/135/95) and with the ethical principles stated in the Declaration of Helsinki 1964, as revised in 2013. Permission to conduct this study was obtained from the local Ethical Committee for Clinical Research.

Before inclusion in the study, all men were given an information sheet explaining the purpose of the test and the aim of the investigation; the patients could discuss their participation with a physician unrelated to the study, and written consent to participate was obtained before enrollment. This study was conducted on a consecutive cohort of eight couples experiencing failed fertilization (i.e., <15% of mature oocytes fertilized after ICSI): four individuals enrolled after an egg reception cycle and four enrolled after an in vitro fertilization cycle with their partner's eggs (**Supplementary Tables I and II**).

Sample processing

Semen samples were obtained by masturbation after 2–5 days of abstinence. After 30 min of liquefaction at room temperature, sperm samples were analyzed with a computer-assisted semen analyzer (Sperm Class analyzer, SCA Human Edition) (Microptic S.L., Barcelona, Spain) and classified following standard criteria (WHO, 2010) (**Supplementary Table I**). The whole ejaculate

from donors and part of the ejaculate from patients was cryopreserved in straws with Sperm Cryoprotect II (Nidacon, Molndal, Sweden), and stored in liquid nitrogen until sample preparation. Eggs were denuded in hyaluronidase (HYASE-10X®) (Vitrolife, Göteborg, Sweden), and ICSI was performed following standard procedures on metaphase-II eggs (Palermo et al., 1992). After ICSI, samples were cultured independently at 37 °C, 6% CO₂ in 25-µl drops of G1® medium (Vitrolife, Göteborg, Sweden) covered with mineral oil (OVOIL®) (Vitrolife). Proper fertilization was assessed 16-19 hr post-ICSI by visualization of two pronuclei and two polar bodies. Fertilization failure was defined as <15% fertilization.

Gene analysis of *PAWP/WBP2NL*

Sperm were washed, and at least 3×10^6 spermatozoa were centrifuged at 15,000g for 2 min at room temperature. Genomic DNA (gDNA) was isolated with QIAamp DNA Blood Mini Kit (QIAGEN, Hilden, Germany), following the manufacturer's instructions. Fragments of *PAWP/WBP2NL* were amplified by PCR using Phusion High-Fidelity DNA polymerase (New England Biolabs, MA) using a CX96 automated thermal cycler (BioRad Laboratories, Hercules, CA) in a final volume of 50 µl. Amplification conditions were: 30 s at 98 °C (initial denaturation) followed by 36 cycles of 5 s at 98 °C (denaturation), 10 s at 57 °C (annealing), and 30 s at 72 °C (extension), and then a final extension for 30 s at 72 °C. PCR fragments were purified with a gel extraction kit (QIAGEN), and the sequence was determined by BigDye Terminator v3.1 using a Sanger ABI 3730xl (GATC Biotechnologies AG, Germany) and analyzed with Chromas Software (Technelysium Ltd., Australia). Basic local alignment search tool (BLAST) analysis was performed against the published sequence of the genomic *PAWP/WBP2NL* locus (Human DNA sequence, from clone CTA-250D10 on chromosome 22, complete sequence).

PCR amplification was designed to cover all coding exons and neighboring intronic regions of the *PAWP/WBP2NL* gene (see **Table III** for primer sequences). The genomic region surrounding exon 1 was amplified using semi-nested PCR, following the same cycle conditions detailed above: first round amplification was directly from the isolated gDNA using primers 1F and 1R, and the second round used 1 µl from the first round amplification in a final volume of 50 µl using primers 1bF and 1R. Single-round PCR was used to amplify exons 2 to 6 using the paired primers.

PCR fragments were purified with a gel extraction kit (QIAGEN). The fragment sequence was determined by BigDye Terminator v3.1 at Sanger ABI 3730xl (GATC Biotechnologies AG, Germany) and analyzed with Chromas Software (Technelysium Ltd., Australia). BLAST analysis

was performed against the published sequence of the genomic *PAWP/WBP2NL* locus (Human DNA sequence from clone CTA-250D10 on chromosome 22) complete sequence.

Table III. Primers used for genomic amplification of *PAWP/WBP2NL*.

Target name	Primer name	Sequence
Exon 1	PAWP 1F	5' -TCTTCAGTTGGCGTCAGGTC
	PAWP 1bF	5' -TGACAGGACCAACCCAAGTC
	PAWP 1R	5' -CTCTCTTCGAAGGACACACG
Exon 2 - 4	PAWP 2bF	5' -TTGTGTGCCGTCTGTTCCCTC
	PAWP 4bR	5' -GCATCACTTACCAGCAGAGG
Exon 5	PAWP 5F	5' -AGATAGGGTCTTGCCATGTTG
	PAWP 5R	5' -ACCCATTTCAGTAGCAGTGG
Exon 6	PAWP 6F	5' -TCCCTGCACAACAGGAAGTG
	PAWP 6R	5' -TACTGGGGAATTAGCCCCAC

Western blot

PAWP/WBP2NL protein abundance was analyzed following previously described protocols (Freour et al., 2017). Briefly, cryopreserved sperm cells were thawed for 10 min at room temperature, and then washed in phosphate-buffered saline (PBS). At least 5×10^6 spermatozoa were pelleted at 15,000 g for 2 min, washed in PBS, resuspended in 100 μ l of Laemmli Buffer, and lysed using three cycles of freezing/boiling (-20 °C, 98 °C). Cell lysates corresponding to 5×10^5 sperm cells (~ 10 μ l) were separated on a 10% sodium dodecyl sulphate polyacrylamide gel, and then transferred to polyvinylidene fluoride membranes (Millipore, Billerica, MA). Membranes were blocked in 5% milk powder in Tris-buffered saline containing 0.1% Tween (TBS-T), and then probed at 4 °C overnight with rabbit anti-human-PAWP/WBP2NL polyclonal antibody (1:1,000 dilution of ab170115 in blocking buffer) (Abcam, Cambridge, UK), followed by incubation with horseradish peroxidase-conjugated anti-rabbit antibody (1:10,000 dilution of NA934 in blocking buffer) (Amersham GE Healthcare, Amersham, UK). Immunoreactivity was detected using chemiluminescent substrate (Luminata Classico, Millipore) and exposure to X-ray films. After development, blots were immediately incubated with an anti- α -tubulin antibody (1:2,000 dilution of T6199) (Sigma, St. Louis, MO) as a loading control.

Validation of the polyclonal antibody to human-PAWP/WBP2NL was performed comparing spermatozoa extracts with OV-90 cell extract. Bands with apparent molecular masses of 35 kDa (upper band), 31 kDa (middle band), and 28 kDa (lower band) were detected, which should correspond to PAWP/WBP2NL isoform 1 (theoretical mass of 31.9 kDa), WBP2 (theoretical mass of 28.1 kDa; 49% identity with the PAWP/WBP2NL amino terminus), and PAWP/WBP2NL

isoform 2 (theoretical mass of 23.7 kDa), respectively. Relative semiquantification of PAWP/WBP2NL abundance was performed by comparative densitometry analysis, measuring the upper (35 kDa) and lower bands (28 kDa) with a specific plug-in of ImageJ software (National Institutes of Health, Bethesda, MD).

Immunofluorescence staining

Immunofluorescence experiments were performed as described elsewhere (Freour et al., 2017). Briefly, at least 10^6 spermatozoa were fixed in PBS containing 4% paraformaldehyde (Sigma-Aldrich, St. Louis, MO) for each patient and donor. Fixed sperm cells were loaded on poly-lysine-coated slides, permeabilized with 0.5% Triton X-100 in PBS, blocked in 3% bovine serum albumin (BSA) in PBS, and incubated overnight at 4 °C with 500 µg/ml of anti-human-PAWP/WBP2NL antibody (1:200 dilution of ab170115 in 0.05% BSA in PBS) (Abcam, Cambridge, UK). Samples were subsequently incubated in 5 µg/ml of Alexa Fluor 568-conjugated goat anti-rabbit IgG Fab2 fragment (Invitrogen, Paisley, UK). Slides were counterstained for 15 min at 37 °C, in the dark, with 20 µg/ml fluorescein-labeled peanut agglutinin (FITC-PNA) and 2 µg/ml Hoechst 33342 (Sigma-Aldrich).

Localization of PAWP/WBP2NL was determined by laser scanning confocal microscopy using a 63× objective on a Sp5 (Leica, Heidelberg, Germany). Images were analyzed with ImageJ software, and the proportion of cells showing PAWP/WBP2NL staining was calculated in all sperm cells with stained nucleus. Among these cells, the same calculation was made in sperm with a clear acrosome status (either intact or reacted, based on the FITC-PNA staining) (**Figure 3a**).

Statistical analysis

PAWP/WBP2NL protein expression was compared between patients and donors using the Student *t*-test. Medcalc software, versión 15.11.4 (MedCalc Software, Ostend, Belgium.), was used for statistical analysis. $p < 0.05$ was considered statistically significant.

ACKNOWLEDGEMENTS

The authors wish to thank the clinical embryology laboratory staff for their assistance with sample collection and analysis and Désirée Garcia for helpful comments. This work was supported by intramural funding of Clinica EUGIN. MTM is partially supported by the Secretary for Universities and Research of the Ministry of Economy and Knowledge of the Government of Catalonia (2015 DI 049).

AUTHORS' CONTRIBUTIONS

TF designed the study, performed experiments, interpreted the data, and drafted the manuscript; MB performed some experiments, interpreted the data, helped to draft the manuscript, and provided critical discussion; MTM performed some experiments interpreted the data and provided critical discussion; AFV performed some experiments and provided critical discussion; RV made substantial contributions to conception and design, interpretation of results and discussion, critical review, and editing of the final version of the manuscript.

REFERENCES

- Aarabi M, Balakier H, Bashar S, Moskovtsev SI, Sutovsky P, Librach CL, Oko R. 2014a. Sperm-derived WW domain-binding protein, PAWP, elicits calcium oscillations and oocyte activation in humans and mice. *FASEB journal : official publication of the Federation of American Societies for Experimental Biology* 28(10):4434-4440.
- Aarabi M, Balakier H, Bashar S, Moskovtsev SI, Sutovsky P, Librach CL, Oko R. 2014b. Sperm content of postacrosomal WW binding protein is related to fertilization outcomes in patients undergoing assisted reproductive technology. *Fertility and sterility* 102(2):440-447.
- Aarabi M., Sutovsky P, Oko R. 2015. Re:Is PAWP the 'real' sperm factor? *Asian Journal of Andrology* 17:446-449.
- Amdani SN, Jones C, Coward K. 2013. Phospholipase C zeta (PLCzeta): oocyte activation and clinical links to male factor infertility. *Advances in biological regulation* 53(3):292-308.
- Amdani SN, Yeste M, Jones C, Coward K. 2015. Sperm Factors and Oocyte Activation: Current Controversies and Considerations. *Biology of reproduction* 93(2):50, 1-8.
- Calhaz-Jorge C, de Geyter C, Kupka MS, de Mouzon J, Erb K, Mocanu E, Motrenko T, Scaravelli G, Wyns C, Goossens V. European IVF-Monitoring Consortium (EIM) for the European Society of Human Reproduction and Embryology (ESHRE), 2016. Assisted reproductive technology in Europe, 2012: results generated from European registers by ESHRE. *Human reproduction* 31(8):1638-1652.
- Chansel-Debordeaux L, Dandieu S, Bechoua S, Jimenez C. 2015. Reproductive outcome in globozoospermic men: update and prospects. *Andrology* 3(6):1022-1034.
- Escoffier J, Yassine S, Lee HC, Martinez G, Delaroche J, Coutton C, Karaouzène T, Zouari R, Metzler-Guillemain C, Pernet-Gallay K, Hennebicq S, Ray PF, Fissore R, Arnoult C. 2015. Subcellular localization of phospholipase C ζ in human sperm and its absence in DPY19L2-deficient sperm are consistent with its role in oocyte activation. *Molecular Human Reproduction* 21(2):157-168.
- Escoffier J, Lee HC, Yassine S, Zouari R, Martinez G, Karaouzène T, Coutton C, Kherraf Z, Halouani L, Triki C, Nef S, Thierry-Mieg N, Savinov SN, Fissore R, Ray PF, Arnoult C. 2016. Homozygous mutation of PLCZ1 leads to defective human oocyte activation and infertility that is not rescued by the WW-binding protein PAWP. *Human Molecular Genetics* 25(5):878-891.
- Esfandiari N, Javed MH, Gotlieb L, Casper RF. 2005. Complete failed fertilization after intracytoplasmic sperm injection--analysis of 10 years' data. *International journal of fertility and women's medicine* 50(4):187-192.

- Ferrer-Vaquero A, Barragan M, Freour T, Vernaev V, Vassena R. 2016. PLCzeta sequence, protein levels, and distribution in human sperm do not correlate with semen characteristics and fertilization rates after ICSI. *Journal of assisted reproduction and genetics* 33(6):747-756.
- Flaherty SP, Payne D, Matthews CD. 1998. Fertilization failures and abnormal fertilization after intracytoplasmic sperm injection. *Human reproduction* 13 Suppl 1:155-164.
- Freour T, Barragan M, Ferrer-Vaquero A, Rodríguez A, Vassena R. 2017. WBP2NL/PAWP mRNA and protein expression in sperm cells are not related to semen parameters, fertilization rate, or reproductive outcome. *Journal of assisted reproduction and genetics* 34(6):803-810.
- Goksan Pabuccu E, Sinem Caglar G, Dogus Demirkiran O, Pabuccu R. 2016. Uncommon but devastating event: total fertilisation failure following intracytoplasmic sperm injection. *Andrologia* 48(2):164-170.
- Hachem A, Godwin J, Ruas M, Lee HC, Ferrer Buitrago M, Ardestani G, Bassett A, Fox S, Navarrete F, de Sutter P, Heindryckx B, Fissore R, Parrington J. 2017. PLCzeta is the physiological trigger of the Ca²⁺ oscillations that induce embryogenesis in mammals but conception can occur in its absence. *Development* 144(16):2914-2924.
- Heytens E, Parrington J, Coward K, Young C, Lambrecht S, Yoon SY, Fissore RA, Hamer R, Deane CM, Ruas M, Grasa P, Soleimani R, Cuvelier CA, Gerris J, Dhont M, Deforce D, Leybaert L, De Sutter P. 2009. Reduced amounts and abnormal forms of phospholipase C zeta (PLCzeta) in spermatozoa from infertile men. *Human reproduction* 24(10):2417-2428.
- Kashir J, Jones C, Lee HC, Rietdorf K, Nikiforaki D, Durrans C, Ruas M, Tee ST, Heindryckx B, Galione A, De Sutter P, Fissore RA, Parrington J, Coward K. 2011. Loss of activity mutations in phospholipase C zeta (PLCzeta) abolishes calcium oscillatory ability of human recombinant protein in mouse oocytes. *Human reproduction* 26(12):3372-3387.
- Kashir J, Konstantinidis M, Jones C, Heindryckx B, De Sutter P, Parrington J, Wells D, Coward K. 2012. Characterization of two heterozygous mutations of the oocyte activation factor phospholipase C zeta (PLCzeta) from an infertile man by use of minisequencing of individual sperm and expression in somatic cells. *Fertility and sterility* 98(2):423-431.
- Kashir J, Deguchi R, Jones C, Coward K, Stricker SA. 2013. Comparative biology of sperm factors and fertilization-induced calcium signals across the animal kingdom. *Molecular reproduction and development* 80(10):787-815.
- Kline D, Kline JT. 1992. Repetitive calcium transients and the role of calcium in exocytosis and cell cycle activation in the mouse egg. *Developmental biology* 149(1):80-89.
- Nomikos M, Elgmati K, Theodoridou M, Calver BL, Cumbes B, Nounesis G, Swann K, Lai FA. 2011. Male infertility-linked point mutation disrupts the Ca²⁺ oscillation-inducing and PIP(2) hydrolysis activity of sperm PLCzeta. *The Biochemical journal* 434(2):211-217.
- Nomikos M, Sanders JR, Theodoridou M, Kashir J, Matthews E, Nounesis G, Lai FA, Swann K. 2014. Sperm-specific post-acrosomal WW-domain binding protein (PAWP) does not cause Ca²⁺ release in mouse oocytes. *Molecular human reproduction* 20(10):938-947.
- Nomikos M, Sanders JR, Kashir J, Sanusi R, Buntwal L, Love D, Ashley P, Sanders D, Knaggs P, Bunkheila A, Swann K, Lai FA. 2015. Functional disparity between human PAWP and PLCzeta in the generation of Ca²⁺ oscillations for oocyte activation. *Molecular human reproduction* 21(9):702-710.
- Nomikos M, Stamatiadis P, Sanders JR, Beck K, Calver BL, Buntwal L, Lofty M, Sideratou Z, Swann K, Lai FA. 2017. Male infertility-linked point mutation reveals a vital binding role for the C2 domain of sperm PLCzeta. *The Biochemical journal* 474(6):1003-1016.
- Palermo G, Joris H, Devroey P, Van Steirteghem AC. 1992. Pregnancies after intracytoplasmic injection of single spermatozoon into an oocyte. *Lancet* 340(8810):17-18.

- Rawe VY, Olmedo SB, Nodar FN, Doncel GD, Acosta AA, Vitullo AD. 2000. Cytoskeletal organization defects and abortive activation in human oocytes after IVF and ICSI failure. *Molecular human reproduction* 6(6):510-516.
- Satouh Y, Nozawa K, Ikawa M. 2015. Sperm postacrosomal WW domain-binding protein is not required for mouse egg activation. *Biology of reproduction* 93(4):94, 1-7.
- Saunders CM, Larman MG, Parrington J, Cox LJ, Royse J, Blayney LM, Swann K, Lai FA. 2002. PLC zeta: a sperm-specific trigger of Ca²⁺ oscillations in eggs and embryo development. *Development* 129(15):3533-3544.
- Shinar S, Almog B, Levin I, Shwartz T, Amit A, Hasson J. 2014. Total fertilization failure in intra-cytoplasmic sperm injection cycles--classification and management. *Gynecological endocrinology* 30(8):593-596.
- Tavalaee M, Nasr-Esfahani MH. 2016. Expression profile of PLCzeta, PAWP, and TR-KIT in association with fertilization potential, embryo development, and pregnancy outcomes in globozoospermic candidates for intra-cytoplasmic sperm injection and artificial oocyte activation. *Andrology* 4(5):850-856.
- WHO. 2010. WHO laboratory manual for the examination and processing of human semen 5th edition.
- Wu YG, Liu Y, Zhou P, Lan GC, Han D, Miao DQ, Tan JH. 2007. Selection of oocytes for in vitro maturation by brilliant cresyl blue staining: a study using the mouse model. *Cell research* 17(8):722-731.
- Yeste M, Jones C, Amdani SN, Patel S, Coward K. 2016. Oocyte activation deficiency: a role for an oocyte contribution? *Human reproduction update* 22(1):23-47.

SUPPLEMENTARY INFORMATION

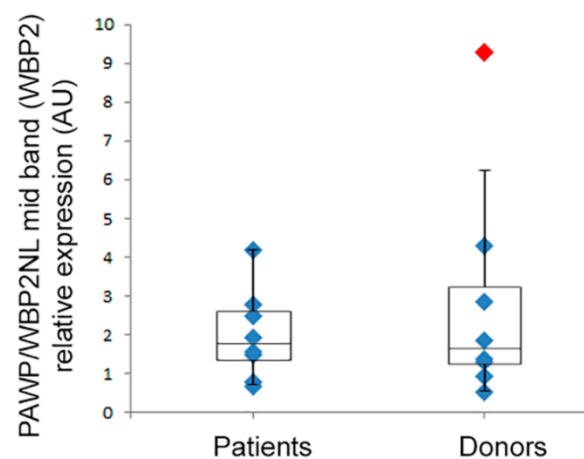
Supplementary Table I. Demographic characteristics of individual patients and donors. A, asthenozoospermia; BMI, body-mass index; D, donor; FR, fertilization rate (%); N, normozoospermia; ND, not determined; NF, non-fertilized; OA, oligoasthenozoospermia; OAT, oligoasthenozoospermia; P, patient; REPA, receipt of egg from partner, or partner-assisted reproduction.

	male age	Female partner age	Egg source	egg age	sperm diagnosis	Volume of ejaculate (ml)	sperm concentration (x10 ⁶ /ml)	total sperm cell number in the ejaculate (x10 ⁹)	Progressive motility (%)	Non Progressive motility (%)	Immotile cells (%)	normal forms	# injected oocytes	FR	1PN	3PN	degenerated	NF	male BMI	female BMI
P1	55	45	Donor	33	N	6.1	59.2	361.12	70.2	1.3	28.5	6	6	0%	2	1	3	0	25.83	18.7
P2	41	37	Partner	37	N	2.2	117.9	259.38	63.3	10.1	26.6	9	4	0%	0	2	0	2	ND	25.0
P3	31	30	Partner	30	N	3.5	205.8	720.3	55.1	4.2	40.7	12	9	0%	ND	ND	ND	ND	27.68	21.8
P4	52	44	Donor	26	N	2.1	24.5	51.45	53.8	2	44.1	8	7	14%	1	4	0	1	30.48	25.2
P5	40	40	Donor	32	N	3.5	62.9	220.15	62.4	2.8	35	4	7	14%	0	3	3	0	23.92	21.8
P6	43	38	Partner	38	A	4.2	142.8	599.76	16.1	3.7	80.3	13	13	15%	ND	ND	ND	ND	23.66	31.5
P7	48	44	Partner	44	OA	1	7.7	7.7	7.3	2.4	90.3	4	2	0%	0	1	1	0	ND	25.0
P8	51	46	Donor	31	OAT	1.8	2.6	4.68	0	3.2	96.8	2	6	0%	0	0	1	5	ND	22.6
D1	32	26	REPA	37	N	ND	28.3	ND	7.77	ND	ND	ND	2	100%	0	0	0	0	23.24	23.7
D2	20	35	Partner	35	N	ND	101.7	ND	24	ND	ND	ND	7	86%	0	0	1	0	26.29	19.38
D3	22	37	Partner	37	N	ND	87.7	ND	39.34	ND	ND	ND	6	83%	0	0	0	1	23.37	30.4
D4	28	42	Partner	42	N	ND	121.8	ND	44.42	ND	ND	ND	6	50%	0	1	2	0	21.15	26.9
D5	19	44	Donor	21	N	ND	72.4	ND	17.26	ND	ND	ND	6	67%	0	1	1	0	22.72	19
D6	34	48	Donor	34	N	ND	59.9	ND	29.89	ND	ND	ND	9	44%	1	1	2	1	21.45	27.6
D7	29	40	Partner	40	N	ND	17.3	ND	18.5	ND	ND	ND	2	100%	0	0	0	0	25.88	27.5
D8	30	31	Partner	31	N	ND	74	ND	90	ND	ND	ND	20	65%	1	2	2	2	22.89	27.46

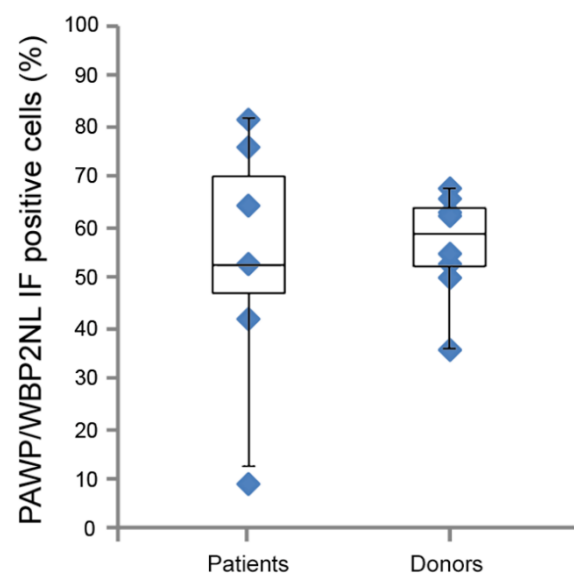
Supplementary Table II: Results of the previous cycle outcome from which we selected the patients. IUI, Intrauterine insemination; IVF, In vitro fertilization; NA, Not applicable; ND, Not determined; P, patient.

	Years of infertility	Previous cycles	Fertilization rate	Past reproductive results	Reason for oocyte donation
P1	2	0	NA	NA	Ovarian failure
P2	4	1	NA	no pregnancy	NA
P3	3	2 IVF	0/9	no pregnancy	NA
P4	9	0	NA	NA	Ovarian failure
P5	6	7 IUI 6 IVF	0	no pregnancy	Ovarian failure
P6	14	3 IUI 5 IVF	2/13	no pregnancy	NA
P7	12	1 IVF	NA	no pregnancy	NA
P8	ND	0	NA	NA	Ovarian failure

Supplementary Figure 1: Comparison of the relative expression in WB of WBP2 versus α -tubulin in patients and donor samples. Results are presented as individual values (blue diamond) and box-plot distribution. Red diamond represents outliers. Comparisons were not statistically significant ($p > 0.05$), Student t-test.



Supplementary Figure 2: Proportion of positive PAWP/WBP2NL sperm cells among sperm with visible acrosome in patients and donors samples. Results are presented as individual values (blue diamond) and box-plot distribution. Comparisons were not statistically significant ($p > 0.05$), Student t-test.



CHAPTER 2: Novel phospholipase C zeta 1 mutations associated with fertilization failures after ICSI

ACCEPTED FOR PUBLICATION AS:

Torra-Massana M, Cornet-Bartolomé D, Barragán M, Durban M, Ferrer-Vaquer A, Zambelli F, Rodríguez A, Oliva R, Vassena R. **Novel phospholipase C zeta 1 mutations associated with fertilization failures after ICSI.** *Hum Reprod* 2019.

Partial contents of this chapter were included in the following oral presentation:

M. Barragan, M. Torra, D. Cornet, A. Ferrer-Vaquer, A. Rodríguez, R. Vassena. **High prevalence of PLC ζ mutations among cases of failed oocyte activation, but not anomalous fertilization, after IVF/ICSI.** ESHRE Annual Meeting 2017, Geneva, Switzerland. O-019. Human Reproduction, Vol.32, No.Suppl pp. 509–539, 2017.

TITLE: Novel PLCZ1 mutations associated with fertilization failures after ICSI

RUNNING TITLE: PLCZ1 mutation in fertilization failure

AUTHORS:

Marc Torra-Massana ^{1, 2, #}, David Cornet-Bartolomé ^{1, #}, Montserrat Barragán ¹, Mercè Durban ¹, Anna Ferrer-Vaquer ¹, Filippo Zambelli ¹, Amelia Rodriguez ¹, Rafael Oliva ^{2,3}, Rita Vassena ^{1, *}

ADDRESS:

¹ Clínica EUGIN, Barcelona 08029, Spain.

² Faculty of Medicine, University of Barcelona, Barcelona 08036, Spain.

³ Molecular Biology of Reproduction and Development Group, Institut d'Investigacions Biomèdiques August Pi i Sunyer (IDIBAPS), Fundació Clínic per a la Recerca Biomèdica, Faculty of Medicine, University of Barcelona, Barcelona 08036, Spain.

These authors contributed equally to this work.

***Correspondence:** Clínica EUGIN, Travessera de les Corts 322, 08029, Barcelona, Spain. Email: rvassena@eugin.es

ABSTRACT

Study question: Are phospholipase C zeta 1 (*PLCZ1*) mutations associated with fertilization failure (FF) after ICSI?

Summary answer: New mutations in the *PLCZ1* sequence are associated with fertilization failures after ICSI.

What is known already: FF occurs in 1-3% of ICSI cycles, mainly due to oocyte activation failure. The sperm PLC ζ /PLCZ1 protein hydrolyzes phosphatidylinositol (4,5)-bisphosphate (PIP₂) in the oocyte, leading to intracellular calcium release and oocyte activation. To date, few *PLCZ1* point mutations causing decreased protein levels or activity have been linked to FF. However, functional alterations of PLC ζ /PLCZ1 in response to both described and novel mutations have not been investigated.

Study design, size, duration: We performed a study including 37 patients presenting total or partial FF ($\leq 25\%$ fertilization rate) after ICSI occurring between 2014 and 2018.

Participants/materials, setting, and methods: Patients were divided into two groups based on oocyte evaluation 19h post ICSI: FF due to a defect in oocyte activation (oocyte activation failure (OAF), n= 22); and FF due to other causes (“no-OAF”, n= 15). Samples from 13 men with good fertilization ($>50\%$ fertilization rate) were used as controls. PLC ζ /PLCZ1 protein localization and levels in sperm were evaluated by immunofluorescence and Western Blot, respectively. Sanger sequencing on genomic DNA was used to identify *PLCZ1* mutations in exonic regions. The effect of the mutations on protein functionality was predicted *in silico* using the MODICT algorithm. Functional assays were performed by cRNA injection of *wild-type* and mutated forms of *PLCZ1* into human *in vitro* matured metaphase II oocytes, and fertilization outcomes (2nd polar body extrusion, pronucleus appearance) scored 19h after injection.

Main results and the role of chance: In the OAF group, 12 (54.6 %) patients carried at least one mutation in the *PLCZ1* coding sequence, versus one patient out of 15 (6.7%) in the no-OAF group ($p < 0.05$), and none of the 13 controls ($p < 0.05$). A total of six different mutations were identified. Five of them were single nucleotide missense mutations: p.I120M, located at the end of the EF-hand domain; p.R197H, p.L224P and p.H233L, located at the X catalytic domain; and p.S500L, located at the C2 domain. The sixth mutation, a frameshift variant (p.V326K fs*25), generates a truncated protein at the X-Y linker region. *In silico* analysis with MODICT predicted all the mutations except p.I120M to be potentially deleterious for PLC ζ /PLCZ1 activity. After *PLCZ1* cRNA injection, a significant decrease in the percentage of activated oocytes was observed for

three mutations (p.R197H, p.H233L, and p.V326K fs*25), indicating a deleterious effect on enzymatic activity. *PLCZ1* protein localization and expression levels in sperm were similar across groups. Fertilization rates were restored (to >60%) in patients carrying *PLCZ1* mutations (n=10) after assisted oocyte activation (AOA), with seven patients achieving pregnancy and live birth.

Limitations, reasons for caution: Caution should be exerted when comparing the cRNA injection results with fertilization outcomes after ICSI, especially in patients presenting mutations in heterozygosis.

Wider implications of the findings: *PLCZ1* mutations were found in a high frequency in patients presenting OAF. Functional analysis of three mutations in human oocytes confirms alteration of PLC ζ /PLCZ1 activity, and their likely involvement in impaired oocyte activation. Our results suggest that *PLCZ1* gene sequencing could be useful as a tool for the diagnosis and counseling of couples presenting fertilization failure after ICSI due to OAF.

Study funding/competing interest(s): This work was supported by intramural funding of Clínica EUGIN, by the Secretary for Universities and Research of the Ministry of Economy and Knowledge of the Government of Catalonia (GENCAT 2015 DI 049 to M. T-M and GENCAT 2015 DI 048 to D. C-B), and by the Torres Quevedo Program from the Spanish Ministry of Economy and Competitiveness to A. F.-V. No competing interest declared.

KEYWORDS: sperm, ICSI, phospholipase C zeta 1, fertilization failure, assisted oocyte activation

INTRODUCTION

In the last 20 years, there has been an increase in the use of ICSI for non-male factor infertility (Neri et al., 2014; Li et al., 2018). Although mean fertilization rates (FR) are around 70-80% for ICSI, total fertilization failure (FF) still occurs in up to 3% of cases (Flaherty et al., 1998; Rawe et al., 2000).

FF has a high emotional and economic impact on patients, its molecular pathogenesis is not completely understood, and research on the topic suffers from ethical and technical limitations. Assisted oocyte activation (AOA) is an experimental technique designed to overcome FF after ICSI. While several live births have been reported after using this technique, its efficiency is still under debate (Vanden Meerschaut et al., 2012; Sfontouris et al., 2015).

Successful fertilization is dependent on a specific pattern of intracellular calcium oscillations in the oocytes, which promotes oocyte activation, including prevention of polyspermy by cortical granule exocytosis, cytoskeletal reorganization, and resumption of meiosis (Kline and Kline, 1992; Ducibella et al., 2002; Yeste et al., 2016). FF is characterized by either abnormally fertilized oocytes (abnormal number of pronuclei (PN)) or, more often, oocyte activation failure (OAF), particularly in cases of repeated FF (≥ 2 ICSI cycles), where $>90\%$ of inseminated oocytes remain at metaphase II (MII) (Flaherty et al., 1998; Yeste et al., 2016). While FF cases may be caused by asynchrony between nuclear and cytoplasmic maturation, spindle abnormalities, and deficiencies in key proteins involved in oocyte activation, such as calcium/calmodulin-dependent protein kinase type II (CamKII), mitogen-activated protein kinase (MAPK) or Wee1-like protein kinase 2 (WEE2) (Sang et al., 2018), most FF after ICSI are linked to defects in sperm-borne oocyte activation factors (SOAFs) (Yeste et al., 2016).

Phospholipase C zeta (PLC ζ /PLCZ1) has emerged as an essential SOAF (Saunders et al., 2002). Microinjection of human *PLCZ1* cRNA or recombinant PLC ζ /PLCZ1 protein into human oocytes triggers calcium oscillations and development to the blastocyst stage (Rogers et al., 2004; Yoon et al., 2012). Moreover, *PLCZ1* knock-out mouse sperm present severe problems with triggering fertilization, oocyte activation and calcium signaling after ICSI even if natural conceptions can occasionally be achieved (Hachem et al., 2017; Nozawa et al., 2018).

The smallest member of PLC family (~70 kDa in humans), PLC ζ /PLCZ1 is a sperm-specific soluble enzyme (Saunders et al., 2002). This protein possesses four main domains: the EF-hand region, important to confer high calcium sensitivity; the X and Y catalytic domains, responsible for enzymatic activity (hydrolysis of PIP₂ from the oocyte intracellular cytoplasmic vesicles); the XY-linker, suggested to be the region of the protein that interacts with PIP₂; and C2, a domain required for PLC ζ /PLCZ1 binding to PI(3)P and PI(5)P-containing liposomes (Saunders et al., 2002; Kouchi et al., 2005; Nomikos et al., 2011; Sanders et al., 2018).

The presence of certain mutations in the coding sequence of *PLCZ1* gene has been shown to affect calcium oscillations and oocyte activation. Four point mutations have been found in patients with FF to date: p.H398P (located in the Y-catalytic domain) and p.H233L (located in the X-catalytic domain) were identified in compound heterozygosis in a non-globozoospermic patient (Heytens et al., 2009; Kashir et al., 2012). Recently, a mutation located in the C2 domain (p.I489F) has been found in homozygosis in two infertile brothers (Escoffier et al., 2016). These mutated forms of PLC ζ /PLCZ1, injected as cRNA or recombinant protein, failed to produce normal calcium oscillations in mouse oocytes (Kashir et al., 2011; Kashir et al., 2012; Escoffier et al., 2016).

Another missense mutation, p.S500L, was described in patients with FF, although functional assays were not performed (Yoon et al., 2008; Ferrer-Vaquer et al., 2016).

Despite this clear association between *PLCZI* sequence and FF, studies on large cohorts of patients have not been published to date. For this reason, the frequency of *PLCZI* mutations and the potential benefit of gene sequencing for FF patients in fertility clinics have not been established. The objective of this study was to use a large cohort of patients with FF to identify mutations in the *PLCZI* gene and determine if they can cause altered protein function and FF after ICSI. Our results showed a clear association between deleterious *PLCZI* mutations and OAF.

MATERIALS AND METHODS

Ethical considerations

Approval to conduct this research was obtained from the local Ethical Committee for Clinical Research and written informed consent was obtained from all patients enrolled in the study.

Study population

Patients were recruited between January 2014 and August 2018. Inclusion criteria were: low fertilization rate (greater than 0% but lower than or equal to 25%) to total (0% FR) FF after one or more ICSI cycles, and a minimum of four MII oocytes injected. Patients with severe male factor (cryptozoospermia, and / or <1% progressive motility) were excluded. In total, 37 patients were included in the study. Patients were divided in two groups for the analysis of PLC ζ /PLCZ1: the OAF group, including 22 patients presenting a previous history of repetitive FF (≥ 2 ICSI cycles) in other clinics or OAF, defined by 100% of oocytes without visible pronuclei among the non-fertilized oocytes; and the no-OAF group, including 15 patients not meeting these criteria, all of them with abnormal fertilization (1PN, 3PN and / or >3PN). As a control group, 13 normozoospermic sperm donors with proven fertility and FR above 50% were included. All semen samples were evaluated according to World Health Organization (WHO, 2010) recommendations. Sperm concentration and motility were assessed using the Integrated Semen Analysis System (ISAS[®], PROiSER, Valencia, Spain), and samples were frozen according to the manufacturer's instructions (CryoProtecII, Nidacon, Mölndal, Sweden) for future use.

Genomic analysis of *PLCZI*

Genomic analysis was performed as previously described (Grasa et al., 2008). Briefly, after sperm genomic DNA isolation, amplification and purification of *PLCZI* exonic regions, the gene

sequence was determined by BigDye Terminator v3.1 at Sanger ABI 3730xl (GATC Biotechnologies AG, Ebersberg, Germany), and analyzed with Chromas (Technelysium Ltd., South Brisbane QLD, Australia). BLAST analysis was performed against the public sequence of the genomic *PLCZ1* locus (*Homo sapiens* 12 BAC RP11-361I14, Roswell Park Cancer Institute Human BAC Library) complete sequence. Only variants in the coding region were considered for analysis.

PLC ζ /PLCZ1 protein levels and localization

PLC ζ /PLCZ1 protein expression levels were analyzed by western blot as previously described (Ferrer-Vaquero et al., 2016). Briefly, whole-cell lysates of 500,000 sperm were loaded per lane, and blots were incubated with 10 μ g/ml of anti-human-PLC ζ /PLCZ1 antibody (pab0367-P, Covalab, Villerbanne, France) at 4°C overnight, followed by incubation in anti-rabbit secondary antibody (horse-radish peroxidase-conjugated, NA934, GE Healthcare, Chicago, IL, USA). Anti- α -tubulin antibody (T6199, Sigma-Aldrich, Spain) was used as a loading control.

Immunofluorescence was performed as previously described (Ferrer-Vaquero et al., 2016). Briefly, sperm were incubated with anti-human-PLC ζ /PLCZ1 antibody (pab0367-P, Covalab) at 4°C overnight, followed by incubation with secondary antibody (Alexa Fluor 568 goat anti-rabbit IgG; Invitrogen, USA). Slides were counterstained with 20 μ g/ml FITC-Peanut Agglutinin (PNA) and 2 μ g/ml Hoechst-33342 (Sigma-Aldrich) for 15 min at 37°C in the dark. The localization of PLC ζ /PLCZ1, PNA, and the sperm nucleus were analyzed by confocal microscopy (LSM780, Carl Zeiss AG, Oberkochen, Germany), scoring for state of the acrosome (intact acrosome, reacted acrosome or unlabeled acrosome) and PLC ζ /PLCZ1 localization (acrosomal, equatorial or postacrosomal).

***In silico* analysis of PLC ζ mutations**

SWISS-MODEL was used to compare structural changes between the PLC ζ /PLCZ1 *wild-type* and frameshift p.V326K fs*25 mutant. To predict the functional effect of the point mutations, the MODICT pipeline was used (Tanyalcin et al., 2016). Briefly, three-dimensional (3D) *wild type* and mutant proteins were modelled using PLCD1 (PDB ID: c1djyB) as a template by Phyre2 (Kelley et al., 2015), and further refined by ModRefiner (Xu and Zhang, 2011). Swiss-PdbViewer was used to obtain RMSD values from the *wild type* / mutant comparisons, and the generated values were used by MODICT to predict the impact of the mutations on protein activity. Thresholds were built using *wild-type* and a previously published mutation, p.H398P, known to negatively affect PLC ζ /PLCZ1 function (Heytens et al., 2009). Briefly, the MODICT scores of the known protein

models were obtained (S_c = wild type score, S_k = known deleterious score). Then, as described in Tanyalcin et al., 2016, we generated an imaginary benign score (SI), by combining the deleterious and wild type score, with the formula: $SI = (2 * S_k + 3.24 * S_c) / 5.24$. Finally, we generated the different thresholds by combining the scores of the wildtype (S_c) and imaginary benign (SI) with the formulas: $T1 = ((S_c + SI) / 2) + 3 * k / 100 * \text{stdev}(SI, S_c)$, for the detrimental threshold; and $T2 = ((S_c + SI) / 2) + 1.5 * k / 100 * \text{stdev}(SI, S_c)$, for the non-detrimental threshold ($k = 55$, default value).

***PLCZ*/*PLCZI* cloning, directed mutagenesis and cRNA synthesis**

Two fragments of human *PLCZI* wild-type cDNA were amplified from a human testis mRNA cDNA library (636533, Clontech, Mountain View, CA, USA) by using the following primer pairs: 5'-CATCATGGATCCATGGAAATGAGATGGTTTTTGTC-3' (forward) and 5'-ACTCCAGGTAACTTTTTTACCCC-3' (reverse), for the 5' *PLCZI* fragment; and 5'-GCATTCATGACATCTGACTAC-3' (forward) and 5'-CATCATTCTAGATTATCTGACGTACCAAACATAAAC-3' (reverse), for the 3' *PLCZI* fragment. PCR amplification conditions were: denaturation at 98°C for 30 s, followed by 35 cycles of amplification (98°C for 30 s, 57°C for 30 s and 72°C for 1 min) and an elongation step at 72°C for 10 min. Both fragments were ligated into a pJET1.2 plasmid (ThermoFisher Scientific, Waltham, MA, USA) to obtain full-length wild-type cDNA (pJET1.2-*PLCZI*^{WT}). Next, pJET1.2-*PLCZI*^{WT} was subjected to site-directed mutagenesis (Q5[®] Site-Directed Mutagenesis Kit, New England Biolabs, Ipswich, MA, USA) to generate *PLCZI*^{I120M}, *PLCZI*^{R197H}, *PLCZI*^{L224P}, *PLCZI*^{H233L}, *PLCZI*^{V326K fs*25} and *PLCZI*^{S500L} mutants, using the primer pairs listed in **Supplementary Table I**. In order to prepare templates for cRNA synthesis, all *PLCZI* cDNAs were subcloned in a pT7CFE1-CHis expression vector (88860, ThermoFisher Scientific). Successful mutagenesis and cloning of the constructs was confirmed by Sanger sequencing. The pT7CFE1-CHis constructs were linearized by SpeI, and cRNA was transcribed *in vitro* using the mMessage/mMachine capping kit (Invitrogen) and a poly(A) tailing kit (Invitrogen), following manufacturer's instructions. Capped and poly (A)-tailed cRNAs were purified from the reaction mixture using the MEGA clear Kit (Invitrogen). cRNA quality was tested by agarose gel electrophoresis, and quantified using Qubit RNA HS Assay Kit (Q32852, Life Technologies, Carlsbad, CA, USA) and the Qubit 2.0 Fluorometer (Life Technologies) following the manufacturer's instructions. *PLCZI* cRNA was diluted at 100 ng/μl in injection buffer (150 mM KCl RNase-free solution) and stored in single-use aliquots at -80°C.

Source of oocytes and IVM

Functional assays for *PLCZI* mutations were performed using *in vitro* matured MII oocytes donated for research purposes, obtained from oocyte donors between 18 and 35 years old. Oocyte donors were stimulated using a short antagonist protocol and a GnRH agonist trigger in all cycles. All oocytes were denuded within 30 minutes after retrieval by gentle pipetting and with 80-IU/ml hyaluronidase (HYASE-10x, Vitrolife, Göteborg, Sweden) in G-MOPSTTM PLUS buffered medium (Vitrolife). Once denuded, oocytes were scored for PB presence. Immature oocytes (metaphase I and germinal vesicle oocytes) were cultured in G-2TM PLUS (Vitrolife) for 36 and 48 hours respectively. Oocytes that reached MII stage (IVM-MII) were subsequently used for cRNA injection tests.

cRNA microinjection and fertilization outcome assessment

A total of 126 human *in vitro* matured MII oocytes were injected with approx. 4 pl of the different *PLCZI* cRNA forms at 100ng/μl, set as the optimal concentration to achieve oocyte activation by Yamaguchi et al. (2017); as control, 21 IVM-MII oocytes were sham-injected with approx. 4 pl of injection buffer. The injected volume was calculated by measuring the equivalent distance (173 μm for around 4 pl volume, in 5-5.7 μm ICSI micropipettes) on the computer screen while performing the injection, by using RI Viewer Imaging Software (Research Instruments, Falmouth, UK). cRNA microinjection was performed with 30°-angled ICSI micropipettes (MIC-35-30, Origio, Måløv, Denmark). Each injection round included oocytes injected with *PLCZI*^{WT} as controls. Presence of oocyte activation was determined by evaluating 2nd PB extrusion and PN appearance 19 hours after injection. Degenerated oocytes were discarded, and different rounds of injection were performed to evaluate a minimum of 10 oocytes per mutation.

AOA

AOA was performed as previously described (Durban, et al., 2015). Briefly, 30 min after ICSI oocytes were treated by two rounds of Ionomycin (MP Biomedical, USA) at 10 μmol/l in G-1 PLUSTM (Vitrolife) for 10 min followed by 30 min washing in G-1 PLUSTM. Afterwards, oocytes were cultured in a time-lapse system incubator under 37°C, 6% CO₂, 5% O₂ conditions. Fertilization assessment was performed 16-19 hours after the last washing and fertilized oocytes were cultured until transfer or freezing.

Statistical analysis

GraphPad Software (GraphPad, San Diego, CA, USA) was used for statistical analysis. The two-tailed Mann–Whitney U test was used to analyse differences in sperm parameters between both FF

groups. Kruskal-Wallis test was used to analyse protein localization patterns and levels between study groups, and between patients with and without a *PLCZI* mutation. Chi-Square test was applied to analyse differences in incidence of *PLCZI* mutations between groups, and to evaluate the percentages of activated oocytes after cRNA injection for each mutation compared to *wild-type*. Statistical significance was set at a p-value < 0.05.

RESULTS

Semen parameters and ICSI cycles

Demographic, sperm and cycle variables for each patient included in the study are reported in **Supplementary Table II**. Sperm parameters were comparable between no-OAF and OAF groups (**Table I**); concentration and motility in controls could be only determined in frozen thawed samples. Patients' semen parameters ranged from normozoospermia to oligoasthenoteratozoospermia and were similar between OAF and no-OAF groups (**Supplementary Table II**).

Table I. Sperm variables of fertilization failure patients included in the study: OAF and no-OAF groups. Values are presented as mean \pm standard deviation [range]. *Two-tailed Mann–Whitney U test. OAF; oocyte activation failure. a+b; sperm with progressive motility. NS; not significant.

Variable; units	OAF (n= 22)	no-OAF (n= 15)	p*
Sperm motility (a+b); %	36.93 \pm 24.8 [1.0-87.12]	46.23 \pm 21.7 [5.9-70.2]	NS
Sperm concentration; million/ml	59.29 \pm 61.5 [0.1-190.9]	42.67 \pm 36.9 [7.4-117.9]	NS
Sperm normal morphology; %	6.6 \pm 4.0 [1-15]	6.5 \pm 3.3 [3-15]	NS
Ejaculate volume; ml	3.7 \pm 1.4 [0.6-6.8]	4.1 \pm 2.6 [1-10.7]	NS

The number (mean \pm SD) of injected oocytes per ICSI cycle was comparable between the three study groups: 6.18 \pm 2.6, 6 \pm 1.2, and 7.54 \pm 2.2, for OAF, no-OAF and controls, respectively. In addition, no significant differences were observed in the mean age of the oocytes used for ICSI between the three study groups: 32.92 \pm 5.5, 29.87 \pm 7.1, and 28.62 \pm 5.9, for OAF, no-OAF and controls, respectively.

Mean FR in OAF (6.4%) and no-OAF (10.6%) groups was lower than in the control group (77.6%). In addition, among the non-fertilized oocytes evaluated (non-degenerated), OAF patients presented 100% of not-activated oocytes (absence of visible PN), while the no-OAF group presented 70.4% of abnormally fertilized oocytes (1PN + 3PN + >3PN) (**Supplementary Table II**).

***PLCZ1* gene sequence**

Thirteen (35.1%) FF patients carried at least one mutation in the coding region of *PLCZ1*. Six different mutations (four of them not previously described) were identified in FF patients (**Table II** and **Supplementary Figure 1**). Five of them were single nucleotide missense mutations: p.I120M, p.R197H, p.L224P, p.H233L, and p.S500L; one mutation was a frameshift caused by a deletion of two nucleotides (p.V326K fs*25). All six mutations were located in protein domains important for enzymatic activity: p.I120M was located at the c-terminus of EF-hand domain; p.R197H, p.L224P and p.H233L were located at the X catalytic domain; p.S500L was found at C2 N-terminal domain; and the p.V326K fs*25 mutation results in a protein truncated at the X-Y linker region, lacking both the Y- and C2 domains (**Table II, Figure 1A**).

Table II. *PLCζ* gene mutations detected in fertilization failure patients. *Patient in which mutation was detected in homozygosis

Mutation (protein)	Mutation (coding sequence)	Gene location	Protein location	Mutation	Variation (dbSNP)	Minor allele frequency (ExAc)	N° cases (patients)
p.I120M	c.360 C>G	Exon 4	EF hand domain	missense	rs79487790	0.0029 / 293	1 (P30)
p.R197H	c.590 G>A	Exon 6	X Catalytic domain	missense	rs781075636	0.00002 / 2	1 (P5)
p.L224P	c.671 T>C	Exon 6	X Catalytic domain	missense	rs144902254	0.0002 / 30	1 (P26)
p.H233L	c.698 A>T	Exon 6	X Catalytic domain	missense	rs200061726	0.0007 / 85	1 (P8)
p.V326K fs*25	c.972_973 delAG	Exon 9	X-Y linker	frameshift	rs777169092	0.00006 / 7	1 (P12)
p.S500L	c.1499 C>T	Exon 13	C2 domain	missense	rs10505830	0.0314 / 3793	9 (P5, P22, P24, P27, P28, P29*, P32, P36, P37)

All mutations were found in heterozygosis, except in patient 29, who carried p.S500L in homozygosis (**Table II**). Moreover, p.S500L was the most frequent mutation, found in nine FF patients, and in heterozygosis with p.R197H in patient 5.

Mutations were unevenly distributed between the two FF (OAF and no-OAF) and control groups (**Figure 1B**). Twelve out of 22 (54.55%) patients in the OAF group had at least one mutation in *PLCZ1* coding sequence, versus one out of 15 (6.67%; $p < 0.05$) patients in the no-OAF group, who presented p.S500L in heterozygosis. None of the 13 controls presented mutations in *PLCZ1* coding sequence ($p < 0.05$).

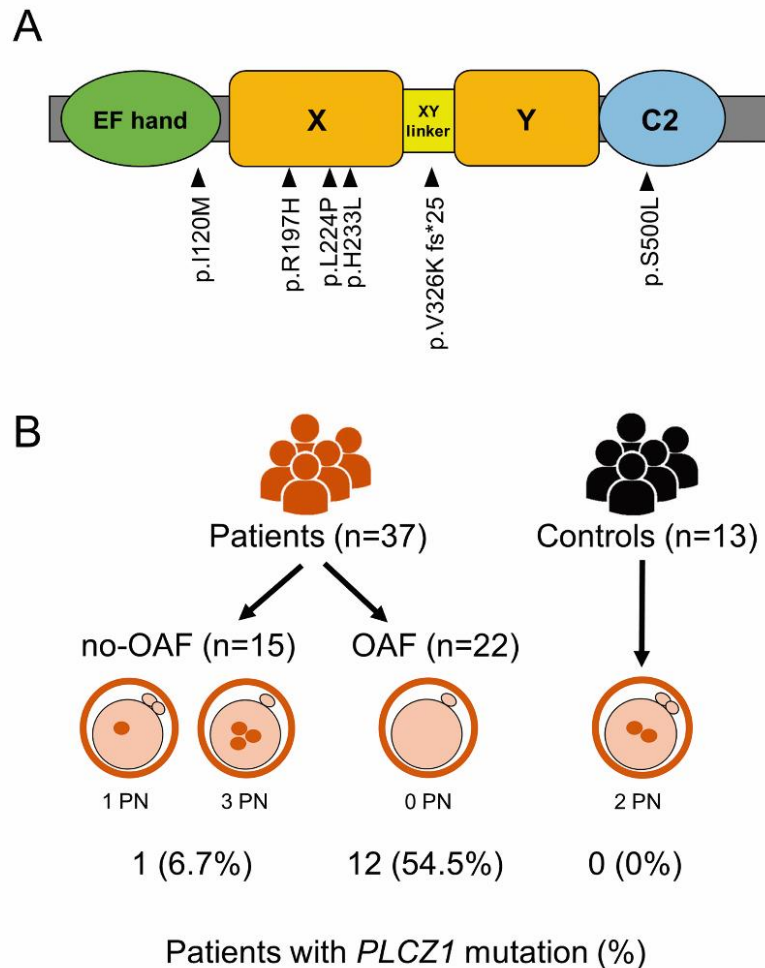


Figure 1: PLC ζ /PLCZ1 mutations detected in fertilization failure patients. (A) Protein structure of phospholipase C zeta 1 (PLC ζ /PLCZ1) indicating the position of mutations (arrowheads). (B) Distribution of PLC ζ /PLCZ1 mutations among study groups. OAF: oocyte activation failure; no-OAF: no oocyte activation failure; PN: pronuclei.

***PLCZ1* mutations are not associated with protein distribution and levels.**

Localization of PLC ζ /PLCZ1 protein within the sperm head was evaluated in nine donors (control group), in patients with no-OAF (n=15) and OAF (n=19). As previously described (Ferrer-Vaquero et al., 2016) in whole sperm of controls, the postacrosomal region was found to be the main subcellular localization (42.9%) of PLC ζ /PLCZ1, followed by acrosomal (24.5%), and equatorial (12.7%) localizations; however, protein staining could not be detected in 24.5% of cells (**Supplementary Figure 2**). Regardless, these localization patterns vary depending on the subpopulation of sperm analyzed (intact acrosome, reacted acrosome, or no acrosome staining). For example, in sperm with an intact acrosome, PLC ζ /PLCZ1 was localized mainly to the acrosome (52.9%) and the postacrosomal region (29.1%) (**Supplementary Figure 2**). In general,

a wide range of PLC ζ /PLCZ1 localization patterns were observed, with no significant differences between groups (**Supplementary Figure 3** and **Supplementary Table III**).

No significant differences were observed in PLC ζ /PLCZ1 localization when comparing OAF patients carrying a mutation with *wild-type* OAF patients and controls (**Figure 2**; $p > 0.05$).

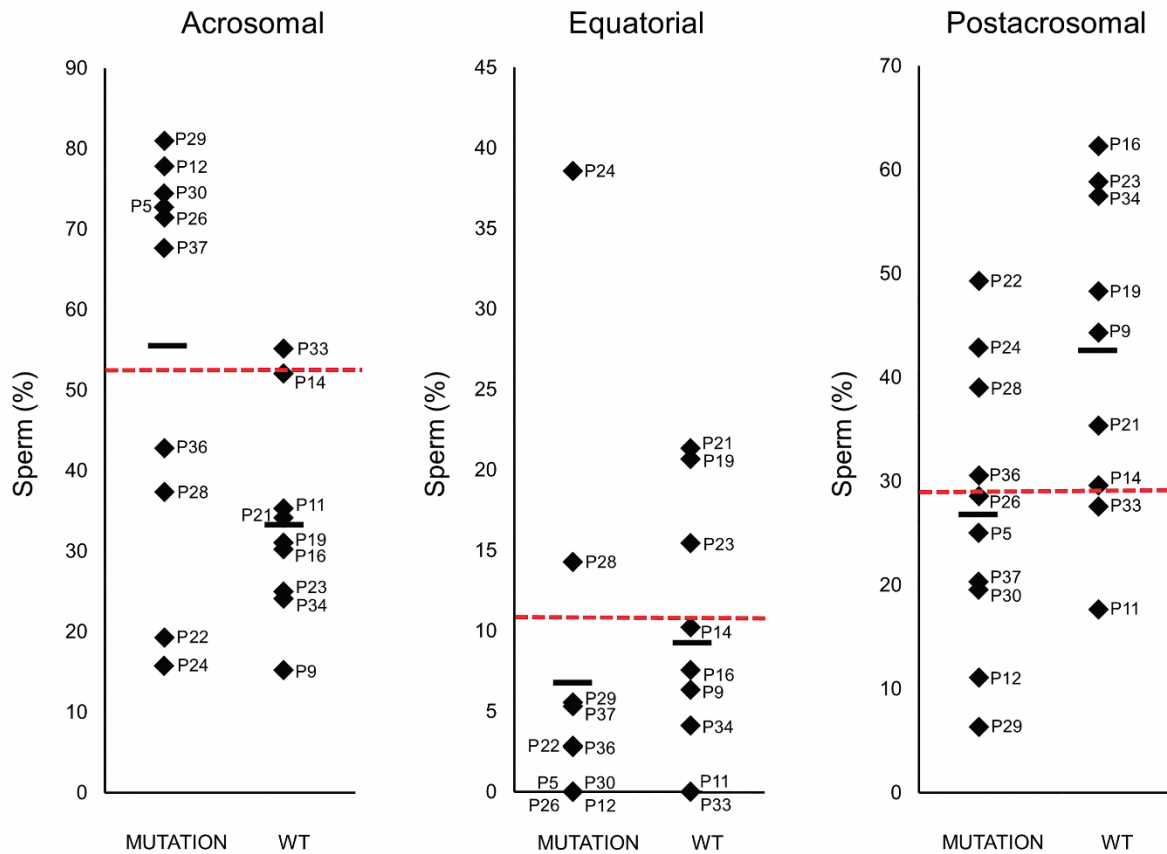


Figure 2. Percentage of sperm with an intact acrosome presenting acrosomal, equatorial and postacrosomal PLC ζ /PLCZ1 localization in OAF patients with and without *PLCZ1* mutations. Immunofluorescent analysis was performed. Red dotted line indicates the mean percentage obtained for the control group. WT: *wild type*.

PLC ζ /PLCZ1 protein levels were analyzed in 19 of the 37 FF patients, and in all the controls ($n=13$) by Western blot. In general, samples analyzed displayed a wide range of PLC ζ /PLCZ1 levels. No significant differences were observed in mean PLC ζ /PLCZ1 protein quantity between the control group (0.58 ± 0.49) and patients presenting FF (0.78 ± 0.47 and 0.63 ± 0.49 , for OAF and no-OAF respectively) (**Supplementary Figure 4** and **Supplementary Figure 5**).

In silico analysis

Bioinformatics modelling showed that V326K fs*25 generates a stop codon 25 residues downstream of the mutated amino acid, and results in a truncated protein at the X-Y linker region missing both the Y- and C2-domains (**Figure 3A**). Phyre2 could successfully build 3D models for all PLC ζ /PLCZ1 variants, all of them with >97% residues covered and >90% confidence. The MODICT algorithm predicted four of the point mutations to be detrimental for PLC ζ /PLCZ1 function (p.H233L, p.S500L, p.L224P and p.R197H), while p.I120M was predicted to have no effect (**Supplementary Figure 6**).

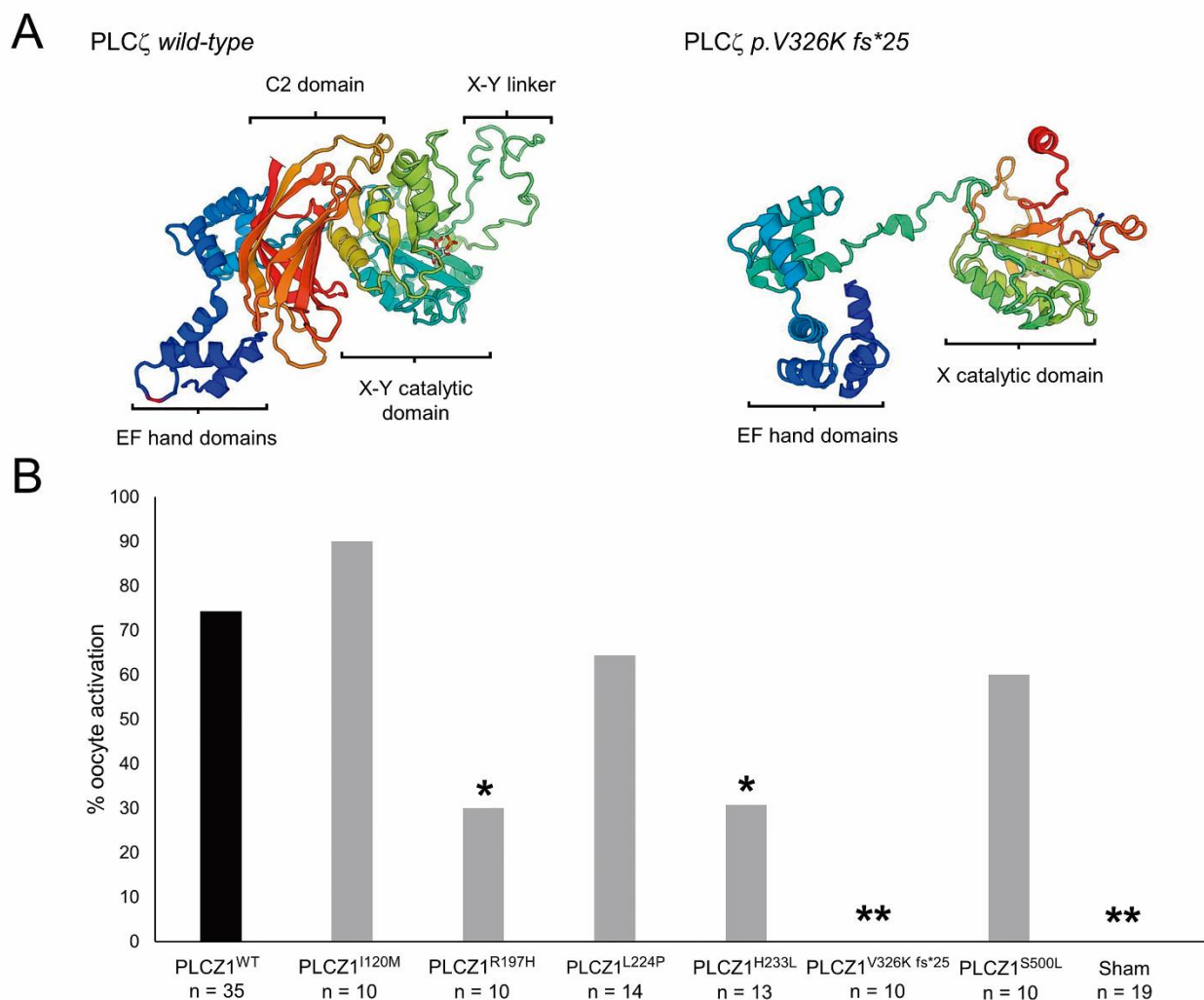


Figure 3. Functional characterization of PLC ζ /PLCZ1 mutations. (A) Three-dimensional protein structure models for PLC ζ /PLCZ1 *wild type* and frameshift p.V326K fs*25 mutant, generated by SWISS-MODEL. The structures are rainbow coloured with blue at the N-terminal, gradually changing to red at C-terminal. (B) Percentage of activated oocytes observed after cRNA injection of *PLCZ1 wild-type*, *PLCZ1* mutants (p.I120M, p.R197H, p.L223P, p.H233L, p.V326Kfs*25, and p.S500L) and sham injection. Chi-Square test: *, $p < 0.05$; **, $p < 0.0001$.

Functional assays of *PLCZ1* mutations

cRNA was synthesized for *PLCZ1* wild-type and all six mutants described in **Table II**. In total, 156 human *in vitro* matured MII oocytes were injected (≥ 10 for each mutation, 135 with cRNA, and 21 sham-injected). We observed 28 oocytes (17.95%) lysed during or shortly after injection, equally distributed among experiments, and these were discarded. As shown in **Figure 3B**, sham injection did not result in oocyte activation. Injection of *PLCZ1*^{WT} cRNA resulted in a high percentage of oocyte activation (74.29%, 26/35). Three *PLCZ1* mutations resulted in a significantly lower percentage of oocyte activation: p.R197H (30%, 3/10), p.H233L (30.77%, 4/13), and the frameshift mutation p.V326K fs*25, which resulted in total failure (0%, 0/10) to trigger oocyte activation. On the other hand, three mutations did not result in a significant decrease of PLC ζ /PLCZ1 activity: p.I120M (90%, 9/10), p.L224P (64.29%, 9/14) and p.S500L (60%, 6/10) (**Figure 3B**).

Table III. Clinical intervention by AOA use and reproductive outcomes of patients with presence of *PLCZ1* gene sequence mutations in ICSI cycles following fertilization failure. FF; Fertilization Failure. AOA; Assisted Oocyte Activation. ET; Embryo Transfer. NA; not applicable

Patient	PLCZ1 mutation	Oocyte source	Fertilization FF cycle/s	Cycle post-FF	Fertilization cycle post-FF	Reproductive outcome
P5	p.R197H p.S500L	Donor	0/7	Donor oocytes- AOA	9/12	Live Birth
P8	p.H233L	Partner	0/2, 0/5	NA	NA	NA
P12	p.V326K fs*25	Donor	0/5	Donor oocytes - AOA	6/9	Live Birth
P22	p.S500L	Partner	0/11, 0/2, 0/3, 2/3	Donor oocytes - AOA	3/11	Live Birth
P24	p.S500L	Partner	0/1, 0/4, 2/3, 0/8, 3/5, 0/7	Donor oocytes - AOA	8/9	Live Birth
P26	p.L224P	Partner	0/5, 1/3	Same gametes	3/4	Live Birth
P27	p.S500L	Donor	1/7	Donor oocytes - AOA	7/9	Live Birth
P28	p.S500L	Partner	0/4	Same gametes - AOA	0/3	No ET
				Donor oocytes - AOA	2/4	Live birth
P29	p.S500L	Partner	0/6, 1/12, 0/13	Same gametes - AOA	6/15	No pregnancy
				Same gametes - AOA	4/6	No pregnancy

AOA treatment for patients with *PLCZ1* mutation

AOA was recommended to patients carrying *PLCZ1* mutations for the next ICSI cycle. Ten out of 13 patients continued ART treatment with AOA (**Table III**). AOA treatment restored fertilization rates (mean FR: 60.48%, range [27-89]), and seven (70%) patients achieved a live birth in the same cycle. AOA was not applied in the post-FF cycle in patient 26, who presented the p.L224P mutation. Interestingly, the second cycle using partner's own oocytes resulted in a good fertilization rate (75%, 3/4) and a live birth.

DISCUSSION

Evidence supporting a crucial role for PLC ζ /PLCZ1 in human oocyte activation has accumulated in the last decade, making it a diagnostic and prognostic marker candidate for FF after ICSI. Nevertheless, while PLC ζ /PLCZ1 has been clearly associated with FF, studies on large cohorts of FF patients are still lacking.

Our study analyzed 37 cases of FF due to either OAF or other reasons (no-OAF). The 25% threshold to define partial FF correspond to a clear minority of fertilized oocytes (one out of four, the minimum number of inseminated oocytes in our study), as well as a cutoff used by several authors in the literature (van der Westerlaken et al., 2005; Yoon et al., 2008; Li et al., 2014). We hypothesized that PLC ζ /PLCZ1 alterations are the main cause of FF due to impaired oocyte activation, while cases with abnormal fertilization could be related to other unknown factors acting in downstream events. By using gene sequencing, we found six mutations (four of which are novel) mapping to relevant domains for PLC ζ /PLCZ1 function, as previously demonstrated using protein chimeras to study discrete protein domains contribution to calcium release in mouse oocytes (Nomikos et al., 2014; Theodoridou et al., 2013). Furthermore, we found that almost 60% of OAF patients included in our study presented *PLCZ1* mutations, in agreement with the role of PLC ζ /PLCZ1 as a SOAF (Saunders et al., 2002).

Our results show that none of the *PLCZ1* mutations detected caused alteration in protein levels or subcellular localization patterns, and confirmed that FF can occur throughout a wide range of PLC ζ /PLCZ1 distributions (and not different from controls), as previously described (Kashir et al., 2013; Ferrer-Vaquero et al., 2016).

In all cases except one (patient 29) the mutations were found in heterozygosis. As transcription in the male germline is completely stopped from spermiogenesis onwards and that genes required for

the correct function of spermatozoa are transcribed earlier during germ cell differentiation (diploid cells), translationally repressed, and finally translated (reviewed in Kleene, 2013), our observations suggested haploinsufficiency for PLC ζ /PLCZ1. As a consequence, mutations found in heterozygosis would reduce the amount of functional protein across total levels (which seemed to be not altered) in all sperm, and be sufficient to cause FF after ICSI.

PLC ζ /PLCZ1 is composed of two main regions, which have different functions and can be distinguished in the protein 3D structure: the catalytic domain (composed of X- and Y-domains), and the regulatory region (including EF-hands and C2- domains). This information needs to be considered when analyzing the effect of the identified mutations on protein function, as tested by *in silico* analysis and cRNA injection into human oocytes after IVM.

Point mutations found in the catalytic domain of PLC ζ /PLCZ1 would be expected to affect enzymatic activity with high probability. One of the mutations detected in our study, p.H233L, was found in heterozygosis (P8) and resulted in a complete inability to activate oocytes (n=7) after ICSI, showing total OAF; these results are in agreement with a previous report (Kashir et al., 2012). We found two additional mutations in the X-domain of PLC ζ /PLCZ1 (P5 (p.R197H) and P26 (p.L224P)), both of them potentially detrimental according to *in silico* predictions. Functional analysis confirmed that p.R197H decreases oocyte activation significantly. When analyzing the 3D model, we observed that this specific residue (R197) is part of a beta sheet near the catalytic core of the enzyme. Conversely, p.L224P may not have such a clear effect on enzymatic function, as its cRNA presented an oocyte activation rate comparable to the *wild type*. This specific leucine (L224) is not associated with a defined secondary structure and allocates outside the catalytic center of the protein.

Focusing on regulatory domains of PLC ζ /PLCZ1, two missense variants were found. One of them, p.I120M, mapping at the C-terminus end of EF-hand domains, does not affect PLC ζ /PLCZ1 ability to trigger oocyte activation by both *in silico* and functional analysis. Nonetheless, this particular patient (P30) underwent two cycles of total FF (0/8; 0/10), suggesting an alternative underlying cause, perhaps related to the critical role of this domain for regulating the high Ca²⁺ sensitivity of PLC ζ /PLCZ1. Although this specific point mutation has no effect on oocyte activation, the fact that this patient could not properly activate his partner's oocytes could be due in part to decreases in egg endoplasmic reticulum Ca²⁺ stores with time after ovulation (Jones and Whittingham, 1996; Takahashi et al., 2009). Another explanation could be the presence of alterations in distal regulatory regions of *PLCZ1* gene or in other sperm mechanisms related to fertilization.

The second missense variant, p.S500L, maps to the C2-domain, which interacts with intracellular vesicles containing the PLC ζ /PLCZ1 substrate PI(4,5)P₂. This mutation was found in nine patients experiencing FF, eight of which presented OAF. In one patient (P29), homozygosity correlated with severe FF in three cycles (0/6, 1/12, 0/13), consistent with a previous report that sperm homozygous for this mutation failed to trigger calcium oscillations when injected into mouse oocytes (Yoon et al., 2008). *In silico* analysis predicted a detrimental effect for this mutation, while functional analysis, by injection of 0.1 mg/ml of p.S500L, resulted in a non-significant decrease in oocyte activation rate compared to *wild-type* PLCZ1. Similar results were obtained for a previously described mutation in homozygosity (p.I489F) in C2-domain, which resulted in diminished oocyte activation if injected at physiological levels, but normal activation if higher levels of cRNA were injected (Nomikos et al., 2017) in mouse oocytes. We used *in vitro* matured human oocytes for the injection test and the cRNA concentration that is known to activate oocytes when injecting wild-type cRNA (Yamaguchi et al., 2017), however, we cannot exclude the possibility that this amount of cRNA exceeds physiological levels in human oocytes.

Altogether, these results suggest that point mutations in EF-hand and C2 domains of PLC ζ /PLCZ1 could affect its regulatory capability. Further studies on binding specificity, calcium dependence, and regulation ability are required to understand the physiological significance of point mutations in the EF-hand and C2 domains of PLC ζ /PLCZ1.

In addition, in the present study we have reported a new mutation produced by deletion of two nucleotides in exon 9. This mutation causes a frameshift, which in turn generates a premature stop codon (p.V326K fs*25) at the X-Y linker, resulting in loss of the Y and C2 domains, and severely disrupting the catalytic function of PLC ζ /PLCZ1. The patient suffered total FF and concordantly, injection of p.V326K fs*25 cRNA into oocytes totally failed to induce activation.

AOA is currently used to overcome FF cases. While its efficacy and safety are still debated (Vanden Meerschaut et al., 2012; Sfontouris et al., 2015), children born after AOA do not seem to present long-term consequences (D'Haeseleer et al., 2014; Vanden Meerschaut et al., 2014; Deemeh et al., 2015). Recent data indicates that AOA does not benefit patients whose sperm shows a normal capacity to generate calcium oscillations in the oocyte (Ferrer-Buitrago et al., 2018). Our results show that PLCZ1 gene sequence analysis could help in identifying cases carrying a deleterious genetic mutation, providing a basis to recommend AOA.

We recognize some limitations of our study. We cannot exclude the possibility that some of the FF cases included are caused by an oocyte-related problem, especially in those FF cases using partner oocytes, and where subsequently a good FR was obtained with donated oocytes. Moreover, we

used *in vitro* matured MII oocytes for the cRNA injection tests, and IVM is a process that may affect the calcium oscillation pattern (Nikiforaki et al., 2014). However, it is exceedingly difficult to gather *in vivo* matured MII for research purposes, as those oocytes are invariably (and rightly) reserved for reproductive treatment.

Overall, our results confirm the essential role of PLC ζ /PLCZ1 in human oocyte activation, and indicate that *PLCZ1* mutations are diverse and frequent in patients experiencing OAF. As observed, *PLCZ1* mutations are likely to reduce the ability of sperm to fertilize the egg, generating infertility or subfertility in some cases. Therefore, *PLCZ1* gene sequencing can represent a useful diagnostic marker, and should be recommended to patients experiencing OAF.

ACKNOWLEDGMENTS

We would like to thank the laboratory staff from Clínica Eugin for their help in sample handling, Désirée García for statistical support, and Gustavo Tiscornia for critical revision of the manuscript.

AUTHOR'S ROLES

M.T-M., D.C-B., M.B.: study design, experimental procedures, data collection and analysis, results interpretation and manuscript preparation. M.D. cRNA injection experiments, manuscript discussion. A.F-V: experimental procedures, data collection, manuscript discussion. F.Z.: *in silico* analysis and manuscript critical discussion. A.R.: expert knowledge, critical discussion. R.O.: study supervision and manuscript discussion. R.V.: study implementation and supervision, expert knowledge, manuscript preparation.

FUNDING

This work was supported by intramural funding of Clínica EUGIN, by the Secretary for Universities and Research of the Ministry of Economy and Knowledge of the Government of Catalonia (GENCAT 2015 DI 049 to M. T-M and GENCAT 2015 DI 048 to D. C-B), and by the Torres Quevedo Program from the Spanish Ministry of Economy and Competitiveness to A. F-V.

CONFLICT OF INTEREST

No competing interest declared.

REFERENCES

D'Haeseleer E, Vanden Meerschaut F, Bettens K, Luyten A, Gysels H, Thienpont Y, De Witte G, Heindryckx B, Oostra A, Roeyers H et al. Language development of children born following

- intracytoplasmic sperm injection (ICSI) combined with assisted oocyte activation (AOA). *Int J Lang Commun Disord* 2014; **49**:702-709.
- Deemeh MR, Tavalae M, Nasr-Esfahani MH. Health of children born through artificial oocyte activation: a pilot study. *Reprod Sci* 2015; **22**:322-328.
- Ducibella T, Huneau D, Angelichio E, Xu Z, Schultz RM, Kopf GS, Fissore R, Madoux S, Ozil JP. Egg-to-embryo transition is driven by differential responses to Ca(2+) oscillation number. *Dev Biol* 2002; **250**:280-291.
- Durban M, Barragan M, Colodron M, Ferrer-Buitrago M, De Sutter P, Heindryckx B, Vernaev V, Vassena R. PLCzeta disruption with complete fertilization failure in normozoospermia. *J Assist Reprod Genet* 2015; **32**:879-886.
- Escoffier J, Lee HC, Yassine S, Zouari R, Martinez G, Karaouzene T, Coutton C, Kherraf ZE, Halouani L, Triki C et al. Homozygous mutation of PLCZ1 leads to defective human oocyte activation and infertility that is not rescued by the WW-binding protein PAWP. *Hum Mol Genet* 2016; **25**:878-891.
- Ferrer-Buitrago M, Dhaenens L, Lu Y, Bonte D, Vanden Meerschaut F, De Sutter P, Leybaert L, Heindryckx B. Human oocyte calcium analysis predicts the response to assisted oocyte activation in patients experiencing fertilization failure after ICSI. *Hum Reprod* 2018; **33**:416-425.
- Ferrer-Vaquer A, Barragan M, Freour T, Vernaev V, Vassena R. PLCzeta sequence, protein levels, and distribution in human sperm do not correlate with semen characteristics and fertilization rates after ICSI. *J Assist Reprod Genet* 2016; **33**:747-756.
- Flaherty SP, Payne D, Matthews CD. Fertilization failures and abnormal fertilization after intracytoplasmic sperm injection. *Hum Reprod* 1998; **13 Suppl 1**:155-164.
- Grasa P, Coward K, Young C, Parrington J. The pattern of localization of the putative oocyte activation factor, phospholipase C zeta, in uncapacitated, capacitated, and ionophore-treated human spermatozoa. *Hum Reprod* 2008; **23**:2513-2522.
- Hachem A, Godwin J, Ruas M, Lee HC, Ferrer Buitrago M, Ardestani G, Bassett A, Fox S, Navarrete F, de Sutter P et al. PLCzeta is the physiological trigger of the Ca(2+) oscillations that induce embryogenesis in mammals but conception can occur in its absence. *Development* 2017; **144**:2914-2924.
- Heytens E, Parrington J, Coward K, Young C, Lambrecht S, Yoon SY, Fissore RA, Hamer R, Deane CM, Ruas M et al. Reduced amounts and abnormal forms of phospholipase C zeta (PLCzeta) in spermatozoa from infertile men. *Hum Reprod* 2009; **24**:2417-2428.
- Jones KT, Whittingham DG. A comparison of sperm- and IP3-induced Ca²⁺ release in activated and aging mouse oocytes. *Dev Biol* 1996; **178**:229-237.
- Kashir J, Jones C, Lee HC, Rietdorf K, Nikiforaki D, Durrans C, Ruas M, Tee ST, Heindryckx B, Galione A et al. Loss of activity mutations in phospholipase C zeta (PLCzeta) abolishes calcium oscillatory ability of human recombinant protein in mouse oocytes. *Hum Reprod* 2011; **26**:3372-3387.
- Kashir J, Konstantinidis M, Jones C, Lemmon B, Lee HC, Hamer R, Heindryckx B, Deane CM, De Sutter P, Fissore RA et al. A maternally inherited autosomal point mutation in human phospholipase C zeta (PLCzeta) leads to male infertility. *Hum Reprod* 2012; **27**:222-231.
- Kashir J, Jones C, Mounce G, Ramadan WM, Lemmon B, Heindryckx B, de Sutter P, Parrington J, Turner K, Child T et al. Variance in total levels of phospholipase C zeta (PLC-zeta) in human sperm may limit the applicability of quantitative immunofluorescent analysis as a diagnostic indicator of oocyte activation capability. *Fertil Steril* 2013; **99**:107-117.
- Kelley LA, Mezulis S, Yates CM, Wass MN, Sternberg MJ. The Phyre2 web portal for protein modeling, prediction and analysis. *Nat Protoc* 2015; **10**:845-858.
- Kleene KC. Connecting cis-elements and trans-factors with mechanisms of developmental regulation of mRNA translation in meiotic and haploid mammalian spermatogenic cells. *Reproduction* 2013; **146**:R1-19.

- Kline D, Kline JT. Repetitive calcium transients and the role of calcium in exocytosis and cell cycle activation in the mouse egg. *Dev Biol* 1992; **149**:80-89.
- Kouchi Z, Shikano T, Nakamura Y, Shirakawa H, Fukami K, Miyazaki S. The role of EF-hand domains and C2 domain in regulation of enzymatic activity of phospholipase C ζ . *J Biol Chem* 2005; **280**:21015-21021.
- Li LJ, Zhang FB, Liu SY, Tian YH, Le F, Wang LY, Lou HY, Xu XR, Huang HF, Jin F. Human sperm devoid of germinal angiotensin-converting enzyme is responsible for total fertilization failure and lower fertilization rates by conventional in vitro fertilization. *Biol Reprod* 2014; **90**:125.
- Li Z, Wang AY, Bowman M, Hammarberg K, Farquhar C, Johnson L, Safi N, Sullivan EA. ICSI does not increase the cumulative live birth rate in non-male factor infertility. *Hum Reprod* 2018; **33**:1322-1330.
- Neri QV, Lee B, Rosenwaks Z, Machaca K, Palermo GD. Understanding fertilization through intracytoplasmic sperm injection (ICSI). *Cell calcium* 2014; **55**:24-37.
- Nikiforaki D, Vanden Meerschaut F, Qian C, De Croo I, Lu Y, Deroo T, Van den Abbeel E, Heindryckx B, De Sutter P. Oocyte cryopreservation and in vitro culture affect calcium signalling during human fertilization. *Hum Reprod* 2014; **29**:29-40.
- Nomikos M, Elgmati K, Theodoridou M, Calver BL, Nounesis G, Swann K, Lai FA. Phospholipase C ζ binding to PtdIns(4,5)P₂ requires the XY-linker region. *J Cell Sci* 2011; **124**:2582-2590.
- Nomikos M, Theodoridou M, Elgmati K, Parthimos D, Calver BL, Buntwal L, Nounesis G, Swann K, Lai FA. Human PLC ζ exhibits superior fertilization potency over mouse PLC ζ in triggering the Ca(2+) oscillations required for mammalian oocyte activation. *Mol Hum Reprod* 2014; **20**:489-498.
- Nomikos M, Stamatiadis P, Sanders JR, Beck K, Calver BL, Buntwal L, Lofty M, Sideratou Z, Swann K, Lai FA. Male infertility-linked point mutation reveals a vital binding role for the C2 domain of sperm PLC ζ . *Biochem J* 2017; **474**:1003-1016.
- Nozawa K, Satouh Y, Fujimoto T, Oji A, Ikawa M. Sperm-borne phospholipase C zeta-1 ensures monospermic fertilization in mice. *Sci Rep* 2018; **8**:1315.
- Rawe VY, Olmedo SB, Nodar FN, Doncel GD, Acosta AA, Vitullo AD. Cytoskeletal organization defects and abortive activation in human oocytes after IVF and ICSI failure. *Mol Hum Reprod* 2000; **6**:510-516.
- Rogers NT, Hobson E, Pickering S, Lai FA, Braude P, Swann K. Phospholipase C ζ causes Ca²⁺ oscillations and parthenogenetic activation of human oocytes. *Reproduction* 2004; **128**:697-702.
- Sanders JR, Ashley B, Moon A, Woolley TE, Swann K. PLC ζ Induced Ca(2+) Oscillations in Mouse Eggs Involve a Positive Feedback Cycle of Ca(2+) Induced InsP₃ Formation From Cytoplasmic PIP₂. *Front Cell Dev Biol* 2018; **6**:36.
- Sang Q, Li B, Kuang Y, Wang X, Zhang Z, Chen B, Wu L, Lyu Q, Fu Y, Yan Z et al. Homozygous Mutations in WEE2 Cause Fertilization Failure and Female Infertility. *Am J Hum Genet* 2018; **102**:649-657.
- Saunders CM, Larman MG, Parrington J, Cox LJ, Royse J, Blayney LM, Swann K, Lai FA. PLC zeta: a sperm-specific trigger of Ca(2+) oscillations in eggs and embryo development. *Development* 2002; **129**:3533-3544.
- Sfontouris IA, Nastri CO, Lima ML, Tahmasbpourmarzouni E, Raine-Fenning N, Martins WP. Artificial oocyte activation to improve reproductive outcomes in women with previous fertilization failure: a systematic review and meta-analysis of RCTs. *Hum Reprod* 2015; **30**:1831-1841.
- Takahashi T, Igarashi H, Kawagoe J, Amita M, Hara S, Kurachi H. Poor embryo development in mouse oocytes aged in vitro is associated with impaired calcium homeostasis. *Biol Reprod* 2009; **80**:493-502.
- Tanyalcin I, Stouffs K, Daneels D, Al Assaf C, Lissens W, Jansen A, Gheldof A. Convert your favorite protein modeling program into a mutation predictor: "MODICT". *BMC Bioinformatics* 2016; **17**:425.

Theodoridou M, Nomikos M, Parthimos D, Gonzalez-Garcia JR, Elgmati K, Calver BL, Sideratou Z, Nounesis G, Swann K, Lai FA. Chimeras of sperm PLCzeta reveal disparate protein domain functions in the generation of intracellular Ca²⁺ oscillations in mammalian eggs at fertilization. *Mol Hum Reprod* 2013; **19**:852-864.

Vanden Meerschaut F, Nikiforaki D, De Gheselle S, Dullaerts V, Van den Abbeel E, Gerris J, Heindryckx B, De Sutter P. Assisted oocyte activation is not beneficial for all patients with a suspected oocyte-related activation deficiency. *Hum Reprod* 2012; **27**:1977-1984.

Vanden Meerschaut F, D'Haeseleer E, Gysels H, Thienpont Y, Dewitte G, Heindryckx B, Oostra A, Roeyers H, Van Lierde K, De Sutter P. Neonatal and neurodevelopmental outcome of children aged 3-10 years born following assisted oocyte activation. *Reprod Biomed Online* 2014; **28**:54-63.

van der Westerlaken L, Helmerhorst F, Dieben S, Naaktgeboren N. Intracytoplasmic sperm injection as a treatment for unexplained total fertilization failure or low fertilization after conventional in vitro fertilization. *Fertil Steril* 2005; **83**:612-7.

WHO. World Health Organization. WHO laboratory manual for the examination and processing of human semen. Fifth edition, 2010. 2010.

Xu D, Zhang Y. Improving the physical realism and structural accuracy of protein models by a two-step atomic-level energy minimization. *Biophys J* 2011; **101**:2525-2534.

Yamaguchi T, Ito M, Kuroda K, Takeda S, Tanaka A. The establishment of appropriate methods for egg-activation by human PLCZ1 RNA injection into human oocyte. *Cell calcium* 2017; **65**:22-30.

Yeste M, Jones C, Amdani SN, Patel S, Coward K. Oocyte activation deficiency: a role for an oocyte contribution? *Hum Reprod Update* 2016; **22**:23-47.

Yoon SY, Jellerette T, Salicioni AM, Lee HC, Yoo MS, Coward K, Parrington J, Grow D, Cibelli JB, Visconti PE et al. Human sperm devoid of PLC, zeta 1 fail to induce Ca(2+) release and are unable to initiate the first step of embryo development. *J Clin Invest* 2008; **118**:3671-3681.

Yoon SY, Eum JH, Lee JE, Lee HC, Kim YS, Han JE, Won HJ, Park SH, Shim SH, Lee WS et al. Recombinant human phospholipase C zeta 1 induces intracellular calcium oscillations and oocyte activation in mouse and human oocytes. *Hum Reprod* 2012; **27**:1768-1780.

SUPPLEMENTARY INFORMATION

Supplementary Table I. Primer pairs used for *PLCZ1* site-directed mutagenesis. Point mutations are indicated as red letters.

Mutant	Forward (5'-3')	Reverse (5'-3')
<i>PLCZ1</i> ^{I120M}	ACGAGCCTATGGAAGAAGTTAG	ATTTCTGAATGATCTCAAAGC
<i>PLCZ1</i> ^{R197H}	GAAAGGATGCCATTGTTTGGAGATTG	ACAAGGGCACTTACATATC
<i>PLCZ1</i> ^{L224P}	AAGCAAACCTCCGTTTAAACTGTTATCC	GTGAGTGTGTAGCCATGATATAC
<i>PLCZ1</i> ^{H233L}	CCAAGCTATACTCAAGTATGCATTC	ATAACAGTTTTAAACAGAAGTTTG
<i>PLCZ1</i> ^{V326K fs*25}	GGGTAAAAAAGTTACCTGG	GTTTCCTTGTCTTGATTGTC
<i>PLCZ1</i> ^{S500L}	TACTCATTCACTATCTAACAAAGGTGATTC	AGAGGCAACTGGATACCAC

Supplementary Table II. Main demographic, semen and ICSI cycle/s variables individualized for each man included in the study (37 patients. 13 controls). A: asthenozoospermia; a+b: sperm with progressive motility; BMI: Body Mass Index; C: control; D: donor; Deg: degenerated; FF: fertilization failure; FR: fertilization rate; N: normozoospermia; ND: not determined; O: oligozoospermia; OAF: oocyte activation failure; Pa: partner; PN: pronuclei; T: teratozoospermia.

Patient	GROUP	Male age (years)	Female age (years)	Conc. (million/ml)	Motility (% a+b)	Morphology (% normal)	Volume (ml)	Diagnostic	Male BMI	Oocyte	Oocyte age (years)	N° cycles with FF (n)	Total oocytes (n)	2PN (n)	OAF (n)	IPN + 3PN + >3PN (n)	Deg (n)	FR (%)
P1	OAF	51	45	120.5	44.5	6	4.3	N	27.43	D	24	2	11	0	11	0	0	0.0%
P2	No-OAF	45	42	59.2	70.2	6	6.1	N	25.83	D	32	1	6	0	0	3	3	0.0%
P3	No-OAF	42	42	92.5	44.2	15	6.8	N	27.43	D	22	1	5	1	0	3	1	20.0%
P4	No-OAF	40	43	77.4	64.4	5	2.2	N	30.35	D	35	1	5	0	0	2	3	0.0%
P5	OAF	40	44	9.9	38.9	4	3.2	O	25.96	D	28	1	7	0	7	0	0	0.0%
P6	No-OAF	46	42	7.7	7.3	4	1	OA	ND	Pa	42	1	8	0	2	2	4	0.0%
P7	No-OAF	40	38	117.9	63.3	9	2.2	N	ND	Pa	38	1	4	0	2	2	0	0.0%
P8	OAF	44	44	0.11	14	ND	0.6	OA	ND	Pa	44	2	7	0	6	0	1	0.0%
P9	OAF	50	46	0.57	1	ND	2.9	OA	ND	D	29	1	6	0	5	0	1	0.0%
P10	No-OAF	52	45	24.5	53.8	8	2.1	N	30.48	D	27	1	7	1	1	5	0	14.3%
P11	OAF	49	46	14	19.8	1	3	OAT	26.23	D	30	1	11	2	7	0	2	18.2%
P12	OAF	36	39	35.1	29.6	5	3	A	22.2	D	28	1	5	0	3	0	2	0.0%
P13	No-OAF	43	38	13.4	67.9	4	4.4	O	29.26	D	23	1	6	1	1	3	1	16.7%
P14	OAF	40	34	142.8	16.1	13	4.2	A	23.66	Pa	34	4	13	2	ND	ND	ND	15.4%
P15	No-OAF	41	41	16.7	51.9	6	4.8	N	23.92	D	32	1	7	1	0	3	3	14.3%
P16	OAF	35	32	14.4	49.7	4	3	O	ND	Pa	32	1	11	1	9	0	1	9.1%
P17	No-OAF	43	48	7.7	64.6	4	6.2	O	22.53	D	34	1	7	0	3	2	2	0.0%
P18	No-OAF	54	50	28.8	52.1	4	2.1	N	25.11	D	22	1	6	1	0	3	2	16.7%
P19	OAF	46	45	22.2	8.6	1	3.8	AT	26.88	D	31	1	6	0	4	0	2	0.0%
P20	No-OAF	42	44	7.4	28.4	5	4.5	OA	ND	D	21	1	7	1	0	1	5	14.3%
P21	OAF	54	45	71	49.5	6	3.2	N	27.43	D	26	1	6	0	1	0	5	0.0%
P22	OAF	34	27	17.8	23.8	7	4.7	A	22.88	Pa	27	4	17	0	ND	ND	ND	0.0%
P23	OAF	37	32	52.3	35	12	2.6	N	ND	Pa	32	3	28	2	ND	ND	ND	7.1%
P24	OAF	47	43	57.7	25	4	6.8	A	ND	Pa	43	6	30	5	ND	ND	ND	16.7%
P25	No-OAF	43	45	26	5.9	7	10.7	A	24.93	D	22	1	6	1	1	2	2	16.7%
P26	OAF	35	31	6.6	27.4	5	4.1	OA	ND	Pa	31	2	8	1	ND	ND	ND	12.5%
P27	No-OAF	34	45	26.8	22.3	6	2	A	25.25	D	28	1	7	1	2	3	1	14.3%

Supplementary Table II (cont.).

Patient	GROUP	Male age (years)	Female age (years)	Conc. (million/ml)	Motility (% a+b)	Morphology (% normal)	Volume (ml)	Diagnostic	Male BMI	Oocyte	Oocyte age (years)	N° cycles with FF (n)	Total oocytes (n)	2PN (n)	OAF (n)	IPN + 3PN + >3PN (n)	Deg (n)	FR (%)
P28	OAF	31	41	153.4	58.6	ND	2	N	21.88	Pa	41	1	4	0	4	0	0	0.0%
P29	OAF	42	36	168.62	72.91	9	4.1	N	22.46	Pa	36	3	31	1	ND	ND	ND	3.2%
P30	OAF	34	34	11.29	19.13	4	3.4	OA	24.02	Pa	34	2	18	0	ND	ND	ND	0.0%
P31	No-OAF	51	42	98.67	62.82	12	1.8	N	24.54	D	29	1	5	1	2	1	1	20.0%
P32	OAF	43	42	1.02	5.88	ND	5.6	OA	23.66	Pa/D	36	3	14	3	ND	ND	ND	21.4%
P33	OAF	43	39	39.72	71.68	15	2.8	N	ND	Pa	39	2	5	0	ND	ND	ND	0.0%
P34	OAF	39	37	125.05	81.3	12	5.1	N	22.35	Pa	37	5	43	1	ND	ND	ND	2.3%
P35	No-OAF	38	41	35.41	34.26	3	4.4	T	ND	Pa	41	1	8	1	2	3	2	12.5%
P36	OAF	39	35	49.47	32.95	7	2.3	N	26.26	D	28	1	7	1	6	0	0	14.3%
P37	OAF	35	34	190.96	87.12	4	6.4	N	24.49	Pa	35	3	9	0	ND	ND	ND	0.0%
D1	C	24	32	45	13.11	ND	ND	ND	22.87	Pa	32	1	8	6	0	1	1	75.0%
D2	C	30	47	75.3	10.62	ND	ND	ND	22.89	D	19	1	7	6	1	0	0	85.7%
D3	C	21	42	28.8	29.51	ND	ND	ND	25.08	D	25	1	6	4	1	1	0	66.7%
D4	C	21	41	30.8	19.16	ND	ND	ND	23.48	Pa	41	1	3	2	1	0	0	66.7%
D5	C	19	39	53.3	13.7	ND	ND	ND	23.66	D	22	1	6	4	0	1	1	66.7%
D6	C	ND	46	46.5	35.7	ND	ND	ND	ND	D	23	1	9	9	0	0	0	100%
D7	C	20	43	40.4	18.07	ND	ND	ND	24.56	D	30	1	8	5	0	0	3	62.5%
D8	C	21	43	42.3	13	ND	ND	ND	23.35	D	32	1	9	9	0	0	0	100%
D9	C	33	39	51.1	15.46	ND	ND	ND	27.11	D	31	1	7	6	0	1	0	85.7%
D10	C	19	44	35.3	5.95	ND	ND	ND	23.3	D	34	1	12	7	1	0	4	58.3%
D11	C	34	39	52.8	9.47	ND	ND	ND	23.33	D	31	1	10	8	1	0	1	80.0%
D12	C	27	39	85.6	23.48	ND	ND	ND	22.99	D	27	1	6	6	0	0	0	100%
D13	C	ND	50	63.4	28.08	ND	ND	ND	26.3	D	25	1	7	4	0	0	3	57.1%

Supplementary Table III. Results of the analysis of Phospholipase C zeta 1 subcellular localization by immunofluorescence. All cell and three different acrosomal status (intact, reacted and no acrosome staining) and four different Phospholipase C zeta 1 localizations (acrosomal, equatorial, postacrosomal and no Phospholipase C zeta 1 staining) were considered.

ALL CELLS							
PATIENT	Group	PLCz antibody # lot	Sperm counted	% Acrosomal	% Equatorial	% Postacrosomal	% No staining
P1	OAF	12E1	NA	NA	NA	NA	NA
P2	No-OAF	12E1	304	19,41	21,38	29,93	29,28
P3	No-OAF	12E1	309	34,30	22,65	34,95	8,09
P4	No-OAF	12E1	313	37,06	24,60	25,88	12,46
P5	OAF	12E1	212	16,51	2,83	52,83	27,83
P6	No-OAF	12E1	368	15,49	15,22	39,13	30,16
P7	No-OAF	12E1	337	16,32	4,45	33,23	45,99
P8	OAF	14F2	NA	NA	NA	NA	NA
P9	OAF	14F2	169	8,28	4,73	36,69	50,30
P10	No-OAF	14F2	376	32,98	8,78	41,76	18,62
P11	OAF	14F2	115	5,22	3,48	12,17	79,13
P12	OAF	14F2	67	26,87	0,00	28,36	44,78
P13	No-OAF	14F2	348	21,84	7,18	35,92	35,06
P14	OAF	14F2	254	24,41	17,32	57,48	16,54
P15	No-OAF	14F2	357	19,33	9,24	42,86	29,97
P16	OAF	14F2	136	12,50	6,62	77,94	2,94
P17	No-OAF	14F2	121	20,66	17,36	59,50	2,48
P18	No-OAF	14F2	219	21,92	11,87	63,01	3,20
P19	OAF	14F2	98	13,27	11,22	75,51	0,00
P20	No-OAF	14F2	250	21,60	35,60	42,40	0,40
P21	OAF	14F2	323	18,27	14,24	36,84	30,65
P22	OAF	14F2	372	7,80	1,08	36,02	55,11
P23	OAF	14F2	381	13,81	11,00	63,43	9,21
P24	OAF	14F2	174	6,32	30,46	60,92	2,30
P25	No-OAF	14F2	231	8,66	10,39	67,10	13,85
P26	OAF	14F2	15	33,33	0,00	60,00	6,67
P27	No-OAF	14F2	226	22,12	10,18	56,19	11,50
P28	OAF	14F2	375	18,13	15,47	41,33	25,07
P29	OAF	15J4	310	39,03	4,84	20,32	35,81
P30	OAF	15J4	268	26,49	1,87	41,42	30,22
P31	No-OAF	15J4	353	22,10	3,97	37,39	36,54
P32	OAF	15J4	NA	NA	NA	NA	NA
P33	OAF	15J4	163	34,36	1,84	39,88	23,93
P34	OAF	15J4	381	12,60	2,10	55,64	29,66
P35	No-OAF	15J4	182	17,03	10,99	37,36	34,62
P36	OAF	15J4	368	23,37	1,90	32,61	42,12
P37	OAF	15J4	360	38,89	5,56	29,17	26,39
D1	C	14F2	347	26,80	14,41	40,35	18,73

D2	C	14F2	NA	NA	NA	NA	NA
D3	C	14F2	352	26,99	18,47	38,92	15,63
D4	C	14F2	NA	NA	NA	NA	NA
D5	C	14F2	335	16,42	4,18	61,79	17,61
D6	C	14F2	NA	NA	NA	NA	NA
D7	C	14F2	407	30,22	7,62	35,87	26,29
D8	C	14F2	359	37,05	12,26	43,45	7,24
D9	C	14F2	NA	NA	NA	NA	NA
D10	C	14F2	336	18,45	4,46	43,15	33,93
D11	C	14F2	340	22,65	10,88	35,29	31,18
D12	C	14F2	363	22,04	20,66	40,50	16,80
D13	C	14F2	363	19,83	21,49	46,83	9,09

INTACT ACROSOME							
PATIENT	Group	PLCz antibody # lot	Sperm counted	% Acrosomal	% Equatorial	% Postacrosomal	% No staining
P1	OAF	12E1	NA	NA	NA	NA	NA
P2	No-OAF	12E1	77	70,13	7,79	22,08	0,00
P3	No-OAF	12E1	193	51,30	27,98	18,65	2,07
P4	No-OAF	12E1	135	69,63	12,59	15,56	2,22
P5	OAF	12E1	44	72,73	0,00	25,00	2,27
P6	No-OAF	12E1	88	53,41	4,55	39,77	2,27
P7	No-OAF	12E1	90	44,44	3,33	41,11	11,11
P8	OAF	14F2	NA	NA	NA	NA	NA
P9	OAF	14F2	79	15,19	6,33	44,30	34,18
P10	No-OAF	14F2	135	52,41	5,52	34,48	7,59
P11	OAF	14F2	17	35,29	0,00	17,65	47,06
P12	OAF	14F2	18	77,78	0,00	11,11	11,11
P13	No-OAF	14F2	107	64,49	6,54	24,30	4,67
P14	OAF	14F2	98	52,04	10,20	29,59	8,16
P15	No-OAF	14F2	188	30,85	5,85	40,96	22,34
P16	OAF	14F2	53	30,19	7,55	62,26	0,00
P17	No-OAF	14F2	58	39,66	18,97	41,38	0,00
P18	No-OAF	14F2	69	49,28	7,25	43,48	0,00
P19	OAF	14F2	29	31,03	20,69	48,28	0,00
P20	No-OAF	14F2	162	48,72	16,67	34,62	0,00
P21	OAF	14F2	164	34,15	21,34	35,37	9,15
P22	OAF	14F2	140	19,29	2,86	49,29	28,57
P23	OAF	14F2	136	25,00	15,44	58,82	0,74
P24	OAF	14F2	70	15,71	38,57	42,86	2,86
P25	No-OAF	14F2	43	41,86	6,98	41,86	9,30
P26	OAF	14F2	7	71,43	0,00	28,57	0,00
P27	No-OAF	14F2	80	51,25	6,25	36,25	6,25
P28	OAF	14F2	182	37,36	14,29	39,01	9,34

P29	OAF	15J4	126	80,95	5,56	6,35	7,14
P30	OAF	15J4	82	74,39	0,00	19,51	6,10
P31	No-OAF	15J4	175	41,14	6,29	36,00	16,57
P32	OAF	15J4	NA	NA	NA	NA	NA
P33	OAF	15J4	98	55,10	0,00	27,55	17,35
P34	OAF	15J4	195	24,10	4,10	57,44	14,36
P35	No-OAF	15J4	99	29,29	20,20	38,38	12,12
P36	OAF	15J4	180	42,78	2,78	30,56	23,89
P37	OAF	15J4	207	67,63	5,31	20,29	6,76
D1	C	14F2	138	43,48	15,94	32,61	7,97
D2	C	14F2	NA	NA	NA	NA	NA
D3	C	14F2	169	51,48	24,26	18,34	5,92
D4	C	14F2	NA	NA	NA	NA	NA
D5	C	14F2	87	44,83	8,05	37,93	9,20
D6	C	14F2	NA	NA	NA	NA	NA
D7	C	14F2	187	59,02	9,84	21,86	9,29
D8	C	14F2	144	68,75	9,03	21,53	0,69
D9	C	14F2	NA	NA	NA	NA	NA
D10	C	14F2	95	61,05	4,21	24,21	10,53
D11	C	14F2	88	77,27	3,41	13,64	5,68
D12	C	14F2	149	44,97	17,45	35,57	2,01
D13	C	14F2	163	25,15	11,66	56,44	6,75

REACTED ACROSOME							
PATIENT	Group	PLCz antibody # lot	Sperm counted	% Acrosomal	% Equatorial	% Postacrosomal	% No staining
P1	OAF	12E1	NA	NA	NA	NA	NA
P2	No-OAF	12E1	69	1,45	14,49	50,72	33,33
P3	No-OAF	12E1	62	11,29	19,35	59,68	9,68
P4	No-OAF	12E1	29	0,00	17,24	55,17	27,59
P5	OAF	12E1	69	2,90	8,70	72,46	15,94
P6	No-OAF	12E1	60	1,67	13,33	53,33	31,67
P7	No-OAF	12E1	33	6,06	3,03	60,61	30,30
P8	OAF	14F2	NA	NA	NA	NA	NA
P9	OAF	14F2	18	5,56	5,56	38,89	50,00
P10	No-OAF	14F2	68	5,88	2,94	76,47	14,71
P11	OAF	14F2	20	0,00	10,00	25,00	65,00
P12	OAF	14F2	7	14,29	0,00	57,14	28,57
P13	No-OAF	14F2	97	0,00	14,43	57,73	27,84
P14	OAF	14F2	103	6,80	25,24	55,34	12,62
P15	No-OAF	14F2	73	6,85	15,07	64,38	13,70
P16	OAF	14F2	37	0,00	5,41	94,59	0,00
P17	No-OAF	14F2	30	0,00	16,67	83,33	0,00
P18	No-OAF	14F2	37	5,41	5,41	89,19	0,00

P19	OAF	14F2	98	0,00	0,00	100,00	0,00
P20	No-OAF	14F2	52	22,22	13,89	63,89	0,00
P21	OAF	14F2	42	7,14	14,29	61,90	16,67
P22	OAF	14F2	49	4,08	0,00	46,94	48,98
P23	OAF	14F2	103	0,00	2,91	87,38	9,71
P24	OAF	14F2	46	0,00	26,09	73,91	0,00
P25	No-OAF	14F2	112	1,79	16,07	75,89	6,25
P26	OAF	14F2	5	0,00	0,00	100,00	0,00
P27	No-OAF	14F2	73	4,11	20,55	73,97	1,37
P28	OAF	14F2	83	0,00	27,71	46,99	25,30
P29	OAF	15J4	31	3,23	16,13	32,26	48,39
P30	OAF	15J4	16	0,00	6,25	81,25	12,50
P31	No-OAF	15J4	33	3,03	0,00	66,67	30,30
P32	OAF	15J4	NA	NA	NA	NA	NA
P33	OAF	15J4	20	0,00	15,00	65,00	20,00
P34	OAF	15J4	82	1,22	0,00	74,39	24,39
P35	No-OAF	15J4	24	0,00	0,00	58,33	41,67
P36	OAF	15J4	34	17,65	5,88	41,18	35,29
P37	OAF	15J4	51	0,00	17,65	54,90	27,45
D1	C	14F2	72	13,89	9,72	63,89	12,50
D2	C	14F2	NA	NA	NA	NA	NA
D3	C	14F2	78	5,13	7,69	78,21	8,97
D4	C	14F2	NA	NA	NA	NA	NA
D5	C	14F2	127	2,36	1,57	91,34	4,72
D6	C	14F2	NA	NA	NA	NA	NA
D7	C	14F2	124	7,26	6,45	66,94	19,35
D8	C	14F2	70	7,14	17,14	72,86	2,86
D9	C	14F2	NA	NA	NA	NA	NA
D10	C	14F2	145	0,00	4,83	66,21	28,97
D11	C	14F2	35	2,86	5,71	85,71	5,71
D12	C	14F2	19	5,26	5,26	73,68	15,79
D13	C	14F2	32	21,88	40,63	28,13	9,38

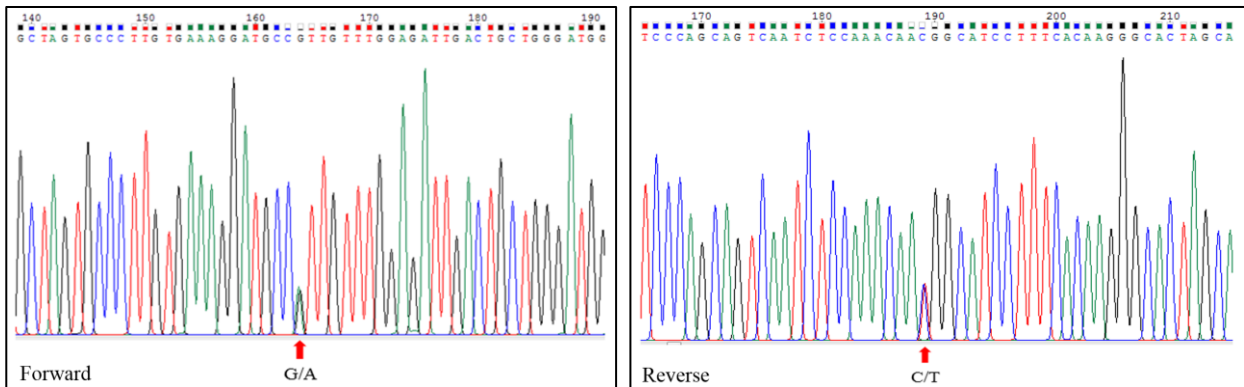
NO ACROSOME STAINING							
PATIENT	Group	PLCz antibody # lot	Sperm counted	% Acrosomal	% Equatorial	% Postacrosomal	% No staining
P1	OAF	12E1	NA	NA	NA	NA	NA
P2	No-OAF	12E1	158	2,53	31,01	24,68	41,77
P3	No-OAF	12E1	54	0,00	7,41	64,81	27,78
P4	No-OAF	12E1	149	14,77	36,91	29,53	18,79
P5	OAF	12E1	99	1,01	0,00	51,52	47,47
P6	No-OAF	12E1	220	4,09	20,00	35,00	40,91
P7	No-OAF	12E1	214	6,07	5,14	25,70	63,08
P8	OAF	14F2	NA	NA	NA	NA	NA

P9	OAF	14F2	72	1,39	2,78	27,78	68,06
P10	No-OAF	14F2	173	25,73	13,45	32,16	28,65
P11	OAF	14F2	78	0,00	2,56	7,69	89,74
P12	OAF	14F2	42	7,14	0,00	30,95	61,90
P13	No-OAF	14F2	144	4,86	2,78	29,86	62,50
P14	OAF	14F2	53	4,30	8,60	64,52	22,58
P15	No-OAF	14F2	96	5,94	10,89	28,71	54,46
P16	OAF	14F2	46	2,17	6,52	82,61	8,70
P17	No-OAF	14F2	33	6,06	15,15	69,70	9,09
P18	No-OAF	14F2	113	10,62	16,81	66,37	6,19
P19	OAF	14F2	48	8,33	10,42	81,25	0,00
P20	No-OAF	14F2	196	5,88	52,21	41,18	0,74
P21	OAF	14F2	117	0,00	4,27	29,91	65,81
P22	OAF	14F2	183	0,00	0,00	22,95	77,05
P23	OAF	14F2	142	14,08	13,38	54,93	17,61
P24	OAF	14F2	58	0,00	24,14	72,41	3,45
P25	No-OAF	14F2	76	0,00	3,95	68,42	27,63
P26	OAF	14F2	3	0,00	0,00	66,67	33,33
P27	No-OAF	14F2	73	8,22	4,11	60,27	27,40
P28	OAF	14F2	110	0,00	8,18	40,91	50,91
P29	OAF	15J4	153	11,76	1,96	29,41	56,86
P30	OAF	15J4	170	5,88	2,35	48,24	43,53
P31	No-OAF	15J4	145	3,45	2,07	32,41	62,07
P32	OAF	15J4	NA	NA	NA	NA	NA
P33	OAF	15J4	45	4,44	0,00	55,56	40,00
P34	OAF	15J4	104	0,00	0,00	37,50	62,50
P35	No-OAF	15J4	59	3,39	0,00	27,12	69,49
P36	OAF	15J4	154	1,95	0,00	33,12	64,94
P37	OAF	15J4	102	0,00	0,00	34,31	65,69
D1	C	14F2	138	16,67	15,22	35,51	32,61
D2	C	14F2	NA	NA	NA	NA	NA
D3	C	14F2	105	3,81	17,14	42,86	36,19
D4	C	14F2	NA	NA	NA	NA	NA
D5	C	14F2	121	10,74	4,13	47,93	37,19
D6	C	14F2	NA	NA	NA	NA	NA
D7	C	14F2	100	6,00	5,00	23,00	66,00
D8	C	14F2	145	20,00	13,10	51,03	15,86
D9	C	14F2	NA	NA	NA	NA	NA
D10	C	14F2	96	4,17	4,17	27,08	64,58
D11	C	14F2	217	3,69	14,75	35,94	45,62
D12	C	14F2	195	6,15	24,62	41,03	28,21
D13	C	14F2	158	15,19	29,11	43,67	12,03

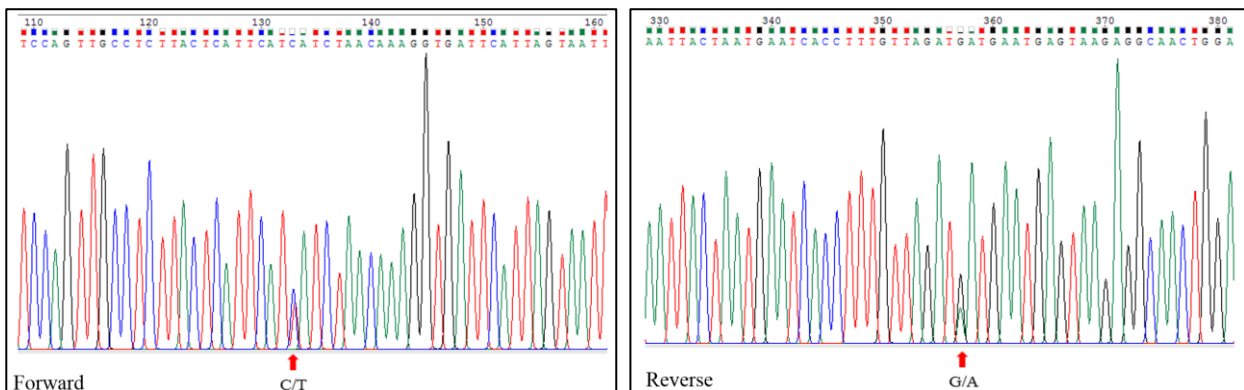
Supplementary Figure 1. Electropherograms showing the nucleotide changes identified by Sanger sequencing in the patients carrying phospholipase C zeta 1 (*PLCZ1*) genetic variants.

Patient 5

c.590 G>A / p.R197H (heterozygosity) – *PLCZ1* exon 6

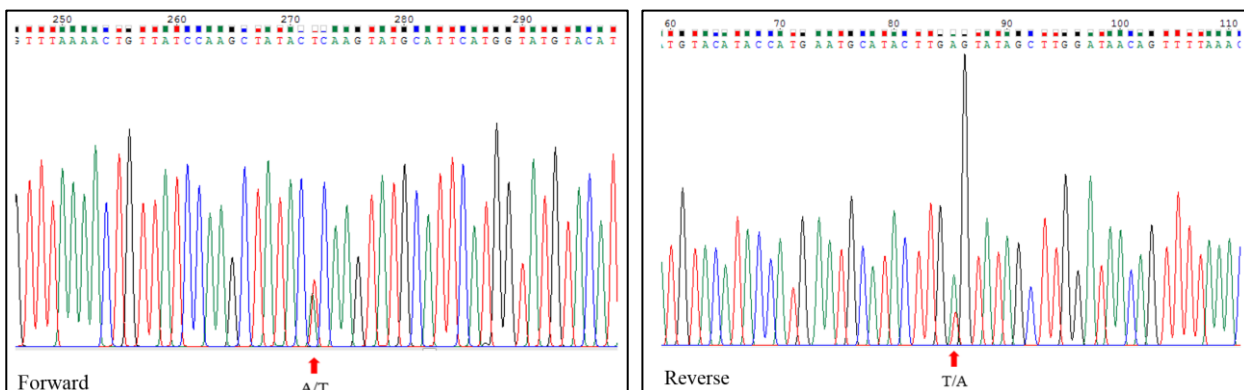


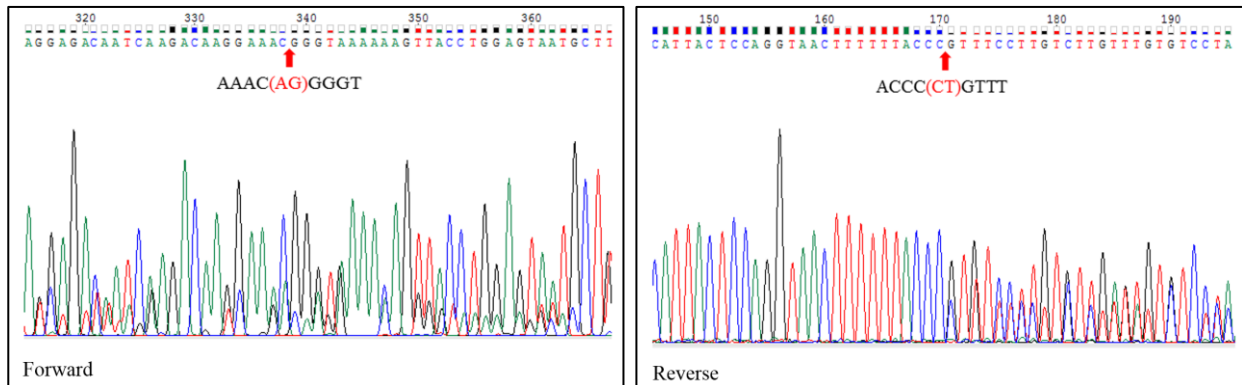
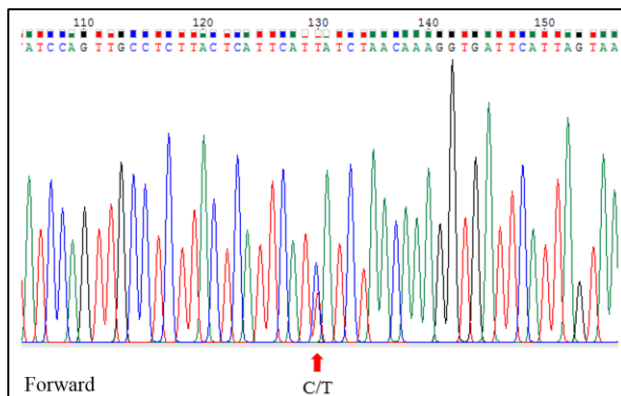
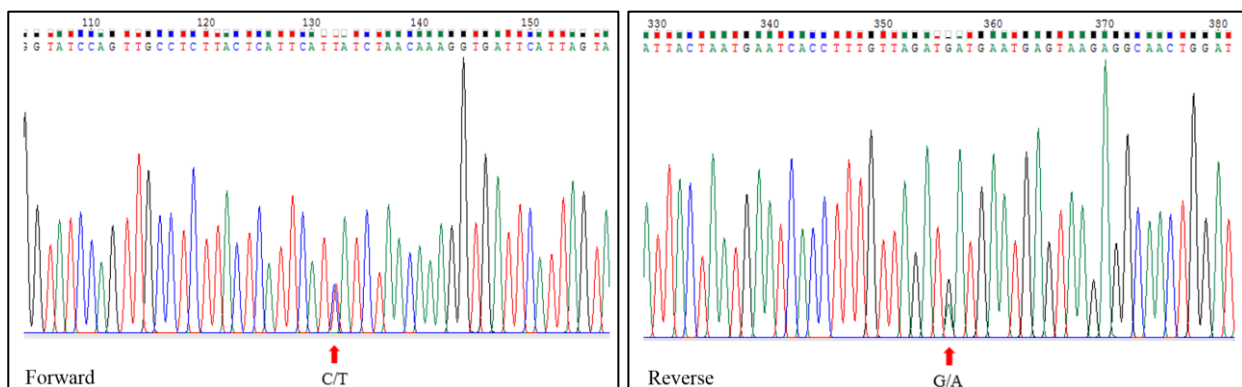
c.1499 C>T / p.S500L (heterozygosity) – *PLCZ1* exon 13

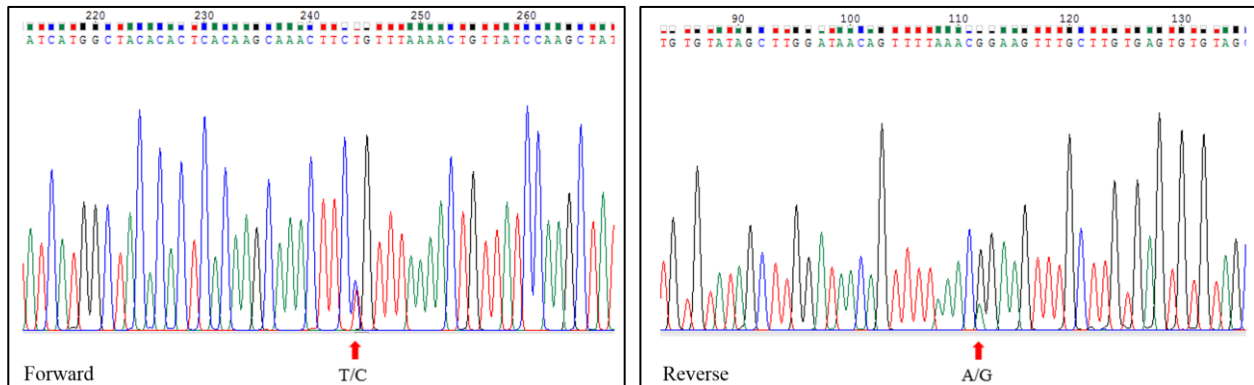
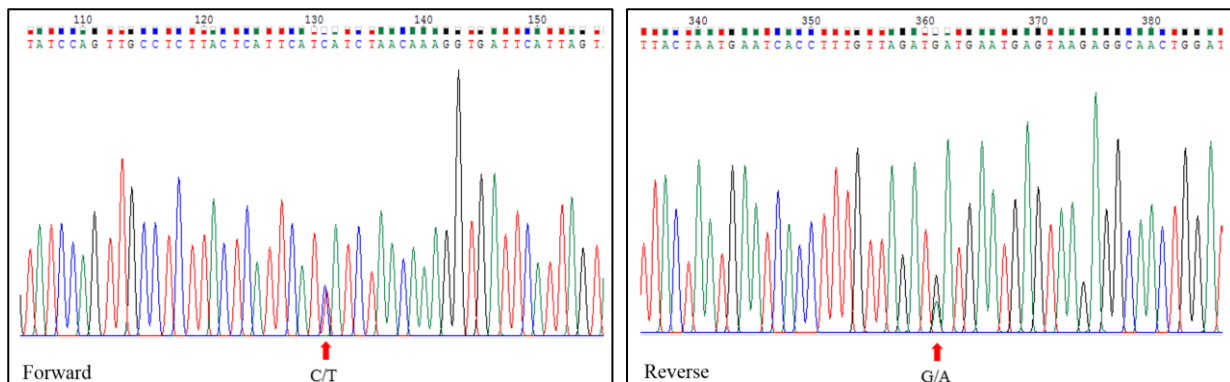
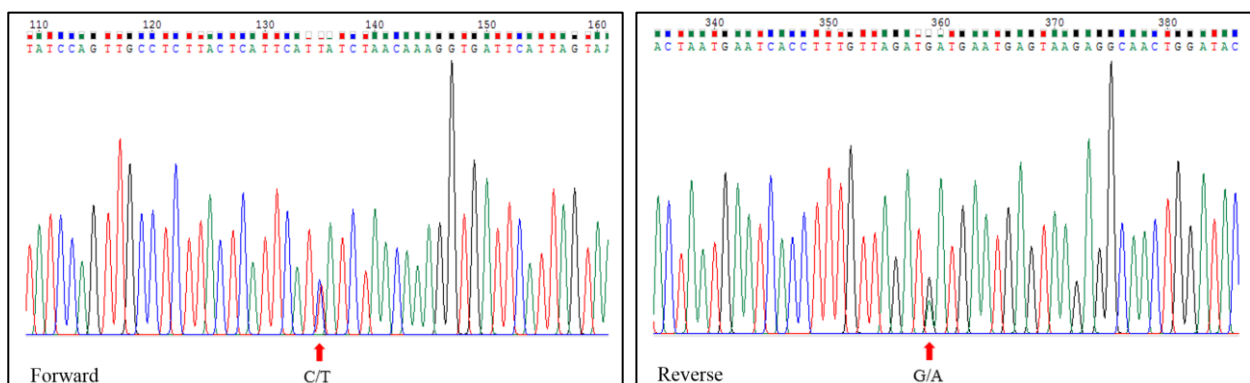


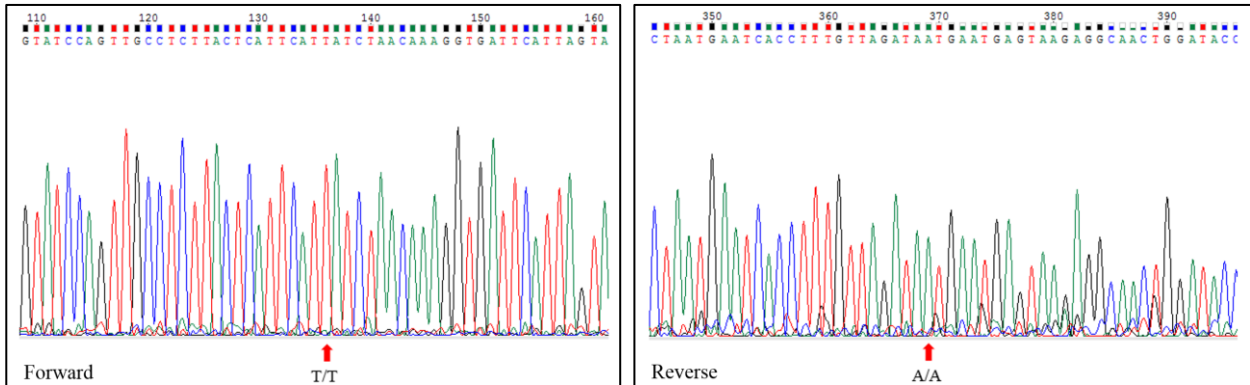
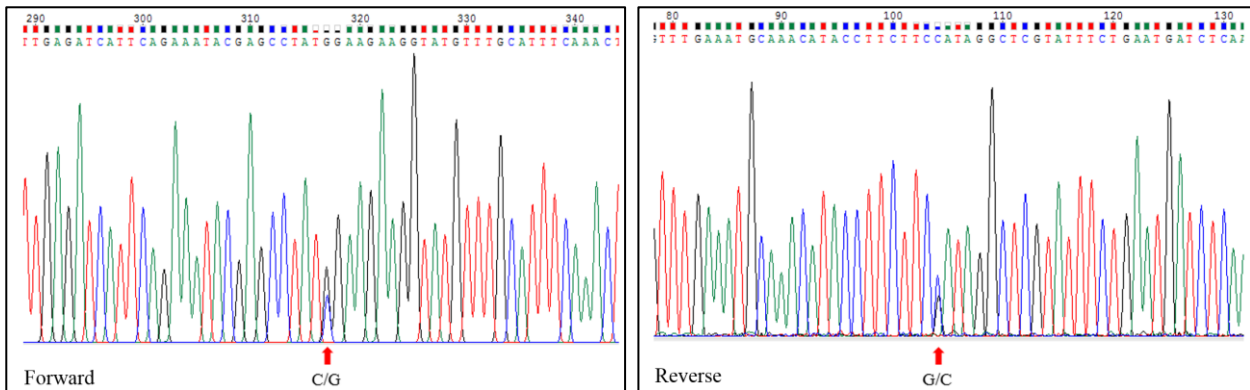
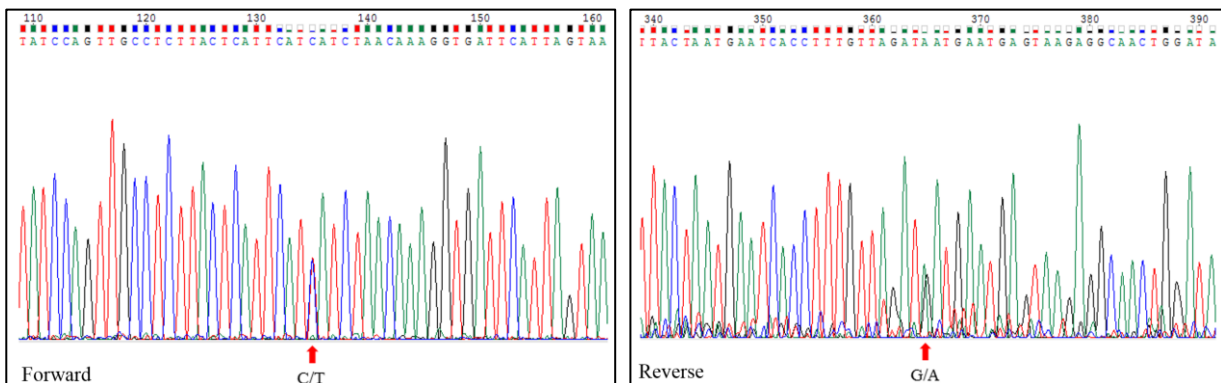
Patient 8

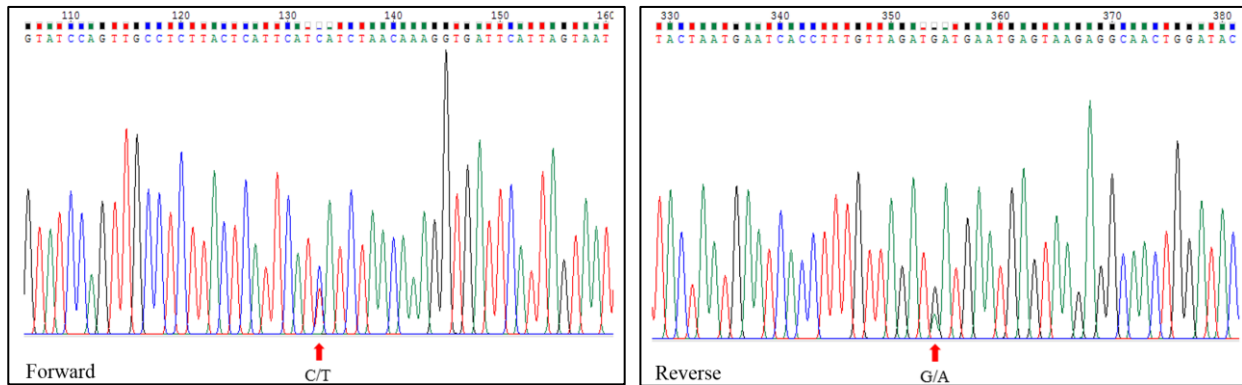
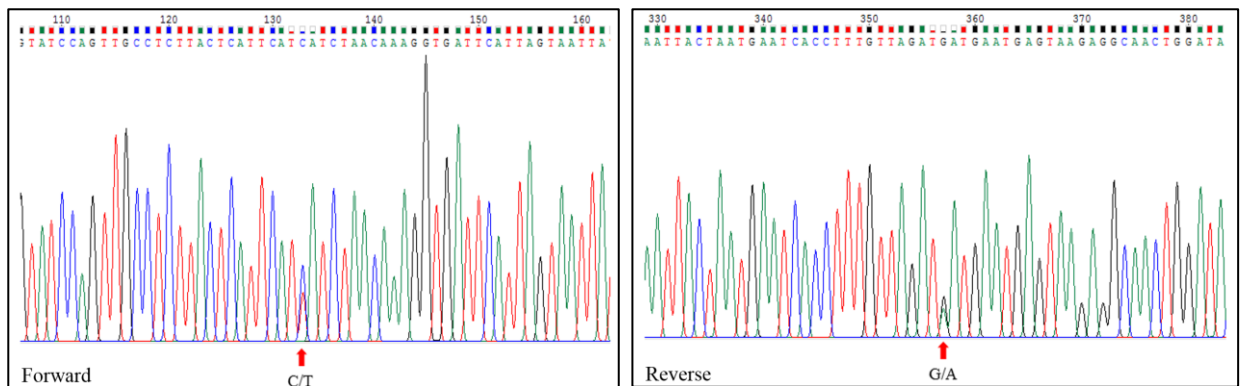
c.698 A>T / p.H233L (heterozygosity) – *PLCZ1* exon 6



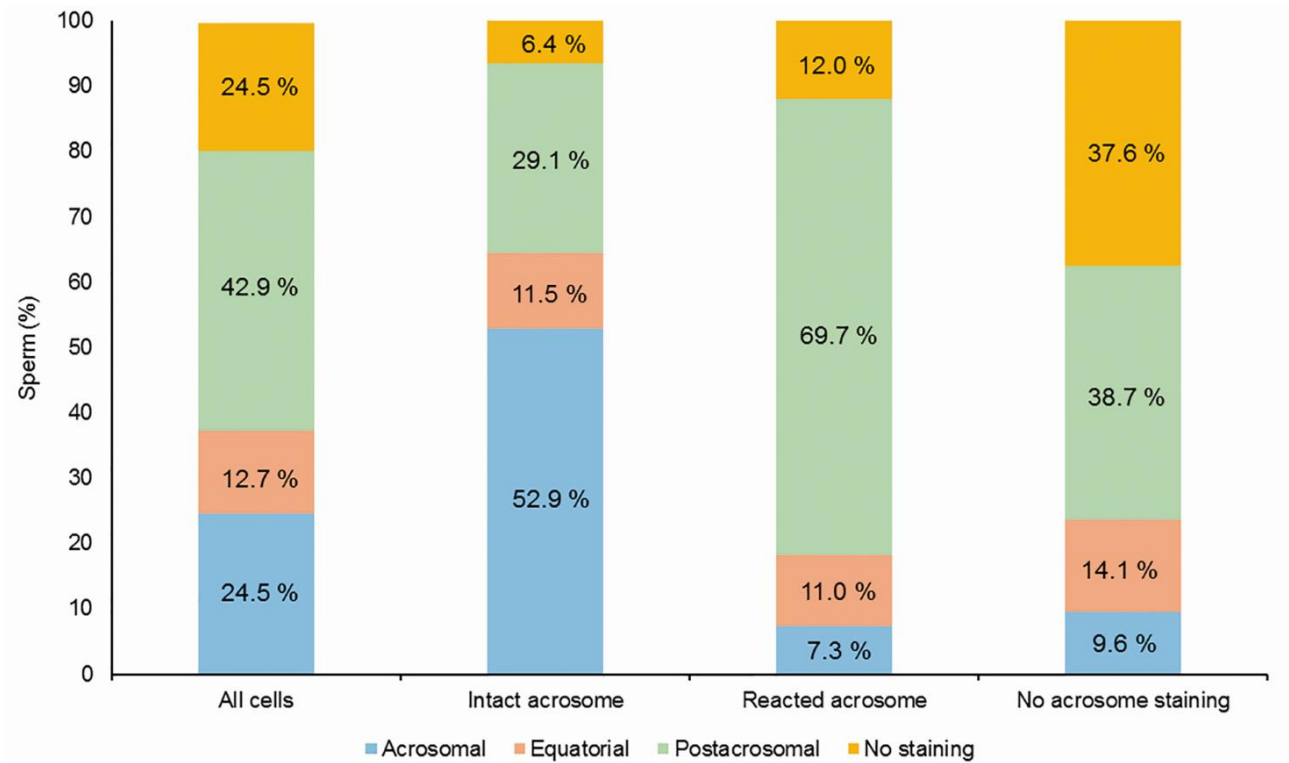
Supplementary Figure 1 (cont.).**Patient 12**c.972_973 delAG / p.V326K fs*25 (heterozygosity) – *PLCZ1* exon 9**Patient 22**c.1499 C>T / p.S500L (heterozygosity) – *PLCZ1* exon 13*Not available***Patient 24**c.1499 C>T / p.S500L (heterozygosity) – *PLCZ1* exon 13

Supplementary Figure 1 (cont.).**Patient 26**c.671 T>C / p.L224P (heterozygosis) – *PLCZ1* exon 6**Patient 27**c.1499 C>T / p.S500L (heterozygosis) – *PLCZ1* exon 13**Patient 28**c.1499 C>T / p.S500L (heterozygosis) – *PLCZ1* exon 13

Supplementary Figure 1 (cont.).**Patient 29**c.1499 C>T / p.S500L (homozygosity) – *PLCZ1* exon 13**Patient 30**c.360 C>G / p.I120M (heterozygosity) – *PLCZ1* exon 4**Patient 32**c.1499 C>T / p.S500L (heterozygosity) – *PLCZ1* exon 13

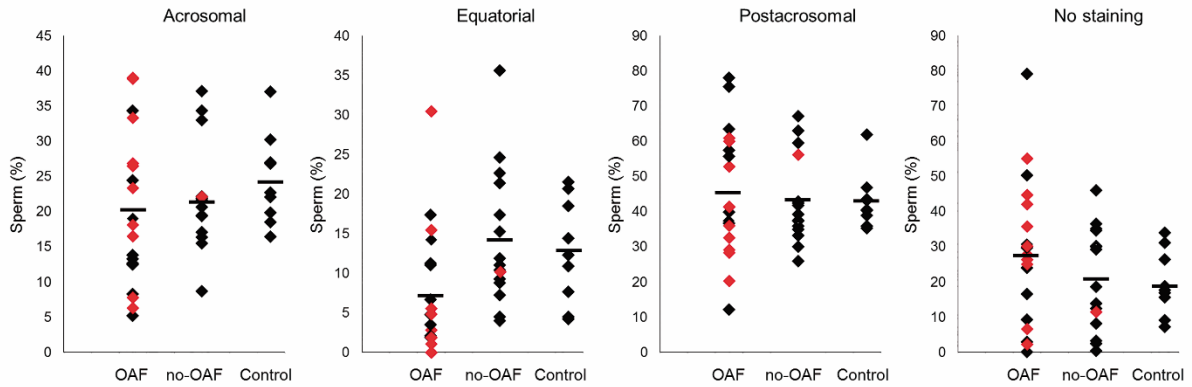
Supplementary Figure 1 (cont.).**Patient 36**c.1499 C>T / p.S500L (heterozygosity) – *PLCZ1* exon 13**Patient 37**c.1499 C>T / p.S500L (heterozygosity) – *PLCZ1* exon 13

Supplementary Figure 2. Percentages of cells for each PLC ζ /PLCZ1 subcellular localization by immunofluorescence (acrosomal, equatorial, postacrosomal and no staining) in all cells and within the three acrosome states considered (intact, reacted, and no acrosome staining).

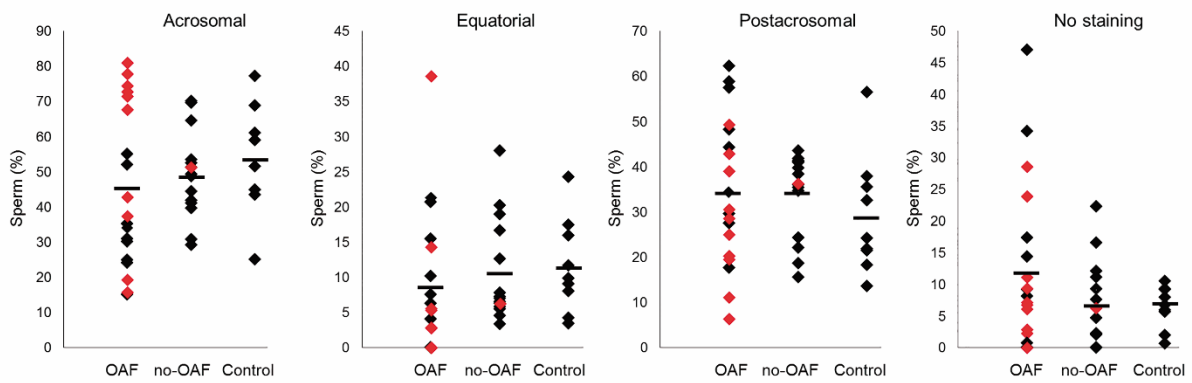


Supplementary Figure 3. Distribution of PLC ζ /PLCZ1 protein staining (acrosomal, equatorial, postacrosomal and no staining) expressed as percentage of cells. Immunofluorescence analysis was performed. Comparison of distribution data in three study groups (OAF: oocyte activation failure; no-OAF; control) are shown for (A) all sperm, (B) sperm with intact acrosome, (C) reacted acrosome and (D) no acrosome stained. Red dots indicate those patients carrying PLCZ1 mutation.

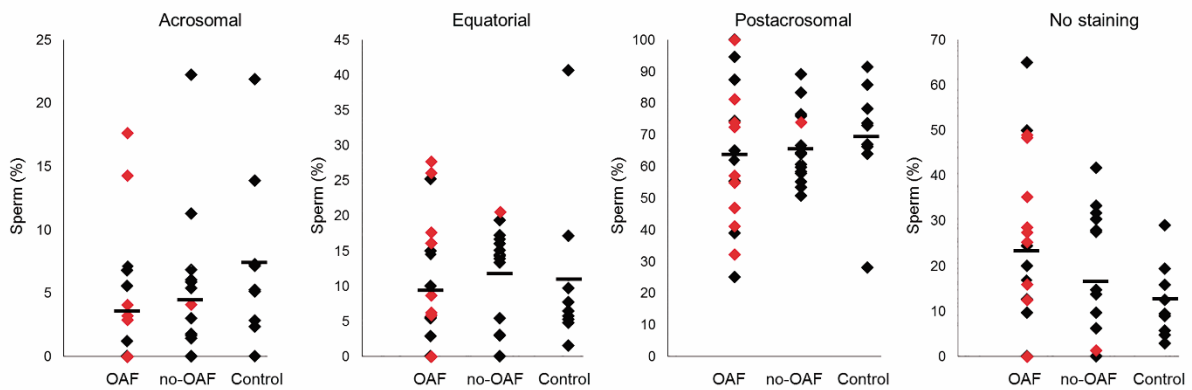
A. All sperm



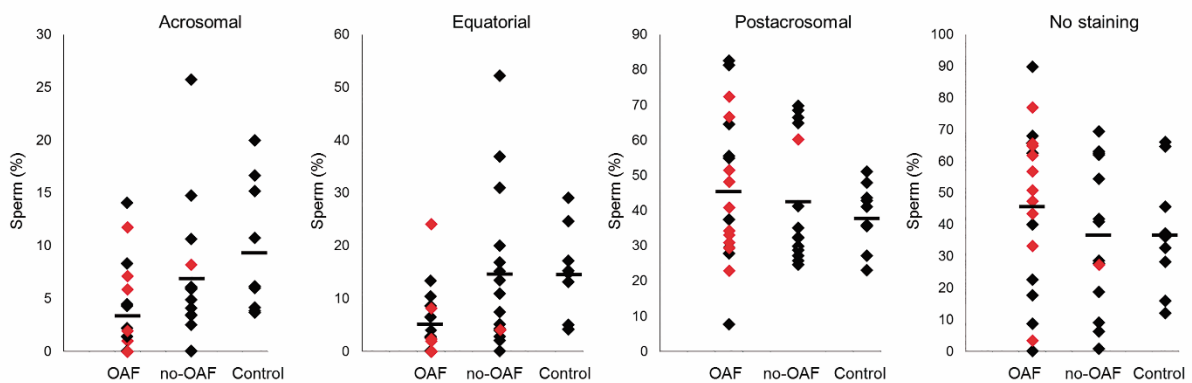
B. Intact acrosome



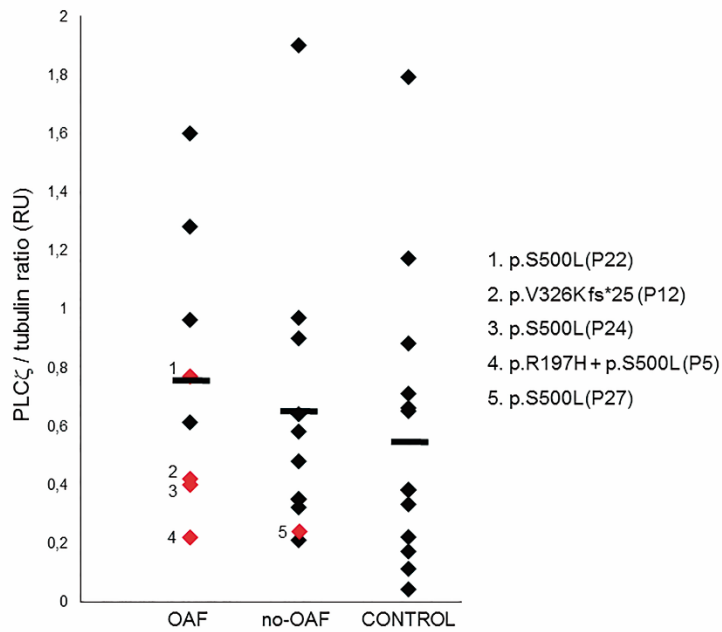
C. Reacted acrosome



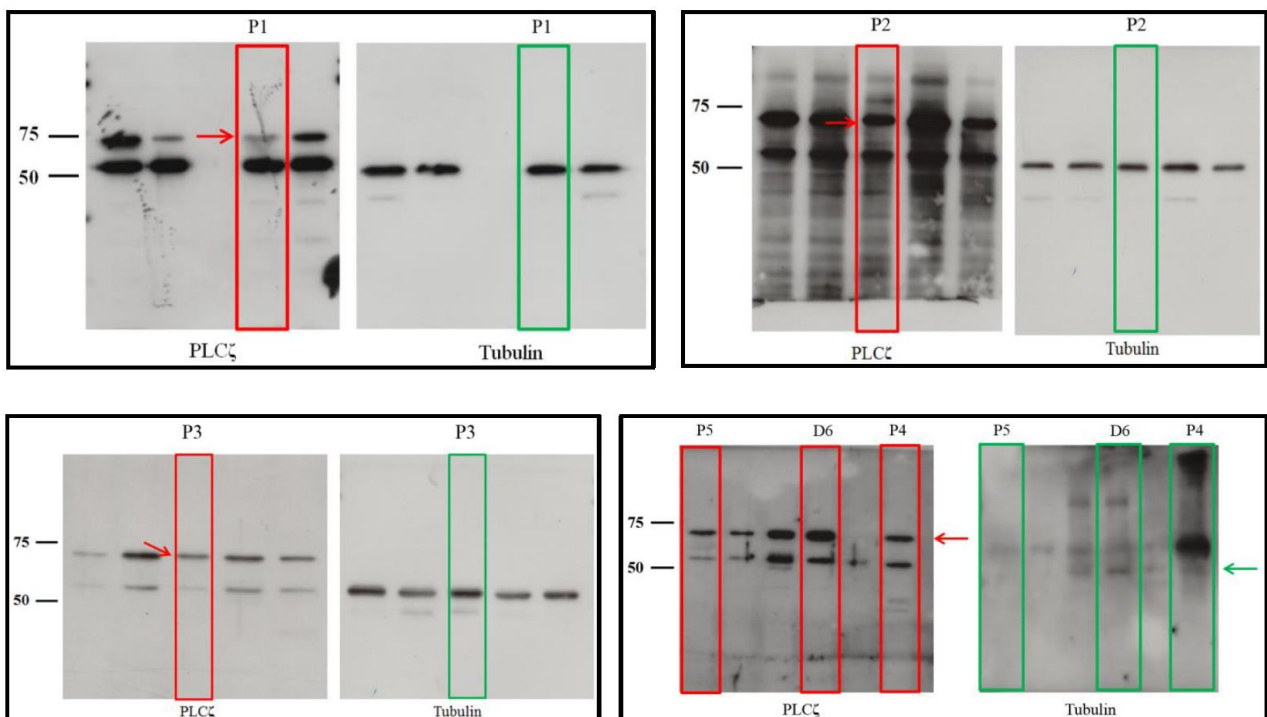
D. No acrosome



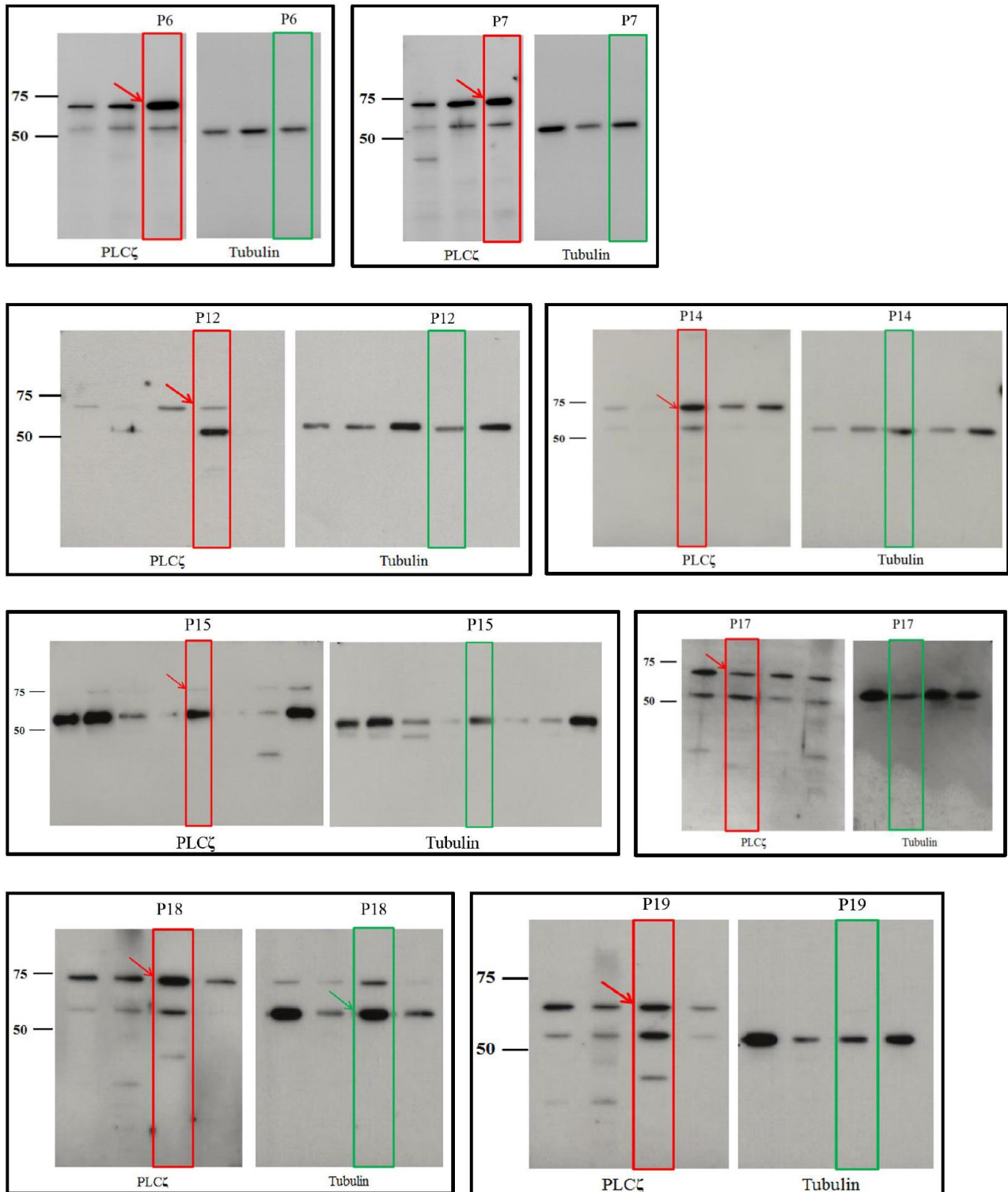
Supplementary Figure 4. Western blot analysis of PLC ζ /PLCZ1 protein levels in the three study groups. Data for the three study groups (OAF: oocyte activation failure; no-OAF; control) are expressed as PLC ζ /tubulin ratio (RU: relative units). Numbers indicate the specific variant in the patients carrying *PLCZ1* variants (indicated by red dots).



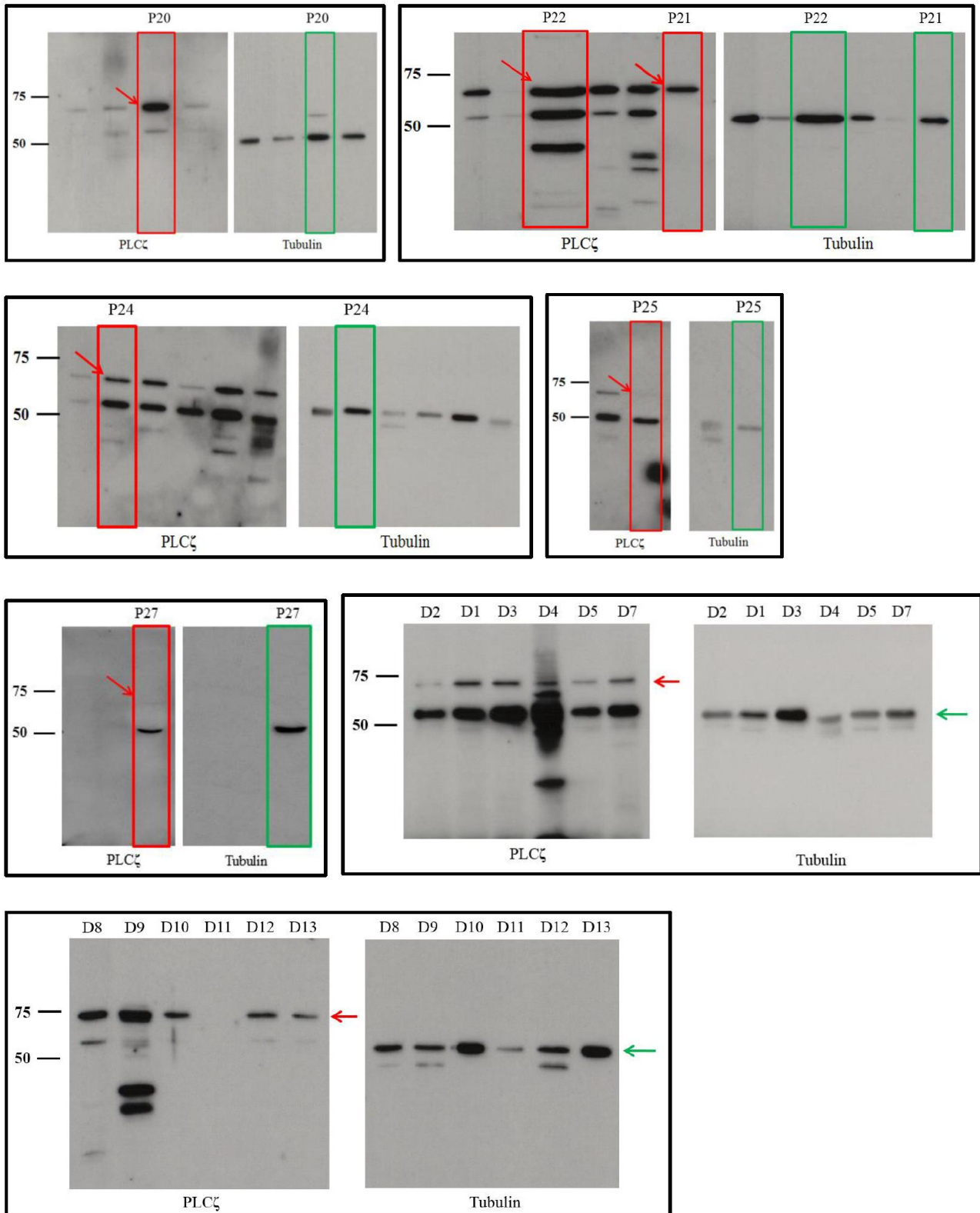
Supplementary Figure 5. Original uncut western blot images for all patients with fertilization failure and controls (D1-D13) in which PLC ζ protein levels (red arrow) were determined by semiquantitative densitometry, using tubulin (green arrow) as a normalizer.



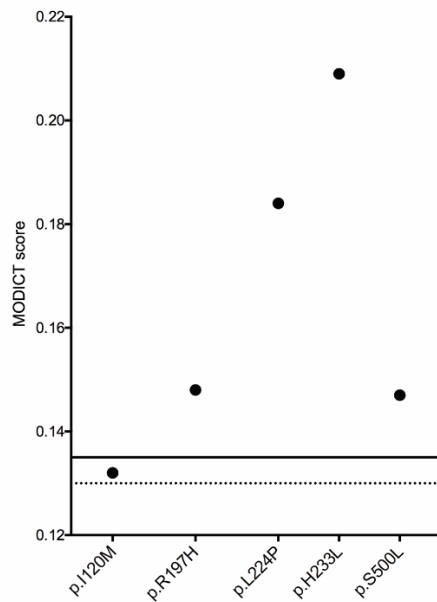
Supplementary Figure 5 (cont.).



Supplementary Figure 5 (cont.).



Supplementary Figure 6. MODICT scores predicting the impact of mutations on PLC ζ /PLCZ1 activity for the five missense variants (p.I120M, p.R197H, p.L223P, p.H233L, and p.S500L). Thresholds to assess the detrimental potential of the variants (continuous line: detrimental, discontinuous line: potentially detrimental) were built by combining the MODICT scores of the wild type (functional) and p.H398P (known detrimental) models, to generate first an imaginary benign mutation, and later derive the thresholds with the calculations reported in Tanyalcin et al. (2016).



CHAPTER 3: Sperm telomere length in donor samples is not related to ICSI outcome

PUBLISHED AS:

Torra-Massana M, Barragán M, Bellu E, Oliva R, Rodríguez A, Vassena R. **Sperm telomere length in donor samples is not related to ICSI outcome.** *J Assist Reprod Genet* 2018; 35:649-657.

Partial contents of this chapter were included in the following oral presentation:

M. Torra, M. Barragán, E. Bellu, A. Rodríguez, R. Oliva, R. Vassena. **Sperm telomere length is not related to reproductive outcomes up to live birth when analyzed independently from female variables.** ESHRE Annual Meeting 2017, Geneva, Switzerland. O-288. Human Reproduction, Vol.32, No.Suppl pp. 509–539, 2017.

Partial contents of this chapter were included in the following poster presentation:

M Torra-Massana, M Barragán Monasterio, E Bellu, A Rodríguez Aranda, R Oliva Virgili, R Vassena. **La longitud telomérica en espermatozoides no está relacionada con el resultado del embarazo hasta niño nacido.** IX Congreso ASEBIR 2017, Madrid, Spain. P-35.

NOTE: This chapter includes all the material included in the publication previously mentioned (Torra-Massana et al., 2018), as well as the results from additional experiments performed in our laboratory (not published). This additional information includes the analysis of sperm telomere length in samples with previous fertilization failure after ICSI.

TITLE

Sperm telomere length in donor samples is not related to ICSI outcome

CAPSULE

Measurement of sperm telomere length in donor normozoospermic men is not useful to predict fertilization rates, embryo morphology or reproductive outcomes in ICSI cycles, regardless of its relationship to other sperm parameters and independently from female variables.

ABSTRACT**Purpose**

Variations in sperm telomere length (STL) have been associated to altered sperm parameters, poor embryo quality, and lower pregnancy rates; but normozoospermic men STL relevance in IVF/ICSI is still uncertain. Moreover, in all studies reported so far, each man STL was linked to the corresponding female partner characteristics. Here we study STL in sperm donor samples, each used for up to 12 women, in order to isolate and determine the relationship between STL and reproductive outcomes.

Methods

Relative STL was determined by qPCR in 60 samples used in a total of 676 ICSI cycles. Univariable and multivariable statistical analysis were used to study STL effect on fertilization rate, embryo morphology, biochemical, clinical, and ongoing pregnancy rates, and live birth (LB) rates.

Results

The average STL value was 4.5 (relative units; SD 1.9; range 2.4-14.2). LOWESS regression and Rho-Spearman test did not reveal significant correlations between STL and the outcomes analyzed. STL was not different between cycles resulting or not in pregnancy and LB (Mann Whitney U-test, $p>0.05$). No significant effect of STL on reproductive outcomes was found, with OR for each unit increase in STL (95% CI) of 0.94 (0.86-1.04), 0.99 (0.9-1.09), 0.98 (0.89-1.09) and 0.93 (0.8-1.06) for biochemical, clinical, ongoing pregnancy and LB, respectively. The multilevel analysis confirmed that the effect of STL on fertilization, biochemical, clinical, ongoing pregnancy and LB was not significant ($p>0.05$).

Conclusion

After addressing STL independently from female variables, results show that STL measurement is not useful to predict reproductive outcomes in ICSI cycles using normozoospermic semen.

Keywords: IVF/ICSI; embryo morphology; sperm telomere length; live birth

INTRODUCTION

Telomeres are evolutionary conserved structures composed of non-coding hexameric tandem repeats (5'-TTAGGG-3') of genomic DNA. Located at the ends of eukaryotic chromosomes, telomeres play a role in maintaining genomic integrity, prevent chromosome end joining, and facilitate homologue pairing and synapsis in meiosis [1]. In most cell types, telomere length decreases with each cell division, as DNA replication mechanisms are unable to replicate the end of their 3' sequence [2]. In fact, when telomeres reach a critical length, chromosome uncapping, apoptosis or cell-cycle arrest occur, thus affecting genome stability, cell division, and meiosis [3, 4].

In male germ cells, telomeres progressively increase in length during spermatogenesis, although further research is necessary to understand the molecular background and regulatory systems involved in this process [5]. Telomere length in spermatozoa increases with man's age, and positively correlates with parental age at conception [6-8]. Conversely, telomeres in oocytes decrease with woman age [4], and telomeres shorten during oocyte maturation [9].

Human sperm telomere length (STL) is around 10–20kb [10], and considerable variability in STL exists among individuals and even among spermatozoa from the same ejaculate [11]. Telomere length can be affected by oxidative stress, which can lead to DNA damage and telomere shortening [12], environmental chemicals [13], smoking, obesity, stress, and diet [14]. Additionally, there seem to be ethnical differences in STL [15].

STL has been proposed as a novel marker of IVF outcomes, and some studies indicate that shorter telomeres are concurrent with altered sperm parameters. For example, oligozoospermic or asthenozoospermic samples have lower STL than normozoospermic ones [8, 11, 16]. Additionally, recent studies indicate a positive correlation between STL, progressive sperm motility, vitality, and protamination, as well as a negative correlation between STL, DNA fragmentation and diploidy

[17, 18]. Other authors did not find correlation between STL and sperm DNA fragmentation, concentration or motility [9].

Moreover, STL has been positively correlated with embryo morphology in IVF cycles [16]. On the other hand, the role of normozoospermic men STL in pregnancy and live birth rates is uncertain, and it remains to be established if it can be used as a reliable marker in fertility clinics.

Inevitably, a significant limitation in all studies reported so far is that each man STL is necessarily linked to his female partner characteristics, making it impossible to assess STL independently from these uncontrolled for variables. This is a significant flaw of current studies, given the relevance of some variables such as woman age for ART outcomes [19, 20]. The aim of this study was to analyze STL in sperm donors, whose samples have been used for several female patients in different cycles, and assess its relationship with reproductive outcomes.

Table I. Baseline characteristics of sperm donor population (n=60), and variables included within cycle level (n=676). Values are presented as mean \pm standard deviation [range]. RU; Relative units. BMI; Body Mass Index. MII; metaphase II oocyte. 2PN; 2 pronuclei zygote. AU; Arbitrary units.

	Variable; units	Overall
Sperm donor level (n=60)	Sperm donor age; years	24.3 \pm 5 [18-35]
	Sperm concentration; million/mL	66.9 \pm 33.2 [15.9-173]
	Sperm motility; %	24.5 \pm 14.1 [5.8-78]
	Sperm telomere length; RU	4.5 \pm 1.9 [2.4-14.2]
Cycle level (n= 676)	Oocyte age; years	32.7 \pm 7.5 [18-49]
	Female patient age; years	40.1 \pm 4.7 [23-50]
	Female patient BMI; kg/m ²	24.3 \pm 4.5 [16.8-41.4]
	Oocyte donor BMI; kg/m ²	22.9 \pm 3.4 [17-33.7]
	MI; number	6.4 \pm 3.1 [1-24]
	2PN; number	4.5 \pm 2.6 [0-21]
	Fertilization rate; %	69.6 \pm 23.9 [0-100]
	Abnormal fertilization rate; %	7.6 \pm 12.9 [0-100]
	Mean embryo morphological score; AU	7 \pm 1.54 [0-10]
	Embryos obtained; number	4.3 \pm 2.4 [0-20]

MATERIALS AND METHODS

Ethical considerations

Permission to conduct this study was obtained from the local Ethical Committee for Clinical Research. All procedures performed were in accordance with the ethical standards of the institutional research committees and with the 1964 Helsinki declaration, as revised in 2013.

Study population

In the present study, 60 normozoospermic sperm donor samples were included after being used for fertility treatments. All samples came from external sperm banks. Demographic data is shown in **Table I**. Semen was thawed, and motility and concentration were determined. Samples used were representative of the whole sperm sample, as were collected by pooling the swim-up fraction (after ICSI) with the pelleted cells. All samples included were assigned to between 6 and 12 ICSI cycles. ICSI cycles were performed using donor sperm with either donor oocytes or patient's own oocytes. All embryo transfers were fresh and on D2-3 of development. A total of 631 women (either oocyte donors or patients) performed the 676 ICSI cycles included in the study, (i.e. 93% of the women were included once). However, only in 2 cases an oocyte donor or patient repeated the cycle with the same sperm donor, representing little to no repetition in the database (99.7% independent cycles/gamete mix). Demographic and clinical variables and reproductive outcomes were collected (**Table I and II**; and **Supplementary Table I**).

Table II. Mean values of oocyte age within study groups, variables included in embryo transfer level (n=626) and reproductive outcomes: pregnancy (biochemical, clinical, ongoing) and live birth rates. Values are presented as mean \pm standard deviation [range] or number (%) when appropriate. RU; Relative units.

Variable; units	Overall	Cycles w/ own oocytes	Cycles w/ donor oocytes
Total ICSI cycles	676	351	325
Oocyte age; years	32.7 \pm 7.5 [18-49]	38.3 \pm 4.4 [23-49]	26.5 \pm 5 [18-35]
Total cycles with transfer	626	316	310
Transferred embryo average morphological score; RU	8 \pm 1.3 [4-10]	7.9 \pm 1.4 [4-10]	8.2 \pm 1.2 [4-10]
Transferred embryos; n			
1	107 (17.1)	65 (20.6)	42 (13.5)
2	461 (73.6)	194 (61.4)	267 (86.1)
3	58 (9.3)	57 (18)	1 (0.3)
Transfer day			
D2	247 (39.5)	167 (52.8)	80 (25.8)
D3	379 (60.5)	149 (47.2)	230 (74.2)
Biochemical pregnancy; %	305/625 (48.8)	123/316 (38.9)	182/309 (58.9)
Clinical pregnancy; %	240/619 (38.8)	103/313 (32.9)	137/306 (44.8)
Ongoing pregnancy; %	187/605 (30.9)	80/305 (26.2)	107/300 (35.7)
Live birth; %	162/586 (27.6)	67/295 (22.7)	95/291 (32.6)
Multiple pregnancy; %	52/619 (8.4)	19/313 (6.1)	33/306 (10.8)

Sperm telomere length determination

Genomic DNA (gDNA) was extracted from 3 to 10 million sperm using QIAMP DNA Blood Mini Kit (QIAGEN, Germany) following the manufacturer's instructions with minor modifications, specifically increasing lysis time up to 2h; gDNA was quantified by measurement of absorbance at $\lambda=260\text{nm}$ (Quawell). Relative STL (relative units; RU) was determined by real-time quantitative

Scatterplot Smoothing (LOWESS) regression, with a fit to 50% of the points and a Epanechnikov weight function (Kernel) [data near the current point receive higher weights than extreme data receive]. The advantage of this regression is that it does not require the specification of a function to fit a model to all of the data in the sample, thus fitting to the data accurately across the whole range of time.

Multivariable statistical analysis

A logistic multilevel regression was used to investigate the effect of STL on the reproductive outcomes (biochemical, clinical, ongoing pregnancy; and live birth). To investigate the effect sperm telomere length on the embryo morphology score, linear multilevel regression was performed, while general linear modelling (logit link function and robust estimation of the standard errors) was employed to investigate the effect of sperm telomere length on fertilization rates. Multilevel analysis allows addressing hierarchical data structures where each donor has several recipients, by decomposing the variance into 2 levels: cycles (level 1) nested within donors (level 2). As level-2 covariates we included sperm concentration (million/mL) and sperm motility (%AB). As level-1 covariates we included: oocyte origin (heterologous vs. autologous), oocyte age (years), female patient BMI (kg/m²), number of injected oocytes (MII), average morphological score of the transferred embryos, transfer day (2 vs. 3) and number of transferred embryos (2-3 vs 1). Analyses were performed using SPSS version 22.0 and MLwiN 2.31 and Stata 13.0/SE (Stata Corp. LT). A p-value <0.05 was set as statistically significant.

Table III. Sperm telomere length (STL) by occurrence of pregnancy (biochemical, clinical and ongoing) and live birth. In this univariate statistical analysis, the effect of maternal age, oocyte origin and other variables were not included as confounding factors. *Mann-Whitney U test. Values are presented as mean \pm standard deviation. STL expressed as Relative Units (RU). CI; confidence interval.

	Negative	Positive	p*	Mean difference	95% CI	
					Lower	Upper
Biochemical	4.43 \pm 1.8	4.27 \pm 1.54	0.23	0.16	-0.10	0.43
Clinical	4.35 \pm 1.7	4.33 \pm 1.6	0.86	0.02	-0.24	0.3
Ongoing	4.35 \pm 1.7	4.3 \pm 1.6	0.75	0.05	-0.24	0.34
Live birth	4.34 \pm 1.7	4.11 \pm 1.26	0.08	0.23	-0.027	0.48

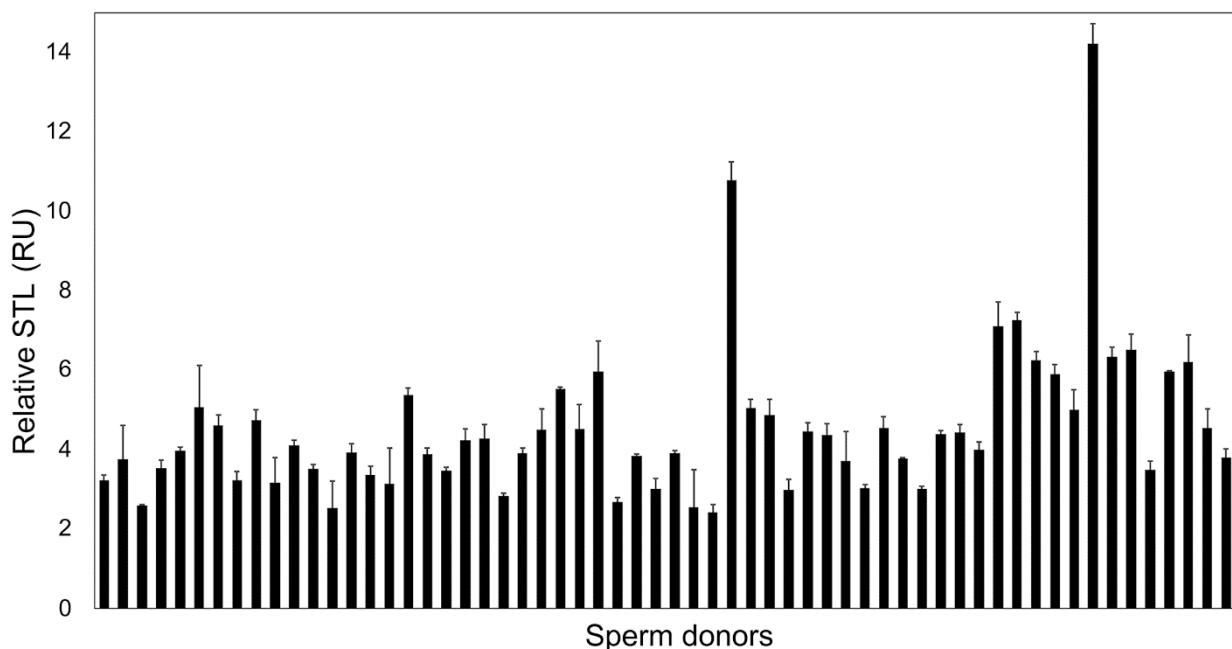
RESULTS

A database including a total of 676 ICSI cycles grouped with 60 different donors was generated. Baseline clinical characteristics of the population are shown in **Table I**, while individualized data for each donor (STL, number of ICSI cycles performed and reproductive outcomes) is indicated in

Supp. **Table III**. A total of 676 ICSI cycles were performed using either donor oocytes (n=325) or patient own oocytes (n=351). 1 (17.1%), 2 (73.6%) or 3 (9.3%) embryos were transferred on D2 (39.5%) or D3 (60.5%) of development.

Overall outcomes were 48.8%, 38.8% and 30.9% for biochemical, clinical, and ongoing pregnancy rates respectively, while live birth rate was 27.6% (**Table II**). As expected, we found some significant differences when comparing those cycles using donor oocytes with cycles using patient's own oocytes, for example in woman age or number of MII oocytes (**Supplementary Table I**).

Figure 1: Distribution of sperm telomere length (STL) among normozoospermic sperm donors by real-time quantitative PCR (qPCR). To obtain the relative STL (relative units, RU), the T/S ratio for each sperm sample (n=60) was normalized against the T/S ratio from a common gDNA sample for the whole study (HeLa gDNA). Data is presented as mean values (black columns) and SD (error bars) of triplicate measurements. T: Amplification value for telomeric region; S: amplification value for a single-copy gene (*36B4*).

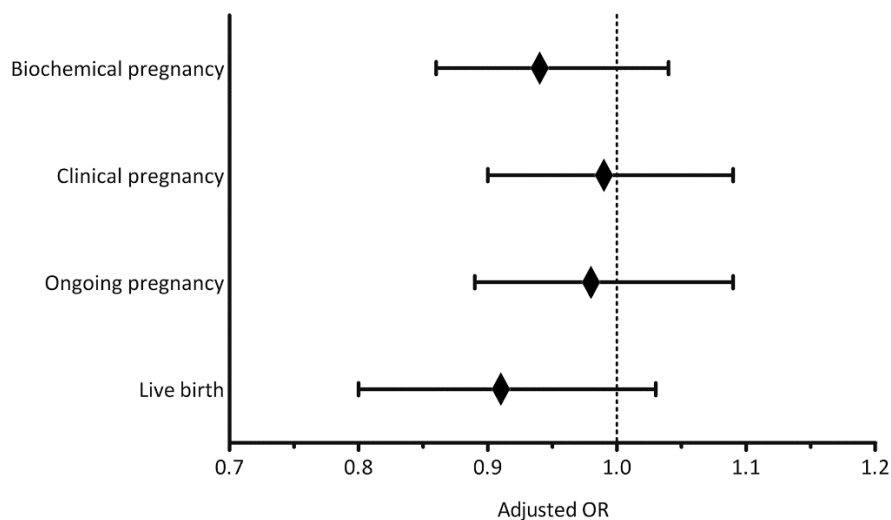


Mean STL was 4.50 RU, with considerable individual variation (SD=1.9; range 2.4-14.2; **Figure 1**). No relevant correlations were found between STL and sperm motility (Rho-spearman coefficient 0.13; p=0.34) and man's age (Rho-spearman coefficient -0.007; p=0.96), while significant correlation was found between STL and sperm concentration (Rho-spearman coefficient 0.28; p=0.03) (**Supplementary Figure 1**).

Mann-Whitney U test revealed that cycles ending in pregnancy and live birth did not differ in STL with those which did not (p>0.05; **Table III**). Additionally, no significant effect of STL was found on reproductive outcomes, with ORs for each unit increase in STL of 0.94 (95% CI 0.86-1.04), 0.99

(95% CI 0.9-1.09), 0.98 (95% CI 0.89-1.09) and 0.93 (95% CI 0.8-1.06) for biochemical, clinical and ongoing pregnancy; and livebirth, respectively (**Figure 2**).

Figure 2: Forest Plot of sperm telomere length (STL) association with reproductive outcomes. A forest plot for STL and reproductive outcomes is shown using rates for pregnancy (biochemical, clinical and ongoing) and live birth. Adjusted odds ratios (95% CIs) for reproductive outcomes by each relative unit increase in STL are denoted by black diamonds (black lines).



There was no significant correlation between STL and the average score of embryo morphology (Rho-spearman coefficient -0.07 ; $p=0.08$), fertilization rate (Rho-spearman coefficient -0.04 ; $p=0.35$) and abnormal fertilization rate (Rho-spearman coefficient 0.02 ; $p=0.65$).

On the other hand, LOWESS regression did not suggest correlation (linear or non-linear) between STL and embryo morphology, fertilization rate, pregnancy rates (biochemical, clinical and ongoing) and live birth rate (**Supplementary Figure 2**).

Table IV(next page). Logistic multilevel regression analysis of the association between STL and reproductive outcomes (1st level: female patient; 2nd level: sperm donor). STL effect on pregnancy (biochemical, clinical and ongoing) and live birth is adjusted by sperm parameters (concentration and motility), female characteristics (oocyte age, oocyte origin and female BMI) and ICSI cycle variables (number of MII, transferred embryo average morphological score, transfer day, number of transferred embryos). Oocyte origin means that the oocytes may come from either a donor or from the own patient. Oocyte age is defined by the age of the patient or the oocyte donor when oocytes are retrieved after hormonal stimulation. Number of MII represents the number of injected oocytes for each cycle. RU; Relative Units. AU; Arbitrary Units. BMI; Body Mass Index. MII; metaphase II oocyte. OR; odd ratio. CI; Confidence interval.

		p	OR	Upper 95% CI	Lower 95% CI
Biochemical pregnancy	Sperm telomere length (RU)	0.411	0.95	0.85	1.068
	Sperm concentration (million/mL)	0.023	0.99	0.99	0.999
	Sperm motility (%)	0.321	0.99	0.97	1.009
	Oocyte age (years)	0.022	0.95	0.91	0.991
	Female patient BMI (kg/m ²)	0.456	0.99	0.95	1.024
	Oocyte origin	<0.001	2.38	1.56	3.620
	Number of MII	0.276	1.04	0.97	1.130
	Transferred embryo average morphological score (AU)	<0.001	1.37	1.18	1.601
	Transfer day (2+ vs. 3+)	0.038	1.57	1.04	2.379
	Number of transferred embryos (2-3 vs. 1)	0.173	1.44	0.86	2.407
	Clinical pregnancy	Sperm telomere length (RU)	0.986	1.00	0.90
Sperm concentration (million/mL)		0.023	0.99	0.99	1.00
Sperm motility (%)		0.508	0.99	0.98	1.01
Oocyte age (years)		0.025	0.95	0.91	0.99
Female patient BMI (kg/m ²)		0.395	0.98	0.94	1.02
Oocyte origin		0.018	1.70	1.11	2.61
Number of MII		0.053	1.08	1.00	1.17
Transferred embryo average morphological score (AU)		<0.001	1.35	1.15	1.58
Transfer day (2+ vs. 3+)		0.140	1.39	0.90	2.12
Number of transferred embryos (2-3 vs. 1)		0.033	1.87	1.07	3.30
Ongoing pregnancy		Sperm telomere length (RU)	0.769	0.98	0.87
	Sperm concentration (million/mL)	0.085	0.99	0.99	0.99
	Sperm motility (%)	0.372	0.99	0.97	0.97
	Oocyte age (years)	0.005	0.93	0.89	0.89
	Female patient BMI (kg/m ²)	0.786	0.99	0.95	0.95
	Oocyte origin	0.012	1.83	1.16	1.16
	Number of MII	0.106	1.07	0.99	0.99
	Transferred embryo average morphological score (AU)	0.002	1.34	1.13	1.13
	Transfer day (2+ vs. 3+)	0.087	1.50	0.95	0.95
	Number of transferred embryos (2-3 vs. 1)	0.216	1.47	0.81	0.81
Live birth	Sperm telomere length (RU)	0.321	0.99	0.97	1.01
	Sperm concentration (million/mL)	0.050	1.00	1.00	1.00
	Sperm motility (%)	0.619	1.00	1.00	1.00
	Oocyte age (years)	0.012	0.99	0.98	1.00
	Female patient BMI (kg/m ²)	0.803	1.00	0.99	1.01
	Oocyte origin	0.035	1.10	1.01	1.19
	Number of MII	0.066	1.02	1.00	1.03
	Transferred embryo average morphological score (AU)	0.006	1.04	1.01	1.08
	Transfer day (2+ vs. 3+)	0.130	1.07	0.98	1.16
	Number of transferred embryos (2-3 vs. 1)	0.372	1.05	0.95	1.15

A logistic multilevel regression analysis showed that the effect of STL on reproductive outcomes analyzed remained non-significant after adjustment for potential confounders and addressing the hierarchical data structure (different cycles within each donor); with p-values of 0.411, 0.986, 0.769 and 0.595 for biochemical, clinical and ongoing pregnancy rates and LB rate, respectively (**Table IV**). General linear modelling showed no significant effect of STL on fertilization rate (p=0.528) and abnormal fertilization rate (p=0.575) (**Table V**). Multilevel analysis showed a statistically significant effect of STL on embryo morphological score (p=0.003, regression coefficient -0.246; **Table V**), although this does not seem to be clinically relevant.

Table V. Multilevel regression analysis of the association between STL and embryo morphological score, fertilization and abnormal fertilization rate. (1st level: female patient; 2nd level: sperm donor). STL effect on embryo morphological score, fertilization rate and abnormal fertilization rate is adjusted by sperm parameters (concentration and motility) and female characteristics (oocyte age, oocyte origin and female BMI) and number of MII. Oocyte origin means that the oocytes may come from either a donor or from the own patient. Oocyte age is defined by the age of the patient or the oocyte donor when oocytes are retrieved after hormonal stimulation. Number of MII is the number of injected oocytes for each cycle. RU; Relative Units. BMI; Body Mass Index. MII; metaphase II oocyte. CI; Confidence interval.

		Coefficient	p	Upper 95% CI	Lower95 % CI
Embryo morphological score	Sperm telomere length (RU)	-0.246	0.003	0.671	0.911
	Sperm concentration (million/mL)	0.009	0.077	0.999	1.019
	Sperm motility (%)	-0.014	0.248	0.963	1.010
	Oocyte age (years)	0.078	0.068	0.996	1.174
	Female patient BMI (kg/m ²)	-0.034	0.292	0.908	1.029
	Oocyte origin	-0.16	0.647	0.431	1.686
	Number of MII	0.237	<0.001	1.127	1.426
Fertilization rate	Sperm telomere length (RU)	0.176	0.528	-0.370	0.722
	Sperm concentration (million/mL)	-0.011	0.131	-0.026	0.003
	Sperm motility (%)	0.013	0.648	-0.044	0.070
	Oocyte age (years)	-0.086	0.324	-0.258	0.085
	Female patient BMI (kg/m ²)	0.034	0.597	-0.091	0.158
	Oocyte origin	-0.674	0.556	-2.920	1.572
	Number of MII	1.107	<0.001	0.622	1.591
Abnormal fertilization rate	Sperm telomere length (RU)	0.045	0.575	-0.113	0.203
	Sperm concentration (million/mL)	0.003	0.613	-0.008	0.014
	Sperm motility (%)	-0.010	0.391	-0.031	0.012
	Oocyte age (years)	0.009	0.794	-0.060	0.079
	Female patient BMI (kg/m ²)	-0.033	0.260	-0.092	0.025
	Oocyte origin	0.074	0.814	-0.545	0.694
	Number of MII	0.363	<0.001	0.221	0.505

DISCUSSION

We present one of the largest studies on normozoospermic STL to date, and the only one addressing STL independently from female factor and other variables associated with ICSI outcomes. Although the relative STL mean value (4.5 RU) obtained in this study was different from the values found in other similar studies, the variation in relative STL found in the samples analyzed is comparable [18, 17]. Differences in relative STL mean value between studies could be explained by different PCR reagents and conditions (e.g. Taq polymerase) and in the reference DNA used (HeLa gDNA in our case).

Although our objective was to study STL effect on reproductive outcomes in normozoospermic donors, some information about other variables was also assessed. We found a slight but significant positive association between sperm concentration and STL, as in previous studies [8]. An explanation for the absence of significant correlation between STL and man's age could be found in the small range of age of our population (18-34 years old).

Given the role of telomeres in chromosomal orientation, synapsis and segregation, STL could affect fertilization and first mitotic division. Sperm telomeres are the first region in the sperm genome to respond to oocyte signals for pronucleus formation [14], and oocytes fertilized with sperm from telomerase-null (TR^{-/-}) mice exhibit high rates of abnormally fertilized oocytes, with increasing percentages of oocytes with one pronucleus [3]. However, we did not find association between STL and fertilization rates and the percentage of zygotes with 1 or 3 pronuclei. Our samples came from sperm donors with high fertilization rates (around 70% on average), and further research using samples from patients with recurrent abnormal fertilization could help understand if there is a role for STL in fertilization.

It has been proposed that sperm with short telomeres may not respond to oocyte signals to form a pronucleus, leading to impaired cleavage, poor-morphology embryos and implantation failure [3]. In fact, STL has been reported as the factor that determines the telomere length of early embryos before telomerase is expressed [23], and short telomeres in the human embryo itself have been associated to higher fragmentation and worse morphology [24]. However, our results from a database of 2993 embryos at D2-3 of development did not support a clinically relevant effect of STL on embryo morphology.

Few studies have been performed addressing the effect of STL on IVF outcomes up to live birth. In 2013, Turner & Hartshorne did not find differences in the average STL between cycles ending in pregnancy and those that did not in 50 patients [9]; while recently, Cariati et al. proposed that

abnormal levels of STL may alter pregnancy rates in normozoospermic patients [18]. However, in both studies, the samples included were used to fertilize oocytes from the partner, making it impossible to isolate the effect of STL from both female and cycle variables. Another limitation of the described reports is that confounding variables such as woman age, BMI, number of MII collected or embryo morphology, were not included in the analysis. After adjusting for these potential confounders, we did not find any effect of STL.

Telomeres lengthen during preimplantation development in both mice and human [3, 9, 23]; perhaps, telomere lengthening in the embryo might compensate for the effect of short STL, and reduce its effect on IVF outcomes. It is also possible that systemic telomere length rather than STL has some role in pregnancy rates, as couples experiencing idiopathic recurrent pregnancy seem to have shorter leukocyte telomeres [14]. Moreover, telomere length in oocytes could also play a role in predicting IVF outcomes [25].

Telomere length measuring in other tissues could be used as a marker to be applied in assisted reproduction. Pathologies like endometriosis and reproductive cancers have been linked to telomere length abnormalities [4], and telomere length in cumulus cells seems to be associated to oocyte and embryo quality [26]. Recently, Xu et al. found that patients with primary ovarian insufficiency had shorter telomeres in granulosa cells, although they did not find association with the quality of the generated embryos [27].

We recognize some limitations of our study: as it was performed in fertile normozoospermic men, associations between STL and reproductive outcomes cannot be discarded in other groups of patients. Only the first fresh embryo transfer was studied, thus no information is available on cumulative pregnancy rates. Although the use of sperm donor samples enabled us to include a high number of ICSI cycles and analyze STL independently (up to 12 women per donor), STL values were determined from a single sample per donor, making it impossible to control possible variations between ejaculates.

In conclusion, although STL might be altered in some groups of patients with clear clinically defined infertility, caution should be exerted when connecting STL results to laboratory or clinical outcomes after ICSI treatment.

COMPLIANCE WITH ETHICAL STANDARDS

Ethical approval

Permission to conduct this study was obtained from the local Ethical Committee for Clinical Research. All procedures performed were in accordance with the ethical standards of the institutional research committees and with the 1964 Helsinki declaration, as revised in 2013.

Conflict of interest

The authors declare that they have no conflict of interest.

REFERENCES

1. O'Sullivan RJ, Karlseder J. Telomeres: protecting chromosomes against genome instability. *Nature reviews Molecular cell biology*. 2010;11(3):171-81. doi:10.1038/nrm2848.
2. Harley CB, Futcher AB, Greider CW. Telomeres shorten during ageing of human fibroblasts. *Nature*. 1990;345(6274):458-60. doi:10.1038/345458a0.
3. Liu L, Blasco M, Trimarchi J, Keefe D. An essential role for functional telomeres in mouse germ cells during fertilization and early development. *Developmental biology*. 2002;249(1):74-84.
4. Kalmbach KH, Fontes Antunes DM, Dracxler RC, Knier TW, Seth-Smith ML, Wang F et al. Telomeres and human reproduction. *Fertil Steril*. 2013;99(1):23-9. doi:10.1016/j.fertnstert.2012.11.039.
5. Ozturk S. Telomerase activity and telomere length in male germ cells. *Biology of reproduction*. 2015;92(2):53. doi:10.1095/biolreprod.114.124008.
6. Kimura M, Cherkas LF, Kato BS, Demissie S, Hjelmberg JB, Brimacombe M et al. Offspring's leukocyte telomere length, paternal age, and telomere elongation in sperm. *PLoS genetics*. 2008;4(2):e37. doi:10.1371/journal.pgen.0040037.
7. Aston KI, Hunt SC, Susser E, Kimura M, Factor-Litvak P, Carrell D et al. Divergence of sperm and leukocyte age-dependent telomere dynamics: implications for male-driven evolution of telomere length in humans. *Molecular human reproduction*. 2012;18(11):517-22. doi:10.1093/molehr/gas028.
8. Ferlin A, Rampazzo E, Rocca MS, Keppel S, Frigo AC, De Rossi A et al. In young men sperm telomere length is related to sperm number and parental age. *Hum Reprod*. 2013;28(12):3370-6. doi:10.1093/humrep/det392.
9. Turner S, Hartshorne GM. Telomere lengths in human pronuclei, oocytes and spermatozoa. *Molecular human reproduction*. 2013;19(8):510-8. doi:10.1093/molehr/gat021.
10. Kozik A, Bradbury EM, Zalensky A. Increased telomere size in sperm cells of mammals with long terminal (TTAGGG)_n arrays. *Molecular reproduction and development*. 1998;51(1):98-104. doi:10.1002/(SICI)1098-2795(199809)51:1<98::AID-MRD12>3.0.CO;2-Q.
11. Antunes DM, Kalmbach KH, Wang F, Dracxler RC, Seth-Smith ML, Kramer Y et al. A single-cell assay for telomere DNA content shows increasing telomere length heterogeneity, as well as increasing mean telomere length in human spermatozoa with advancing age. *Journal of assisted reproduction and genetics*. 2015;32(11):1685-90. doi:10.1007/s10815-015-0574-3.
12. Kawanishi S, Oikawa S. Mechanism of telomere shortening by oxidative stress. *Annals of the New York Academy of Sciences*. 2004;1019:278-84. doi:10.1196/annals.1297.047.

13. Ling X, Zhang G, Chen Q, Yang H, Sun L, Zhou N et al. Shorter sperm telomere length in association with exposure to polycyclic aromatic hydrocarbons: Results from the MARHCS cohort study in Chongqing, China and in vivo animal experiments. *Environment international*. 2016. doi:10.1016/j.envint.2016.08.001.
14. Thilagavathi J, Venkatesh S, Dada R. Telomere length in reproduction. *Andrologia*. 2013;45(5):289-304. doi:10.1111/and.12008.
15. Hansen ME, Hunt SC, Stone RC, Horvath K, Herbig U, Ranciaro A et al. Shorter telomere length in Europeans than in Africans due to polygenetic adaptation. *Human molecular genetics*. 2016. doi:10.1093/hmg/ddw070.
16. Yang Q, Zhao F, Dai S, Zhang N, Zhao W, Bai R et al. Sperm telomere length is positively associated with the quality of early embryonic development. *Hum Reprod*. 2015;30(8):1876-81. doi:10.1093/humrep/dev144.
17. Rocca MS, Speltra E, Menegazzo M, Garolla A, Foresta C, Ferlin A. Sperm telomere length as a parameter of sperm quality in normozoospermic men. *Hum Reprod*. 2016;31(6):1158-63. doi:10.1093/humrep/dew061.
18. Cariati F, Jaroudi S, Alfarawati S, Raberi A, Alviggi C, Pivonello R et al. Investigation of sperm telomere length as a potential marker of paternal genome integrity and semen quality. *Reprod Biomed Online*. 2016;33(3):404-11. doi:10.1016/j.rbmo.2016.06.006.
19. Yan J, Wu K, Tang R, Ding L, Chen ZJ. Effect of maternal age on the outcomes of in vitro fertilization and embryo transfer (IVF-ET). *Science China Life sciences*. 2012;55(8):694-8. doi:10.1007/s11427-012-4357-0.
20. Cardozo ER, Karmon AE, Gold J, Petrozza JC, Styer AK. Reproductive outcomes in oocyte donation cycles are associated with donor BMI. *Hum Reprod*. 2016;31(2):385-92. doi:10.1093/humrep/dev298.
21. Cawthon RM. Telomere measurement by quantitative PCR. *Nucleic acids research*. 2002;30(10):e47.
22. Coroleu B, Barri PN, Carreras O, Belil I, Buxaderas R, Veiga A et al. Effect of using an echogenic catheter for ultrasound-guided embryo transfer in an IVF programme: a prospective, randomized, controlled study. *Hum Reprod*. 2006;21(7):1809-15. doi:10.1093/humrep/del045.
23. de Frutos C, Lopez-Cardona AP, Fonseca Balvis N, Laguna-Barraza R, Rizos D, Gutierrez-Adan A et al. Spermatozoa telomeres determine telomere length in early embryos and offspring. *Reproduction*. 2016;151(1):1-7. doi:10.1530/REP-15-0375.
24. Keefe DL, Franco S, Liu L, Trimarchi J, Cao B, Weitzen S et al. Telomere length predicts embryo fragmentation after in vitro fertilization in women--toward a telomere theory of reproductive aging in women. *American journal of obstetrics and gynecology*. 2005;192(4):1256-60; discussion 60-1. doi:10.1016/j.ajog.2005.01.036.
25. Keefe DL, Liu L, Marquard K. Telomeres and aging-related meiotic dysfunction in women. *Cellular and molecular life sciences : CMLS*. 2007;64(2):139-43. doi:10.1007/s00018-006-6466-z.
26. Cheng EH, Chen SU, Lee TH, Pai YP, Huang LS, Huang CC et al. Evaluation of telomere length in cumulus cells as a potential biomarker of oocyte and embryo quality. *Hum Reprod*. 2013;28(4):929-36. doi:10.1093/humrep/det004.
27. Xu X, Chen X, Zhang X, Liu Y, Wang Z, Wang P et al. Impaired telomere length and telomerase activity in peripheral blood leukocytes and granulosa cells in patients with biochemical primary ovarian insufficiency. *Hum Reprod*. 2017;32(1):201-7. doi:10.1093/humrep/dew283.

SUPPLEMENTARY INFORMATION

Supplementary Table I. Mean values of cycle level (n=676) variables in cycles using patient's own oocytes (n=351) or donor oocytes (n=325). Student's t-test was applied to compare variables between groups. Values are presented as mean \pm standard deviation [range]. BMI; Body Mass Index. MII; metaphase II oocyte. 2PN; 2 pronuclei zygote. NA; not-applicable. NS; non-significant.

Variable; units	Cycles with own oocytes (n=351)	Cycles with donor oocytes (n=325)	p value
Cycles; %	51.9	48.1	NA
Oocyte age; years	38.3 \pm 4.4 [23-49]	26.5 \pm 5 [18-35]	p < 0.001
Patient age; years	38.3 \pm 4.4 [23-49]	42.1 \pm 4.1 [24-50]	p < 0.001
Female patient BMI; kg/m ²	24.4 \pm 4.4 [16.8-37.6]	24.3 \pm 4.8 [16.9-41.4]	NS
Oocyte donor BMI; kg/m ²	NA	22.9 \pm 3.4 [17-33.7]	NA
MI	6 \pm 4 [1-24]	6.92 \pm 1.7 [4-15]	p < 0.001
2PN	4.1 \pm 3.1 [0-21]	5 \pm 1.8 [0-12]	P < 0.001
Fertilization rate; %	68 \pm 26 [0-100]	72 \pm 21 [0-100]	p = 0.029
Abnormal fertilization rate; %	8.1 \pm 14.9 [0-100]	7.2 \pm 10.3 [0-50]	NS
Mean embryo morphological score	7.2 \pm 1.48 [0-10]	6.75 \pm 1.56 [0-10]	NS
Embryos obtained	4 \pm 2.9 [0-20]	4.6 \pm 1.8 [0-10]	p = 0.001

Supplementary Table II. Statistics for primer pairs used in our study (telomere region, *36B4*). Relationship between Cq values and gDNA concentration was calculated using CFX Manager software (BioRad) to find a slope and intercept which predicts correlation coefficient (R²). qPCR efficiencies (E) were calculated based on the standard curve according to the formula $[E=10^{(-1/\text{slope})}-1] \times 100$ and are expressed as a percentage.

Region/gene	gDNA	Slope	Intercept	Efficiency (%)	R ²	Dilution range
Telomere	HeLa	-2.902	20.32	121.1	0.995	100pg – 10ng
Telomere	Sperm	-3.573	19.39	90.5	0.995	50pg – 5ng
<i>36B4</i>	HeLa	-3.636	29.89	88.4	0.999	100pg – 10ng
<i>36B4</i>	Sperm	-3.580	28.75	90.2	0.998	50pg – 5ng

Supplementary Table III. Information about STL, number of ICSI cycles performed and reproductive outcomes individualized for each sperm donor included in this study (n=60). Reproductive outcomes (biochemical, clinical, ongoing pregnancies, and live birth) are expressed as the ratio of positive results / total number of ICSI cycles with information. Oocyte origin (patient or donor) is indicated between brackets. STL; Sperm telomere length. RU; Relative units. SD; Standard deviation. N; Total number of cycles.

Sperm donor	STL Mean \pm SD (RU)	ICSI cycles N (Patient, Donor)	Biochemical pregnancy Ratio (Patient, Donor)	Clinical pregnancy Ratio (Patient, Donor)	Ongoing pregnancy Ratio (Patient, Donor)	Live birth Ratio (Patient, Donor)
1	3.23 \pm 0.13	12 (7, 5)	4/12 (3/7, 1/5)	4/12 (3/7, 1/5)	4/12 (3/7, 1/5)	4/12 (3/7, 1/5)
2	3.76 \pm 0.84	12 (7, 5)	3/12 (1/7, 2/5)	2/11 (1/7, 1/4)	2/11 (1/7, 1/4)	2/11 (1/7, 1/4)
3	2.59 \pm 0.03	12 (5, 7)	9/12 (3/5, 6/7)	7/12 (2/5, 5/7)	7/12 (2/5, 5/7)	7/12 (2/5, 5/7)
4	3.54 \pm 0.19	12 (4, 8)	3/12 (0/4, 3/8)	1/12 (0/4, 1/8)	1/12 (0/4, 1/8)	1/12 (0/4, 1/8)
5	3.97 \pm 0.10	12 (4, 8)	9/12 (4/4, 5/8)	7/12 (2/4, 5/8)	4/12 (1/4, 3/8)	3/12 (1/4, 2/8)
6	5.08 \pm 1.03	12 (4, 8)	4/12 (0/4, 4/8)	1/12 (0/4, 1/8)	1/12 (0/4, 1/8)	1/12 (0/4, 1/8)
7	4.61 \pm 0.26	12 (6, 6)	5/12 (2/6, 3/6)	3/12 (1/6, 2/6)	3/12 (1/6, 2/6)	3/12 (1/6, 2/6)
8	3.24 \pm 0.20	12 (8, 4)	4/12 (1/8, 3/4)	3/12 (1/8, 2/4)	2/12 (1/8, 1/4)	1/12 (0/8, 1/4)
9	4.74 \pm 0.27	12 (5, 7)	8/12 (3/5, 5/7)	8/12 (3/5, 5/7)	5/12 (1/5, 4/7)	5/12 (1/5, 4/7)
10	3.17 \pm 0.63	12 (8, 4)	7/12 (4/8, 3/4)	5/12 (2/8, 3/4)	5/12 (2/8, 3/4)	5/12 (2/8, 3/4)
11	4.10 \pm 0.13	12 (9, 3)	6/11 (4/8, 2/3)	6/11 (4/8, 2/3)	4/9 (3/7, 1/2)	3/8 (2/6, 1/2)
12	3.51 \pm 0.10	12 (3, 9)	6/11 (1/3, 5/8)	3/11 (1/3, 2/8)	2/11 (1/3, 1/8)	2/11 (1/3, 1/8)
13	2.53 \pm 0.69	12 (6, 6)	6/12 (3/6, 3/6)	3/12 (2/6, 1/6)	3/12 (2/6, 1/6)	3/12 (2/6, 1/6)
14	3.94 \pm 0.20	12 (8, 4)	5/11 (3/7, 2/4)	2/11 (2/7, 0/4)	1/11 (1/7, 0/4)	1/11 (1/7, 0/4)
15	3.36 \pm 0.21	12 (5, 7)	6/10 (2/4, 4/6)	3/9 (1/3, 2/6)	3/9 (1/3, 2/6)	3/9 (1/3, 2/6)
16	3.14 \pm 0.90	12 (7, 5)	7/12 (3/7, 4/5)	5/12 (2/7, 3/5)	5/12 (2/7, 3/5)	4/11 (2/7, 2/4)
17	5.38 \pm 0.16	12 (6, 6)	4/11 (1/5, 3/6)	4/11 (1/5, 3/6)	4/11 (1/5, 3/6)	4/11 (1/5, 3/6)
18	3.89 \pm 0.16	12 (8, 4)	6/11 (3/7, 3/4)	4/11 (1/7, 3/4)	3/11 (1/7, 2/4)	3/11 (1/7, 2/4)
19	3.46 \pm 0.09	12 (8, 4)	2/11 (1/7, 1/4)	1/11 (1/7, 0/4)	1/11 (1/7, 0/4)	1/11 (1/7, 0/4)
20	4.23 \pm 0.29	12 (7, 5)	7/12 (4/7, 3/5)	5/12 (4/7, 1/5)	4/12 (3/7, 1/5)	4/12 (3/7, 1/5)
21	4.29 \pm 0.35	12 (4, 8)	8/12 (3/4, 5/8)	8/12 (3/4, 5/8)	7/12 (2/4, 5/8)	6/11 (2/4, 4/7)
22	2.84 \pm 0.06	12 (7, 5)	5/11 (2/6, 3/5)	3/11 (1/6, 2/5)	3/11 (1/6, 2/5)	3/11 (1/6, 2/5)
23	3.90 \pm 0.15	12 (8, 4)	4/12 (3/8, 1/4)	4/12 (3/8, 1/4)	4/12 (3/8, 1/4)	4/12 (3/8, 1/4)
24	4.50 \pm 0.51	12 (2, 10)	9/12 (0/2, 9/10)	7/12 (0/2, 7/10)	6/12 (0/2, 6/10)	6/12 (0/2, 6/10)
25	5.52 \pm 0.05	12 (6, 6)	7/11 (2/6, 5/5)	6/11 (2/6, 4/5)	5/10 (2/6, 3/4)	3/10 (2/6, 1/4)
26	4.51 \pm 0.62	12 (9, 3)	3/10 (3/7, 0/3)	1/9 (1/6, 0/3)	0/9 (0/5, 0/4)	0/8 (0/5, 0/3)
27	5.98 \pm 0.76	12 (3, 9)	7/12 (1/3, 6/9)	4/12 (1/3, 3/9)	3/11 (1/3, 2/8)	3/11 (1/3, 2/8)
28	2.69 \pm 0.12	12 (1, 11)	6/11 (1/1, 5/10)	4/11 (0/1, 3/10)	3/11 (0/1, 3/10)	3/11 (0/1, 3/10)
29	3.84 \pm 0.06	12 (7, 5)	6/12 (2/7, 4/5)	5/12 (2/7, 3/5)	4/12 (1/7, 3/5)	4/12 (1/7, 3/5)
30	3.00 \pm 0.27	12 (6, 6)	4/9 (1/3, 3/6)	2/9 (1/3, 1/6)	1/9 (0/3, 1/6)	1/9 (0/3, 1/6)
31	3.90 \pm 0.08	12 (6, 6)	8/12 (3/6, 5/6)	7/12 (3/6, 4/6)	6/12 (3/6, 3/6)	6/12 (3/6, 3/6)
32	2.54 \pm 0.95	12 (5, 7)	5/12 (0/5, 5/7)	5/12 (0/5, 5/7)	3/12 (0/5, 3/7)	3/12 (0/5, 3/7)
33	2.42 \pm 0.20	12 (7, 5)	8/12 (4/7, 4/5)	6/12 (3/7, 3/5)	2/9 (0/5, 2/4)	2/9 (0/5, 2/4)

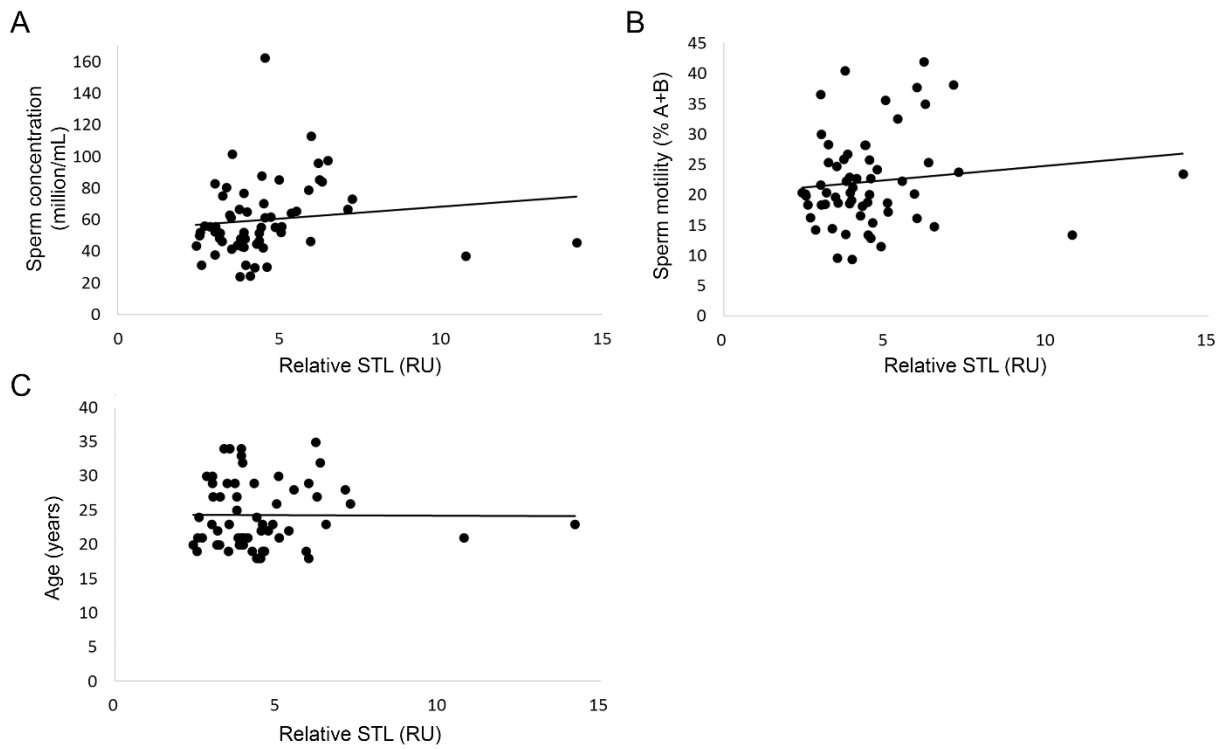
Supplementary Table III (cont.).

Sperm donor	STL Mean \pm SD (RU)	ICSI cycles N (Patient, Donor)	Biochemical pregnancy Ratio (Patient, Donor)	Clinical pregnancy Ratio (Patient, Donor)	Ongoing pregnancy Ratio (Patient, Donor)	Live birth Ratio (Patient, Donor)
34	10.78 \pm 0.46	12 (4, 8)	3/12 (2/4, 1/8)	3/12 (2/4, 1/8)	2/12 (2/4, 0/8)	2/12 (2/4, 0/8)
35	5.06 \pm 0.20	12 (8, 4)	6/12 (3/8, 3/4)	6/12 (3/8, 3/4)	5/12 (3/8, 2/4)	5/12 (3/8, 2/4)
36	4.87 \pm 0.40	12 (8, 4)	3/9 (2/5, 1/4)	3/9 (2/5, 1/4)	3/9 (2/5, 1/4)	3/9 (2/5, 1/4)
37	3.00 \pm 0.25	12 (4, 8)	7/12 (3/4, 4/8)	6/12 (3/4, 3/8)	6/12 (3/4, 3/8)	6/12 (3/4, 3/8)
38	4.46 \pm 0.22	12 (8, 4)	5/11 (3/7, 2/4)	5/11 (3/7, 2/4)	3/11 (2/7, 1/4)	3/11 (2/7, 1/4)
39	4.37 \pm 0.29	6 (4, 2)	2/5 (2/4, 0/1)	2/5 (2/4, 0/1)	2/5 (2/4, 0/1)	1/5 (1/4, 0/1)
40	3.70 \pm 0.74	6 (3, 3)	0/5 (0/2, 0/3)	0/5 (0/2, 0/3)	0/5 (0/2, 0/3)	0/5 (0/2, 0/3)
41	3.02 \pm 0.09	12 (6, 6)	6/12 (2/6, 4/6)	6/12 (2/6, 4/6)	2/12 (1/6, 1/6)	2/12 (1/6, 1/6)
42	4.55 \pm 0.28	12 (5, 7)	6/10 (3/5, 3/5)	5/10 (2/5, 3/5)	4/10 (2/5, 2/5)	4/10 (2/5, 2/5)
43	3.77 \pm 0.03	12 (8, 4)	2/7 (1/3, 1/4)	2/7 (1/3, 1/4)	1/6 (1/2, 0/4)	0/5 (0/2, 0/3)
44	3.01 \pm 0.07	12 (5, 7)	8/12 (3/5, 5/7)	7/12 (3/5, 4/7)	5/12 (1/5, 4/7)	5/12 (1/5, 4/7)
45	4.38 \pm 0.09	11 (5, 6)	7/10 (3/5, 4/5)	5/10 (3/5, 2/5)	5/10 (3/5, 2/5)	5/10 (3/5, 2/5)
46	4.44 \pm 0.19	12 (7, 5)	4/12 (2/7, 2/5)	4/12 (2/7, 2/5)	4/12 (2/7, 2/5)	4/12 (2/7, 2/5)
47	3.99 \pm 0.21	12 (10, 2)	4/11 (3/9, 1/2)	4/11 (3/9, 1/2)	4/11 (3/9, 1/2)	2/10 (1/8, 1/2)
48	7.11 \pm 0.60	8 (2, 6)	3/7 (0/2, 3/5)	2/7 (0/2, 2/5)	2/7 (0/2, 2/5)	2/7 (0/2, 0/5)
49	7.26 \pm 0.18	10 (7, 3)	4/6 (3/5, 1/1)	2/5 (1/4, 1/1)	0/4 (0/3, 0/1)	0/4 (0/3, 0/1)
50	6.24 \pm 0.23	8 (4, 4)	1/5 (0/3, 1/2)	1/5 (0/3, 1/2)	1/5 (0/3, 1/2)	0/4 (0/3, 0/1)
51	5.90 \pm 0.25	12 (6, 6)	6/11 (2/5, 4/6)	5/10 (2/5, 3/5)	4/9 (1/4, 3/5)	1/6 (0/3, 1/3)
52	4.99 \pm 0.51	7 (3, 4)	4/7 (1/3, 3/4)	3/7 (1/3, 2/4)	1/7 (1/3, 0/4)	1/7 (1/3, 0/4)
53	14.21 \pm 0.50	7 (5, 2)	2/5 (1/3, 1/2)	2/5 (1/3, 1/2)	2/5 (1/3, 1/2)	0/3 (0/2, 0/1)
54	6.33 \pm 0.24	12 (5, 7)	5/12 (2/5, 3/7)	5/12 (2/5, 3/7)	3/10 (0/4, 3/6)	1/8 (0/3, 1/5)
55	6.51 \pm 0.40	12 (7, 5)	6/11 (3/7, 3/4)	5/11 (3/7, 2/4)	2/9 (1/6, 1/3)	0/7 (0/5, 0/2)
56	3.50 \pm 0.21	12 (8, 4)	5/11 (1/7, 4/4)	5/11 (1/7, 4/4)	3/11 (1/7, 2/4)	3/11 (1/7, 2/4)
57	5.97 \pm 0.02	12 (6, 6)	6/12 (2/6, 4/6)	6/12 (2/6, 4/6)	6/12 (2/6, 4/6)	6/12 (2/6, 4/6)
58	6.20 \pm 0.69	6 (4, 2)	1/2 (0/1, 1/1)	1/2 (0/1, 1/1)	0/2 (0/1, 0/1)	0/2 (0/1, 0/1)
59	4.55 \pm 0.48	7 (2, 5)	4/6 (1/2, 3/4)	2/5 (1/2, 1/3)	2/5 (1/2, 1/3)	1/5 (0/2, 1/3)
60	3.79 \pm 0.24	12 (11, 1)	4/10 (4/9, 0/1)	4/10 (4/9, 0/1)	4/10 (4/9, 0/1)	1/7 (1/6, 0/1)

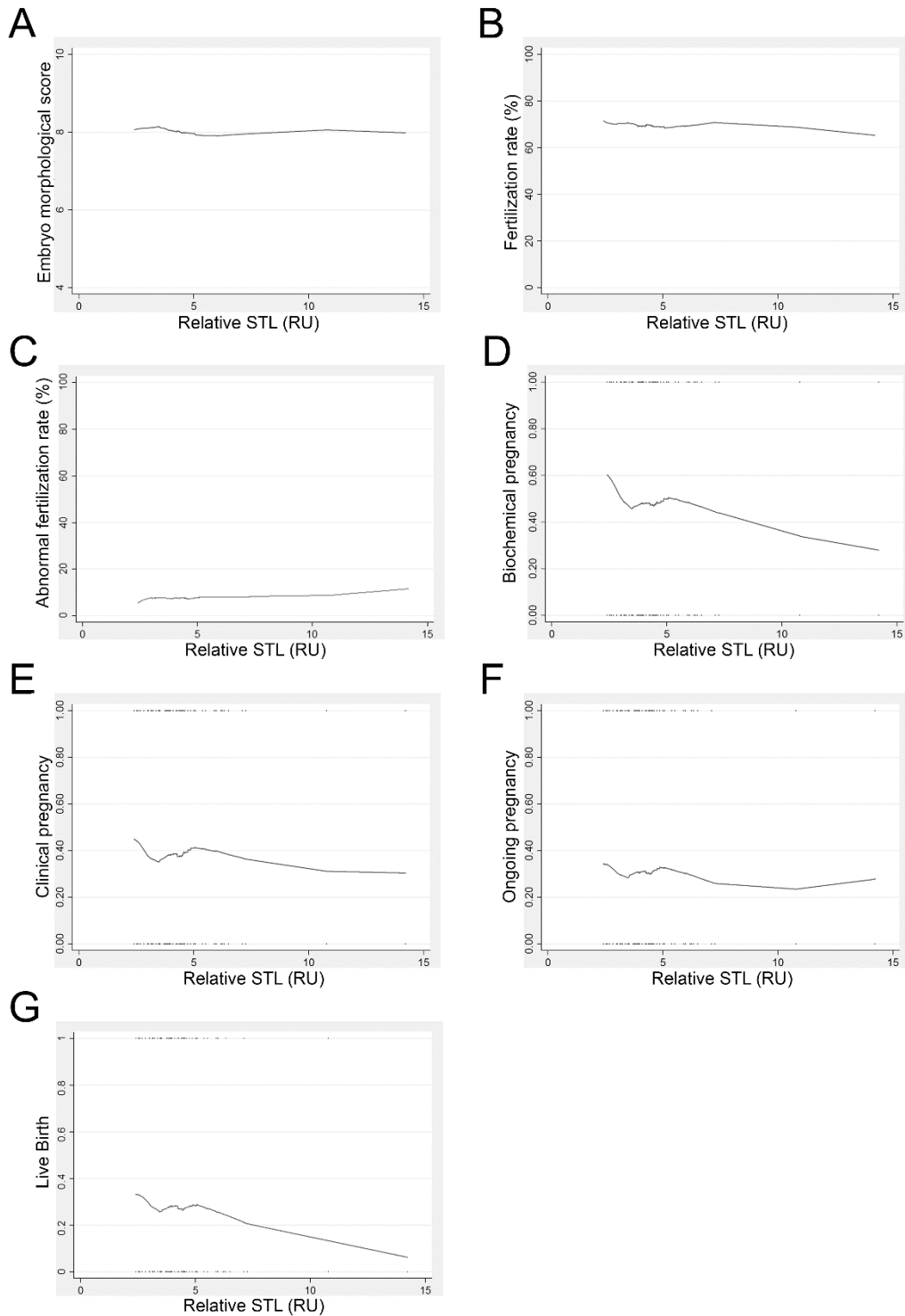
Note:

The decrease observed in the total number of cycles between ICSI cycles (third column) and biochemical pregnancy results (fourth column) is due to absence of embryo transfer (because of fertilization failure, embryo arrest, or embryo freezing without transfer). The decrease observed in the total number of cycles along reproductive outcomes results (fourth to seventh columns) is due to incomplete information about their outcome.

Supplementary Figure 1: Correlation between STL (RU) and sperm concentration (million/mL) (A), sperm motility (% A+B) (B) and sperm donor age (years) (C). n=60 samples.



Supplementary figure 2: Locally Weighted Scatterplot Smoothing (LOWESS) regression of STL (RU) against embryo morphological score (A), fertilization rate (B), abnormal fertilization rate (C), pregnancy rates (biochemical (D), clinical (E) and ongoing (F)) and live birth rate (G).



ADDITIONAL INFORMATION

Analysis of sperm telomere length in samples with previous FF after ICSI

As a complementary study, we tested whether sperm samples with previous FF after ICSI present different levels of sperm telomere length compared to sperm donors with good fertilization rates.

In our previous study (Torra-Massana et al., 2018), we could isolate the statistical effect of the sperm telomere length variable from the female factor, by including samples from men whose sperm was used in between 6 and 12 ICSI cycles. This kind of analysis could not be performed in this complementary study, as the samples with previous FF are from infertile patients (not sperm donors), who perform only one or few ICSI cycles, usually using the oocytes from their partner every time. Nevertheless, we considered appropriate to compare STL in both groups, as FF samples could hide an altered mechanism in telomeres.

A total of 67 sperm donors with good fertilization rates and 26 patients with previous FF after ICSI. STL was determined by qPCR, as described in Torra-Massana et al., 2018. STL differences between groups were evaluated by unpaired t-test comparison, considering $p < 0.05$ as significant.

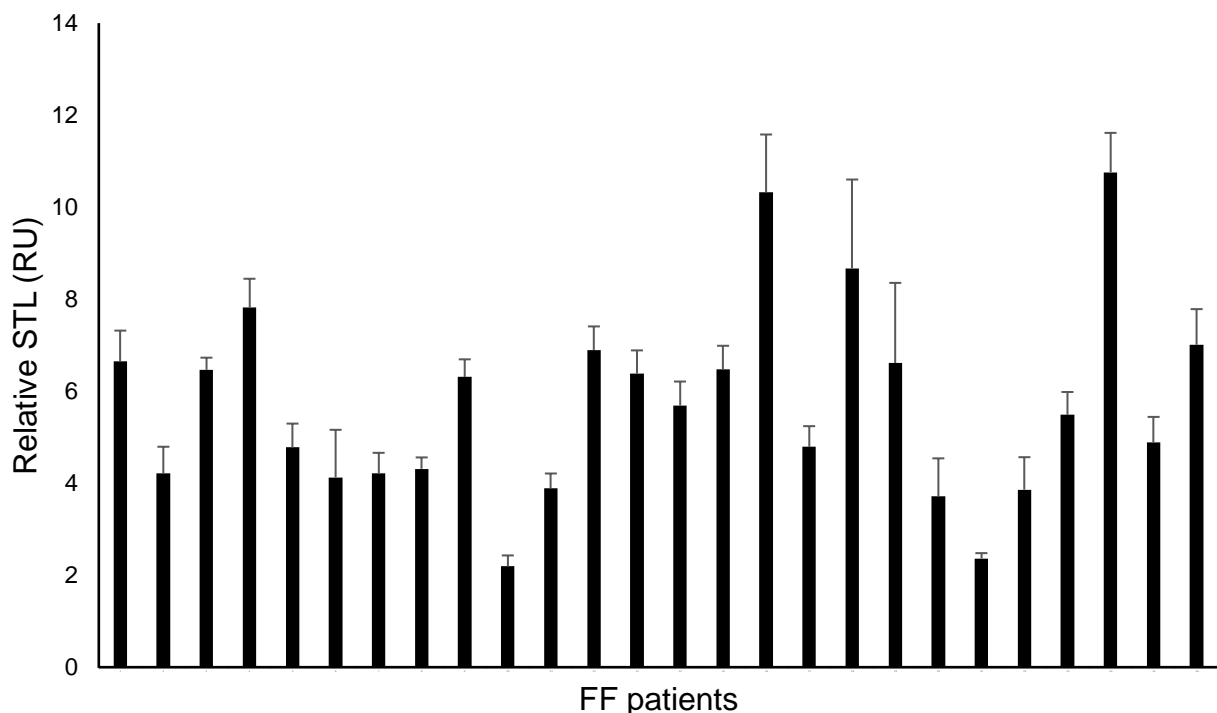


Figure A1. Distribution of sperm telomere length (STL) among FF patients. The T/S ratio (T, amplification value for the telomeric region; S, amplification value for a single copy gene (36B4)) for each FF sample ($n = 26$) was normalized against the T/S ratio from a common gDNA sample (HeLa gDNA). Data is presented as mean values (black columns) and SD (error bars) of triplicate measurements.

The mean STL value in the FF patients was $5.73 \text{ RU} \pm 2.12$ [2.19 – 10.76] (**Figure A1**). The STL obtained in FF patients was significantly higher than the mean STL value obtained in the controls with good fertilization rates: $4.62 \text{ RU} \pm 2.32$ [2.56 – 14.15] ($p = 0.015$) (**Figure A2**).

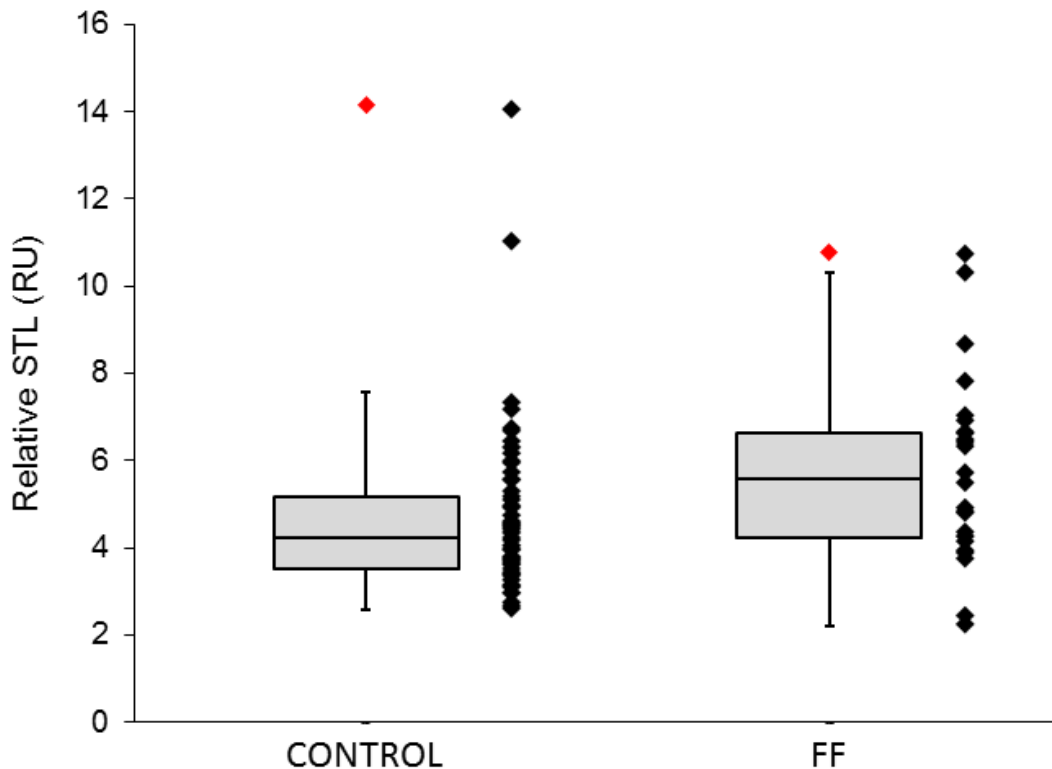


Figure A2. Comparison of relative STL values (expressed in relative units, RU) obtained in both groups (FF and controls). Black dots indicate the STL value for each sperm sample included, while red dots indicate the STL values detected as outliers.

Our results indicate that abnormal STL values could be associated with infertility and, in particular, with fertilization failure after ICSI. Nevertheless, STL levels were higher in samples with FF, which is against the general idea that shorter STL is associated with infertility. There is the possibility that both too long and too short STL may affect fertility, as suggested by Cariati et al., 2016.

Further research is required to assess if STL can be useful as a marker for FF after ICSI. Nevertheless, considering the complexity and diversity of mechanisms potentially explaining FF, the different approaches available for STL measurement, and the high STL variability observed not only between individuals but also between cells in the same ejaculate (Antunes et al., 2015); we hypothesize that STL abnormalities account for very little FF cases (if any), and thus it is difficult to consider STL measurement as a reliable clinical marker.

CHAPTER 4: Prediction of sperm markers involved in oocyte activation by *in silico* analysis of protein-protein interactions

Partial contents of this chapter were included in the following oral presentation:

Marc Torra Massana, Montserrat Barragán Monasterio, Rafael Oliva Virgili, Amelia Rodríguez Aranda, Rita Vassena. **Predicción de marcadores espermáticos de fallo de activación ovocitaria mediante análisis *in silico* de interacciones proteicas.** 32º Congreso Nacional de la Sociedad Española de Fertilidad (SEF) 2018, Madrid, Spain.

INTRODUCTION

Fertilization failure after ICSI is mainly caused by oocyte activation failure (OAF). Some alterations in specific protein factors (either in sperm or the oocyte) have been documented as causes of OAF (Alazami et al., 2015; Sang et al., 2018). However, oocyte activation is a complex process yet to be fully explained, and, in many cases, the alterations leading to FF cannot be identified.

All initial steps of oocyte activation and egg-to-zygote transition occur in the absence of transcription (Evsikov et al., 2006), with proteins and signalling events playing essential roles. The sperm protein phospholipase C zeta (PLC ζ) triggers a specific Ca²⁺ signalling that induces oocyte activation. The mechanism of calcium regulation is tightly controlled in the oocyte, with different protein and membrane channels involved. Most downstream events (cortical granule exocytosis, meiotic resumption and pronuclear formation, among others) depend on different kinases, such as CAMKII, Emi2, or MAPK (Yeste et al., 2016).

As research on human fertilization is a process with intrinsic ethical and legal restrictions, and human oocytes are difficult samples to obtain in most cases (usually reserved for reproductive purposes), most of the knowledge comes from animal models. For this reason, *in silico* approaches can be useful to better characterize the human fertilization process. For example, previous studies used bioinformatic softwares to predict protein-protein interactions (PPI) between sperm and oocyte membrane proteins (Sabetian et al., 2014), implicated in fertilization *in vivo*. Recently, other *in silico* approaches predicted the sperm contribution to fertilization and embryo development from proteomics or transcriptomics libraries, in the mouse model using prediction of PPI (Ntostis et al., 2017), or in humans using gene ontology analysis (Castillo et al., 2018).

To date, few sperm proteins have been described to play essential roles in fertilization though ICSI. Other sperm factors different from PLC ζ could participate in generating calcium signalling in the oocyte, as PLC ζ -KO mice are able to produce some calcium signalling in the oocyte, as well as being able to generate offspring (Nozawa et al., 2018). Moreover, FF can still occur in the clinic when using sperm without any apparent PLC ζ protein defect, even in oocyte donation cycles (Ferrer-Vaquer et al., 2016). Specific sperm proteins could regulate the mechanisms acting downstream of the initial calcium rise, such as MAPK pathway or calcium homeostasis system. While the oocyte is considered to drive these early fertilization events (Yeste et al., 2016), the need of paternal factors is demonstrated by the low efficiencies of parthenogenetic embryo development or somatic nuclear cloning, and the presence of several embryo proteins of suspected male origin (Castillo et al., 2018).

Our hypothesis is that sperm-specific or sperm-enriched proteins are able to participate in the regulation of oocyte activation events. By using *in silico* analysis of protein-protein interactions (PPI), we predicted different potential PPI between sperm proteins and oocyte proteins involved in oocyte activation signalling. We expect that this analysis will be useful as a starting point in the search of new male fertility markers to be used in assisted reproduction, especially for fertilization failure cases due to OAF.

MATERIAL AND METHODS

Generation of sperm proteins list

To identify sperm proteins which could play a role during fertilization, we focused on those genes which were specific to -or enriched in- sperm. We predicted that this subset of genes would be expressed predominantly during spermatogenesis, increasing the chance to find proteins with an important role in sperm function. To this aim, the total list of genes defined as elevated in the testis was downloaded from ProteinAtlas database (n=2,237). We only considered sperm proteins identified by MS proteomics technology, using the most comprehensive proteomics catalogue available, which includes a total of 6,871 sperm proteins found by mass spectrometry (Castillo et al., 2018). Of the 2,237 proteins downloaded, 917 were confirmed by sperm proteomics studies (**Figure 1**). Additionally, the list was manually evaluated, and those proteins with evidence of expression in female tissues and/or without clear enrichment in the testis were eliminated. Finally, we eliminated the proteins found in oocyte proteomics studies. Checking protein lists of the two only far-reaching oocyte proteome analysis available to date: Wang et al., 2010 (mouse oocyte proteome) and Virant-Klun et al., 2016 (human oocyte proteome). For comparison of protein lists and generation of Venn diagrams we used Venny's on-line (<http://bioinfogp.cnb.csic.es/tools/venny/>).

Generation of oocyte activation proteins list

To create a subset of proteins participating in oocyte activation signalling and early fertilization events, the complete list of proteins present in the “Oocyte meiosis” signalling pathway was downloaded from KEGG database (http://www.genome.jp/kegg-bin/show_pathway?hsa04114) (Kanehisa et al., 2016). To have a list as complete as possible, a bibliographic search was conducted, looking for proteins reported to play a role in the early signalling of the oocyte from articles retrieved from PubMed (**Figure 1**). Some of the extra proteins added to the final list include phospholipases different from PLC ζ (PLC β , γ), different members of the PKC family, members

of the store-operated calcium entry system (SOCE) such as STIM1 and ORAI1, Wee1-like protein kinases 1 and 2, SRC family kinases (Fyn, Yes, Src), calcium channels which could play a role in calcium homeostasis in the oocyte (Ryr2, TRPV3 and 4, membrane ATPases), as well as other kinases like PTK2 and PTK2B (Schmitt and Nebreda, 2002; Ducibella and Fissore, 2008; Yeste et al., 2016; Martin et al., 2016; Xu and Yang, 2017). As we wanted to focus on the processes happening after sperm-entry into the oocyte, membrane or zona-pellucida proteins reported to have a role in sperm-egg binding were not included in the list (i.e. JUNO, ZPs, etc.).

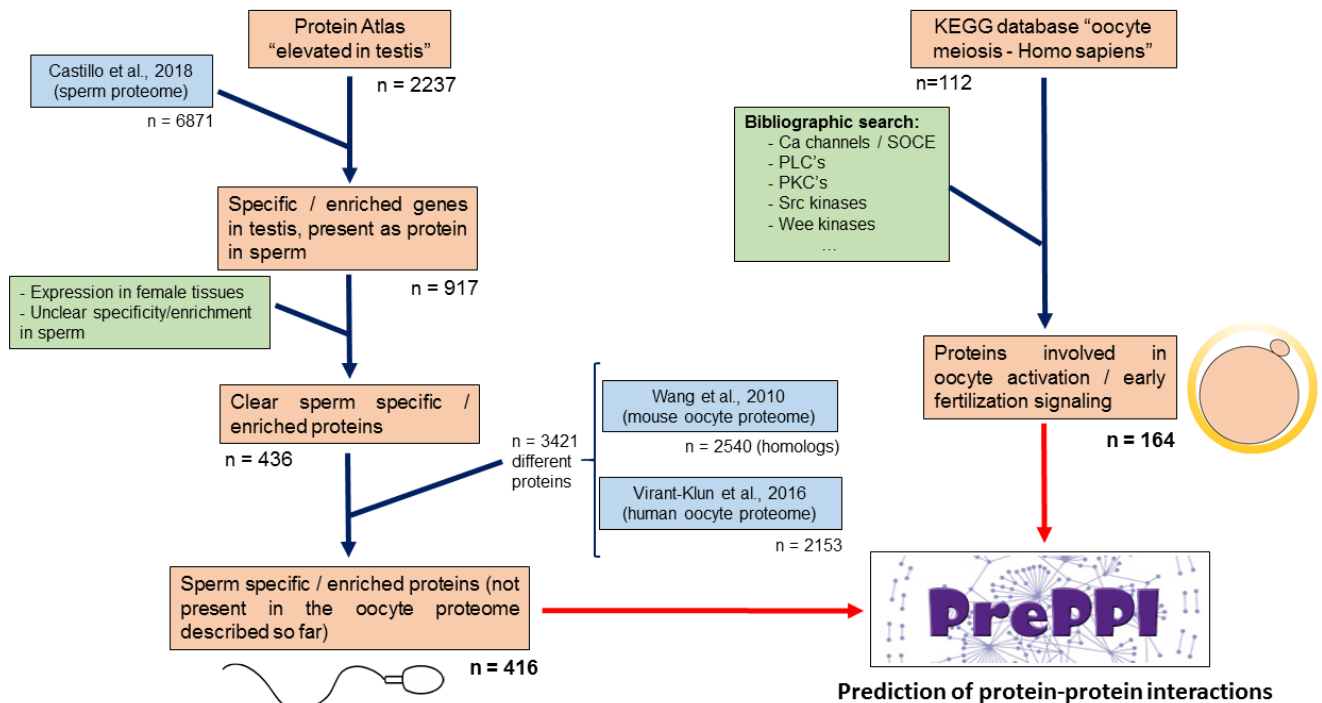


Figure 1. General strategy used to generate lists of sperm-specific proteins and oocyte proteins involved in the oocyte activation signalling pathway. ProteinAtlas was used as the main source of testis-enriched proteins, this data was combined with the available information from the sperm and oocyte proteomes described in the literature, and manually annotated to eliminate proteins with potential expression in female tissues. KEGG database was used as the main source of oocyte proteins.

Prediction of protein-protein interactions

The PrePPI database was used to predict PPI between sperm and oocyte proteins (<https://honiglab.c2b2.columbia.edu/PrePPI/>) (Zhang et al., 2013). PrePPI is a database of predicted and experimentally determined protein-protein interactions (PPI) for the human proteome. Predicted interactions in the database are determined using a Bayesian framework that combines structural, functional, and evolutionary and expression information. The main advantage of this method is that protein 3D structural information is included in the prediction of PPI.

The PrePPI database uses all separate prediction parameters to assign a final probability to each PPI (0.5 - 1). Only those interactions with an assigned final probability of ≥ 0.85 were annotated in our analysis.

Analysis of protein candidates and PPI network

In order to validate the list of sperm candidates selected, we compared the list of sperm proteins with previous studies which reported list of testis-enriched genes / proteins (Djureinovic et al., 2014).

The major molecular functions of our candidate list and interactors found after PrePPI analysis were identified using the ClueGo plugin of Cytoscape (Bindea et al., 2009), a tool able to visualize the non-redundant biological terms for large clusters of genes.

Relevance of predicted interactions was assessed considering their associated final probability, the predicted score value, and the molecular and biological function reported in the bibliography of the interactors involved for each PPI.

RESULTS

Selection of sperm and oocyte interaction candidates

The final list of sperm candidates contained 416 proteins. In 2014, Djureinovic and colleagues reported a list of 364 genes highly expressed in testis, 188 of which were present in the sperm proteome (reported in Castillo et al., 2018), of which 167 (88.8 %) were present in our final sperm list. This comparison indicates that our list contains a high percentage of sperm-specific proteins previously described using experimental techniques and confirmed by other authors.

ClueGo analysis revealed that the main biological processes in the list of sperm proteins are fertilization, cilium movement and sexual reproduction (**Figure 2A**). Other relevant sperm functions are sperm capacitation, acrosome assembly, sperm motility or penetration to zona pellucida.

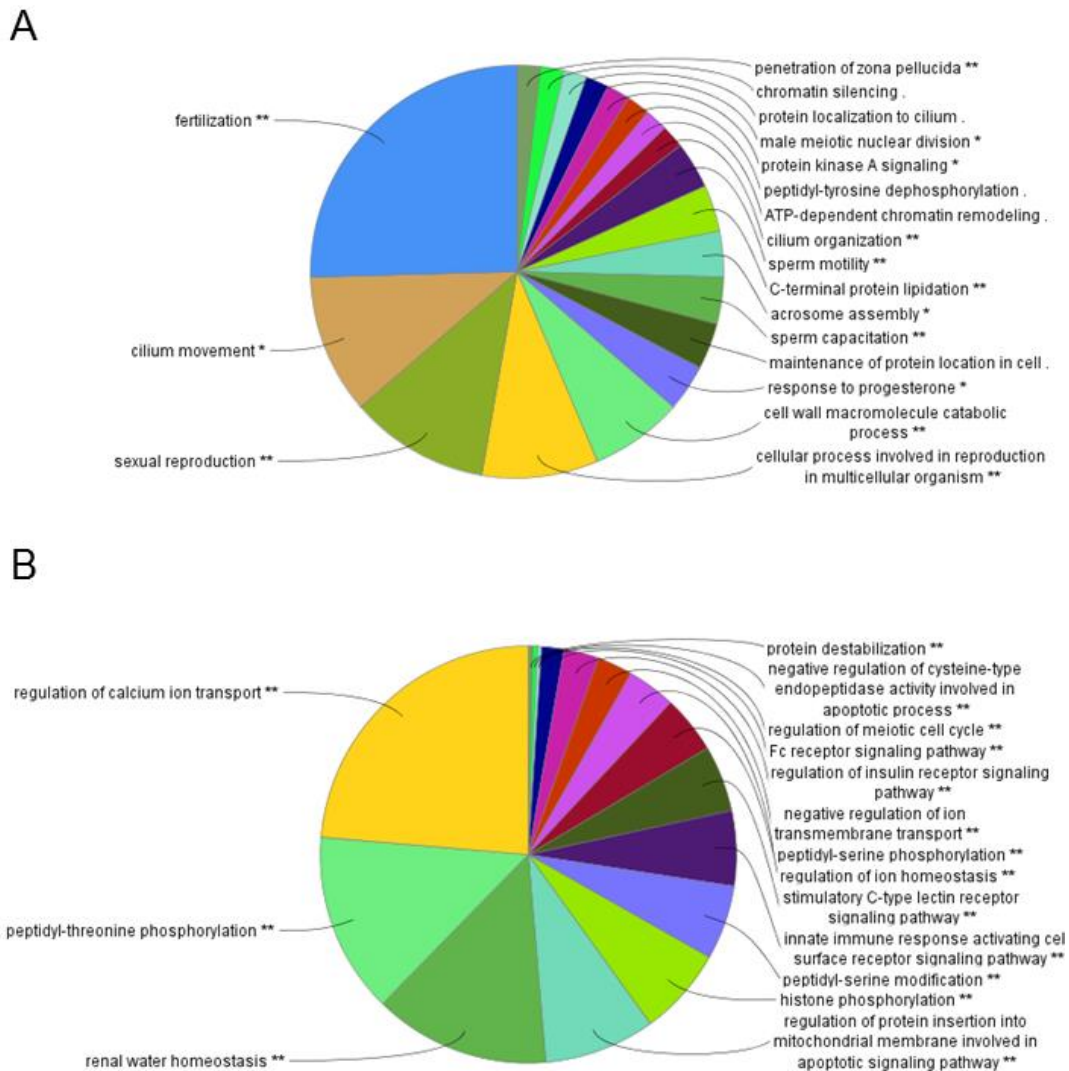


Figure 2. Gene ontology analysis of non-redundant biological terms performed using ClueGO plug-in in Cytoscape, for all sperm specific proteins included in the study (**A**), and the oocyte activation proteins involved in the predicted PPI (**B**).

The final list of potential interactors participating in oocyte activation signalling and early fertilization contained a total of 163 proteins. 80 of these proteins were not present in the complete sperm proteome, meaning that they have more chances to be “oocyte exclusive” and interactions involved less likely to occur during spermatogenesis or other sperm functions prior to oocyte activation.

Prediction and analysis of protein-protein interactions

By using the PrePPI database, a total of 151 PPIs with an assigned final probability ≥ 0.85 were predicted to occur between paternal and maternal proteins in pathways involved in oocyte activation (**Supplementary Table I**), 46 of them (30.5 %) with an interaction probability above

0.95. The predicted interactions comprise 69 different sperm proteins and 57 proteins involved in oocyte activation. The two main biological functions found in oocyte interactors were regulation of calcium transport and peptidyl-threonine phosphorylation, both functions essential to oocyte activation (**Figure 2B**).

The sperm proteins which participated in more interactions were TSSK2 (14 interactions), TSSK6 (11 interactions), TSSK1B (9 interactions), CSNK1A1L (9 interactions), SUV39H2 (8 interactions), CATSPER1 (6 interactions), and TEX14 (6 interactions). Conversely, the oocyte activation proteins participating in a higher number of interactions were proto-oncogene tyrosine-protein kinase SRC kinase (27 interactions), cyclin-dependent kinase 2 (11 interactions), tyrosine-protein kinase Fyn (8 interactions), serine/threonine-protein kinase PLK1 (5 interactions), and calmodulin-1 (5 interactions).

Table 1. Sperm-specific or enriched kinases and phosphatases predicted to interact with proteins participating in oocyte activation signalling cascade by using PrePPi database (final probability of the interaction > 0.85).

Protein symbol	Protein name	Oocyte interactors (protein name)
CSNK1A1L	Casein kinase I isoform alpha-like	BTRC, CDK1, CDK2, PLK1, PPP2CA, PRKACA, PRKCD, PRKCQ, SRC
DUSP15	Dual specificity protein phosphatase 15	PLCG1, FYN, SRC
GK2	Glycerol kinase 2	PLCG2
GK3P	Glycerol kinase 3	PLCG2
STKLD1	Serine/threonine kinase-like domain-containing protein STKLD1	PRKCB, PRKCQ, SRC
TEX14	Inactive serine/threonine-protein kinase TEX14	CDK2, FYN, PRKCD, PRKCE, SRC, YES1
TPTE	Putative tyrosine-protein phosphatase TPTE	SRC
TSSK1B	Testis-specific serine/threonine-protein kinase 1	CCNB1, CDK2, MOS, PLK1, PRKACA, PRKACG, PRKCA, RPS6KA3, SRC
TSSK2	Testis-specific serine/threonine-protein kinase 2	CAMK2A, CAMK2B, CCNB1, CDK2, MAPK1, MAPK12, PLK1, PRKACA, PRKACG, PRKCA, PRKCB, PRKCQ, PRKCZ, SRC
TSSK3	Testis-specific serine/threonine-protein kinase 3	CDK2, SRC, AURKA, CCNB1
TSSK6	Testis-specific serine/threonine-protein kinase 6	CAMK2D, CCNB1, CDK1, CDK2, PRKACG, PRKCA, PRKCB, PRKCE, PRKCZ, PTK2B, SRC

34 out of 151 predicted PPI (23.2 %) were previously validated experimentally, as indicated in **Supplementary Table I**. As some interesting examples, the interaction between sperm ODF2 and

PLK1 could be involved in centrosome function (Soung et al., 2009), or the interaction between Mos kinase and sperm CCDC136.

Finally, we considered it relevant to focus on the specific group of sperm proteins able to participate in phosphorylation events. A total of 11 different sperm kinases and phosphatases appeared in our interaction network, participating in 62 PPI (**Table I**). Interestingly, different members of the TSSK kinases family appeared in our analysis in a recurrent manner, participating in up to 38 PPI, including oocyte interactors such as PKC, CDK1, Mos kinase or CAMKII.

DISCUSSION

Overall, our analysis uncovered a list of sperm proteins with potential function during oocyte activation. We hypothesize that sperm function in oocyte activation is not limited to the initial calcium signalling triggered by PLC ζ . Despite most of the signalling cascade observed in oocyte activation is carried by oocyte protein, specific sperm kinases and other proteins could contribute to early fertilization events required to start embryo development. Previous efforts were made to characterize the function of testis-enriched genes with unknown role during the fertilization process. In Miyata et al., 2016, 54 genes were demonstrated to have little impact on fertility in mice. Some of these sperm genes were found in the PPI predicted, for example Ubqln3, the proteinase Capn11, and some members of the lysozyme-like superfamily (Lyzl1, Lyzl4, Spaca3). Although the role of these genes in human male fertility is unknown, they are likely to have little or absent effect on fertilization.

Although oocyte proteome studies are scarce and the oocyte proteome is still incompletely characterized, we did not include proteins demonstrated to be present in the oocyte by mass-spectrometry techniques, in order to increase the probability of finding sperm-oocyte PPI and to reduce the probability of predicting oocyte-oocyte PPI. Proteins eliminated include some factors previously reported to play important roles in the oocyte, such as pachytene checkpoint protein 2 homolog (Rinaldi et al., 2017) or DDX4 (Silvestris et al., 2018), among others.

The PrePPI analysis results involved some proteins which, despite participating in several interactions, are not likely to play essential roles during fertilization or have high chances to be occurring in other biological processes. For example, Src kinase binds to different sperm partners, but Src kinase role in the oocyte is still discussed (Kinsey, 2014). Another example is CATSPER, a sperm protein which participates in some predicted PPI, but both the molecular characteristics of the protein (membrane calcium receptor essential for sperm motility) and the fact that sperm from

CATSPER-KO mice are able to fertilize zona-pellucida free eggs suggest little importance of this protein in signalling events after sperm-entry into the oocyte.

Different sperm proteins could play a more relevant role in oocyte signalling. For example, TSSK family is a group of proteins particularly represented in our prediction (TSSK1B, TSSK2, TSSK3 and TSSK6 in our analysis), forming part of up to 38 interactions with oocyte proteins. Previous studies have demonstrated an important role of these kinases in spermatogenesis. Interestingly, some of these proteins are present in the mature sperm (Li et al., 2011), indicating a possible role for sperm function. Mice-KO studies indicate that TSSK6 is essential for fertilization, being the responsible of Izumo relocalization during acrosome reaction (Sosnik et al., 2009). Although sperm from this TSSK6-KO mice are able to activate the oocyte when doing ICSI, additional post-sperm-entry functions for this or other TSSK kinases are still a possibility taking into account their predicted interactions with PKC, PLK1, MAPK members such as MOS, CamKII, aurora kinase A, or CDK2, among other factors. Other sperm kinases participating in different interactions were STKLD1 kinase, Casein kinase I, or dual specificity protein phosphatase 15.

Additionally, some protein with protease activity are also present. For example, acrosin interaction with adenylate cyclase could play a role in fertilization, as previously reported (Adeniran et al., 1995). However, acrosin KO mice are fertile, and the only important role for this acrosomal protease has been described in sperm penetration.

CCDC136, a testis-specific protein recently reported to play important roles in acrosome formation and fertilization (Geng et al., 2016), was found to interact with MOS, a kinase responsible for MAPK signaling triggering. Inhibition of CCDC136 results in reduced fertilization rates though IVF (Geng et al., 2016).

Our analysis presents some limitations. First, the molecular mechanisms and specific proteins from the oocyte participating in the oocyte activation process are not completely described, and KEGG “oocyte meiosis” pathway was constructed taking into account experimental data from animals models such as *Xenopus*; we estimate that many other proteins may participate in the signalling process. For example, in addition to the different calcium channels included, others still unknown channels are expected to be involved. Second, we focused on a very specific signalling within oocyte activation, including several kinases and calcium regulation, but other cellular processes occur which are expected to comprise many other proteins, from both sperm and oocyte: pronuclear formation, meiotic resumption and gene expression regulation, etc. Third, and as previously mentioned, it is possible that some of the specific interactions detected occur in previous processes such as spermatogenesis. In this case, despite the interactions have potential to be established, they

may not occur during fertilization, or may not have any biological relevance. Fourth, other mechanisms of regulation different from direct PPI may participate during fertilization: post-translational modifications, regulation of gene expression, etc.

Our analysis suggests the existence of paternal proteins with potential to be involved in early stages of fertilization. Future research will be necessary to confirm these PPI in the fertilized oocyte, as well as to assess if some sperm proteins can be used as fertility markers for patients undergoing assisted reproduction.

REFERENCES

- Adeniran AJ, Shoshani I, Minuth M, Awad JA, Elce JS, Johnson RA. Purification, characterization, and N-terminal amino acid sequence of the adenylyl cyclase-activating protease from bovine sperm. *Biol Reprod* 1995; 52:490-9.
- Alazami AM, Awad SM, Coskun S, Al-Hassan S, Hijazi H, Abdulwahab FM, Poizat C, Alkuraya FS. TLE6 mutation causes the earliest known human embryonic lethality. *Genome Biol* 2015; 16:240.
- Bindea G, Mlecnik B, Hackl H, Charoentong P, Tosolini M, Kirilovsky A, Fridman WH, Pagès F, Trajanoski Z, Galon J. ClueGO: a Cytoscape plug-in to decipher functionally grouped gene ontology and pathway annotation networks. *Bioinformatics* 2009; 25:1091-3.
- Castillo J, Jodar M, Oliva R. The contribution of human sperm proteins to the development and epigenome of the preimplantation embryo. *Hum Reprod Update* 2018; 24:535-555.
- Djureinovic D, Fagerberg L, Hallström B, Danielsson A, Lindskog C, Uhlén M, Pontén F. The human testis-specific proteome defined by transcriptomics and antibody-based profiling. *Mol Hum Reprod* 2014; 20:476-88.
- Ducibella T, Fissore R. The roles of Ca²⁺, downstream protein kinases, and oscillatory signaling in regulating fertilization and the activation of development. *Dev Biol* 2008; 315:257-79.
- Evsikov AV, Graber JH, Brockman JM, Hampl A, Holbrook AE, Singh P, Eppig JJ, Solter D, Knowles BB. Cracking the egg: molecular dynamics and evolutionary aspects of the transition from the fully grown oocyte to embryo. *Genes Dev* 2006; 20:2713-27.
- Ferrer-Vaquero A, Barragan M, Freour T, Vernaev V, Vassena R. PLC ζ sequence, protein levels, and distribution in human sperm do not correlate with semen characteristics and fertilization rates after ICSI. *J Assist Reprod Genet* 2016; 33:747-56.
- Geng Q, Ni L, Ouyang B, Hu Y, Zhao Y, Guo J. A Novel Testis-Specific Gene, Ccdc136, Is Required for Acrosome Formation and Fertilization in Mice. *Reprod Sci* 2016; 23:1387-96.
- Kanehisa M, Furumichi M, Tanabe M, Sato Y, Morishima K. KEGG: new perspectives on genomes, pathways, diseases and drugs. *Nucleic Acids Res* 2017; 45:D353-D361.
- Kinsey WH. SRC-family tyrosine kinases in oogenesis, oocyte maturation and fertilization: an evolutionary perspective. *Adv Exp Med Biol* 2014; 759:33-56.
- Li Y, Sosnik J, Brassard L, Reese M, Spiridonov NA, Bates TC, Johnson GR, Anguita J, Visconti PE, Salicioni AM. Expression and localization of five members of the testis-specific serine kinase (Tssk) family in mouse and human sperm and testis. *Mol Hum Reprod* 2011; 17:42-56.

- Martin JH, Bromfield EG, Aitken RJ, Nixon B. Biochemical alterations in the oocyte in support of early embryonic development. *Cell Mol Life Sci* 2017; 74:469-485.
- Miyata H, Castaneda JM, Fujihara Y, Yu Z, Archambeault DR, Isotani A, Kiyozumi D, Kriseman ML, Mashiko D, Matsumura T, Matzuk RM, Mori M, Noda T, Oji A, Okabe M, Prunskaitė-Hyyryläinen R, Ramirez-Solis R, Satouh Y, Zhang Q, Ikawa M, Matzuk MM. Genome engineering uncovers 54 evolutionarily conserved and testis-enriched genes that are not required for male fertility in mice. *Proc Natl Acad Sci USA* 2016; 113:7704-10.
- Nozawa K, Satouh Y, Fujimoto T, Oji A, Ikawa M. Sperm-borne phospholipase C zeta-1 ensures monospermic fertilization in mice. *Sci Rep* 2018; 8:1315.
- Ntostis P, Carter D, Iles D, Huntriss J, Tzetis M, Miller D. Potential sperm contributions to the murine zygote predicted by in silico analysis. *Reproduction* 2017; 154:777-788.
- Rinaldi VD, Hsieh K, Munroe R, Bolcun-Filas E, Schimenti JC. Pharmacological Inhibition of the DNA Damage Checkpoint Prevents Radiation-Induced Oocyte Death. *Genetics* 2017; 206:1823-1828.
- Sabetian S, Shamsir MS, Abu Naser M. Functional features and protein network of human sperm-egg interaction. *Syst Biol Reprod Med* 2014; 60:329-37.
- Sang Q, Li B, Kuang Y, Wang X, Zhang Z, Chen B, Wu L, Lyu Q, Fu Y, Yan Z, Mao X, Xu Y, Mu J, Li Q, Jin L, He L, Wang L. Homozygous Mutations in WEE2 Cause Fertilization Failure and Female Infertility. *Am J Hum Genet* 2018; 102(4):649-657.
- Schmitt A, Nebreda AR. Signalling pathways in oocyte meiotic maturation. *J Cell Sci* 2002; 115:2457-9.
- Silvestris E, Cafforio P, D'Oronzo S, Felici C, Silvestris F, Loverro G. In vitro differentiation of human oocyte-like cells from oogonial stem cells: single-cell isolation and molecular characterization. *Hum Reprod* 2018; 33:464-473.
- Sosnik J, Miranda PV, Spiridonov NA, Yoon SY, Fissore RA, Johnson GR, Visconti PE. Tssk6 is required for Izumo relocalization and gamete fusion in the mouse. *J Cell Sci* 2009; 122:2741-9.
- Soung NK, Park JE, Yu LR, Lee KH, Lee JM, Bang JK, Veenstra TD, Rhee K, Lee KS. Plk1-dependent and -independent roles of an ODF2 splice variant, hCenexin1, at the centrosome of somatic cells. *Dev Cell* 2009; 16:539-50.
- Virant-Klun I, Leicht S, Hughes C, Krijgsveld J. Identification of Maturation-Specific Proteins by Single-Cell Proteomics of Human Oocytes. *Mol Cell Proteomics* 2016; 15:2616-27.
- Wang S, Kou Z, Jing Z, Zhang Y, Guo X, Dong M, Wilmut I, Gao S. Proteome of mouse oocytes at different developmental stages. *Proc Natl Acad Sci USA* 2010; 107:17639-44.
- Xu YR, Yang WX. Calcium influx and sperm-evoked calcium responses during oocyte maturation and egg activation. *Oncotarget* 2017; 8:89375-89390.
- Yeste M, Jones C, Amdani SN, Patel S, Coward K. Oocyte activation deficiency: a role for an oocyte contribution? *Hum Reprod Update* 2016; 22:23-47.
- Zhang QC, Petrey D, Garzón J, Deng L, Honig B. PrePPI: a structure-informed database of protein-protein interactions. *Nucleic Acids Res* 2013; 41:D828-33.

SUPPLEMENTARY MATERIAL

Supplementary Table I. List of predicted protein-protein interactions by PrePPI database. Each line includes one interaction between a sperm-specific protein and a protein involved in oocyte activation signalling. PrePPI algorithm assigns a final probability (FP) between (from 0 to 1) to each PPI, based on experimental evidence, 3D protein structure and gene ontology information. The interactions previously experimentally demonstrated are indicated in the last column with the letter “EXP”.

OOCYTE ACTIVATION PROTEINS		SPERM SPECIFIC PROTEINS		
Protein symbol	Protein name	Protein symbol	Protein name	FP
CUL1	Cullin-1	CAND2	Cullin-associated NEDD8-dissociated protein 2	1 EXP
PRKCA	Protein kinase C alpha type	HIST1H1T	Histone H1t	1 EXP
CALM1	Calmodulin-1	CETN1	Centrin-1	1 EXP
CCNE1	G1/S-specific cyclin-E1	CETN1	Centrin-1	1 EXP
PLK1	Serine/threonine-protein kinase PLK1	ODF2	Outer dense fiber protein 2	1 EXP
SRC	Proto-oncogene tyrosine-protein kinase Src	SPACA3	Sperm acrosome membrane-associated protein 3	1
CDK2	Cyclin-dependent kinase 2	RPL10L	60S ribosomal protein L10-like	1 EXP
SRC	Proto-oncogene tyrosine-protein kinase Src	DUSP15	Dual specificity protein phosphatase 15	1 EXP
PLCG1	1-phosphatidylinositol 4,5-bisphosphate phosphodiesterase gamma-1	DUSP15	Dual specificity protein phosphatase 15	1
CUL1	Cullin-1	LYAR	Cell growth-regulating nucleolar protein	1 EXP
FYN	Tyrosine-protein kinase Fyn	CELSR3	Cadherin EGF LAG seven-pass G-type receptor 3	1 EXP
CDK2	Cyclin-dependent kinase 2	HIST1H1T	Histone H1t	0,99
SRC	Proto-oncogene tyrosine-protein kinase Src	KLHL10	Kelch-like protein 10	0,99
SRC	Proto-oncogene tyrosine-protein kinase Src	TEX14	Inactive serine/threonine-protein kinase TEX14	0,99
MOS	Proto-oncogene serine/threonine-protein kinase mos	SPERT	Spermatid-associated protein	0,99 EXP
SMC1A	Structural maintenance of chromosomes protein 1A	DDI1	Protein DDI1 homolog 1	0,99 EXP
MOS	Proto-oncogene serine/threonine-protein kinase mos	CCDC136	Coiled-coil domain-containing protein 136	0,99 EXP
CUL1	Cullin-1	RPL10L	60S ribosomal protein L10-like	0,99 EXP
FYN	Tyrosine-protein kinase Fyn	SUV39H2	Histone-lysine N-methyltransferase SUV39H2	0,99 EXP
PLCG1	1-phosphatidylinositol 4,5-bisphosphate phosphodiesterase gamma-1	SUV39H2	Histone-lysine N-methyltransferase SUV39H2	0,99 EXP
FYN	Tyrosine-protein kinase Fyn	TSKS	Testis-specific serine kinase substrate	0,99 EXP
PRKCQ	Protein kinase C theta type	CETN1	Centrin-1	0,98
SRC	Proto-oncogene tyrosine-protein kinase Src	LYZL4	Lysozyme-like protein 4	0,98
CACNA1H	Voltage-dependent T-type calcium channel subunit alpha-1H	CATSPER2	Cation channel sperm-associated protein 2	0,98

RYR3	Ryanodine receptor 3	CATSPER2	Cation channel sperm-associated protein 2	0,98
PRKCA	Protein kinase C alpha type	TSSK1B	Testis-specific serine/threonine-protein kinase 1	0,98
PRKACG	cAMP-dependent protein kinase catalytic subunit gamma	DHH	Desert hedgehog protein	0,97
SRC	Proto-oncogene tyrosine-protein kinase Src	LYZL1	Lysozyme-like protein 1	0,97
SRC	Proto-oncogene tyrosine-protein kinase Src	LYZL2	Lysozyme-like protein 2	0,97
PPP2CA	Serine/threonine-protein phosphatase 2A catalytic subunit alpha isoform	CSNK1A1L	Casein kinase I isoform alpha-like	0,97
SKP1	S-phase kinase-associated protein 1	TTC21A	Tetratricopeptide repeat protein 21A	0,97 EXP
RYR3	Ryanodine receptor 3	CATSPER1	Cation channel sperm-associated protein 1	0,97
SRC	Proto-oncogene tyrosine-protein kinase Src	CAPZA3	F-actin-capping protein subunit alpha-3	0,97
SKP1	S-phase kinase-associated protein 1	FBXO24	F-box only protein 24	0,96
SRC	Proto-oncogene tyrosine-protein kinase Src	UBL4B	Ubiquitin-like protein 4B	0,96
TRPV3	Transient receptor potential cation channel subfamily V member 3	CATSPER1	Cation channel sperm-associated protein 1	0,96
PRKCA	Protein kinase C alpha type	TSSK2	Testis-specific serine/threonine-protein kinase 2	0,96
PRKCA	Protein kinase C alpha type	TSSK6	Testis-specific serine/threonine-protein kinase 6	0,96
PTK2B	Protein-tyrosine kinase 2-beta	TSSK6	Testis-specific serine/threonine-protein kinase 6	0,96
CDK2	Cyclin-dependent kinase 2	SUV39H2	Histone-lysine N-methyltransferase SUV39H2	0,96
FBXO5	F-box only protein 5	SUV39H2	Histone-lysine N-methyltransferase SUV39H2	0,96
PRKCD	Protein kinase C delta type	ART3	Ecto-ADP-ribosyltransferase 3	0,95 EXP
CAMK2D	Calcium/calmodulin-dependent protein kinase type II subunit beta	IQCF1	IQ domain-containing protein F1	0,95 EXP
CALM1	Calmodulin-1	CATSPER1	Cation channel sperm-associated protein 1	0,95
PRKCQ	Protein kinase C theta type	TSSK2	Testis-specific serine/threonine-protein kinase 2	0,95
CDK2	Cyclin-dependent kinase 2	TSSK3	Testis-specific serine/threonine-protein kinase 3	0,95
ADCY8	Adenylate cyclase type 8	ACR	Acrosin	0,94
FYN	Tyrosine-protein kinase Fyn	TEX14	Inactive serine/threonine-protein kinase TEX14	0,94
FYN	Tyrosine-protein kinase Fyn	SPACA3	Sperm acrosome membrane-associated protein 3	0,94
CAMK2A	Calcium/calmodulin-dependent protein kinase type II subunit alpha	TSSK2	Testis-specific serine/threonine-protein kinase 2	0,94
FYN	Tyrosine-protein kinase Fyn	SH3GL3	Endophilin-A3	0,94
SRC	Proto-oncogene tyrosine-protein kinase Src	SH3GL3	Endophilin-A3	0,94
RPS6KA3	Ribosomal protein S6 kinase alpha-3	TSSK1B	Testis-specific serine/threonine-protein kinase 1	0,94
FYN	Tyrosine-protein kinase Fyn	DUSP15	Dual specificity protein phosphatase 15	0,94 EXP
CDK2	Cyclin-dependent kinase 2	POTEF	POTE ankyrin domain family member F	0,93
STIM2	Stromal interaction molecule 2	CATSPER1	Cation channel sperm-associated protein 1	0,93

SRC	Proto-oncogene tyrosine-protein kinase Src	TSSK2	Testis-specific serine/threonine-protein kinase 2	0,93
SRC	Proto-oncogene tyrosine-protein kinase Src	TSSK3	Testis-specific serine/threonine-protein kinase 3	0,93
SRC	Proto-oncogene tyrosine-protein kinase Src	TSSK1B	Testis-specific serine/threonine-protein kinase 1	0,93
PRKACG	cAMP-dependent protein kinase catalytic subunit gamma	TSSK1B	Testis-specific serine/threonine-protein kinase 1	0,93
ADCY5	Adenylate cyclase type 5	ACR	Acrosin	0,92
ADCY1	Adenylate cyclase type 1	ACR	Acrosin	0,92
PRKCE	Protein kinase C epsilon type	TEX14	Inactive serine/threonine-protein kinase TEX14	0,92
CCNB1	G2/mitotic-specific cyclin-B1	TSSK2	Testis-specific serine/threonine-protein kinase 2	0,92
PRKCB	Protein kinase C beta type	TSSK6	Testis-specific serine/threonine-protein kinase 6	0,92
PRKCE	Protein kinase C epsilon type	TSSK6	Testis-specific serine/threonine-protein kinase 6	0,92
CAMK2D	Calcium/calmodulin-dependent protein kinase type II subunit beta	TSSK6	Testis-specific serine/threonine-protein kinase 6	0,92
CDK1	Cyclin-dependent kinase 1	SUV39H2	Histone-lysine N-methyltransferase SUV39H2	0,92
SRC	Proto-oncogene tyrosine-protein kinase Src	TPTE	Putative tyrosine-protein phosphatase TPTE	0,91
CDK2	Cyclin-dependent kinase 2	TEX14	Inactive serine/threonine-protein kinase TEX14	0,91
PRKCD	Protein kinase C delta type	TEX14	Inactive serine/threonine-protein kinase TEX14	0,91
SRC	Proto-oncogene tyrosine-protein kinase Src	CSNK1A1L	Casein kinase I isoform alpha-like	0,91
PLK1	Serine/threonine-protein kinase PLK1	CSNK1A1L	Casein kinase I isoform alpha-like	0,91
BTRC	F-box/WD repeat-containing protein 1A	CSNK1A1L	Casein kinase I isoform alpha-like	0,91
SRC	Proto-oncogene tyrosine-protein kinase Src	STKLD1	Serine/threonine kinase-like domain-containing protein STKLD1	0,91
PRKACG	cAMP-dependent protein kinase catalytic subunit gamma	TSSK2	Testis-specific serine/threonine-protein kinase 2	0,91
PRKCZ	Protein kinase C zeta type	TSSK2	Testis-specific serine/threonine-protein kinase 2	0,91
CDK1	Cyclin-dependent kinase 1	TSSK6	Testis-specific serine/threonine-protein kinase 6	0,91
SRC	Proto-oncogene tyrosine-protein kinase Src	TSSK6	Testis-specific serine/threonine-protein kinase 6	0,91
PRKCZ	Protein kinase C zeta type	TSSK6	Testis-specific serine/threonine-protein kinase 6	0,91
GPR3	G-protein coupled receptor 3	ACR	Acrosin	0,9
PLCG2	1-phosphatidylinositol 4,5-bisphosphate phosphodiesterase gamma-2	GK3P	Glycerol kinase 3	0,9
PLCG1	1-phosphatidylinositol 4,5-bisphosphate phosphodiesterase gamma-1	PLCZ1	1-phosphatidylinositol 4,5-bisphosphate phosphodiesterase zeta-1	0,9
YES1	Tyrosine-protein kinase Yes	TEX14	Inactive serine/threonine-protein kinase TEX14	0,9
PRKCQ	Protein kinase C theta type	STKLD1	Serine/threonine kinase-like domain-containing protein STKLD1	0,9
CDK2	Cyclin-dependent kinase 2	TSSK2	Testis-specific serine/threonine-protein kinase 2	0,9
PRKACG	cAMP-dependent protein kinase catalytic subunit gamma	TSSK6	Testis-specific serine/threonine-protein kinase 6	0,9

CDK2	Cyclin-dependent kinase 2	TSSK6	Testis-specific serine/threonine-protein kinase 6	0,9
SRC	Proto-oncogene tyrosine-protein kinase Src	UBQLN3	Ubiquilin-3	0,9
RBX1	E3 ubiquitin-protein ligase RBX1	PRAME	Melanoma antigen preferentially expressed in tumors	0,89 EXP
FYN	Tyrosine-protein kinase Fyn	TUBA3C	Tubulin alpha-3 chain	0,89 EXP
SRC	Proto-oncogene tyrosine-protein kinase Src	AKAP4	A-kinase anchor protein 4	0,89
PPP1CC	Serine/threonine-protein phosphatase PP1-gamma catalytic subunit	TEX36	Testis-expressed protein 36	0,89 EXP
CDC20	Cell division cycle protein 20 homolog	SPATC1	Speriolin	0,89 EXP
PLK1	Serine/threonine-protein kinase PLK1	RGPD4	RanBP2-like and GRIP domain-containing protein 4	0,89 EXP
CAMK2D	Calcium/calmodulin-dependent protein kinase type II subunit beta	SPATA24	Spermatogenesis-associated protein 24	0,89 EXP
FYN	Tyrosine-protein kinase Fyn	LOXHD1	Lipoxygenase homology domain-containing protein 1	0,89
CPEB2	Cytoplasmic polyadenylation element-binding protein 4	DND1	Dead end protein homolog 1	0,89
CDK2	Cyclin-dependent kinase 2	CSNK1A1L	Casein kinase I isoform alpha-like	0,89
SRC	Proto-oncogene tyrosine-protein kinase Src	IQUB	IQ and ubiquitin-like domain-containing protein	0,89
CDC23	Cell division cycle protein 23 homolog	SPERT	Spermatid-associated protein	0,89 EXP
CALM1	Calmodulin-1	C11orf65	Uncharacterized protein C11orf65	0,89 EXP
CALML3	Calmodulin-like protein 3	C11orf65	Uncharacterized protein C11orf65	0,89 EXP
MOS	Proto-oncogene serine/threonine-protein kinase mos	DYDC1	DPY30 domain-containing protein 1	0,89 EXP
PRKACA	cAMP-dependent protein kinase catalytic subunit alpha	TSSK2	Testis-specific serine/threonine-protein kinase 2	0,89
CALM1	Calmodulin-1	IQCN	IQ domain-containing protein N	0,89 EXP
CALML3	Calmodulin-like protein 3	IQCN	IQ domain-containing protein N	0,89 EXP
CCNB2	G2/mitotic-specific cyclin-B2	SUV39H2	Histone-lysine N-methyltransferase SUV39H2	0,89
CCNB1	G2/mitotic-specific cyclin-B1	SUV39H2	Histone-lysine N-methyltransferase SUV39H2	0,89
ANAPC11	Anaphase-promoting complex subunit 11	CAPN11	Calpain-11	0,89 EXP
SRC	Proto-oncogene tyrosine-protein kinase Src	PRSS38	Serine protease 38	0,88
ADCY5	Adenylate cyclase type 5	GRID2	Glutamate receptor ionotropic, delta-2	0,88
PLCG2	1-phosphatidylinositol 4,5-bisphosphate phosphodiesterase gamma-2	GK2	Glycerol kinase 2	0,88
SRC	Proto-oncogene tyrosine-protein kinase Src	GALNTL5	Inactive polypeptide N-acetylgalactosaminyltransferase-like protein 5	0,88
PLCB1	1-phosphatidylinositol 4,5-bisphosphate phosphodiesterase beta-1	PLCZ1	1-phosphatidylinositol 4,5-bisphosphate phosphodiesterase zeta-1	0,88
SRC	Proto-oncogene tyrosine-protein kinase Src	PRSS58	Serine protease 58	0,88
CPEB4	Cytoplasmic polyadenylation element-binding protein 4	DND1	Dead end protein homolog 1	0,88
PRKCQ	Protein kinase C theta type	CSNK1A1L	Casein kinase I isoform alpha-like	0,88

PRKCD	Protein kinase C delta type	CSNK1A1L	Casein kinase I isoform alpha-like	0,88
PLCG2	1-phosphatidylinositol 4,5-bisphosphate phosphodiesterase gamma-2	CATSPER1	Cation channel sperm-associated protein 1	0,88
PTK2B	Protein-tyrosine kinase 2-beta	CATSPER2	Cation channel sperm-associated protein 2	0,88
PLK1	Serine/threonine-protein kinase PLK1	TSSK2	Testis-specific serine/threonine-protein kinase 2	0,88
MAPK12	Mitogen-activated protein kinase 12	TSSK2	Testis-specific serine/threonine-protein kinase 2	0,88
CAMK2B	Calcium/calmodulin-dependent protein kinase type II subunit beta	TSSK2	Testis-specific serine/threonine-protein kinase 2	0,88
AURKA	Aurora kinase A	TSSK3	Testis-specific serine/threonine-protein kinase 3	0,88
PTK2	Focal adhesion kinase 1	SH3GL3	Endophilin-A3	0,88
CCNB1	G2/mitotic-specific cyclin-B1	TSSK1B	Testis-specific serine/threonine-protein kinase 1	0,88
CDK2	Cyclin-dependent kinase 2	TSSK1B	Testis-specific serine/threonine-protein kinase 1	0,88
PLK1	Serine/threonine-protein kinase PLK1	TSSK1B	Testis-specific serine/threonine-protein kinase 1	0,88
PRKCG	Protein kinase C gamma type	TEX15	Testis-expressed protein 15	0,88
ADCY4	Adenylate cyclase type 4	ACR	Acrosin	0,87
PRKACA	cAMP-dependent protein kinase catalytic subunit alpha	FSCB	Fibrous sheath CABYR-binding protein	0,87
CALM1	Calmodulin-1	SEPT12	Septin-12	0,87
SRC	Proto-oncogene tyrosine-protein kinase Src	FBXO39	F-box only protein 39	0,87
CCNB1	G2/mitotic-specific cyclin-B1	TSSK6	Testis-specific serine/threonine-protein kinase 6	0,87
MOS	Proto-oncogene serine/threonine-protein kinase mos	TSSK1B	Testis-specific serine/threonine-protein kinase 1	0,87
SRC	Proto-oncogene tyrosine-protein kinase Src	TXNDC2	Thioredoxin domain-containing protein 2	0,86
PRKACA	cAMP-dependent protein kinase catalytic subunit alpha	CSNK1A1L	Casein kinase I isoform alpha-like	0,86
PRKCB	Protein kinase C beta type	STKLD1	Serine/threonine kinase-like domain-containing protein STKLD1	0,86
PRKACA	cAMP-dependent protein kinase catalytic subunit alpha	TSSK1B	Testis-specific serine/threonine-protein kinase 1	0,86
CDC20	Cell division cycle protein 20 homolog	SUV39H2	Histone-lysine N-methyltransferase SUV39H2	0,86
CDK2	Cyclin-dependent kinase 2	POTEI	POTE ankyrin domain family member I	0,85
SRC	Proto-oncogene tyrosine-protein kinase Src	PRSS55	Serine protease 55	0,85
CHERP	Calcium homeostasis endoplasmic reticulum protein	FTMT	Ferritin, mitochondrial	0,85
CDK1	Cyclin-dependent kinase 1	CSNK1A1L	Casein kinase I isoform alpha-like	0,85
CACNA1H	Voltage-dependent T-type calcium channel subunit alpha-1H	CATSPER1	Cation channel sperm-associated protein 1	0,85
PRKCB	Protein kinase C beta type	TSSK2	Testis-specific serine/threonine-protein kinase 2	0,85
MAPK1	Mitogen-activated protein kinase 1	TSSK2	Testis-specific serine/threonine-protein kinase 2	0,85
CCNB1	G2/mitotic-specific cyclin-B1	TSSK3	Testis-specific serine/threonine-protein kinase 3	0,85
ANAPC2	Anaphase-promoting complex subunit 2	LYAR	Cell growth-regulating nucleolar protein	0,85 EXP
SRC	Proto-oncogene tyrosine-protein kinase Src	PRSS50	Probable threonine protease PRSS50	0,85

CHAPTER 5: Comparative proteomics uncovers differentially expressed proteins related to mitochondrial and proteasomal function in sperm samples producing fertilization failure after ICSI

UNDER PREPARATION AS:

Torra-Massana M, Jodar M, Barragán M, Soler-Ventura A, Delgado-Dueñas D, Rodríguez A, Oliva R, Vassena R. **Comparative proteomics uncovers differentially expressed proteins related to mitochondrial and proteasomal function in sperm samples producing fertilization failure after ICSI.**

Partial contents of this chapter were included in the following oral presentation:

M. Torra, M. Jodar, M. Barragán, A. Soler-Ventura, D. Delgado-Dueñas, A. Rodriguez, R. Oliva, R. Vassena. **Mitochondrial and proteasomal genes associated with fertilization failure after ICSI identified by high-throughput differential sperm proteomics.** ESHRE Campus Symposium: ‘The Holy Grail of gamete and embryo assessment’, 2018, Nice, France.

Partial contents of this chapter will be included in the following oral presentation:

Torra-Massana, M.; Jodar, M.; Barragán, M.; Soler-Ventura, A.; Delgado-Dueñas, D.; Rodríguez, A.; Oliva, R.; Vassena, R. **High-throughput differential proteomics identifies altered mitochondrial and proteasomal sperm function in repeated fertilization failure.** ESHRE Annual Meeting 2019, Viena, Austria. Accepted abstract for oral presentation.

TITLE: Comparative proteomics uncovers differentially expressed proteins related to mitochondrial and proteasomal function in sperm samples producing fertilization failure after ICSI

RUNNING TITLE: Sperm proteomics and ICSI fertilization failure

AUTHORS: Marc Torra-Massana^{1,2,3}, Meritxell Jodar^{1,3}, Montserrat Barragán^{1,2}, Ada Soler-Ventura^{1,3}, David Delgado-Dueñas^{1,3}, Amelia Rodríguez^{1,2}, Rafael Oliva^{1,3,*}, Rita Vassena^{1,2,*}

ADDRESS:

¹ EUGIN-UB Research Excellence Program

² Clínica EUGIN, Travessera de les Corts 322, 08029, Barcelona, Spain.

³ Molecular Biology of Reproduction and Development Group, Institut d'Investigacions Biomèdiques August Pi i Sunyer (IDIBAPS), Fundació Clínic per a la Recerca Biomèdica, Faculty of Medicine, University of Barcelona, Casanova, Barcelona, Spain.

***Correspondence:**

Clínica EUGIN, Travessera de les Corts 322, 08029 Barcelona, Spain. Email: rvassena@eugin.es
Molecular Biology of Reproduction laboratory, Faculty of Medicine, Casanova 143, 08036 Barcelona, Spain. Email: roliva@ub.edu

INTRODUCTION

During recent years, the use of intracytoplasmic sperm injection (ICSI) in fertility clinics has increased, in particular for non-male factor infertility (Boulet et al., 2015). This technique is very efficient, resulting in a mean fertilization rate around 70-80%, but total fertilization failure (TFF) still occurs in 1-3% of ICSI cycles, even when inseminating a good number of oocytes (Yanagida 2004). Moreover, there is a reasonable percentage of ICSI cycles with fertilization rates below 50% (>25% of all cases), implying reduced probability of obtaining good quality embryos and achieving pregnancy (Flaherty et al., 1998). Both situations, caused by mechanisms not completely understood yet, cannot be easily diagnosed nor predicted, implying not only difficult clinical management and counseling, but also high economic and emotional burden on patients.

A number of molecular and cellular factors have been involved in the fertilization process during ICSI. Regarding the oocyte, nucleus-cytoplasmic maturation asynchrony, spindle defects or abnormalities in factors participating in oocyte activation signaling cascade could explain some ICSI FF cases (Neri et al., 2014; Yeste et al., 2016). For example, the “store-operated calcium entry” (SOCE) system, CamKII, MAPK, or, as recently demonstrated, mutations in TLE6 or WEE2 kinase, are oocyte molecular factors that explain problems in undergoing fertilization and MII exit (Alazami et al., 2015; Yeste et al., 2016; Sang et al., 2018).

On the other hand, sperm defects are considered the leading cause of OAF after ICSI (Neri et al., 2014; Yeste et al., 2016). Sperm triggers calcium oscillations leading to oocyte activation, and subsequent meiotic resumption, cortical granule extrusion, and pronuclei formation. Poor nuclear chromatin condensation or protamine deficiency, centrosomal dysfunction, or deficient sperm head–tail attachment may lead to diminished sperm fertilizing ability (Nasr-Esfahani et al., 2007; Rawe et al., 2008; Terada et al., 2010). Moreover, different sperm-borne oocyte activating factors (SOAF) have been proposed to play a role in oocyte activation (Sette et al., 1998; Aarabi et al., 2014). During the last decade, evidence has accumulated proposing PLC ζ as the main SOAF (Rogers et al., 2004; Yoon et al., 2012). However, knock-out mice for PLC ζ are still able to generate offspring (Nozawa et al., 2018), and FF can still occur in the clinic when using sperm without any apparent PLC ζ protein defect (Ferrer-Vaquer et al., 2016). For this reason, other sperm mechanisms could play a role during the early fertilization events after ICSI.

The sperm proteome is predicted to contain around 7,000 proteins (Castillo et al., 2018). During recent years, proteomics techniques have emerged as an efficient approach to understand and characterize the mechanisms underlying male infertility. Mass spectrometry (MS) has been used to study the sperm proteome in different groups of infertile patients: asthenozoospermia (Amaral et

al., 2014), globozoospermia (Liao et al., 2009), high oxidative stress (Sharma et al., 2013), high DNA fragmentation (Intasqui et al., 2013), varicocele (Fariello et al., 2012) or IVF failure (Zhu et al., 2013), as some examples. So far, four studies have addressed FF in conventional IVF (Pixton et al., 2004; Frapsauce et al., 2014; Légaré et al., 2014; Liu et al., 2018), identifying differentially expressed proteins mainly related to sperm motility and gamete interactions. However, to our knowledge, no proteomics approach using samples which failed to fertilize after ICSI has been published.

Currently, high-throughput approaches based on liquid chromatography coupled to tandem mass spectrometry are available, and both the use of isobaric tandem mass tags (TMTs) and the introduction of novel methodologies for the analysis of quantitative proteomic data have offered good results in previous sperm comparative proteomics studies (Azpiazu et al., 2014; Bogle et al., 2017; Barrachina et al., 2018). Using these approaches, our objective was to study the molecular mechanisms leading to FF after ICSI, by comparing samples with good fertilization rate (>75%) and samples with repetitive FF. Some of the proteins and mechanisms identified could be useful as clinical markers for FF in assisted reproduction.

MATERIALS AND METHODS

Ethical approval

Approval to conduct this research was obtained from the local Ethical Committee for Clinical Research and written consent was obtained from all patients enrolled in the study.

Study population and sperm sample collection

The patient recruitment and sample collection period was from January 2016 to January 2018. A total of 17 couples with similar clinical characteristics but different fertilization outcomes after ICSI consented to be included in this study. For the control group (n = 12, C1 - C12), patients had an overall fertilization rate above 75 % after ICSI with a total of, at least, 6 inseminated oocytes. For the FF group (n = 5, F1 - F5), patients had experienced repetitive FF in 3 consecutive ICSI cycles or more, comprising at least 6 inseminated oocytes, and did not have any previous IVF cycle with good fertilization rate. For both groups, men above 45 years old, <15 % progressive motility or <10 million/ml sperm count were excluded.

Semen samples were obtained by masturbation after a minimum of 2 days of abstinence. After 30 min of liquefaction at room temperature, sperm samples were analyzed with an integrated semen

analysis system (ISAS, Proiser), and classified following standard criteria (WHO 2010). Part of the ejaculate not going to be processed for ICSI was cryopreserved in either straws (0.5 ml semen per straw) or cryotubes (up to 1.5 ml per cryotube) using Sperm Cryoprotect II (Nidacon) according to manufacturer's instructions, and stored in liquid nitrogen until further processing.

For proteomics approaches, 8 controls and 4 FF samples were used. For functional characterization of mitochondrial and proteasomal function, 5 controls and 4 FF samples were included (**Supplementary Table I**).

Oocytes and ICSI

Female patient stimulation was based on either long agonist or antagonist protocol depending on medical history, clinical characteristics, and ovarian reserve; while short antagonist and GnRH agonist trigger was the protocol for oocyte donors. Oocytes were denuded with 80 U hyaluronidase (HYASE-10X[®]) (Vitrolife, Sweden), and ICSI was performed following standard procedures on metaphase-II oocytes (Palermo et al., 1992). After ICSI, inseminated oocytes were cultured independently at 37°C, 6% CO₂ in 25 µl drops of G1[®] medium (Vitrolife, Sweden) covered with mineral oil (OVOIL[®]) (Vitrolife, Sweden). Fertilization was assessed for 2 PN formation at 16 to 19 h post-ICSI.

Sperm processing and protein solubilization

The general strategy used in our study is depicted in **Figure 1**. Sperm samples cryopreserved in straws were thawed for 5 min at 37 °C and sperm samples cryopreserved in cryotubes were thawed for 3 min at 40 °C in a water bath, as per the clinical routine. Once thawed, sperm samples were centrifuged at 500 g x 10 min to eliminate the cryoprotectant and resuspended with 1 ml PureSperm Buffer (Nidacon). After assessing the post-thawed concentration and round cell contamination, samples were purified through 50 % density gradient (DG) separation (Puresperm, Nidacon) at 300 g without brakes for 20 min at room temperature. After DG, sperm concentration assessment was repeated, and all samples contained <1 % contaminating round cells after DG and were further processed. Samples were pelleted at 2500 g for 5 min, the recovered sperm pellet was solubilized in lysis buffer (2 % SDS, 1 mM phenylmethylsulphonyl fluoride (PMSF), in PBS), and protein extracts were stored at -80 °C until further processing.

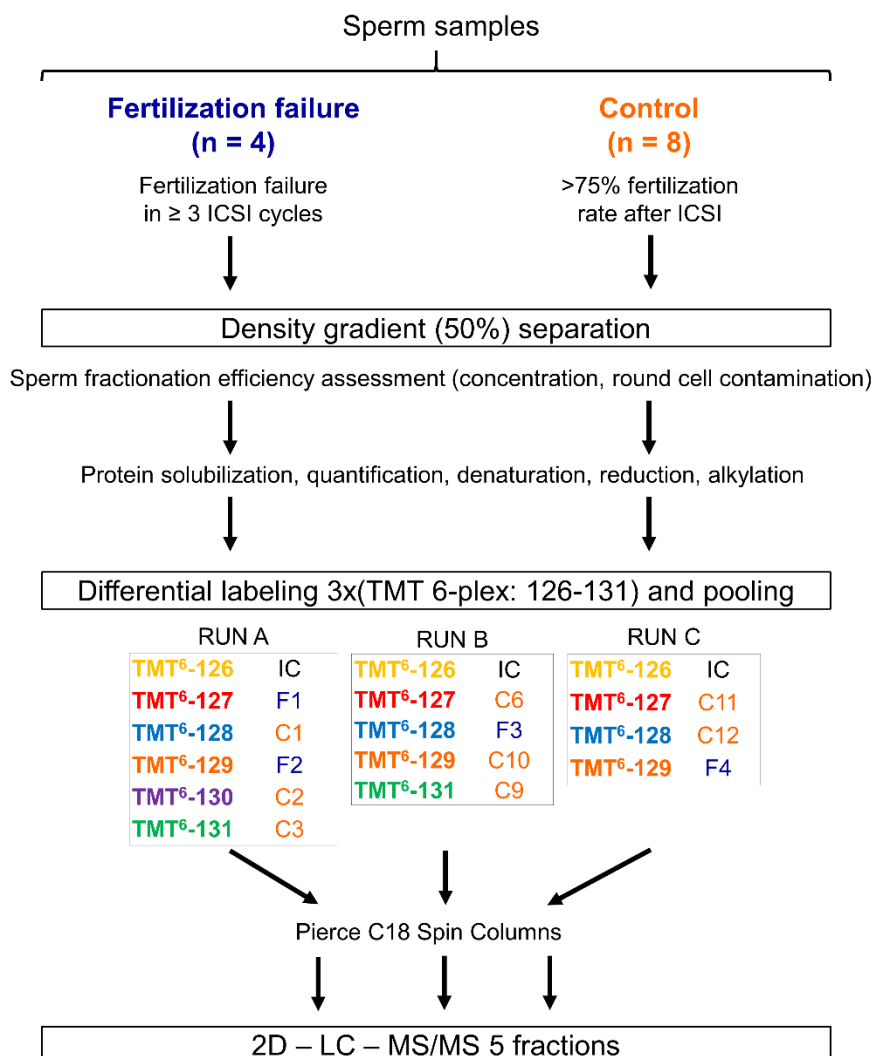


Figure 1. Schematic representation of the strategy used for the identification of proteomic changes between study groups (FF and controls). Samples were thawed and processed by 50 % density gradient. After quality assessment (concentration and round cell contamination), the soluble proteins were digested, reduced, alkylated, and labeled with TMT 6-plex isobaric tags. Prior to labelling, equal amounts of peptides from each sample were pooled and divided into three to serve as the internal controls for all three independent multiplex runs. Labeled peptides were separated by liquid chromatography with fraction collection and proteins were quantified through MS/MS.

Sperm peptide isotopic labeling (TMT-6plex)

Individual protein extracts were thawed at room temperature for 10 min followed by 30 minutes at 4 °C with constant shaking, and quantified using microBCA™ Protein Assay Kit (PIERCE, Thermo Fisher Scientific) following the manufacturer's instructions. Subsequently, TMT-6-plex (Thermo Fisher Scientific) labeling was used, following manufacturer's instructions with minor modifications. Briefly, 25 µg of protein from each sample was resuspended in 100 mM TEAB (triethyl ammonium bicarbonate; pH 8.5, Thermo Fisher Scientific) to reach a protein concentration

of 0.6 $\mu\text{g}/\mu\text{l}$. Afterwards, proteins were reduced with 9.5 mM TCEP (tris(2-carboxyethyl) phosphine) for one hour at 55 °C, and alkylated with a final concentration of 17 mM iodoacetamide for 30 min in the dark. Proteins were precipitated overnight at -20 °C with cold 100 % acetone to reach a final concentration of 87.5 %. Samples were centrifuged at 17500 g 10 min at 4 °C and protein pellets were resuspended with 50 mM TEAB to obtain a protein concentration of 0.6 $\mu\text{g}/\mu\text{l}$, and trypsinized overnight at 37 °C with constant shaking, in 1:20 protease-to-protein ratio. Prior to labeling, an aliquot (4.8 μg) was taken from each sample and combined together at equal amounts to establish the internal control sample. The purpose of this internal control sample is to allow comparing the results of the three multiplex (A, B and C runs; **Figure 1**). Approximately 20 μg of peptides from each sample (including 72 μg for the internal control common for each run) were labeled with TMT isobaric tags (Product number: 90064; Lot: PL198866, Thermo Fisher Scientific). 6-plex TMT label reagents (0.8 mg each) were equilibrated at room temperature and dissolved in 41 μl of anhydrous acetonitrile (ACN, Sigma-Aldrich), and the two vials of each TMT label reagent were mixed in a single tube to avoid any bias (reporter ions intensity from m/z 126 to m/z 131: TMT-126, -127, -128, -129, -130, -131). 51.35 μl of TMT was added to the internal control, while 16.4 μl of each TMT label reagent was added to the samples as described in **Figure 1**. After incubation for 1 h at room temperature, reactions were quenched by incubating for 15 min in a final concentration of 0.29% hydroxylamine. The TMT-labeled samples were combined at equal volumes (10 μg per sample; 60 μg total) within each multiplex, each one containing at least one FF sample and 2 controls (**Figure 1**). Labeled peptides were dried in a speed-vacuum centrifuge, and 30 μg of each multiplex was resuspended in 50 μl of 0.5 % trifluoroacetic acid (TFA) in 5% ACN, cleaned up with reversed-phase C18 Spin Columns (Pierce C18 Spin Columns, Thermo Fisher Scientific) following manufacturer's instructions, and eluted in 40 μl of 70 % ACN.

Strong-cation exchange chromatography fractionation

Labeled peptides from each multiplex (A, B and C) were fractionated using an Oasis MCX cartridge (1 cc, 10 mg, 30 μm , 80 Å, Waters). Starting with an activation step with 1 ml of 100% ACN (Acetonitrile) and an equilibration step with 5 mM FA / 25 % ACN (FA: Amonium Formiate, pH=3), 5 μl of each multiplex was loaded to the column and washed twice with equilibration buffer (5 mM FA / 25 % ACN). After that, in order to compile 5 different fractions, sequential elution steps were performed by gravity as follows: 5 mM FA / 25 % ACN, 200 mM FA / 25 % ACN, 350 mM FA / 25 % ACN, 1000 mM FA / 25 % ACN, 500 mM FA / 25 % ACN / 1500 mM KCl, 1000 mM FA / 50 % ACN. The collected fractions for each multiplex (5 fraction per multiplex, 15 fractions in total) were desalted using a reversed-phase C18 Spin Columns (Pierce C18 Spin Columns, Thermo Fisher Scientific) following manufacturer's instructions.

Protein identification and quantification by liquid chromatography - tandem mass spectrometry (LC-MS/MS)

Desalted fractions were brought to dryness and reconstituted with 5 μ l of 0.1 % FA and 4.5 μ l from each fraction was loaded onto a trap column C18 (L 2 cm, 200 μ m ID, 5 μ m, 120 Å , Nanoseparations). For separation a linear gradient was applied together with the analytical column (L 15 cm, 75 μ m ID, 3 μ m, 100 Å , Thermo Fisher Scientific). Buffer A (97 % H₂O, 3 % ACN, 0.1 % FA) and buffer B (97 % ACN, 3 % H₂O, 0.1 % FA) were used for a 80 min linear gradient (0-5 min 0 % to 0 % B, 5-60 min 0 % to 37 % B, 60-65 min 37 % to 100 % B, 65-80 min 100 % to 100 % B) for elution at a rate of 400 nl / min to separate the peptides. The MS/MS analysis was performed by a nano-LC ultra 2D eksigent (AB Sciex) attached to a LTQ-Orbitrap Velos coupled to a nanospray ion source (Thermo Fisher Scientific). The LTQ Orbitrap Velos (Thermo Fisher Scientific) settings included 30000 of resolution for the MS1 scans at 400 m/z for precursor ions followed by 7500 of resolution for the MS2 scans of the 15 most intense precursor ions at 400 m/z, in positive ion mode. The mass range was set 380-1500 m/z. The acquisition of MS/MS data was performed using Xcalibur 2.2 (Thermo Fisher Scientific). Normalized collision energy for HCD-MS2 was set to 42 %.

LC-MS/MS data was analyzed using Proteome Discoverer 1.4.1.14 (Thermo Fisher Scientific). For database searching, raw MS files were submitted to the in-house *Homo sapiens* UniProtKB/Swiss-Prot database with *Sus scrofa* Trypsin added to it (HUMAN_PIG_Uniprot_R_2017_06.fasta; released June 2017, 23064 protein entries) using SEQUEST HT version 28.0 (Thermo Fisher Scientific). For re-scoring, percolator search node was used. The following parameters were applied in order to perform the searches: two maximum missed cleavage sites for trypsin, as dynamic modifications, TMT-labeled lysine, histidine, serine, threonine and N-terminus (+229.163 Da) and methionine oxidation (+15.995 Da), as static modification cysteine carbamido methylation (+57.021 Da), 20 ppm precursor mass tolerance, 0.1 Da fragment mass tolerance, 10 mmu peak integration tolerance, and most confident centroid peak integration method. Percolator was used for protein identification with the following identification criteria: at least one unique peptide per protein with a FDR of 1%. Different isoforms of the same protein were treated as ungrouped to avoid any possible ambiguity (Amaral et al., 2014; Bogle et al., 2018).

For protein quantification data, normalized TMT quantitative values were obtained from each identified spectrum derived from the ratio of the intensity of reporter ions from HCD MS2 spectra corresponding to each individual samples (TMT-127 to TMT-131) with the internal control (TMT-126), obtained by Proteome Discoverer software (**Supplementary Figure 1**). Only those proteins

with at least 1 unique peptide identified with a FDR <1 %, quantified by ≥ 2 PSMs in all the samples, and with a coefficient of variation <50 % in at least 75 % of the samples were considered for further statistical analyses. Significant statistical differences between the controls and FF groups were evaluated after the normalization of the relative proteomic quantification values by log₂ transformation.

Group and individualized statistical analyses

All statistical analyses were performed using R software version 3.4.4 (<http://www.r-project.org>) or GraphPad Prism software version 7.01 (GraphPad Software Inc., San Diego, CA, USA). In addition to a principal component analysis, gene ontology enrichment analysis was carried out using Gene Ontology Consortium database (<http://www.geneontology.org/>) based on PANTHER v. 14 database in order to predict the potential pathways involved.

For the group analysis, the differences between FF and controls were determined by a student's t-test two tailed, and null hypothesis was rejected at the 0.05 level. For individualized analysis of each FF sample, two different approaches were considered: (i) Rout's test was performed in order to establish the outliers profile for each individualized sample. (ii) Stable-protein pairs was applied as previously described (Barrachina 2018). Briefly, the intensity values from HCD MS2 spectra corresponding to each individual sample (TMT-127 to TMT-131), excluding the internal control (TMT-126), were used to establish the stable-protein pairs for controls and FF groups. Stable-protein pairs were determined by applying the statistical principle of 2 proteins (with more than 1 peptide quantified for each one) were highly-correlated when $\geq 75\%$ of the possible peptide combinations had a Pearson correlation coefficient ≥ 0.9 . In this analysis, only those proteins with 2 or more associated peptides were considered (n=113). Those proteins which lost more than 50% of correlations in a specific FF sample when compared to controls were considered as dysregulated or altered.

Western blotting

Western Blot and relative semiquantification of protein abundance by comparative densitometry were carried as previously described (Freour et al., 2018). Protein extracts corresponding to 1 million sperm were used to this aim. Two different antibodies were used at indicated dilutions as normalizers: anti- α -tubulin antibody (T6199, Sigma-Aldrich, 1:5000) and anti-SDHA antibody (ab14715, Abcam, 1:5000).

The following antibodies were used at the listed dilutions: PSMA1 (HPA037646, Sigma-Aldrich, 1:2000), DLAT (ab110333, Abcam, 1:1000) as primary antibodies; and peroxidase labeled anti-

mouse (NIF825, GE Healthcare Bio-Sciences, USA) and anti-rabbit (NIF824, GE Healthcare Bio-Sciences, USA) as secondary antibodies at 1:10,000. Before using the antibodies for validation, different dilutions of primary antibodies were tested on different amounts of protein to determine its sensitivity and to ensure that the semi-quantification was performed within the linear range.

Determination of sperm mitochondrial DNA copy number

Genomic DNA (gDNA) was extracted from 2 million sperm (after DG processing) and quantified as previously described (Torra-Massana et al., 2018). Mitochondrial DNA (mtDNA) copy number was determined by real-time quantitative PCR (qPCR). Two different mtDNA genes (MT-ND1 and MT-ND4) were amplified and normalized relative to the amplification of a single-copy nuclear gene B2M. Primer sequences and target locus are shown in **Supplementary Table II**. Each qPCR included 1 ng of DNA, 10 µl of 2× SsoAdvanced Universal SYBR Green Supermix (BioRad, USA), and 0.1 µl of each primer (100 µM), in a 20 µl final reaction volume. The qPCR program used consisted of an initial denaturalization step of 30 s at 95 °C and 40 cycles of 95 °C for 5 s and 60 °C for 30 s. All qPCRs were carried out in triplicate in 96-well plates using CFX96 (BioRad, USA). Analysis was performed considering the primer pair efficiencies, which were evaluated using sequential dilutions of sperm gDNA samples (**Supplementary Table II**).

Analysis of mitochondrial membrane potential by flow cytometry

Sperm mitochondrial membrane potential (MMP) was measured by using JC-1 (Sigma-Aldrich), as previously described (Fernandez & O’Flaherty 2018). Briefly, 2 million sperm previously processed by DG were stained with 2 µM JC-1 for 15 min at 37°C. JC-1 forms J-aggregates inside the mitochondria in sperm with high MMP, producing red fluorescence, while it will remain as a monomer in sperm with low MMP, emitting in green. Before flow cytometry evaluation, SYTOXTM Blue (Thermo Fisher Scientific) was added at the cell suspension at 1 µM, a viability indicator which allows to exclude dead cells. All samples were analyzed using a Sony SA3800 flow cytometer (Sony Biotechnology, San Jose, California, USA), and data analyzed using FlowJo software v. 10.5.2 (LLC, Ashland, Oregon, USA). Results for MMP were expressed as the ratio of red/green fluorescence in live sperm (expressed as relative units, RU); a decrease in this ratio indicates mitochondrial depolarization.

Determination of sperm proteasome activity

Proteasome activity in sperm samples was determined using the Proteasome Activity Assay Kit (ab107921, Abcam) following the manufacturer’s instructions. This kit utilizes an AMC-tagged peptide substrate which releases fluorescent AMC in the presence of proteolytic activity. Briefly,

for each sample, 2 million sperm (previously processed by 50% DG) were resuspended in 20 μ l 1% NP-40 and centrifuged for 15 min at 4°C 13,000 rpm, recovering the soluble extract (supernatant). A standard curve was prepared using AMC standard, and all samples were assayed in duplicate, with and without proteasome inhibitor (MG-132, Abcam), in a 96-well plate for fluorimetric quantitative assay (88378, Thermo Fisher Scientific). The plate was incubated at 37°C in FLx800™ microplate reader (BioTek), for 70 minutes, and the fluorescence of released AMC monitored at time intervals of 10 min at an excitation wavelength of 360 nm and an emission wavelength of 460 nm. Results are expressed as proteasome activity units (PAU), each unit defined as the amount of proteasome in 400.000 live sperm which generates 1.0 nmol of AMC per minute at 37°C.

Table I. Demographic and semen parameters, ICSI cycle/s variables (number of oocytes and fertilization outcomes) and density gradient processing information for the two groups included in the study (FF and controls). Results are indicated as mean \pm SD [range]. Oocyte age is considered the age of the female partner, or the age of the oocyte donor when using donor oocytes. NS, not significant. SD, Standard deviation. FR, Fertilization rate. DG, Density gradient.

	FF group (n = 5)	Control group (n = 12)	p
Male age; years	40.0 \pm 3.7 [36, 43]	37.3 \pm 3.8 [31, 43]	NS
Male BMI	23.3 \pm 1.1 [22.4, 24.5]	24.2 \pm 2.6 [21.3, 29.0]	NS
Volume, ml	5.3 \pm 0.9 [4.1, 6.4]	4.6 \pm 1.4 [1.6, 6.7]	NS
Concentration, million/ml	86.5 \pm 70.3 [21.8, 191.0]	118.6 \pm 64.6 [18.5, 242.2]	NS
Motility, % a+b	54.7 \pm 28.7 [21.3, 87.1]	62.0 \pm 16,6 [34.4, 87.2]	NS
Morphology, % normal	7.8 \pm 2.9 [4, 12]	5.7 \pm 2.8 [2, 13]	NS
Inseminated oocytes per cycle, n	6.0 \pm 3.4 [3.0, 10.8]	7.2 \pm 3.3 [3.0, 16.0]	NS
Oocyte mean age, years	34.9 \pm 4.9 [27, 42]	30.0 \pm 5.0 [20, 40]	NS
FR, % (2PN / injected oocytes)	3.05 (4 / 131)	83.19 (99 / 119)	< 0.0001
Contaminating cells after DG, %	0.21 \pm 0.16 [0, 0.37]	0.23 \pm 0.16 [0, 0.52]	NS
DG recovery, %	38.1 \pm 7.2 [31.2, 43.4]	34.9 \pm 8.9 [18.1, 47.4]	NS

RESULTS

Semen parameters and ICSI cycles

Demographic and semen parameters and fertilization outcomes for all patients included in the study are indicated in **Supplementary Table III**. The only significant difference between both groups was observed in the mean fertilization rate (3.05 % in FF vs. 83.19 % in controls) (**Table I**). No significant differences were observed in age, sperm parameters, the number of inseminated oocytes per cycle and the mean age of the woman providing the oocytes (partner or donor), between FF and controls (**Table I**). All patients were normozoospermic, except F4 and C6 which presented mild asthenozoospermia and teratozoospermia, respectively (**Supplementary Table III**). All samples presented <1% contaminating cells after 50% DG processing prior to proteomics, and the efficiency of purification by DG was similar between both groups (**Table I**).

Global sperm proteome analysis

By using TMT labelling and high-resolution 2D-LC-MS/MS analysis, a total of 1,398 different proteins with at least one unique peptide with <1 % FDR were identified (comprising a total of 6,662 unique peptides). 87 of these proteins were not previously identified in other sperm proteomics studies using specific methods to ensure the proper elimination of potentially contaminating cells (**Supplementary Table IV**).

After applying the previously described criteria (FDR <1 %, ≥ 2 PSMs in all the samples, coefficient of variation <50 % in at least 75 % of the samples), a total of 232 sperm proteins with high confidence quantification values were identified and used for subsequent analyses. A principal component analysis within this group of proteins could differentiate FF samples and controls, as observed in **Supplementary Figure 2**; most controls clustered together, indicating it is a quite homogeneous group. A GO Biological Process term analysis for all these 232 proteins is shown in **Supplementary Figure 3**.

A second analysis in the group of proteins with high confidence quantification values, based on the GO data recently published by Castillo et al., 2018, allowed identification of 14 proteins related to the fertilization process (i.e. IZUMO4, ACR, ZPBP or CRISP1) and 4 sperm proteins with potential roles in preimplantational development (ODF2, TMED10, VCP and RUVBL1), all of them summarized in **Table II**. Any of these proteins were differentially expressed between FF and control samples, suggesting that other factors are involved in fertilization failure after ICSI.

Table II. Sperm proteins detected in proteomics analysis functionally involved in the processes of fertilization and preimplantation embryo development. *T-test.

UniprotKB accession number	Symbol	Protein name	Relative abundance (FF : control)	p-value*
Sperm Protein involved in fertilization				
P10323	ACR	Acrosin	0,936	0,4627
O75969	AKAP3	A-kinase anchor protein 3	0,858	0,2913
P78371	CCT2	T-complex protein 1 subunit beta	1,059	0,7509
P49368	CCT3	T-complex protein 1 subunit gamma	0,903	0,2159
Q99832	CCT7	T-complex protein 1 subunit eta	0,864	0,1368
P15529	CD46	Membrane cofactor protein	1,085	0,481
P54107	CRISP1	Cysteine-rich secretory protein 1	0,889	0,9713
P34931	HSPA1L	Heat shock 70 kDa protein 1-like	1,061	0,1717
Q1ZYL8	IZUMO4	Izumo sperm-egg fusion protein 4	1,038	0,5191
A4D1T9	PRSS37	Probable inactive serine protease 37	1,26	0,3119
Q6UW49	SPESP1	Sperm equatorial segment protein 1	1,038	0,8369
P20155	SPINK2	Serine protease inhibitor Kazal-type 2	1,03	0,8892
Q9BS86	ZBPB	Zona pellucida-binding protein 1	1,004	0,7991
Sperm proteins potentially involved in preimplantational embryo development				
Q5BJF6	ODF2	Outer dense fiber protein 2	0,985	0,8372
Q9Y265	RUVBL1	RuvB-like 1	1,058	0,7174
P49755	TMED10	Transmembrane emp24 domain-containing protein 10	0,99	0,9105
P55072	VCP	Transitional endoplasmic reticulum ATPase	0,993	0,9463

Group analysis identifies differentially expressed proteins related to mitochondrial and proteasomal function

To identify potential markers of FF, group statistical analysis comparing protein quantification values between FF samples and controls was applied. This analysis identified 9 differentially expressed proteins (t-test, $p < 0.05$), with 4 of them presenting lower levels in the fertilization failure group (**Table III**): three of them seem to be involved in spermatogenesis (FMR1NB,

FAM209B, RAB2B), while proteasome subunit alpha 1 (PSMA1) is essential for proteasome function. On the other hand, 5 mitochondrial proteins involved in sperm metabolism were found at higher levels in FF samples (DLAT, ATP5H, SLC25A3, SLC25A6, and FH) (**Table III**).

Table III. Proteins with differential abundance between samples with repetitive fertilization failure after ICSI and controls (>80% mean fertilization rate) at group level, following strict criteria analysis. *T-test.

UniprotKB accession number	Symbol	Protein name	p-value*	Relative abundance (FF : control)
P10515	DLAT	Dihydrolipoyllysine-residue acetyltransferase component of pyruvate dehydrogenase complex, mitochondrial	0,0033	1.257
Q00325	SLC25A3	Phosphate carrier protein, mitochondrial	0,0075	1.181
Q8N0W7	FMR1NB	Fragile X mental retardation 1 neighbor protein	0,0123	0.868
Q8WUD1	RAB2B	Ras-related protein Rab-2B	0,0187	0.866
Q5JX69	FAM209B	Protein FAM209B	0,0226	0.872
P25786	PSMA1	Proteasome subunit alpha type-1	0,0341	0.893
O75947	ATP5H	ATP synthase subunit d, mitochondrial	0,0407	1.370
P12236	SLC25A6	ADP/ATP translocase 3, mitochondrial	0,0433	1.128
P07954	FH	Fumarate hydratase, mitochondrial	0,0473	1.098

The differential abundance of DLAT and PSMA1 was verified by WB (**Figure 2**), using two proteins commonly used as normalizers for sperm: SDHA and tubulin (Barragan et al., 2015). The purpose of using two independent normalizer proteins located in different subcellular compartments was to increase the reliability of WB validation.

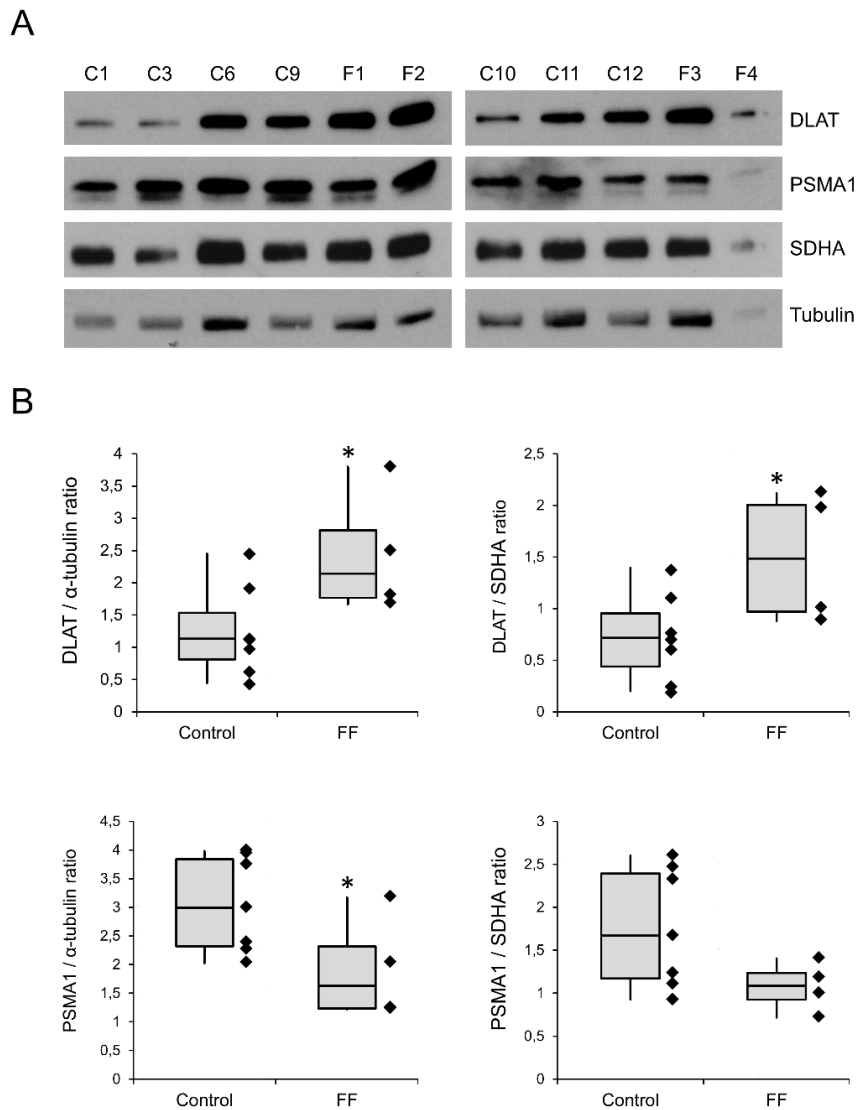


Figure 2. WB validation of differential abundance observed for DLAT and PSMA1 in FF samples and controls. **A.** Original blots indicating the bands used for protein levels semiquantification (for DLAT, PSMA1, SDHA and tubulin) in protein extracts from 4 FF and 5 control samples. **B.** Box plots representing protein levels of DLAT and PSMA1 determined by WB between FF and control samples, for both normalizers used (SDHA and tubulin). Asterisk indicates significant difference (t-test, $p < 0.05$).

Individualized analysis is consistent with group analysis results and provides additional information for each FF sample

Stable-protein pairs and analysis of outliers were applied to better evaluate the proteomic differences between FF and controls. Both analyses not only complement the previous group analysis, but also provide information of the molecular alterations in each specific FF sample.

Table IV. Stable-protein correlations in control population ($\geq 75\%$ fertilization rate after ICSI; n=8) altered in individual FF patients.

Samples	Number of correlations	Correlations in common with control stable-protein pairs	Proteins involved	Proteins that lost $\geq 50\%$ correlations
Stable-protein pairs for the control group (Control group; n=8)				
Control group	146	-	28	
Alterations in individual FF patients				
Control + F2	179	144	28	-
Control + F3	94	92	28	PDHA2, ACRV1, PHB2, RUVBL1, ZPBP, ASRGL1, NUP210L, FAM209B, DECR1, ATP5F1D, PDHB, TEKT2
Control + F4	114	114	28	RPLP2, PHB2, FAM209B, ATP5F1D, TEKT2
Control + F13	84	80	28	CD59, OXCT1, NUP54, CCT3, ACRV1, SPACA4, RPLP2, PHB2, RUVBL1, MPC1L, NUP210L, FAM209B, DECR1, ATP5F1D, PDHB, TEKT2

A total of 146 stable-protein pairs between 28 different proteins were identified for patients with good fertilization rates (controls) (**Supplementary Table V**). These 28 proteins are functionally involved in processes related to metabolism (i.e. PDHA2 or ATP5F1C) or fertilization (SPACA4 and ZPBP), or are involved in specific functions related to sperm subcellular structures such as nucleus or flagella. To assess alterations of stable-protein pairs in individual FF patients, the analysis of the stable-protein pairs for the control group was repeated by adding one single FF patient at a time (**Table IV**). This strategy revealed that the patient F1 had a similar sperm proteomic signature to that found in control men, since most of the stable protein pairs established for control population were maintained. In contrast, some proteins related to the ones detected in the group analysis presented loss of correlations in the other FF patients; for instance, 100% correlations were lost for ATP5F1D (member of the ATP synthase) in 3 out of 4 samples, as well as $>50\%$ correlations for PDHB and PDHA2 (two different subunits of E1 component of PDH complex) in 2 out of 4 samples (**Table IV**).

Other interesting proteins include FAM209B (100% of correlations lost in 3 out of 4 FF samples, also detected in the group analysis), mitochondrial protein PHB2 (>75% correlations lost in 3 out of 4 samples); TEKT2 (100% of correlations lost in 3 out of 4 samples), an important structural protein in sperm, or ACRV1, an acrosomal protein (**Table IV**). In addition, some alterations seem to be present in specific samples; for example, in sample F2, all correlations are lost for ASRGL1 protein. This analysis also uncovered two proteins associated with the nuclear envelope or nuclear pore complex (NUP54 and NUP210L), structures needed for pronucleus formation and interaction with sperm aster during oocyte fertilization (Payne et al., 2003).

The analysis of outliers also provided complementary information on specific FF samples (**Supplementary Table VI**). For example, ROPN1 is present at lower levels in sample F2, a protein which, as it will be discussed, may have potential roles as a marker for FF.

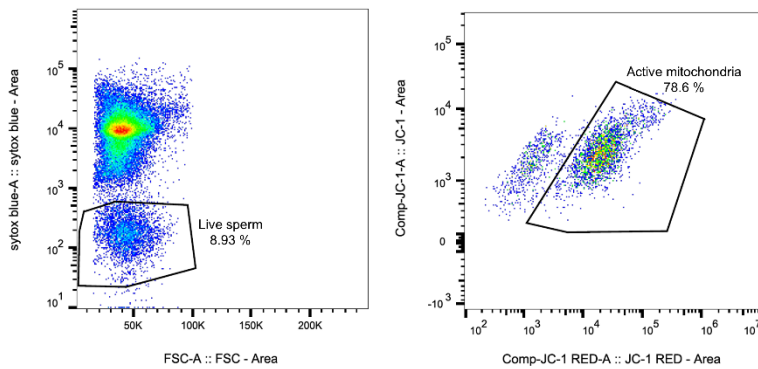
FF samples do not present differences in mitochondrial DNA copy number

To evaluate if the overexpression of mitochondrial proteins observed in FF samples is explained by the presence of a higher number of mitochondria per cell, the mean value of mtDNA_{cn} was determined by qPCR. No significant difference was observed in mtDNA_{cn} between FF samples and controls, for any of the two mitochondrial genes used (MT-ND1 and MT-ND4) (**Supplementary Figure 4**).

FF samples present reduced mitochondrial membrane potential

In order to determine if the altered levels of specific mitochondrial proteins in FF samples is associated with changes in mitochondrial activity, analysis of MMP was performed in both FF and control samples. SYTOXTM Blue staining could clearly distinguish the population of live sperm and, within this population, JC-1 allowed to differentiate between cells emitting red fluorescence, presenting high MMP and mitochondrial activity, and sperm emitting green fluorescence only, presenting mitochondrial depolarization and reduced mitochondrial activity (**Figure 3A**). All FF samples analyzed showed less MMP than 4 out of 5 controls (**Figure 3B**). At group level, MMP was lower in FF (1.64 ± 0.84 RU) when compared to controls (3.75 ± 2.27 RU), but this difference did not reach statistical significance.

A



B

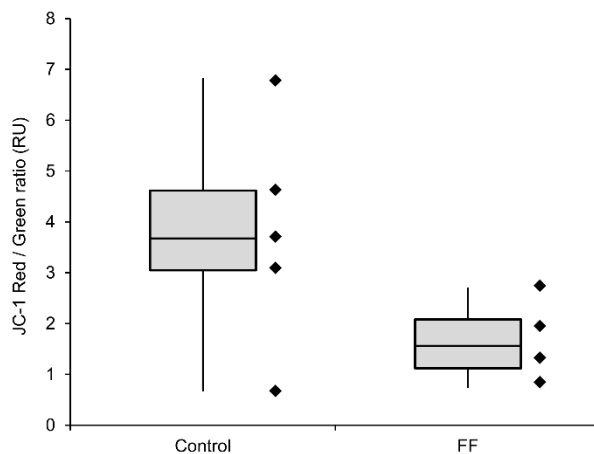


Figure 3. Analysis of sperm mitochondrial membrane potential. **A.** Representative dot plots showing the SYTOX™ Blue negative cells (live sperm, left panel) and, within this cell population, the two cell populations which can be differentiated by JC-1 staining (right panel): sperm emitting red fluorescence (positive mitochondrial activity) and sperm emitting green fluorescence only (without mitochondrial activity). **B.** Box plots indicating the MMP (expressed as the JC-1 ratio of red / green fluorescence, relative units, RU) in FF and control samples.

Proteasome activity is diminished in FF samples

To see if PSMA1 underexpression observed in FF samples can be associated with reduced proteasomal activity in sperm, we used a fluorimetric assay to determine the proteolytic activity in both FF and control samples. In all samples, 70 minutes incubation period resulted in a linear increase of RFU detected ($R > 0.99$), while presence of inhibitor completely blocked proteasome activity (slope close to 0 for all samples) (**Supplementary Figure 5**). Sperm samples presented variable levels of proteasome activity, and the positive control included in the kit (Jurkat cell line lysate) resulted in a higher proteasome activity (0.91 PAU) (**Figure 4A**). At group level, the mean proteasome activity was lower in FF samples (0.21 ± 0.08) when compared to controls (0.35 ± 0.18) (**Figure 4B**).

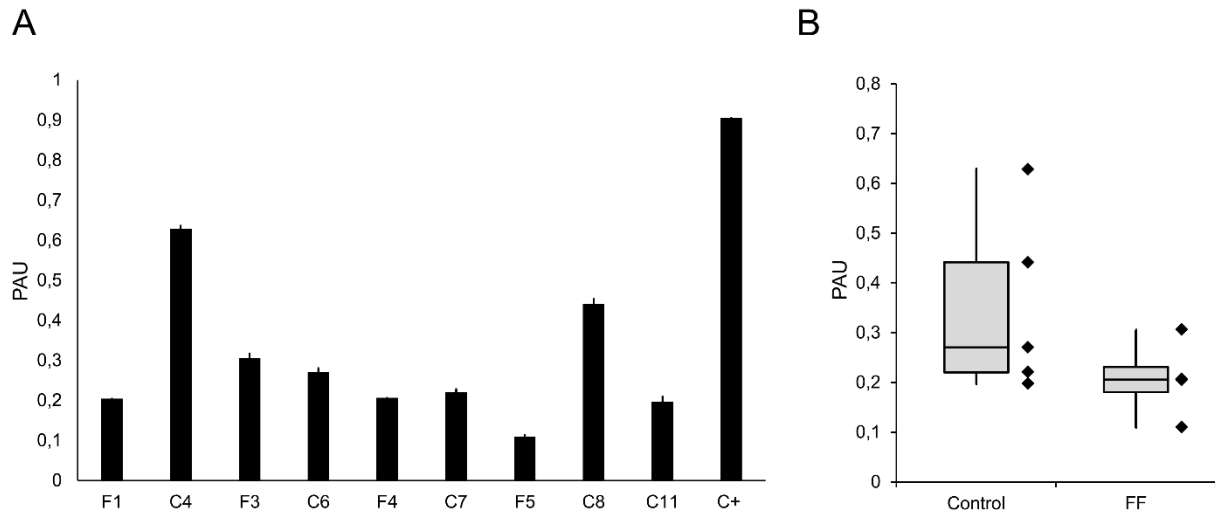


Figure 4. Analysis of proteasome activity in sperm. **A.** Levels of proteasome activity obtained in FF samples, controls, and positive control. **B.** Box plots representing the difference in proteasome activity between samples with fertilization failure (FF) and good fertilization rates (controls) after ICSI. Results are expressed in proteasome activity units (PAU), each unit defined as the amount of proteasome the amount of proteasome which generates 1.0 nmol of AMC per minute at 37°C.

DISCUSSION

As far as we know, this is the first study of comparative proteomics in sperm samples that present fertilization failure after ICSI. Our study combines conventional and novel methodologies for proteomics analysis and contributes to the elucidation of the molecular and cellular mechanisms behind FF.

We identified 14 proteins involved in the fertilization process, as referred in gene ontology databases. However, most of these proteins are involved in fertilization events that occur prior to sperm entry (i.e. capacitation, motility) and oocyte activation, useful FF markers for intrauterine insemination or IVF. For instance, proteins like IZUMO, ZPBP or CRISP1, which have a role in sperm-oocyte fusion, were not altered in our samples with FF after ICSI.

According to our results, PDHA2, PDHB and DLAT were differentially expressed in FF samples. Those proteins have enzymatic activity and belong to the pyruvate dehydrogenase complex (PDC), which forms part of the pyruvate and citric acid cycle at mitochondria. PDC is organized in three main complexes: pyruvate dehydrogenase (E1 subunit: PDHA1, PDHA2, PDHB), dihydrolipoyl transacetylase (E2 subunit: DLAT), and dihydrolipoamide dehydrogenase (E3 subunit: DLD). PDC regulates sperm motility and capacitation (Kumar et al., 2006; Li et al., 2016), and could be considered an essential mechanism for proper sperm fertilization after ICSI. Moreover, it has been described that disruption of PDC function in hamster sperm resulted in fertilization failure due to

inability to elicit calcium oscillation in the oocyte (Siva et al., 2014), a phenotype which is compatible with the one observed in our FF patients. It has been described that one of the main causes of mitochondrial dysfunction could rely on defects on regulation of the mitochondrial PDC and it has been implicated as a potential therapeutic target because of its activity as a key modulator of energy and metabolic homeostasis (Byron and Lindsay, 2016; Park et al., 2018).

Our approaches (grouped and individualized analysis) identified other proteins which alterations would result in inaccurate sperm metabolism, as most of them participate in oxidative respiration. For example, we found a dysregulation of different components of ATP synthase complex, which is essential for sperm capacitation (Rogers et al., 1977; Ramió-Lluch et al., 2014). Altered mitochondrial function could lead to FF after ICSI by generating higher sperm apoptosis rates, impaired calcium signalling, incorrect capacitation, higher DNA damage caused by abnormal pH and ROS levels, compromised centriolar function, or inability of sperm to undergo first steps inside the oocyte after sperm-entry (i.e. formation of male pronucleus, Reyes et al., 1993), as some examples. The lower MMP that we observed in FF samples could be related with a deficient mitochondrial function, and seems to be consistent with recent reports associating higher sperm MMP with better fertilization parameters (Zhang et al., 2018).

Sperm carry around 100 mitochondria per cell, located in the midpiece, but this number is variable (Amaral et al., 2013). It could be possible that an excessive mitochondrial load could be damaging sperm function as higher levels of sperm mtDNAcn were recently associated with lower fertilization rates (Wu et al., 2018). For this reason, we sought to determine if this was the case in our patients, but we did not observe any difference between FF and controls. However, this does not come as a surprise, since there is a high inter-individual variability in the levels of mtDNAcn in the general population, and the small number of patients in the FF group does not allow obtaining a conclusive answer. Moreover, as already reported, the levels of mtDNA do not always correlate to the expression of mitochondrial proteins and the metabolic activity of the cells (cita).

PSMA1, a component of the proteasome core, was underexpressed in FF samples, which could be related to the reduced levels of proteasome activity observed in the fluorimetric assay. Proteasome dependent proteolysis plays key roles not only during spermatogenesis, but also in mature sperm, where proteasomes are essential for sperm capacitation, sperm intracellular calcium signaling, acrosome reaction and oocyte fertilization (Sutovsky 2011; Miles et al., 2013; Kerns et al., 2016; Zigo et al., 2018). Rawe et al. showed that sperm proteasome inhibition resulted in disrupted aster formation and pronuclear development in bovine oocytes (Rawe et al., 2008). The authors also found reduced proteasome activity in sperm from patients with head-tail junction defects (observed

by electron microscopy), and described the role of sperm proteasome proteolysis in releasing the functional sperm centriole (a structure that acts as a microtubule-organizing center needed for early embryo development) by sperm mitochondrial sheath and tail connecting piece degradation. Moreover, more than half of the oocytes failed to fertilize after ICSI presented abnormal accumulations of proteasomes near the non-decondensed male PN (Rawe et al., 2008). Previous sperm proteomics studies on samples with FF after IVF also detected proteasomal proteins as differentially expressed (Frapasauce et al., 2014). For these reasons, deficient proteasome activity could affect the fertilization ability of sperm even after entry into the oocyte, thus possibly explaining part of the FF cases after ICSI.

Mitochondria and proteasome are closely related by maintaining a cross-talk, and different studies report a common dysregulation in both systems. For example, in Parkinson disease or aging, changes in mitochondrial activity can lead to reduced proteasome activity (Branco et al., 2010). Excessive mitochondrial function may be linked to a reduced proteasome system activity, altogether causing cellular dysfunction, cellular stress and impaired cellular homeostasis and viability (Maharjan et al., 2014; Segref et al., 2014; Ross et al., 2015; D'Amico et al., 2017). At the same time, cellular oxidative stress, largely used as a maker of quality in human sperm, can affect mitochondrial function and oxidative respiration in sperm (Ferramosca et al., 2013; Uribe et al., 2015). As shown in animal models, mitochondrial function and cellular stress can affect the autophagy process activated upon fertilization and early developmental steps (Song et al., 2012; Wu et al., 2015).

FAM209B, FMRNB1 and RAB2B were proteins also found as underexpressed in FF patients. The two first, despite little evidence is available about their function, show restricted expression in testicular tissue, suggesting that specific alterations during spermatogenesis could be involved in FF. However, FMRNB1-KO mice do not present fertility problems (Miyata et al., 2016). Regarding RAB2B, a member of GTPase family, could play a role in spermiogenesis as it participates in the protein transport between endoplasmic reticulum and Golgi. If RAB2B shares the function of its close homolog (RAB2A), which is involved in acrosome formation and possibly in anchoring and stabilizing the acrosome to the nucleus in mature sperm (Mountjoy et al., 2008), its deficit could lead to abnormal distribution of acrosomal components (i.e. PLC ζ or other SOAF), as well as some structural defects that could compromise fertilization ability.

Finally, individual analysis of outliers and stable-protein pairs provided valuable information about each specific FF patient. For example, ROPN1, a protein found at lower levels in F2, was recently found as the protein with most reduced abundance in samples with fertilization failure after IVF

when compared to controls (Liu et al., 2018). This protein could be an interesting clinical marker for male infertility and FF, as it participates in sperm PKA signaling, capacitation-induced tyrosine phosphorylation and fibrous sheath integrity (Fiedler et al., 2013; Zhang et al., 2016).

We recognize some limitations of our study. As cases of repetitive fertilization failure after ICSI are very rare, 4 FF samples were included. In addition, in our study we checked quantitative protein alterations; complementary studies on the role of posttranslational modifications alterations, gene sequence variants, or alternative splicing, will be useful to understand all the mechanisms potentially involved in sperm-dependent ICSI fertilization failure. For example, several mitochondrial proteins (such as PDH enzyme) are reported to undergo phosphorylation or acetylation during sperm capacitation (Shivaji et al., 2009).

In conclusion, our study identifies different mechanisms involved in male factor fertilization failure after ICSI, a process which is multifactorial. In addition, we reinforce the idea that molecular and cellular events occurring in sperm before fertilization (such as capacitation or sperm metabolism) can have profound effects not only on sperm ability to reach and penetrate the oocyte, but also on oocyte activation and early development of the embryo. We believe that some of the markers and mechanisms identified in our study could be useful as diagnostic and prognostic factors for fertilization failure after ICSI.

ACKNOWLEDGEMENTS

We would like to thank the laboratory staff from Clínica Eugin for their help in sample handling, Désirée García for statistical support, Judit Castillo, Ferran Barrachina and Filippo Zambelli for experimental counseling, and Gustavo Tiscornia for critical revision of the manuscript.

FUNDING

This work was supported by the EUGIN-UB Research Excellence Program, by intramural funding from Clinica EUGIN, and by the Secretary for Universities and Research of the Ministry of Economy and Knowledge of the Government of Catalonia (GENCAT 2015 DI 049) to M. T-M.

CONFLICT OF INTEREST

No competing interest declared.

REFERENCES

- Aarabi M, Balakier H, Bashar S, Moskovtsev SI, Sutovsky P, Librach CL, Oko R. Sperm-derived WW domain-binding protein, PAWP, elicits calcium oscillations and oocyte activation in humans and mice. *FASEB J* 2014; 28:4434-40.
- Alazami AM, Awad SM, Coskun S, Al-Hassan S, Hijazi H, Abdulwahab FM, Poizat C, Alkuraya FS. TLE6 mutation causes the earliest known human embryonic lethality. *Genome Biol* 2015; 16:240.
- Amaral A, Lourenço B, Marques M, Ramalho-Santos J. Mitochondria functionality and sperm quality. *Reproduction* 2013; 146:163-74.
- Amaral A, Paiva C, Attardo Parrinello C, Estanyol JM, Ballescà JL, Ramalho-Santos J, Oliva R. Identification of proteins involved in human sperm motility using high-throughput differential proteomics. *J Proteome Res* 2014; 13:5670-84.
- Azpiazu R, Amaral A, Castillo J, Estanyol JM, Guimerà M, Ballescà JL, Balasch J, Oliva R. High-throughput sperm differential proteomics suggests that epigenetic alterations contribute to failed assisted reproduction. *Hum Reprod* 2014; 29:1225-37.
- Barrachina F, Jodar M, Delgado-Dueñas D, Soler-Ventura A, Estanyol JM, Mallofré C, Ballesca JL, Oliva R. Novel and conventional approaches for the analysis of quantitative proteomic data are complementary towards the identification of seminal plasma alterations in infertile patients. *Mol Cell Proteomics* 2018.
- Bogle OA, Kumar K, Attardo-Parrinello C, Lewis SE, Estanyol JM, Ballescà JL, Oliva R. Identification of protein changes in human spermatozoa throughout the cryopreservation process. *Andrology* 2017; 5:10-22.
- Boulet SL, Mehta A, Kissin DM, Warner L, Kawwass JF, Jamieson DJ. Trends in use of and reproductive outcomes associated with intracytoplasmic sperm injection. *JAMA* 2015; 313:255-63.
- Branco DM, Arduino DM, Esteves AR, Silva DF, Cardoso SM, Oliveira CR. Cross-talk between mitochondria and proteasome in Parkinson's disease pathogenesis. *Front Aging Neurosci* 2010; 2:17.
- Castillo J, Jodar M, Oliva R. The contribution of human sperm proteins to the development and epigenome of the preimplantation embryo. *Hum Reprod Update* 2018.
- Codina M, Estanyol JM, Fidalgo MJ, Ballescà JL, Oliva R. Advances in sperm proteomics: best-practise methodology and clinical potential. *Expert Rev Proteomics* 2015; 12:255-77.
- D'Amico D, Sorrentino V, Auwerx J. Cytosolic Proteostasis Networks of the Mitochondrial Stress Response. *Trends Biochem Sci* 2017; 42:712-725.
- Fariello RM, Pariz JR, Spaine DM, Gozzo FC, Pilau EJ, Fraietta R, Bertolla RP, Andreoni C, Cedenho AP. Effect of smoking on the functional aspects of sperm and seminal plasma protein profiles in patients with varicocele. *Hum Reprod* 2012; 27:3140-9.
- Fatehi AN, Bevers MM, Schoevers E, Roelen BA, Colenbrander B, Gadella BM. DNA damage in bovine sperm does not block fertilization and early embryonic development but induces apoptosis after the first cleavages. *J Androl* 2006; 27:176-88.
- Fawzy M, Emad M, Mahran A, Sabry M, Fetih AN, Abdelghafar H, Rasheed S. Artificial oocyte activation with SrCl₂ or calcimycin after ICSI improves clinical and embryological outcomes compared with ICSI alone: results of a randomized clinical trial. *Hum Reprod* 2018.
- Fernandez MC, O'Flaherty C. Peroxiredoxin 6 is the primary antioxidant enzyme for the maintenance of viability and DNA integrity in human spermatozoa. *Hum Reprod* 2018.
- Ferramosca A, Pinto Provenzano S, Montagna DD, Coppola L, Zara V. Oxidative stress negatively affects human sperm mitochondrial respiration. *Urology* 2013; 82:78-83.

- Ferrer-Vaquer A, Barragan M, Freour T, Vernaev V, Vassena R. PLC ζ sequence, protein levels, and distribution in human sperm do not correlate with semen characteristics and fertilization rates after ICSI. *J Assist Reprod Genet* 2016; 33:747-56.
- Fiedler SE, Dudiki T, Vijayaraghavan S, Carr DW. Loss of R2D2 proteins ROPN1 and ROPN1L causes defects in murine sperm motility, phosphorylation, and fibrous sheath integrity. *Biol Reprod* 2013; 88:41.
- Flaherty SP, Payne D, Matthews CD. Fertilization failures and abnormal fertilization after intracytoplasmic sperm injection. *Hum Reprod* 1998; Suppl 1:155-64.
- Frapsauce C, Pionneau C, Bouley J, Delarouziere V, Berthaut I, Ravel C, Antoine JM, Soubrier F, Mandelbaum J. Proteomic identification of target proteins in normal but nonfertilizing sperm. *Fertil Steril* 2014; 102:372-80.
- Freour T, Barragan M, Torra-Massana M, Ferrer-Vaquer A, Vassena R. Is there an association between PAWP/WBP2NL sequence, expression, and distribution in sperm cells and fertilization failures in ICSI cycles? *Mol Reprod Dev* 2018; 85:163-170.
- Intasqui P, Camargo M, Del Giudice PT, Spaine DM, Carvalho VM, Cardozo KH, Cedenho AP, Bertolla RP. Unraveling the sperm proteome and post-genomic pathways associated with sperm nuclear DNA fragmentation. *J Assist Reprod Genet* 2013; 30:1187-202.
- Kerns K, Morales P, Sutovsky P. Regulation of Sperm Capacitation by the 26S Proteasome: An Emerging New Paradigm in Spermatology. *Biol Reprod* 2016; 94:117.
- Lee D, Moawad AR, Morielli T, Fernandez MC, O'Flaherty C. Peroxiredoxins prevent oxidative stress during human sperm capacitation. *Mol Hum Reprod* 2017; 23:106-115.
- Légaré C, Droit A, Fournier F, Bourassa S, Force A, Cloutier F, Tremblay R, Sullivan R. Investigation of male infertility using quantitative comparative proteomics. *J Proteome Res* 2014; 13:5403-14.
- Liao TT, Xiang Z, Zhu WB, Fan LQ. Proteome analysis of round-headed and normal spermatozoa by 2-D fluorescence difference gel electrophoresis and mass spectrometry. *Asian J Androl* 2009; 11:683-93.
- Liu X, Liu G, Liu J, Zhu P, Wang J, Wang Y, Wang W, Li N, Wang X, Zhang C, Shen X, Liu F. iTRAQ-based analysis of sperm proteome from normozoospermic men achieving the rescue-ICSI pregnancy after the IVF failure. *Clin Proteomics* 2018; 15:27.
- Maharjan S, Oku M, Tsuda M, Hoseki J, Sakai Y. Mitochondrial impairment triggers cytosolic oxidative stress and cell death following proteasome inhibition. *Sci Rep* 2014; 4:5896.
- Marques M, Sousa AP, Paiva A, Almeida-Santos T, Ramalho-Santos J. Low amounts of mitochondrial reactive oxygen species define human sperm quality. *Reproduction* 2014; 147:817-24.
- Miles EL, O'Gorman C, Zhao J, Samuel M, Walters E, Yi YJ, Sutovsky M, Prather RS, Wells KD, Sutovsky P. Transgenic pig carrying green fluorescent proteasomes. *Proc Natl Acad Sci U S A* 2013; 110:6334-9.
- Miyata H, Castaneda JM, Fujihara Y, Yu Z, Archambeault DR, Isotani A, Kiyozumi D, Kriseman ML, Mashiko D, Matsumura T, Matzuk RM, Mori M, Noda T, Oji A, Okabe M, Prunskaitė-Hyyryläinen R, Ramirez-Solis R, Satouh Y, Zhang Q, Ikawa M, Matzuk MM. Genome engineering uncovers 54 evolutionarily conserved and testis-enriched genes that are not required for male fertility in mice. *Proc Natl Acad Sci U S A* 2016; 113:7704-10.
- Moawad AR, Fernandez MC, Scarlata E, Dodia C, Feinstein SI, Fisher AB4, O'Flaherty C. Deficiency of peroxiredoxin 6 or inhibition of its phospholipase A2 activity impair the in vitro sperm fertilizing competence in mice. *Sci Rep* 2017; 7:12994.
- Nasr-Esfahani MH, Razavi S, Mardani M, Shirazi R, Javanmardi S. Effects of failed oocyte activation and sperm protamine deficiency on fertilization post-ICSI. *Reprod Biomed Online* 2007; 14:422-9.
- Neri QV, Lee B, Rosenwaks Z, Machaca K, Palermo GD. Understanding fertilization through intracytoplasmic sperm injection (ICSI). *Cell calcium* 2014; 55:24-37.

- Nozawa K, Satouh Y, Fujimoto T, Oji A, Ikawa M. Sperm-borne phospholipase C zeta-1 ensures monospermic fertilization in mice. *Sci Rep* 2018; 8:1315.
- Ozkosem B, Feinstein SI, Fisher AB, O'Flaherty C. Advancing age increases sperm chromatin damage and impairs fertility in peroxiredoxin 6 null mice. *Redox Biol* 2015; 5:15-23.
- Ozkosem B, Feinstein SI, Fisher AB, O'Flaherty C. Absence of Peroxiredoxin 6 Amplifies the Effect of Oxidant Stress on Mobility and SCSA/CMA3 Defined Chromatin Quality and Impairs Fertilizing Ability of Mouse Spermatozoa. *Biol Reprod* 2016; 94:68.
- Palermo G, Joris H, Devroey P, Van Steirteghem AC. Pregnancies after intracytoplasmic injection of single spermatozoon into an oocyte. *Lancet* 1992; 340:17-8.
- Pixton KL, Deeks ED, Flesch FM, Moseley FL, Björndahl L, Ashton PR, Barratt CL, Brewis IA. Sperm proteome mapping of a patient who experienced failed fertilization at IVF reveals altered expression of at least 20 proteins compared with fertile donors: case report. *Hum Reprod* 2004; 19:1438-47.
- Qian MX, Pang Y, Liu CH, Haratake K, Du BY, Ji DY, Wang GF, Zhu QQ, Song W, Yu Y, Zhang XX, Huang HT, Miao S, Chen LB, Zhang ZH, Liang YN, Liu S, Cha H, Yang D, Zhai Y, Komatsu T, Tsuruta F, Li H, Cao C, Li W, Li GH, Cheng Y, Chiba T, Wang L, Goldberg AL, Shen Y, Qiu XB. Acetylation-mediated proteasomal degradation of core histones during DNA repair and spermatogenesis. *Cell* 2013; 153:1012-24.
- Ramió-Lluch L, Yeste M, Fernández-Novell JM, Estrada E, Rocha L, Cebrián-Pérez JA, Muiño-Blanco T, Concha II, Ramírez A, Rodríguez-Gil JE. Oligomycin A-induced inhibition of mitochondrial ATP-synthase activity suppresses boar sperm motility and in vitro capacitation achievement without modifying overall sperm energy levels. *Reprod Fertil Dev* 2014; 26:883-97.
- Reyes R, Sánchez-Vázquez ML, Delgado NM. Energy metabolism of spermatozoa during pronucleus formation induced in vitro by heparin-reduced glutathione. I. Glucose uptake. *Arch Androl* 1993; 30:73-7.
- Rogers BJ, Ueno M, Yanagimachi R. Inhibition of hamster sperm acrosome reaction and fertilization by oligomycin, antimycin A, and rotenone. *J Exp Zool* 1977; 199:129-36.
- Rogers NT, Hobson E, Pickering S, Lai FA, Braude P, Swann K. Phospholipase Czeta causes Ca²⁺ oscillations and parthenogenetic activation of human oocytes. *Reproduction* 2004; 128:697-702.
- Ross JM, Olson L, Coppotelli G. Mitochondrial and Ubiquitin Proteasome System Dysfunction in Ageing and Disease: Two Sides of the Same Coin? *Int J Mol Sci* 2015; 16:19458-76.
- Ryu DY, Kim KU, Kwon WS, Rahman MS, Khatun A, Pang MG. Peroxiredoxin activity is a major landmark of male fertility. *Sci Rep* 2017; 7:17174.
- Samanta L, Sharma R, Cui Z, Agarwal A. Proteomic analysis reveals dysregulated cell signaling in ejaculated spermatozoa from infertile men. *Asian J Androl* 2018.
- Sang Q, Li B, Kuang Y, Wang X, Zhang Z, Chen B, Wu L, Lyu Q, Fu Y, Yan Z, Mao X, Xu Y, Mu J, Li Q, Jin L, He L, Wang L. Homozygous Mutations in WEE2 Cause Fertilization Failure and Female Infertility. *Am J Hum Genet* 2018; 102:649-657.
- Segref A, Kevei É, Pokrzywa W, Schmeisser K, Mansfeld J, Livnat-Levanon N, Ensenuer R, Glickman MH, Ristow M, Hoppe T. Pathogenesis of human mitochondrial diseases is modulated by reduced activity of the ubiquitin/proteasome system. *Cell Metab* 2014; 19:642-52.
- Sette C, Bevilacqua A, Geremia R, Rossi P. Involvement of phospholipase Cgamma1 in mouse egg activation induced by a truncated form of the C-kit tyrosine kinase present in spermatozoa. *J Cell Biol* 1998; 142:1063-74.
- Sfontouris IA, Nastri CO, Lima ML, Tahmasbpourmarzouni E, Raine-Fenning N, Martins WP. Artificial oocyte activation to improve reproductive outcomes in women with previous fertilization failure: a systematic review and meta-analysis of RCTs. *Hum Reprod* 2015; 30:1831-41.

- Sharma R, Agarwal A, Mohanty G, Hamada AJ, Gopalan B, Willard B, Yadav S, du Plessis S. Proteomic analysis of human spermatozoa proteins with oxidative stress. *Reprod Biol Endocrinol* 2013; 11:48.
- Shivaji S, Kota V, Siva AB. The role of mitochondrial proteins in sperm capacitation. *J Reprod Immunol* 2009; 83:14-8.
- Siva AB, Panneerdoss S, Sailasree P, Singh DK, Kameshwari DB, Shivaji S. Inhibiting sperm pyruvate dehydrogenase complex and its E3 subunit, dihydrolipoamide dehydrogenase affects fertilization in Syrian hamsters. *PLoS One* 2014; 9:e97916.
- Song BS, Yoon SB, Kim JS, Sim BW, Kim YH, Cha JJ, Choi SA, Min HK, Lee Y, Huh JW, Lee SR, Kim SH, Koo DB, Choo YK, Kim HM, Kim SU, Chang KT. Induction of autophagy promotes preattachment development of bovine embryos by reducing endoplasmic reticulum stress. *Biol Reprod* 2012; 87:8, 1-11.
- Sutovsky P. Sperm proteasome and fertilization. *Reproduction* 2011; 142:1-14.
- Terada Y, Schatten G, Hasegawa H, Yaegashi N. Essential roles of the sperm centrosome in human fertilization: developing the therapy for fertilization failure due to sperm centrosomal dysfunction. *Tohoku J Exp Med* 2010; 220:247-58.
- The Gene Ontology Consortium. Expansion of the gene ontology knowledgebase and resources: the gene ontology consortium. *Nucleic Acids Res* 2017; 45:D331– D338.
- Torra-Massana M, Barragán M, Bellu E, Oliva R, Rodríguez A, Vassena R. Sperm telomere length in donor samples is not related to ICSI outcome. *J Assist Reprod Genet* 2018; 35:649-657.
- Uribe P, Boguen R, Treulen F, Sánchez R, Villegas JV. Peroxynitrite-mediated nitrosative stress decreases motility and mitochondrial membrane potential in human spermatozoa. *Mol Hum Reprod* 2015; 21:237-43.
- Vanden Meerschaut F, D'Haeseleer E, Gysels H, Thienpont Y, Dewitte G, Heindryckx B, Oostra A, Roeyers H, Van Lierde K, De Sutter P. Neonatal and neurodevelopmental outcome of children aged 3-10 years born following assisted oocyte activation. *Reprod Biomed Online* 2014; 28:54-63.
- WHO. 2010. WHO laboratory manual for the examination and processing of human semen 5th edition.
- Wu LL, Russell DL, Wong SL, Chen M, Tsai TS, St John JC, Norman RJ1, Febbraio MA, Carroll J, Robker RL. Mitochondrial dysfunction in oocytes of obese mothers: transmission to offspring and reversal by pharmacological endoplasmic reticulum stress inhibitors. *Development* 2015; 142:681-91.
- Wu H, Whitcomb BW, Huffman A, Brandon N, Labrie S, Tougias E, Lynch K, Rahil T, Sites CK, Pilsner JR. Associations of sperm mitochondrial DNA copy number and deletion rate with fertilization and embryo development in a clinical setting. *Hum Reprod* 2018.
- Yanagida K. Complete fertilization failure in ICSI. *Hum Cell* 2004.
- Yeste M, Jones C, Amdani SN, Patel S, Coward K. Oocyte activation deficiency: a role for an oocyte contribution? *Hum Reprod Update* 2016; 22:23-47.
- Yoon SY, Eum JH, Lee JE, Lee HC, Kim YS, Han JE, Won HJ, Park SH, Shim SH, Lee WS, Fissore RA, Lee DR, Yoon TK. Recombinant human phospholipase C zeta 1 induces intracellular calcium oscillations and oocyte activation in mouse and human oocytes. *Hum Reprod* 2012; 27:1768-80.
- Zhang X, Chen M, Yu R, Liu B, Tian Z, Liu S. FSCB phosphorylation regulates mouse spermatozoa capacitation through suppressing SUMOylation of ROPN1/ROPN1L. *Am J Transl Res* 2016; 8:2776-82.
- Zhang G, Yang W, Zou P, Jiang F, Zeng Y, Chen Q, Sun L, Yang H, Zhou N, Wang X, Liu J, Cao J, Zhou Z, Ao L. Mitochondrial functionality modifies human sperm acrosin activity, acrosome reaction capability and chromatin integrity. *Hum Reprod* 2018.
- Zhu Y, Wu Y, Jin K, Lu H, Liu F, Guo Y, Yan F, Shi W, Liu Y, Cao X, Hu H, Zhu H, Guo X, Sha J, Li Z, Zhou Z. Differential proteomic profiling in human spermatozoa that did or did not result in pregnancy via IVF and AID. *Proteomics Clin Appl* 2013; 7:850-8.

Zigo M, Kerns K, Sutovsky M, Sutovsky P. Modifications of the 26S proteasome during boar sperm capacitation. *Cell Tissue Res* 2018; 372:591-601.

SUPPLEMENTARY INFORMATION

Supplementary Table I. Distribution of FF and control samples across the different experimental approaches performed.

Sample	Proteomics	Western Blot	JC-1 / Proteasome activity
F1	✓	✓	✓
F2	✓	✓	
F3	✓	✓	✓
F4	✓	✓	✓
F5			✓
C1	✓	✓	
C2	✓		
C3	✓	✓	
C4			✓
C5			✓
C6	✓	✓	
C7			✓
C8			✓
C9	✓	✓	
C10	✓	✓	
C11	✓	✓	✓
C12	✓	✓	

Supplementary Table II. mtDNA quantification was performed via real time qPCR with SYBR green chemistry. We used primer pairs targeting two different genes in the mtDNA (MT-ND1 and MT-ND4), that were normalized to a single nuclear gene (B2M) to detect the relative mtDNA copy number per cell using the delta CT method. qPCR efficiencies (E) were calculated on sperm DNA based on the standard curve according to the formula $[E=10(-1/\text{slope})-1] \times 100$ and are expressed as a percentage.

Gene	Target DNA	Forward (5'-3')	Reverse (5'-3')	Efficiency (%)
MT-ND1	Mitochondrial	CACCCAAGAACACGGTT TGT	TGGCCATGGGTATGTTGTAA	96.4
MT-ND4	Mitochondrial	CCTCGCTAACCTCGCCTT A	GGAGAACGTGGTTACTAGCACA	82.6
B2M	Nuclear	TGCTGTCTCCATGTTTGA TGT	TCTCTGCTCCCCACCTCTAAG	85.3

Supplementary Table III. Individualized demographic and clinical variables for each patient included in the study.

ID	Age	Male BMI	Volume (ml)	Conc. (M/ml)	Motility (%a+b)	Morph. (% normal)	ICSI FR (2PN/MI)	Oocyte	Oocyte age	Mean oocyte age	Oocyte /cycle	Mean FR
F1	36	24.49	6.4	190.96	87.12	4	0/2 0/3 0/4	Partner Partner Partner	33 34 34	33.67	3	0% (0/9)
F2	43	22.46	4.1	55.7	49	9	0/12 0/6 1/12 0/13	Partner Partner Partner Partner	35 36 36 36	35.75	10.7	2'3% (1/43)
F3	42	22.35	5.1	125.05	81.3	12	0/20 1/7 0/2 0/2 0/12 0/8	Partner Partner Partner Partner Partner Donor	36 36 36 37 38 31	35.67	8.5	1.96% (1/51)
F4	43	24.44	5.8	21.78	21.3	7	1/5 1/3 0/3	Partner Partner Partner	42 41 42	41.67	3.67	18'2% (2/11)
F5	36	22.88	5.0	39.1	35	7	0/11 0/2 0/3 0/1	Partner Partner Partner Partner	27 27 29 29	28	4.25	0% (0/17)
C1	34	21.27	4.6	118.5	66.7	5	4/4 7/7	Partner Donor	33 33	33	5.5	100% (11/11)
C2	31	23.37	4	109.99	50.85	5	6/6 5/8	Donor Donor	23 27	25	7	78.57%(11/14)
C3	40	22.31	4.6	38.95	48.45	4	5/6	Donor	31	31	6	83'3% (5/6)
C4	35	NA	5.1	18.53	34.37	NA	2/3 9/11	Partner Partner	34 35	34.5	7	78.57% (11/14)
C5	40	29.03	4.8	242.21	87.22	13	8/8	Donor	33	33	8	100% (8/8)
C6	39	21.74	3.4	213.53	81.92	2	6/7	Donor	22	22	7	85'7% (6/7)
C7	36	26.12	6.7	90.36	59.47	5	6/7	Partner	40	40	7	85.7% (6/7)
C8	43	NA	5.7	165.8	39.27	6	12/1 6	Partner	28	28	16	75% (12/16)
C9	33	NA	1.6	118.16	62.84	5	1/1 1/2 5/6	Partner Partner Donor	36 37 23	32	3	77.78% (7/9)
C10	39	NA	3.9	112.13	76.29	4	2/2 2/3 5/6	Partner Partner Donor	36 36 20	30.67	3.67	81.82% (9/11)
C11	42	24.62	6.5	72.81	74.85	6	8/10	Donor	25	25	10	80% (8/10)
C12	35	25.25	4.2	122.63	62.35	8	5/6	Donor	26	26	6	83'3% (5/6)

Supplementary Table IV. List of proteins (n=87) not previously identified in previous sperm proteomics studies.

Uniprot accession	Gene name	Protein name
A0A0C4DH39	IGHV1-58	IGHV1-58
A6H8Y1	BDP1	Transcription factor TFIIB component B" homolog
A6NI56	CCDC154	Coiled-coil domain-containing protein 154
A6NL88	SHISA7	Protein shisa-7
A8MT65	ZNF891	Zinc finger protein 891
O14804	TAAR5	Trace amine-associated receptor 5
O14990	PPP1R2C	Protein phosphatase inhibitor 2 family member C
O15258	RER1	Protein RER1
O43493	TGOLN2	Trans-Golgi network integral membrane protein 2
O43653	PSCA	Prostate stem cell antigen
O75354	ENTPD6	Ectonucleoside triphosphate diphosphohydrolase 6
O75438	NDUFB1	NADH dehydrogenase [ubiquinone] 1 beta subcomplex subunit 1
O95562	SFT2D2	Vesicle transport protein SFT2B
O96006	ZBED1	Zinc finger BED domain-containing protein 1
P00156	MT-CYB	Cytochrome b
P04004	VTN	Vitronectin
P08962	CD63	CD63 antigen
P0CG34	TMSB15A	Thymosin beta-15
P17021	ZNF17	Zinc finger protein 17
P20273	CD22	B-cell receptor CD22
P21554	CNR1	Cannabinoid receptor 1
P24387	CRHBP	Corticotropin-releasing factor-binding protein
P26951	IL3RA	Interleukin-3 receptor subunit alpha
P29536	LMOD1	Leiomodin-1
P30291	WEE1	Wee1-like protein kinase
P31645	SLC6A4	Sodium-dependent serotonin transporter
P32989	TOP1	DNA topoisomerase 1
P33053	RPO147	DNA-directed RNA polymerase 147 kDa polypeptide
P36784	E2	Regulatory protein E2
P42694	HELZ	Probable helicase with zinc finger domain
P47914	RPL29	60S ribosomal protein L29
P54108	CRISP3	Cysteine-rich secretory protein 3

P60568	IL2	Interleukin-2
P62072	TIMM10	Mitochondrial import inner membrane translocase subunit Tim10
P78312	FAM193A	Protein FAM193A
Q02539	HIST1H1A	Histone H1.1
Q08174	PCDH1	Protocadherin-1
Q13972	RASGRF1	Ras-specific guanine nucleotide-releasing factor 1
Q15849	SLC14A2	Urea transporter 2
Q16512	PKN1	Serine/threonine-protein kinase N1
Q29983	MICA	MHC class I polypeptide-related sequence A
Q5J5C9	DEFB121	Beta-defensin 121
Q5QGZ9	CLEC12A	C-type lectin domain family 12 member A
Q5UE93	PIK3R6	Phosphoinositide 3-kinase regulatory subunit 6
Q5VV63	ATRNL1	Attractin-like protein 1
Q6MZM0	HEPHL1	Hephaestin-like protein 1
Q6P0Q8	MAST2	Microtubule-associated serine/threonine-protein kinase 2
Q6UDR6	SPINT4	Kunitz-type protease inhibitor 4
Q6UWE0	LRSAM1	E3 ubiquitin-protein ligase LRSAM1
Q6UXD5	SEZ6L2	Seizure 6-like protein 2
Q6W2J9	BCOR	BCL-6 corepressor
Q6ZN30	BNC2	Zinc finger protein basonuclein-2
Q6ZTR5	CFAP47	Cilia- and flagella-associated protein 47
Q6ZVX9	PAQR9	Membrane progesterin receptor epsilon
Q7L4I2	RSRC2	Arginine/serine-rich coiled-coil protein 2
Q86SQ7	SDCCAG8	Serologically defined colon cancer antigen 8
Q86X29	LSR	Lipolysis-stimulated lipoprotein receptor
Q89489	A29L	Protein A26 homolog
Q8HWS3	RFX6	DNA-binding protein RFX6
Q8IUX4	APOBEC3F	DNA dC->dU-editing enzyme APOBEC-3F
Q8IXR9	C12orf56	Uncharacterized protein C12orf56
Q8IZD9	DOCK3	Dedicator of cytokinesis protein 3
Q8JPR2	L	RNA-directed RNA polymerase L
Q8N895	ZNF366	Zinc finger protein 366
Q8TBR7	FAM57A	Protein FAM57A
Q92562	FIG4	Polyphosphoinositide phosphatase
Q92733	PRCC	Proline-rich protein PRCC

Q96A25	TMEM106A	Transmembrane protein 106A
Q96AC6	KIFC2	Kinesin-like protein KIFC2
Q96N03	VSTM2L	V-set and transmembrane domain-containing protein 2-like protein
Q96RE7	NACC1	Nucleus accumbens-associated protein 1
Q99797	MIPEP	Mitochondrial intermediate peptidase
Q9BPU6	DPYSL5	Dihydropyrimidinase-related protein 5
Q9BQA9	CYBC1	Cytochrome b-245 chaperone 1
Q9BTE7	DCUN1D5	DCN1-like protein 5
Q9C091	GREB1L	GREB1-like protein
Q9C0B2	CFAP74	Cilia- and flagella-associated protein 74
Q9H0U3	MAGT1	Magnesium transporter protein 1
Q9H2C0	GAN	Gigaxonin
Q9H8Y5	ANKZF1	Ankyrin repeat and zinc finger domain-containing protein 1
Q9P2X0	DPM3	Dolichol-phosphate mannosyltransferase subunit 3
Q9UH17	APOBEC3B	DNA dC->dU-editing enzyme APOBEC-3B
Q9UHG2	PCSK1N	ProSAAS
Q9UNW9	NOVA2	RNA-binding protein Nova-2
Q9Y239	NOD1	Nucleotide-binding oligomerization domain-containing protein 1
Q9Y5F9	PCDHGB6	Protocadherin gamma-B6
Q9Y6X5	ENPP4	Bis(5'-adenosyl)-triphosphatase ENPP4

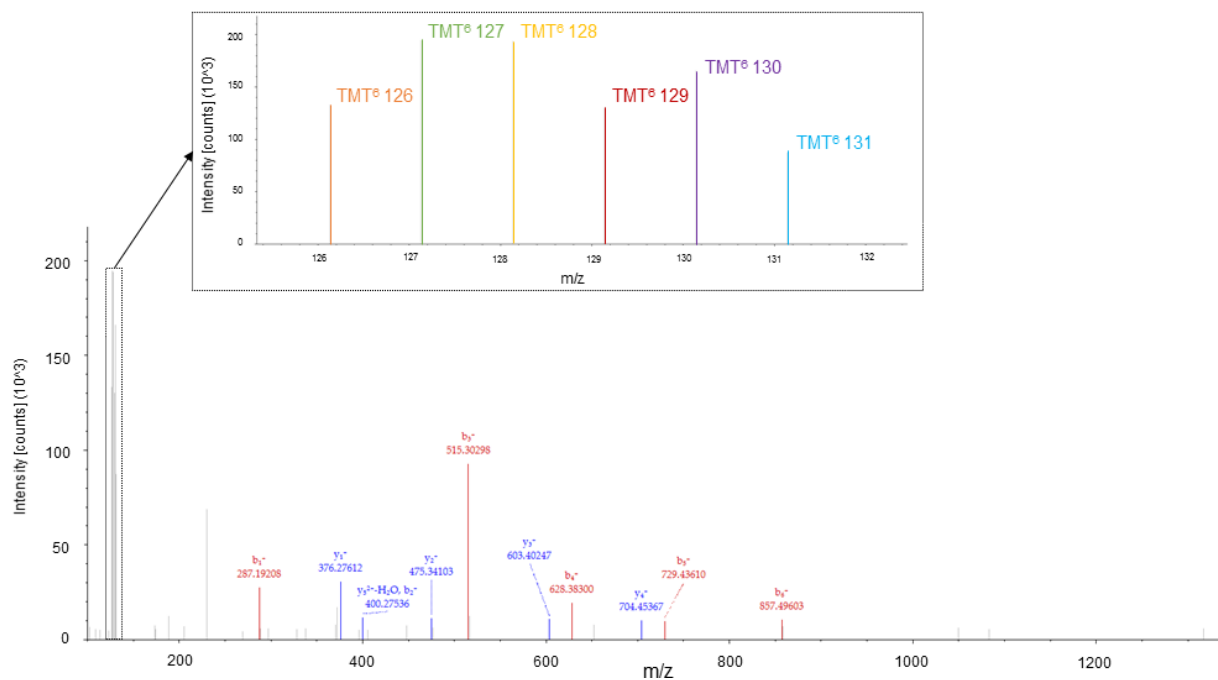
Supplementary Table V. Proteins involved in the stable-protein pairs in the control patients (n = 8). The correlation of two proteins is counted as a single correlation. Colour code refers to protein function: green, metabolism or mitochondrial function; orange, sperm structure-associated; blue, fertilization; yellow, other cellular functions.

Proteins		Number of stable correlations
Metabolism / mitochondrial function	PDHA2	12
	OXCT1	11
	COX6B1	9
	PHB2	4
	ATP5F1C	4
	MPC1L	2
	DECR1	1
	ATP5F1D	1
	PDHB	1
	ATP5O	1
	LDHC	1
Sperm structure -associated	NUP155	11
	NUP54	9
	CFAP45	8
	ACRV1	6
	NUP210L	2
	TEKT2	1
Fertilization	SPACA4	4
	ZPBP	3
Other	CD59	15
	FAM209A	9
	DYNLL2	9
	CCT3	8
	RUVBL1	4
	RPLP2	4
	ASRGL1	3
	FAM209B	2
	SSBP1	1
Total	146	
Correlations	73	
Proteins involved	28	

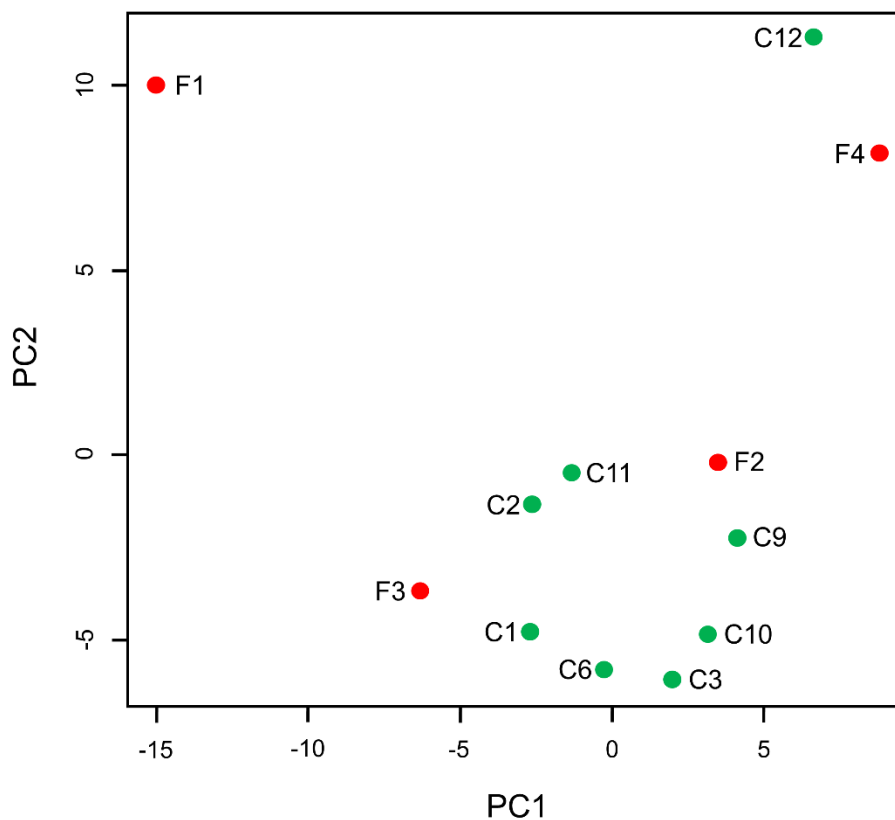
Supplementary Table VI. Results of outliers analysis for each FF sample included in the proteomics study. The proteins overexpressed and underexpressed compared with the control group are indicated in green and red, respectively.

Patient	Uniprot ID	Symbol	
F1	P0DP23	CALM1	1,731
	Q9UII2	ATPIF1	1,048
	P10606	COX5B	0,938
	P61604	HSPE1	0,934
	Q9UIF3	TEKT2	0,799
	O75947	ATP5H	0,608
	P14927	UQCRB	0,58
	Q8WWB3	DYDC1	0,522
	P30049	ATP5F1D	0,454
	Q9UL16	CFAP45	0,437
	P10809	HSPD1	0,296
	P29803	PDHA2	0,281
	F2	Q96KW9	SPACA7
Q14165		MLEC	0,496
Q9HAT0		ROPN1	-0,407
F3	Q9H1X1	RSPH9	0,602
	Q96D96	HVCN1	-0,322
	Q6UXI9	NPNT	-0,918
F4	P13987	CD59	0,46
	O00330	PDHX	0,45
	P22695	UQCRC2	0,428
	P54652	HSPA2	0,382
	Q00325	SLC25A3	0,294
	P0DP23	CALM1	-0,462

Supplementary Figure 1. Example of TMT 6-plex MS/MS spectrum. The spectrum shows a peptide of the differentially expressed protein dihydrolipoyllysine-residue acetyltransferase component of pyruvate dehydrogenase complex (DLAT) (peptide sequence: GIDLTQVK, G1-TMT6plex (229.16293 Da), K8-TMT6plex (229.16293 Da)). The reporter ions (m/z 126-131) are shown in the dotted box, where the intensity of each reporter ion indicates the relative proportion of the peptide in each labelled sample.

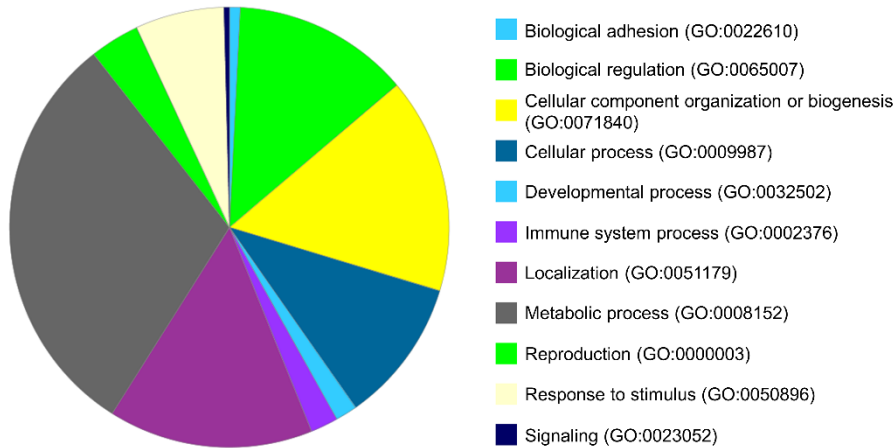


Supplementary Figure 2. PCA analysis performed for all samples included in the proteomics study (4 FF, 8 controls) using the quantification data from the 232 proteins with high-confidence quantification values.

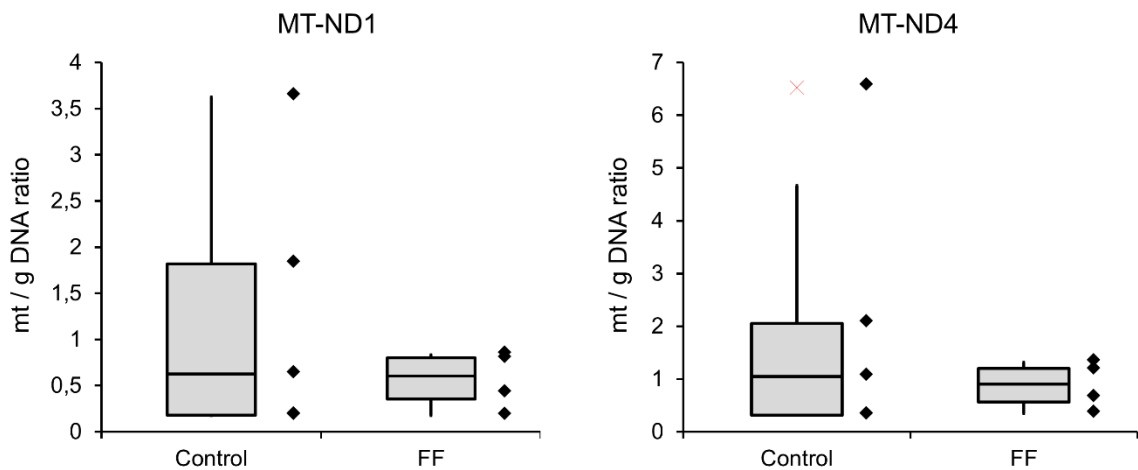


Supplementary Figure 3. Gene ontology - Biological Process analysis performed with PANTHER v. 14 database on the 232 sperm proteins with high confidence quantification values identified (FDR <1 %, ≥ 2 PSMs in all the samples, coefficient of variation <50 % in at least 75 % of the samples).

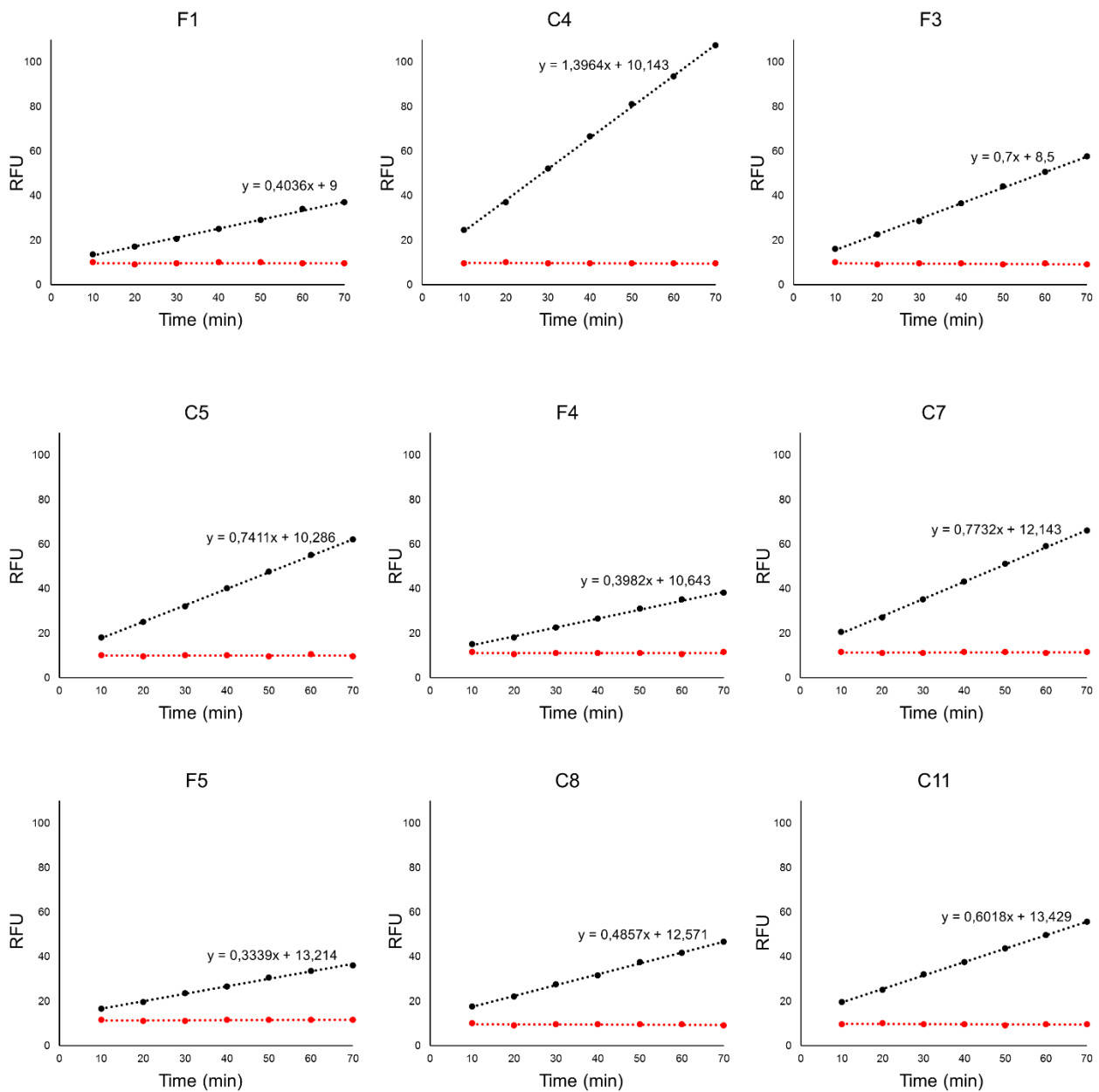
PANTHER GO-Slim Biological Process



Supplementary Figure 4. Relative mitochondrial DNA copy number (mtDNAcn) of 4 samples with FF and 5 controls. The expression levels of two mitochondrial genes (MT-ND1 and MT-ND4) were normalized against a nuclear gene (B2M).



Supplementary Figure 5. Results of the fluorimetric assay used to determine the proteasomal activity in FF samples and controls. Samples were incubated at 37°C for 70 minutes, and fluorescence (expressed as relative fluorescent units, RFU) was monitored every 10 minutes. For each sample, an increase in fluorescent signal was observed upon time (black lines), while any increase was observed when proteasomal inhibitor was added (red lines).



CHAPTER 6: Use of assisted oocyte activation (AOA) after a failed fertilization cycle: where is the evidence?

Partial contents of this chapter were included in the following oral presentation:

Torra-Massana, Marc; Barragán, Montserrat; Rodríguez, Amelia; Vassena, Rita. **Use of assisted oocyte activation (AOA) after a failed fertilization cycle: where is the evidence?** ESHRE Campus Symposium: ‘Evidence-based practice in the IVF laboratory’, 2018, Athens, Greece.

INTRODUCTION

Fertilization failure (FF) occurs in 1-3% of all ICSI cycles, even when using donor oocytes. As FF is a rare event, studies reporting large numbers of cases are scarce, and clinical guidelines in case of FF after ICSI are lacking. Clinical options for the following cycle include: change of one of the gametes, artificial oocyte activation (AOA), or performing a new cycle under the same conditions. Regarding AOA, the use of calcium ionophores (such as ionomycin and calcymycin (A23187)) are the most common strategies. Despite being still considered an experimental technique, AOA combined with ICSI seems to be safe, as numerous live births have been achieved without apparent health problems in the offspring (D'haeseleer et al., 2014; Vanden Meerschaut et al., 2014; Deemeh et al., 2015). Nevertheless, AOA efficiency is still under debate. While several studies report beneficial results (Murugesu et al., 2017; Fawzy et al., 2018), other authors indicate no marked improvement in fertilization and pregnancy rates after AOA (Sfontouris et al., 2015).

Although specific sperm molecular alterations can be associated with complete and repeated FF (e.g. presence of deleterious mutations in sperm PLC ζ), in most cases AOA is performed without a genetic diagnosis, apparently justified by the presence of clinical FF, either total or partial. The semen sample analysis performed in most fertility clinics, based on sperm concentration, motility and morphology, does not allow the identification of clear gamete defects that may explain the origin of fertilization failure. Recently, different studies point out that AOA is not beneficial for all patients or FF cases (Ferrer-Buitrago et al., 2018). For all these reasons, there is a need to analyse in which cases AOA should be recommended, in order to apply this technique only in those. In particular, when facing FF after ICSI in the absence of molecular information about the gametes, there is no consensus on whether to use AOA in the following cycle.

Table I. Baseline characteristics of the included patients, indicated as mean \pm standard deviation [range], and fertilization rate in the first ICSI cycle, expressed as %.

Variable, units	
Woman age, years	41.81 \pm 3.99 [30 - 50]
Man age, years	42.54 \pm 6.17 [25 - 62]
Sperm concentration, million / ml	53.24 \pm 57.73 [0.6 – 369.7]
Sperm motility, % a + b	43.54 \pm 19.81 [3.5 – 91.3]
Fertilization rate (FF cycle), 2PN / MII oocytes (%)	62 / 812 (7.64 %)

The aim of our study is to understand whether the presence of FF in a previous cycle is a sufficient criterion to indicate AOA. As we would like to address this question specifically in relation to the

male contribution to FF, we focused on cases where the oocyte was of high quality (donor oocytes). We further selected patients undergoing a new cycle after FF and compared the laboratory and reproductive results in those who underwent AOA to those who repeated the cycle without additional interventions.

MATERIAL & METHODS

Study design and participants

This is a retrospective consecutive cohort study including couples with a previous oocyte donation cycle with partial or total fertilization failure after ICSI ($\leq 20\%$ fertilization rate) using the patient's own sperm, all of them undergoing a second oocyte donation cycle (with oocytes from a different donor, and the partner own sperm, either fresh or cryopreserved) between June 2012 and March 2018. In all cycles included, a minimum of 5 mature oocyte were inseminated, and all embryo transfers (ET) were performed fresh. Patients with severe male factor (i.e. testicular biopsy, cryptozoospermia, or extreme asthenozoospermia - $<2\%$ progressive motility-), and those who had a previous history of adequate fertilization were excluded. 125 patients met these criteria and were included, 64 of them with total FF. 92% (115/125) of patients repeated the cycle with donor oocytes and partner sperm (OD group) without any additional intervention, while 8% (10/125) underwent oocyte donation with partner sperm + AOA (AOA group). Mean demographic and semen parameters of the patients included in this study are represented in **Table I**.

Ovarian stimulation and laboratory procedures

Ovarian stimulation, trigger of ovulation, and oocyte pick-up and denudation were performed as previously described (Pujol et al., 2018). ICSI was elective, and only MII oocytes were inseminated.

Partner semen (either fresh or frozen) was used in all cycles. Sperm samples were collected or thawed on the day of ICSI. Samples were analyzed by SCA (Sperm Class Analyzer; Microptic), and graded according to the World Health Organization guidelines (WHO, 2010). Sperm selection was performed by swim up, as previously described (Pujol et al., 2018).

Fertilization was assessed 14–19 h post ICSI. Embryo transfer was performed at Day 2 or 3 of embryonic development. Embryos with a higher morphological score were selected for embryo transfer. The ultrasound evidence of a gestational sac with fetal heartbeat was considered as a positive clinical pregnancy.

Assisted oocyte activation

Assisted oocyte activation (AOA) was performed as previously described (Durban, et al., 2015). Briefly, 30 min after ICSI, oocytes were treated by two rounds of Ionomycin (MP Biomedical, USA) at 10 $\mu\text{mol/l}$ in G-1 PLUSTM (Vitrolife) for 10 min followed by 30 min washing in G-1 PLUSTM medium (Vitrolife). Afterwards, oocytes were cultured into a time lapse system incubator under 37 °C, 6% CO₂, 5% O₂ conditions.

Statistical analysis

Age and number of inseminated oocytes were compared between the first and second ICSI cycles by two-tailed Fisher's exact test. Fertilization and pregnancy rates after fresh embryo transfer (FET) were compared between the different study groups by using variables (and reproductive outcomes (fertilization and clinical pregnancy rates) were compared between the different study groups by two-tailed Fisher's exact test. A p-value of 0.05 was set as statistically significant.

RESULTS

Our analysis of different ICSI cycle parameters found no significant difference in the age of the oocyte donors used between the first and the second ICSI cycle for each couple (**Table II**). However, the mean number of inseminated oocytes and the mean fertilization rate of the oocyte donors were higher in the second ICSI cycle (**Table II**). The percentage of oocyte donors with <50% fertilization rate was significantly higher in the first ICSI cycle.

Table II. Statistical comparison of oocyte donor variables (age, historical mean fertilization rate) and ICSI cycle variables (number of inseminated oocytes and fertilization rate) between the first ICSI cycles (FF cycles) and the subsequent ICSI cycle for all the patients included in the study.

	First ICSI cycle (FF, n=125)	Second ICSI cycle (n=125)	p
Oocyte donor age, years	25.76 \pm 4.56 [18 – 35]	26.56 \pm 4.38 [18 – 35]	NS
Oocyte donor mean fertilization rate (historical), %	64.82 \pm 18.34 [0-100]	72.72 \pm 9.01 [47.83 – 89.02]	p < 0.001
Number of oocyte donors with a history of \leq 50% mean fertilization rate; n (%)	15 / 125 (12 %)	3 / 125 (2.4 %)	p < 0.01
Number of inseminated oocytes per cycle, n	6.50 \pm 1.18 [5 – 11]	8.19 \pm 1.51 [5 – 13]	p < 0.001
Fertilization rate, 2PN/MII (%)	62 / 812 (7.64 %)	704 / 1024 (68.75 %)	p < 0.001

In the second ICSI cycle, all patients in which AOA was applied recovered good fertilization rates (> 40% in all cases). The mean fertilization rate when using AOA was similar to that obtained in the cycles post-FF without using AOA (**Table III**). The reproductive outcomes (clinical pregnancy and live birth rate) were slightly higher when using AOA, but this difference did not reach statistical significance. Our results show that most of the patients who suffered FF after ICSI, including those with total FF, recovered good fertilization rates when using good quality donor oocytes in the subsequent cycle. At the same time, we observed that 2 patients (2 / 115, 1.74 %) repeated the FF. This means that some patients, may have clear sperm-related defects, in which AOA is expected to provide a benefit.

Table III. Statistical analysis of the outcomes (fertilization rate, number of cases with FF, clinical pregnancy and live birth rates) in oocyte donation ICSI cycles performed after a previous FF, when using AOA (AOA group) or not (OD group). The information of the patients which had total FF previously (OD-TFF subgroup) is also included.

	OD group (n=115)	OD-TFF subgroup (n=64)	AOA group (n=10)	p (OD vs AOA)	p (TFF vs AOA)
Fertilization rate, 2PN/MII (%)	641 / 929 (69.00 %)	312 / 465 (67.10 %)	63 / 95 (66.32 %)	NS	NS
Cases with FF, n	2	2	0	-	-
Clinical pregnancy, positive cases / cycles with ET (%)	46 / 102 (44.23 %)	23 / 50 (46.00 %)	6 / 10 (60 %)	NS	NS
Live birth rate, positive cases / cycles with ET (%)	39 / 102 (38.24 %)	22 / 50 (44.00 %)	6 / 10 (60 %)	NS	NS

Finally, as AOA is especially recommended in FF caused by oocyte activation failure, we performed an additional subanalysis, analysing the fertilization outcomes in relation to a previous evidence of oocyte activation (**Table IV**). Those patients which had a previous evidence of oocyte activation (presence of at least one oocyte with 1PN, 3PN, or 2PN, n = 85), presented a fertilization rate of 71.39 %, significantly higher than those patients with any evidence of oocyte activation (n = 30, 62.03 %).

Table IV. Statistical analysis of the outcomes (fertilization rate, number of cases with FF, clinical pregnancy and live birth rates) in oocyte donation ICSI cycles performed after a previous FF with and without evidence of oocyte activation (presence of at least one oocyte with 1PN, 2PN, 3PN, or >3PN). FF: fertilization failure; PN: pronuclei.

	Previous evidence of oocyte activation (n = 85)	No previous evidence of oocyte activation (n = 30)	p
Fertilization rate, 2PN/MII (%)	494 / 692 (71.39 %)	147 / 237 (62.03 %)	p < 0.01
Cases with FF, n	0	2	-
Clinical pregnancy, positive cases / total cycles (%)	33 / 76 (43.42 %)	13 / 26 (50.00 %)	NS
Live birth rate, positive cases / total cycles (%)	26 / 76 (34.21 %)	13 / 26 (50.00 %)	NS

DISCUSSION

This is the largest study analysing the outcomes of patients with previous fertilization failure in ICSI cycles with donor oocytes. We expect that our results may be useful for AOA recommendation and clinical management after FF using oocyte donation.

In a clinical context, a failed oocyte donation cycle (either caused by FF or not), it is usually followed by insemination of more oocytes and to use another oocyte donor with higher mean fertilization rates, in order to increase the chance of reproductive success. This explains why there is an increase in the number of inseminated oocytes and the oocyte donor mean fertilization rate in the ICSI cycles post-FF. Even when using donor oocytes, FF can be caused by an oocyte-dependent problem, as suggested by the presence of 12% donors with mean fertilization rate below 50%. Nevertheless, most of the FF cycles included in this study are not expected to be caused by an oocyte factor (88%), and sperm defects or other cycle-specific parameters could be involved.

Almost all patient with FF (either total or partial) recovered good fertilization rates in a subsequent donor oocyte ICSI cycle, and AOA did not result in better fertilization rates or reproductive outcomes. This is in accordance with previous reports, indicating that AOA is not beneficial for all FF cases (Ferrer-Buitrago et al., 2018). However, in 1.74 % of cases (2/115), fertilization failure occurred in two consecutive cycles with high quality oocytes, indicating that this might be the approximate rate of alterations in the male gamete leading to a consistent inability to activate the oocyte after ICSI. These results are similar to the ones obtained by Liu and colleagues: 26 patients

with previous FF after ICSI repeated ICSI treatment without AOA nor additional interventions, of which 22 (84.6%) achieved good fertilization rates.

In fertility clinics, sperm quality evaluation is based on semen parameters (concentration, motility and morphology). We propose that, in a FF situation, a more detailed molecular analysis should be performed to identify the putative functionality of the male gamete (i.e. testing PLC ζ abnormalities), which could be helpful to identify those cases with higher probability of experiencing a repetitive FF, as well as to identify the cases in which AOA should be recommended.

Our results should not be extended to couples where the woman is of advanced reproductive age or where the man has a concomitant severe male factor infertility. It is possible that the good quality of the oocyte used may compensate for hidden or partial sperm defects (i.e. subfertility); therefore, we hypothesize that the percentage of repetitive FF is higher in cycles using oocytes with lower quality, as previously reported (Shinar et al., 2014).

Overall, our results provide evidence that AOA, a technique still considered experimental, provides no benefit in most cases of FF after oocyte donation. Within this group of patients, and in absence of molecular information about the gametes, one instance of low fertilization or total fertilization should not be, alone, indication for AOA.

REFERENCES

- Deemeh MR, Tavalae M, Nasr-Esfahani MH. Health of children born through artificial oocyte activation: a pilot study. *Reprod Sci* 2015; 22:322-8.
- D'haeseleer E, Vanden Meerschaut F, Bettens K, Luyten A, Gysels H, Thienpont Y, De Witte G, Heindryckx B, Oostra A, Roeyers H, Sutter PD, van Lierde K. Language development of children born following intracytoplasmic sperm injection (ICSI) combined with assisted oocyte activation (AOA). *Int J Lang Commun Disord* 2014; 49:702-9.
- Durban M, Barragán M, Colodron M, Ferrer-Buitrago M, De Sutter P, Heindryckx B, Vernaev V, Vassena R. PLC ζ disruption with complete fertilization failure in normozoospermia. *J Assist Reprod Genet* 2015; 32:879-86.
- Fawzy M, Emad M, Mahran A, Sabry M, Fetih AN, Abdelghafar H, Rasheed S. Artificial oocyte activation with SrCl₂ or calcimycin after ICSI improves clinical and embryological outcomes compared with ICSI alone: results of a randomized clinical trial. *Hum Reprod* 2018; 33:1636-1644.
- Ferrer-Buitrago M, Dhaenens L, Lu Y, Bonte D, Vanden Meerschaut F, De Sutter P, Leybaert L, Heindryckx B. Human oocyte calcium analysis predicts the response to assisted oocyte activation in patients experiencing fertilization failure after ICSI. *Hum Reprod* 2018; 33:416-425.
- Liu J, Nagy Z, Joris H, Tournaye H, Smits J, Camus M, Devroey P, Van Steirteghem A. Analysis of 76 total fertilization failure cycles out of 2732 intracytoplasmic sperm injection cycles. *Hum Reprod* 1995; 10:2630-6.

Murugesu S, Saso S, Jones BP, Bracewell-Milnes T, Athanasiou T, Mania A, Serhal P, Ben-Nagi J. Does the use of calcium ionophore during artificial oocyte activation demonstrate an effect on pregnancy rate? A meta-analysis. *Fertil Steril* 2017; 108:468-482.e3.

Pujol A, García D, Obradors A, Rodríguez A, Vassena R. Is there a relation between the time to ICSI and the reproductive outcomes? *Hum Reprod* 2018; 33:797-806.

Sfontouris IA, Nastri CO, Lima ML, Tahmasbpourmarzouni E, Raine-Fenning N, Martins WP. Artificial oocyte activation to improve reproductive outcomes in women with previous fertilization failure: a systematic review and meta-analysis of RCTs. *Hum Reprod* 2015; 30:1831-41.

Shinar S, Almog B, Levin I, Shwartz T, Amit A, Hasson J. Total fertilization failure in intra-cytoplasmic sperm injection cycles--classification and management. *Gynecol Endocrinol* 2014; 30:593-6.

Vanden Meerschaut F, D'Haeseleer E, Gysels H, Thienpont Y, Dewitte G, Heindryckx B, Oostra A, Roeyers H, Van Lierde K, De Sutter P. Neonatal and neurodevelopmental outcome of children aged 3-10 years born following assisted oocyte activation. *Reprod Biomed Online* 2014; 28:54-63.

DISCUSSION



Factors underlying infertility and, more specifically, fertilization failure, are heterogeneous and diverse. For this reason, treatment advice and counselling of patients experiencing FF needs to be individualized for each specific case. However, there is a lack of diagnostic, prognostic and treatment tools to fulfil this objective.

This problem can be explained by two main reasons: i) there is a strong need to improve the sperm quality evaluation and male infertility diagnostic in fertility clinics, including tests which can inform about sperm function and fertilizing ability (clearly not evaluated when using the routine assessment by spermiogram); ii) there is a considerable lack of knowledge about human fertilization (especially in the events occurring during oocyte activation) and the alterations leading to FF after ICSI. Both limitations could be overcome with more research on human fertilization. Considering the complexity of human fertilization and its implications in ART, this research needs to be general and comprehensive, including as many factors and mechanisms as possible, different techniques and approaches, and involving both basic biology and clinical data; something which was pursued along the present thesis.

Since the discovery of the sperm role in triggering oocyte activation, research has focused on identifying the specific factors involved in this function. Two sperm proteins gained special attention after being proposed to be involved in oocyte activation: PLC ζ , described by Saunders et al. in 2002, and PAWP, described by Wu and colleagues in 2007. Since then, several studies characterizing the function of both proteins in fertilization (in animal models and human) have been performed to elucidate which is the real ‘sperm factor’. Some controversy existed on the role of PLC ζ and PAWP in human fertilization, (Nomikos et al., 2014; Aarabi et al., 2014), and despite strong evidence has accumulated in favour of PLC ζ during the last decade, this issue is still an ongoing goal of many researchers. For this reason, we wanted to characterize both proteins as markers for FF after ICSI, including different approaches (protein levels, protein localization and gene sequence) and numerous patients with FF.

PAWP protein localization, protein levels and distribution of most genetic variants were similar between FF and controls, suggesting that PAWP may not be a useful marker for FF after ICSI. Of note, the genetic analysis of PAWP gene resulted in the identification of two missense variants exclusively carried by two FF patients: c.13C>G (p.Q5E) and c.409G>T (p.C170F). However, the functional significance of these variants during fertilization (if any) is very complicated to determine with the current knowledge, as the non-canonical mechanism by which PAWP would trigger oocyte activation (involving PLC γ) has not been demonstrated in humans. Furthermore, it is not known if PAWP could be involved in other fertilization events downstream of the onset of

calcium oscillations (i.e. regulation of the oocyte meiotic spindle or male chromatin remodelling factors), as originally suggested by Wu et al., 2007. Finally, as suggested by a recent report, WBP2, a close homolog of PAWP, could also contain oocyte activation ability and compensate for potential PAWP defects in sperm (Hamilton et al., 2018), something which was not taken into account in most studies addressing PAWP in human fertilization. Both SOAF (PAWP / WBP2 and PLC ζ) could play important roles in human fertilization by acting in synergy (Hamilton et al., 2018). This would make sense from an evolutionary perspective, in which two independent sperm mechanisms would have been selected to maximize the chances of achieving a correct oocyte fertilization.

In the present thesis, by performing the largest analysis of *PLCZI* gene sequencing in patients with FF after ICSI to date, we found a clear association between the presence of *PLCZI* mutations and OAF, the most common cause of FF, in agreement with the described role of PLC ζ . This study also allowed the identification of 4 novel *PLCZI* mutations (only 4 mutations were previously detected in ICSI FF patients in other reports), including the first frameshift mutation reported, and deleterious effects were confirmed for p.R197H, H233L and p.V326K*25.

We consider these results as very promising from a clinical point of view. First, because we confirmed that specific alterations in PLC ζ enzyme can lead to FF after ICSI in a considerable proportion of patients. Second, we demonstrated that *PLCZI* gene sequencing can be a useful tool not only to diagnose FF after ICSI, but also to orientate and facilitate the future treatment of the patient (i.e. providing evidence of a clear gamete defect and the justification to apply AOA). Third, this was the first study reporting that *PLCZI* variants in heterozygosis may be sufficient to generate a phenotype of FF after ICSI, as suggested by the high percentage of patients with mutation in heterozygosis. Nevertheless, further research is needed to determine the exact mechanisms by which mutations in heterozygosis may affect the percentage of functional protein in mature sperm, and the fertilizing ability of sperm through ICSI.

Overall, we believe that *PLCZI* gene sequencing could be incorporated in the clinic as a complementary tool to improve the sperm quality evaluation. Absence or abnormal function of PLC ζ is not expected to cause any problem in spermatogenesis and fertilization events prior to oocyte activation, as demonstrated by *Plcz1*^{-/-} studies (Nozawa et al., 2018), which explains why several cases of FF are unexpected and happening in normozoospermic men, and thus not properly diagnosed in a routine spermiogram.

Although we could not observe significant differences in protein localization when analyzing FF patients at group level, we cannot exclude that, in specific cases, abnormal localization or absence

of PLC ζ can explain FF after ICSI. Similarly, despite not included in the present thesis, we found two FF patients with lack of normally formed acrosomes (as visualized by PNA staining, data not shown). We believe that, in patients with these cellular defects or presence of deleterious mutations in *PLCZ1*, AOA can be beneficial as a treatment for sperm-related FF (as indicated by our results).

On the contrary, when molecular information of the gametes was not considered, the analysis of the outcomes of a big group of patients indicated that one instance of previous FF using donor oocyte did not justify the use of AOA. This again highlights the importance of adding new tests and improve the characterization of sperm quality, to perform fertility treatments based on the evidence.

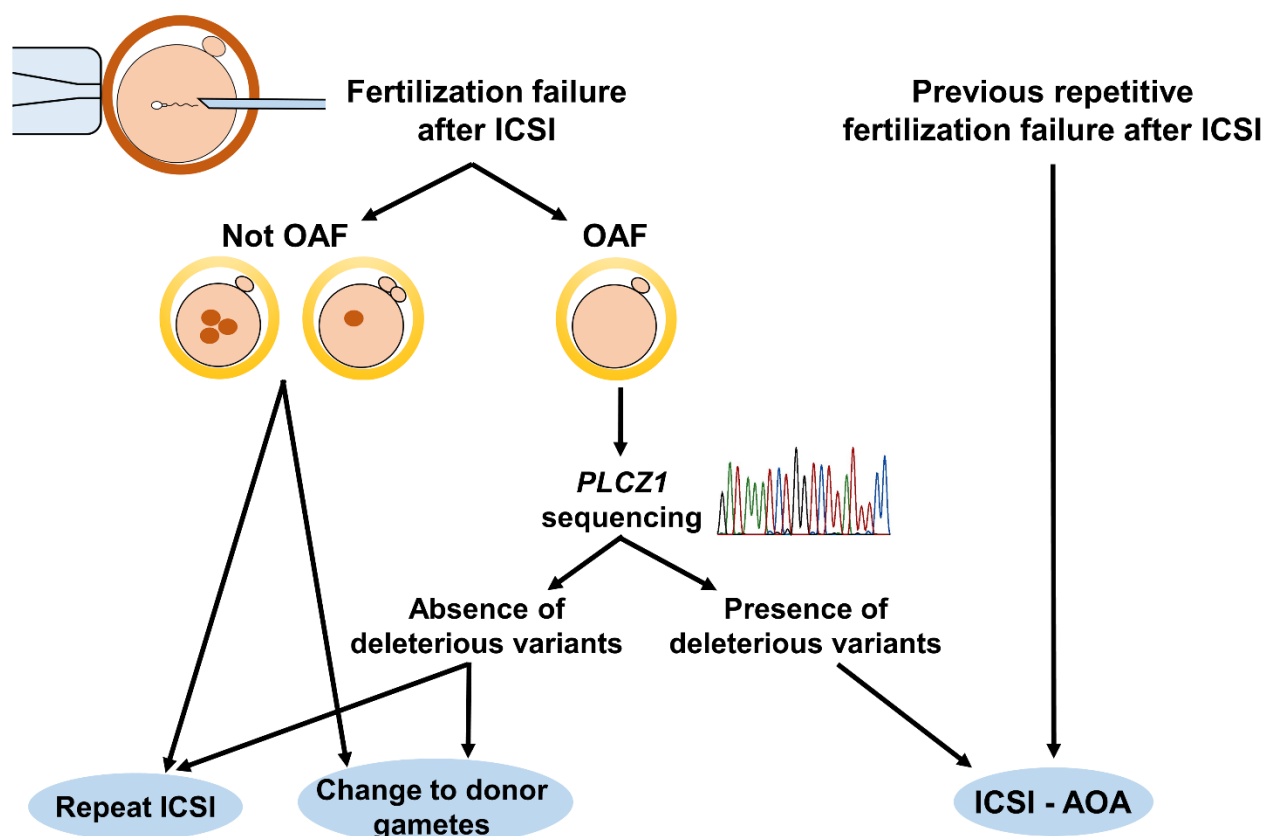


Figure 1. Model for the clinical management of cases with FF after ICSI. *PLCZ1* gene sequencing could help identify patients with deleterious genetic variants in cases of OAF. AOA could be useful for patients carrying *PLCZ1* mutations and for those who have a previous history of recurrent FF. When there is no OAF nor presence of molecular defects in the gametes, there is no evidence to recommend AOA use; repeat the cycle under the same circumstances or changing to donor gametes (sperm, oocyte, or both) should be the strategies evaluated in the subsequent attempt.

By combining the results obtained from *PLCZ1* sequencing and AOA analysis, we performed a model of clinical counselling for FF after ICSI using donor oocytes (**Figure 1**). This model is especially useful for cases of oocyte donation (or high-quality oocytes) and with a minimum of 4-

5 inseminated oocytes; as the female factor may play a role in the FF and increase the complexity of the problem in ICSI cycles when using partner oocytes. In parallel, further research in AOA recommendations and protocols will be required to improve the treatment and counselling of FF patients. For example, different authors have proposed the injection of PLC ζ (either as recombinant protein or cRNA) as more physiological method to perform AOA (Yamaguchi et al., 2017).

It is important to remember that patients carrying deleterious *PLCZI* mutations achieving live birth after AOA will transmit their infertility (inability to activate the oocyte) to their offspring. For this reason, appropriate genetic counselling must be an essential part in the fertility treatment of these patients.

We hypothesize that AOA is not beneficial when one or both gametes generate FF due to problems different from the specific calcium signalling and downstream events. These defects, either from sperm or oocyte origin, may result in abnormal sperm decondensation, aberrant formation of cytoskeletal structures and / or aberrant pronuclear development, migration, and apposition (Combelles et al., 2010). As commented before (see section 7.3.4), sperm nuclear or DNA defects may explain part of these abnormalities in FF. Among the different parameters related to sperm DNA, STL is one of the least investigated in relation to the fertilization process.

Our study of STL involves two main novel aspects. The first one is the inclusion of sperm samples in which multiple ICSI cycles were performed, which allowed us to correct for the female factor and statistically isolate the STL effect on fertilization rates and reproductive outcomes. We applied a multivariate analysis including not only fertilization rate, but also the abnormal fertilization rate (the hypothetic phenotype which we suspected to be caused in part by abnormal STL), but we did not observe any significant effect of STL for any of these variables. On the other hand, we determined STL in different samples with previous FF after ICSI, something not previously performed at the moment of our analysis. Surprisingly, we could observe significantly higher STL values when comparing samples with good fertilization rates and samples with FF after ICSI. However, a recently published study reported that sperm samples with previous FF after ICSI presented significantly lower levels of relative STL (Darmishonnejad et al., 2018). Further research is required to clarify this apparent inconsistency, as well as to determine if STL may play important roles in the fertilization process and / or be used as a clinical marker for male infertility. Nevertheless, we believe that STL will not become a robust marker for FF after ICSI due to different reasons previously anticipated (see chapter 3, additional information).

To date, many reports evaluating the sperm-related causes of FF after ICSI have been published, but a limitation of most studies is their focus on very specific factors, either searching which is

“the real and only SOAF” (PLC ζ or PAWP), or by searching other sperms-specific mechanisms such as STL or sperm chromatin condensation, among others. Few studies address the fertilization failure problem as a complex process of different mechanisms, cellular events and signalling pathways acting together, involving a wide array of molecular factors, organelles and structures. In the present thesis, we tried to overcome this limitation by including the studies of *in silico* PPI prediction in oocyte activation and characterization of whole sperm proteomics in FF samples, both addressing the fertilization process from a general and cellular point of view.

The signalling cascade during oocyte activation is mainly triggered by oocyte proteins, but we hypothesized that sperm protein could contribute to the regulation of this signalling. Our *in silico* study of PPI provides a list of potential sperm specific factors with potential to interact with oocyte proteins, almost a quarter of them (23.2 %) already validated experimentally in other systems. Different sperm-specific kinases of the TSSK family showed a potential ability to interact with different proteins involved in the oocyte activation cascade. The function of these kinases has been described in spermatogenesis and even sperm capacitation, but future research would be interesting to characterize its function in the mature sperm and in fertilization events in the oocyte cytoplasm.

Nevertheless, our *in silico* analysis presents some limitations, as mentioned before (see chapter 4, discussion), including the incomplete knowledge and annotation of factors participating in oocyte activation, as well as the difficulty of discerning if a specific PPI participates in oocyte activation, in previous processes, or in both. In addition, other mechanisms involved in early fertilization were not included, such as pronuclear formation, sperm head decondensation, aster formation, or mitochondrial sheath degradation.

For this reason, we next performed a more sophisticated and robust approach to identify new mechanisms underlying FF. This analysis not only includes samples with clear FF after ICSI (as far as we are concerned, any previous study included up to 5 samples with ≥ 3 ICSI cycles with fertilization failure), but also uses a powerful technology reported to be suitable to study male infertility mechanisms, involves a bioinformatics analysis which combines both conventional and novel approaches, and there is an experimental validation not only for specific sperm markers, but also for whole sperm cellular mechanisms such as mitochondrial and proteasomal activity.

The alterations found in the levels of specific mitochondrial proteins (such PDH enzyme and ATP synthase proteins) or ROPN1 in FF samples suggests that abnormal sperm metabolism or intracellular signalling, usually associated to abnormal capacitation and fertilization problems prior to sperm-oocyte fusion, may be involved in fertilization trough ICSI also (**Figure 2**). In addition, despite not tested in our study, we believe that ROS production may be a consequence of this

altered mitochondrial function. Proteasome dysfunction, indicated by PSMA1 underexpression and reduced proteolytic activity *in vitro* in FF samples, could contribute to FF after ICSI by affecting different mechanisms, such as aster formation and PN dynamics (**Figure 2**). An abnormal spermatogenesis could be the cause of the consequence of abnormal mitochondrial and proteasomal function. Moreover, as previously reported, specific process occurring in spermatogenesis and spermiogenesis (as pointed by the detection of altered markers like RAB2B, FAM209B, and FMR1NB, or factors present in the nuclear envelope such as NUP210L or NUP54) could affect fertilization through ICSI by generating deficient chromatin compaction or microstructural sperm defects not identified by a routine microscopy evaluation (such as correct formation of the acrosome, correct structure of layers surrounding the nucleus, and correct attachment between the head and the midpiece) (**Figure 2**).

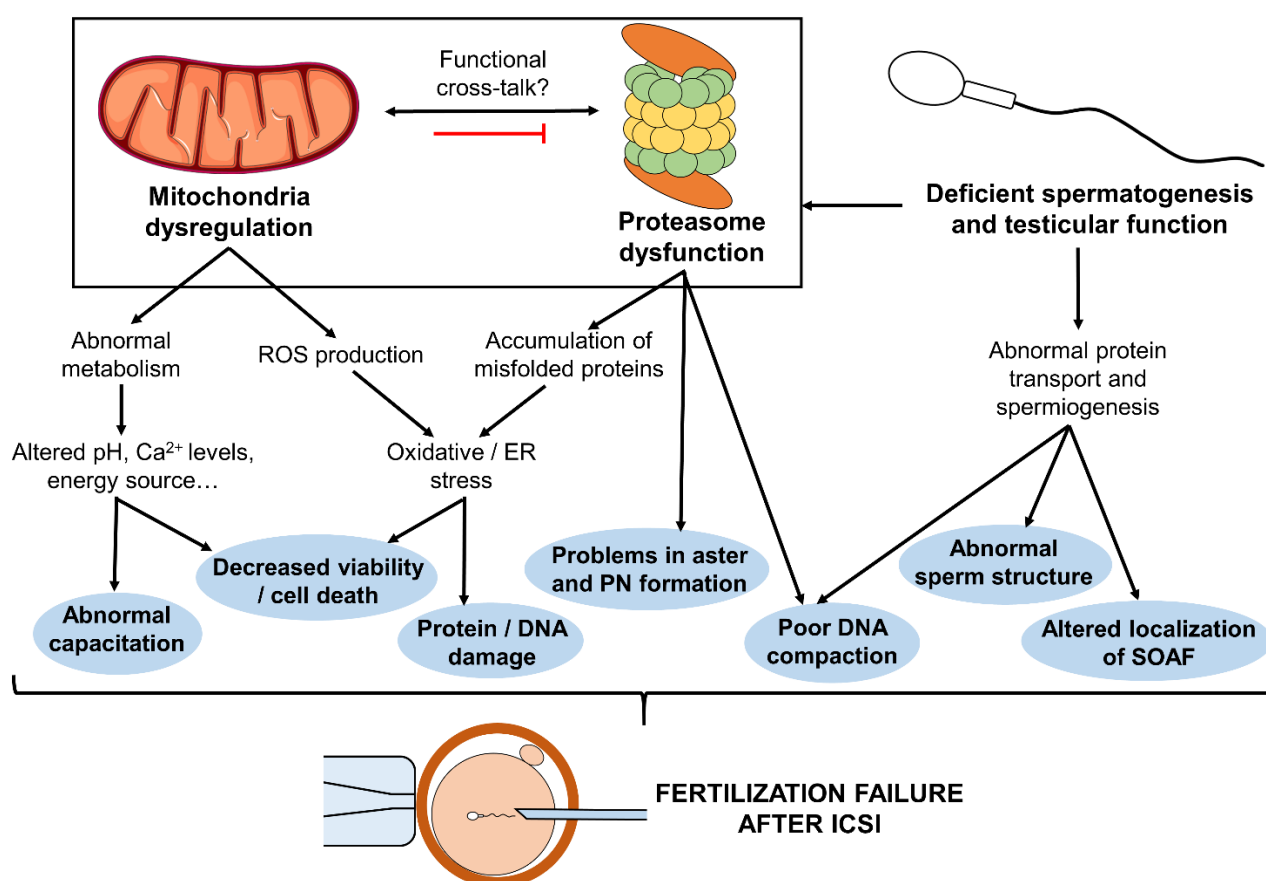


Figure 2. Schematic summary of the potential mechanisms by which abnormal mitochondrial and proteasome function and spermiogenesis could lead to fertilization failure after ICSI. ER: endoplasmic reticulum; PN: pronuclei; ROS: reactive oxygen species; SOAF: sperm-borne oocyte activation factor/s.

Although the sperm mechanisms identified by our proteomics study are not completely novel, as proteasomal and mitochondrial activity in sperm have been studied in different infertile groups. However, this study is the first to address both mechanisms in a group of samples which failed to

fertilize after ICSI. In the present study, the results indicate that both mechanisms could affect oocyte activation, either by directly affecting events occurring in post-sperm entry, or by affecting upstream essential processes such as sperm metabolism and capacitation. In addition, we hypothesise that mitochondrial and proteasomal function are related by maintaining a functional cross-talk (**Figure 2**), in which abnormal mitochondrial function would impair proteasomal function. This has been observed in many models and diseases but has not been demonstrated in sperm yet.

Mitochondrial activity is clearly associated with sperm function and has a high potential to become a new parameter to be included in ART for male infertility diagnosis and selection of sperm with higher fertilization ability. A good option could be to use fluorescent staining coupled with flow cytometry to select sperm populations with high MMP, which present higher percentages of viable sperm, motility, intact acrosome and integral chromatin, as well as higher rate of DNA decondensation after ICSI and thus higher ability to form the male pronucleus and higher fertilization rates (Sousa et al., 2011; Marchetti et al., 2012).

Separation of protein through liquid chromatography has been reported to be more powerful than separation by 2D gels (Amaral et al., 2014). However, a disadvantage of LC-MS/MS approaches is that the information determined by the presence of protein post-translational modifications (PTMs) is lost (Amaral et al., 2014). Glycosilation, acetylation, nitrosylation, SUMOylation and, obviously, phosphorylation, have been reported to happen in sperm proteins and to be important to modulate its function. One-third of the proteins in the human proteome are substrates for phosphorylation, and 30% of the proteins in unfertilized oocytes are phosphorylated (Cohen, 2000; Roux et al., 2006). The role of these changes in the fertilization success though deserves special attention in future studies. In addition, these PTM analysis could be combined with subcellular proteomics, which would allow identification of less abundant proteins and better characterization of the sperm subcellular compartments involved in fertilization through ICSI. Nevertheless, some specific sperm structures (such as the mitochondrial sheath and the perinuclear theca) are difficult to be accessible and isolated, so an approach like this would be really challenging.

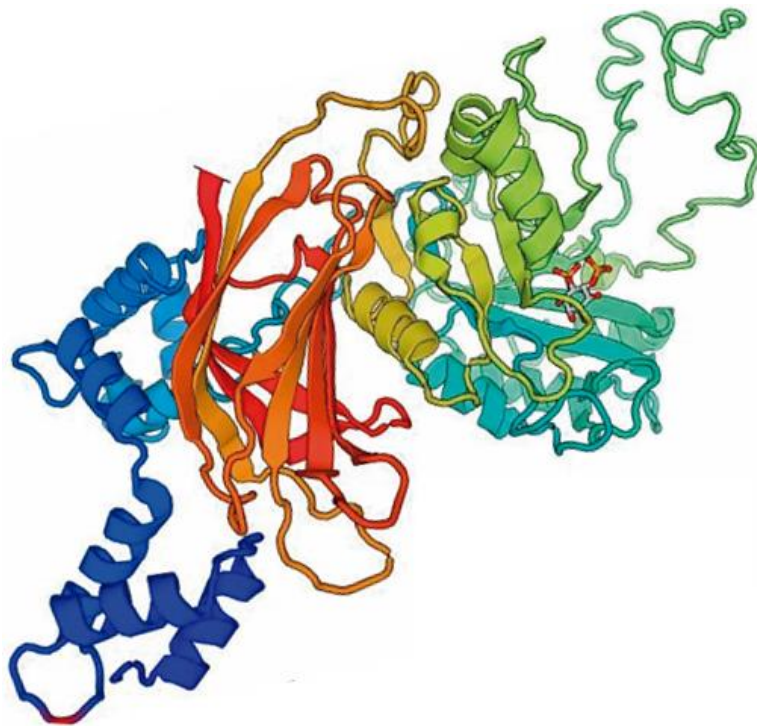
Finally, the specific protocols and techniques applied to process and select sperm in the IVF laboratory may well affect fertilization rates after ICSI. For this reason, we sought to determine if the time of sperm processing and incubation may impact negatively fertilization rates and reproductive outcomes. Different molecular and cellular parameters (such as motility, acrosomal status and DNA damage) are reported to change with time of sperm incubation, for this reason we considered time as an indirect measurement of changes related to sperm quality. Nevertheless, after

a multivariate analysis including different confounding factors, we could not see any significant effect of sperm incubation time prior to ICSI on fertilization and reproductive outcomes. These results suggest that, within the time intervals analysed and using a protocol which separates sperm from seminal fluid shortly after sample collection, sperm incubation time is not a critical factor for ICSI.

While the present thesis has focused on the male factor, the role of the oocyte in FF cannot be underestimated. Future research will be helpful to understand the largely unknown biology of the oocyte, identifying the specific mechanisms and associated alterations which may contribute to FF after ICSI. In addition, it would be interesting to characterize the mechanisms by which sperm contact with oocyte membrane contributes to generate calcium signalling during oocyte activation, as demonstrated by IVF experiments in *Plcz1*^{-/-} mice (Nozawa et al., 2018).

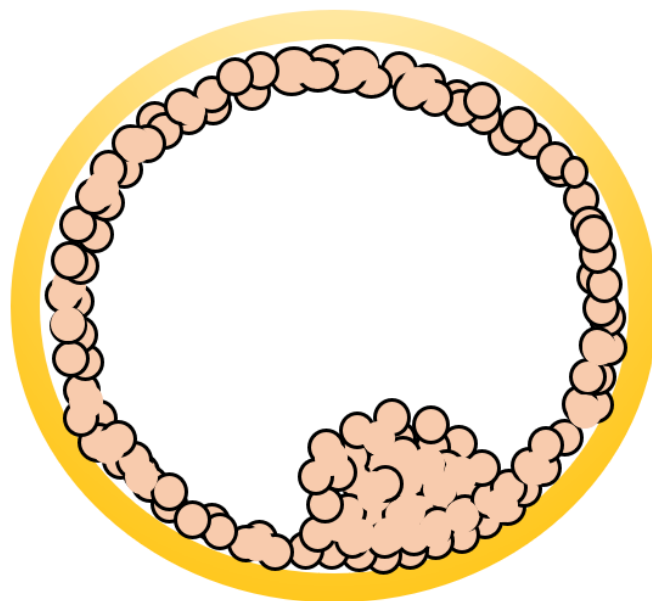
Overall, the results of this thesis provide a better characterization of the mechanisms leading to FF after ICSI. Further efforts will be required to improve the knowledge of these mechanisms and to add a translational value to this research, for example by incorporating novel tests, biomarkers or protocols useful to improve the sperm quality assessment in the routine of fertility clinics. Our results provide a basis for future research studies, and leave some unanswered questions which will for sure be elucidated in a near future, such as: which is the role of PAWP in fertilization and early development? Why do *PLCZI* mutations in heterozygosis cause subfertility or FF after ICSI? Are there any other sperm proteins apart from PLC ζ involved in oocyte activation signalling? Which is the percentage of FF cases characterized by reduced mitochondrial and proteasomal function? Is there any way to improve sperm quality in patients presenting sperm-related FF?

CONCLUSIONS



1. A high percentage (55 %) of patients with oocyte activation failure and repetitive fertilization failure present mutations in *PLCZ1* gene sequence. These mutations can affect protein function and ability to trigger oocyte activation, by affecting different protein domains. In many cases, mutations in heterozygosis seem to be enough to produce a phenotype of FF after ICSI.
2. PAWP protein levels, protein localization and genetic variants do not seem to be associated with fertilization failure after ICSI.
3. Sperm telomere length is a genetic factor not associated with fertilization rates and reproductive outcomes in a population of normozoospermic men without fertilization problems.
4. In the first proteomic analysis including sperm samples with fertilization failure after ICSI, a total of 1,398 proteins were identified. Nine proteins presented quantitative alterations between FF samples and controls. Further validation confirmed the differential abundance of DLAT and PSMA1, which could be used as clinical markers for FF after ICSI.
5. Sperm samples from patients with fertilization failure after ICSI presented lower mitochondrial activity and proteasomal function, both mechanisms needed for successful fertilization.
6. *In silico* PPI analysis predicted that different sperm-specific factors (such as members of the TSSK family) could play a role in oocyte activation and signalling during early fertilization events.
7. The time of sperm incubation before ICSI does not have a significant effect on fertilization rates and reproductive outcomes in cycles using fresh semen processed by swim-up.
8. AOA does not improve reproductive outcomes after iCSI in oocyte donation cycles when the only information is one previous instance of failed fertilization. In-deep analysis of gamete defects and fertilization failure origin should be performed to recommend this technique.

BIBLIOGRAPHY



- Aalberts M, Stout TA, Stoorvogel W. Prostatosomes: extracellular vesicles from the prostate. *Reproduction* 2013; 147:R1-14.
- Aarabi M, Balakier H, Bashar S, Moskovtsev SI, Sutovsky P, Librach CL, Oko R. Sperm-derived WW domain-binding protein, PAWP, elicits calcium oscillations and oocyte activation in humans and mice. *FASEB J* 2014; 28:4434-40.
- Abe KI, Funaya S, Tsukioka D, Kawamura M, Suzuki Y, Suzuki MG, Schultz RM, Aoki F. Minor zygotic gene activation is essential for mouse preimplantation development. *Proc Natl Acad Sci USA* 2018; 115:E6780-E6788.
- Ajduk A, Ilozue T, Windsor S, Yu Y, Seres KB, Bomphrey RJ, Tom BD, Swann K, Thomas A, Graham C, Zernicka-Goetz M. Rhythmic actomyosin-driven contractions induced by sperm entry predict mammalian embryo viability. *Nat Commun* 2011; 2:417.
- Alazami AM, Awad SM, Coskun S, Al-Hassan S, Hijazi H, Abdulwahab FM, Poizat C, Alkuraya FS. TLE6 mutation causes the earliest known human embryonic lethality. *Genome Biol* 2015; 16:240.
- Amaral A, Castillo J, Ramalho-Santos J, Oliva R. The combined human sperm proteome: cellular pathways and implications for basic and clinical science. *Hum Reprod Update* 2014; 20:40-62.
- Amargant F, García D, Barragán M, Vassena R, Vernos I. Functional Analysis of Human Pathological Semen Samples in an Oocyte Cytoplasmic Ex Vivo System. *Sci Rep* 2018; 8:15348.
- Antunes DM, Kalmbach KH, Wang F, Dracxler RC, Seth-Smith ML, Kramer Y, Buldo-Licciardi J, Kohlrausch FB, Keefe DL. A single-cell assay for telomere DNA content shows increasing telomere length heterogeneity, as well as increasing mean telomere length in human spermatozoa with advancing age. *J Assist Reprod Genet* 2015; 32:1685-90.
- Asch R, Simerly C, Ord T, Ord VA, Schatten G. The stages at which human fertilization arrests: microtubule and chromosome configurations in inseminated oocytes which failed to complete fertilization and development in humans. *Hum Reprod* 1995; 10:1897-906.
- ASEBIR. Criterios ASEBIR de Valoración Morfológica de Oocitos, Embriones Tempranos y Blastocistos Humanos. 3a edición. 2015.
- Austin CR. Observations on the penetration of the sperm in the mammalian egg. *Aust J Sci Res B* 1951; 4:581-96.
- Bai GR, Yang LH, Huang XY, Sun FZ. Inositol 1,4,5-trisphosphate receptor type 1 phosphorylation and regulation by extracellular signal-regulated kinase. *Biochem Biophys Res Commun* 2006; 348:1319-27.
- Balakier H, Sojecki A, Motamedi G, Librach C. Time-dependent capability of human oocytes for activation and pronuclear formation during metaphase II arrest. *Hum Reprod* 2004; 19:982-7.
- Baluch DP, Koeneman BA, Hatch KR, McGaughey RW, Capco DG. PKC isotypes in post-activated and fertilized mouse eggs: association with the meiotic spindle. *Dev Biol* 2004; 274:45-55.
- Barragán M, Pons J, Ferrer-Vaquer A, Cornet-Bartolomé D, Schweitzer A, Hubbard J, Auer H, Rodoloso A, Vassena R. The transcriptome of human oocytes is related to age and ovarian reserve. *Mol Hum Reprod* 2017; 23:535-548.
- Barratt CLR, Björndahl L, De Jonge CJ, Lamb DJ, Osorio Martini F, McLachlan R, Oates RD, van der Poel S, St John B, Sigman M, Sokol R, Tournaye H. The diagnosis of male infertility: an analysis of the evidence to support the development of global WHO guidance-challenges and future research opportunities. *Hum Reprod Update* 2017; 23:660-680.
- Beck-Fruchter R, Shalev E, Weiss A. Clinical benefit using sperm hyaluronic acid binding technique in ICSI cycles: a systematic review and meta-analysis. *Reprod Biomed Online* 2016; 32:286-98.

- Borges E Jr, de Almeida Ferreira Braga DP, de Sousa Bonetti TC, Iaconelli A Jr, Franco JG Jr. Artificial oocyte activation using calcium ionophore in ICSI cycles with spermatozoa from different sources. *Reprod Biomed Online* 2009; 18:45-52.
- Calafell JM, Badenas J, Egozcue J, Santaló J. Premature chromosome condensation as a sign of oocyte immaturity. *Hum Reprod* 1991; 6:1017-21.
- Capmany G, Taylor A, Braude PR, Bolton VN. The timing of pronuclear formation, DNA synthesis and cleavage in the human 1-cell embryo. *Mol Hum Reprod* 1996; 2:299-306.
- Cariati F, Jaroudi S, Alfarawati S, Raberi A, Alviggi C, Pivonello R, Wells D. Investigation of sperm telomere length as a potential marker of paternal genome integrity and semen quality. *Reprod Biomed Online* 2016; 33:404-11.
- Castillo J, Jodar M, Oliva R. The contribution of human sperm proteins to the development and epigenome of the preimplantation embryo. *Hum Reprod Update* 2018; 24:535-555.
- Cissen M, Wely MV, Scholten I, Mansell S, Bruin JP, Mol BW, Braat D, Repping S, Hamer G. Measuring Sperm DNA Fragmentation and Clinical Outcomes of Medically Assisted Reproduction: A Systematic Review and Meta-Analysis. *PLoS One* 2016; 11:e0165125.
- Cohen P. The regulation of protein function by multisite phosphorylation--a 25 year update. *Trends Biochem Sci* 2000; 25:596-601.
- Combelles CM, Morozumi K, Yanagimachi R, Zhu L, Fox JH, Racowsky C. Diagnosing cellular defects in an unexplained case of total fertilization failure. *Hum Reprod* 2010; 25:1666-71.
- Cooney MA, Malcuit C, Cheon B, Holland MK, Fissore RA, D'Cruz NT. Species-specific differences in the activity and nuclear localization of murine and bovine phospholipase C zeta 1. *Biol Reprod* 2010; 83:92-101.
- Cooper TG, Noonan E, von Eckardstein S, Auger J, Baker HW, Behre HM, Haugen TB, Kruger T, Wang C, Mbizvo MT, Vogelsong KM. World Health Organization reference values for human semen characteristics. *Hum Reprod Update* 2010; 16:231-45.
- Coticchio G, Mignini Renzini M, Novara PV, Lain M, De Ponti E, Turchi D, Fadini R, Dal Canto M. Focused time-lapse analysis reveals novel aspects of human fertilization and suggests new parameters of embryo viability. *Hum Reprod* 2018; 33:23-31.
- Coward K, Ponting CP, Chang HY, Hibbitt O, Savolainen P, Jones KT, Parrington J. Phospholipase Czeta, the trigger of egg activation in mammals, is present in a non-mammalian species. *Reproduction* 2005; 130:157-63.
- Cox LJ, Larman MG, Saunders CM, Hashimoto K, Swann K, Lai FA. Sperm phospholipase Czeta from humans and cynomolgus monkeys triggers Ca²⁺ oscillations, activation and development of mouse oocytes. *Reproduction* 2002; 124:611-23.
- Darmishonnejad Z, Tavalae M, Izadi T, Tanhaei S, Nasr-Esfahani MH. Evaluation of sperm telomere length in infertile men with failed/low fertilization after intracytoplasmic sperm injection. *Reprod Biomed Online* 2018.
- de Rooij DG, Russell LD. All you wanted to know about spermatogonia but were afraid to ask. *J Androl* 2000; 21:776-98.
- Deemeh MR, Tavalae M, Nasr-Esfahani MH. Health of children born through artificial oocyte activation: a pilot study. *Reprod Sci* 2015; 22:322-8.
- de Mateo S, Castillo J, Estanyol JM, Ballescà JL, Oliva R. Proteomic characterization of the human sperm nucleus. *Proteomics* 2011; 11:2714-26.
- D'haeseleer E, Vanden Meerschaut F, Bettens K, Luyten A, Gysels H, Thienpont Y, De Witte G, Heindryckx B, Oostra A, Roeyers H, Sutter PD, van Lierde K. Language development of children born following

- intracytoplasmic sperm injection (ICSI) combined with assisted oocyte activation (AOA). *Int J Lang Commun Disord* 2014; 49:702-9.
- Dirican EK, Ozgün OD, Akarsu S, Akin KO, Ercan O, Uğurlu M, Camsari C, Kanyilmaz O, Kaya A, Unsal A. Clinical outcome of magnetic activated cell sorting of non-apoptotic spermatozoa before density gradient centrifugation for assisted reproduction. *J Assist Reprod Genet* 2008; 25:375-81.
- Dohle GR, Colpi GM, Hargreave TB, Papp GK, Jungwirth A, Weidner W; EAU Working Group on Male Infertility. EAU guidelines on male infertility. *Eur Urol* 2005; 48:703-11.
- Ducibella T, Huneau D, Angelichio E, Xu Z, Schultz RM, Kopf GS, Fissore R, Madoux S, Ozil JP. Egg-to-embryo transition is driven by differential responses to Ca(2+) oscillation number. *Dev Biol* 2002; 250:280-91.
- Ducibella T, Fissore R. The roles of Ca²⁺, downstream protein kinases, and oscillatory signaling in regulating fertilization and the activation of development. *Dev Biol* 2008; 315:257-79.
- Dumollard R, Marangos P, Fitzharris G, Swann K, Duchen M, Carroll J. Sperm-triggered [Ca²⁺] oscillations and Ca²⁺ homeostasis in the mouse egg have an absolute requirement for mitochondrial ATP production. *Development* 2004; 131:3057-67.
- Duncan FE, Que EL, Zhang N, Feinberg EC, O'Halloran TV, Woodruff TK. The zinc spark is an inorganic signature of human egg activation. *Sci Rep* 2016; 6:24737.
- Ebner T, Moser M, Sommergruber M, Gaiswinkler U, Shebl O, Jesacher K, Tews G. Occurrence and developmental consequences of vacuoles throughout preimplantation development. *Fertil Steril* 2005; 83:1635-40.
- Ebner T, Moser M, Tews G. Is oocyte morphology prognostic of embryo developmental potential after ICSI? *Reprod Biomed Online* 2006; 12:507-12.
- Eddy EM, Toshimori K, O'Brien DA. Fibrous sheath of mammalian spermatozoa. *Microsc Res Tech* 2003; 61:103-15.
- Escoffier J, Lee HC, Yassine S, Zouari R, Martinez G, Karaouzène T, Coutton C, Kherraf ZE, Halouani L, Triki C, Nef S, Thierry-Mieg N, Savinov SN, Fissore R, Ray PF, Arnoult C. Homozygous mutation of PLCZ1 leads to defective human oocyte activation and infertility that is not rescued by the WW-binding protein PAWP. *Hum Mol Genet* 2016; 25:878-91.
- Fatehi AN, Bevers MM, Schoevers E, Roelen BA, Colenbrander B, Gadella BM. DNA damage in bovine sperm does not block fertilization and early embryonic development but induces apoptosis after the first cleavages. *J Androl* 2006; 27:176-88.
- Fawzy M, Emad M, Mahran A, Sabry M, Fetih AN, Abdelghafar H, Rasheed S. Artificial oocyte activation with SrCl₂ or calcimycin after ICSI improves clinical and embryological outcomes compared with ICSI alone: results of a randomized clinical trial. *Hum Reprod*. 2018; 33:1636-1644.
- Ferrer-Vaquer A, Barragan M, Freour T, Vernaev V, Vassena R. PLC ζ sequence, protein levels, and distribution in human sperm do not correlate with semen characteristics and fertilization rates after ICSI. *J Assist Reprod Genet* 2016; 33:747-56.
- Flaherty SP, Payne D, Swann NJ, Matthews CD. Assessment of fertilization failure and abnormal fertilization after intracytoplasmic sperm injection (ICSI). *Reprod Fertil Dev* 1995; 7:197-210.
- Flaherty SP, Payne D, Matthews CD. Fertilization failures and abnormal fertilization after intracytoplasmic sperm injection. *Hum Reprod* 1998; 13 Suppl 1:155-64.
- Frapsauce C, Pionneau C, Bouley J, Delarouziere V, Berthaut I, Ravel C, Antoine JM, Soubrier F, Mandelbaum J. Proteomic identification of target proteins in normal but nonfertilizing sperm. *Fertil Steril* 2014; 102:372-80.

- Fujimoto S, Yoshida N, Fukui T, Amanai M, Isobe T, Itagaki C, Izumi T, Perry AC. Mammalian phospholipase C ζ induces oocyte activation from the sperm perinuclear matrix. *Dev Biol* 2004; 274:370-83.
- Gardner DK, Lane M. Culture of viable human blastocysts in defined sequential serum-free media. *Hum Reprod* 1998; 13 Suppl 3:148-59.
- Gasca S, Reyftmann L, Pellestor F, Rème T, Assou S, Anahory T, Dechaud H, Klein B, De Vos J, Hamamah S. Total fertilization failure and molecular abnormalities in metaphase II oocytes. *Reprod Biomed Online* 2008; 17:772-81.
- Hachem A, Godwin J, Ruas M, Lee HC, Ferrer Buitrago M, Ardestani G, Bassett A, Fox S, Navarrete F, de Sutter P, Heindryckx B, Fissore R, Parrington J. PLC ζ is the physiological trigger of the Ca²⁺ oscillations that induce embryogenesis in mammals but conception can occur in its absence. *Development* 2017; 144:2914-2924.
- Hamilton LE, Suzuki J, Acteau G, Shi M, Xu W, Meinsohn MC, Sutovsky P, Oko R. WBP2 shares a common location in mouse spermatozoa with WBP2NL/PAWP and like its descendent is a candidate mouse oocyte-activating factor. *Biol Reprod* 2018; 99:1171-1183.
- Harada Y, Matsumoto T, Hirahara S, Nakashima A, Ueno S, Oda S, Miyazaki S, Iwao Y. Characterization of a sperm factor for egg activation at fertilization of the newt *Cynops pyrrhogaster*. *Dev Biol* 2007; 306:797-808.
- Heindryckx B, Van der Elst J, De Sutter P, Dhont M. Treatment option for sperm- or oocyte-related fertilization failure: assisted oocyte activation following diagnostic heterologous ICSI. *Hum Reprod* 2005; 20:2237-41.
- Heindryckx B, De Gheselle S, Gerris J, Dhont M, De Sutter P. Efficiency of assisted oocyte activation as a solution for failed intracytoplasmic sperm injection. *Reprod Biomed Online* 2008; 17:662-8.
- Heytens E, Parrington J, Coward K, Young C, Lambrecht S, Yoon SY, Fissore RA, Hamer R, Deane CM, Ruas M, Grasa P, Soleimani R, Cuvelier CA, Gerris J, Dhont M, Deforce D, Leybaert L, De Sutter P. Reduced amounts and abnormal forms of phospholipase C zeta (PLCzeta) in spermatozoa from infertile men. *Hum Reprod* 2009; 24:2417-28.
- Hojnik N, Kovacic B. Oocyte Activation Failure: Physiological and Clinical Aspects. *Embryogenesis* 2019.
- Hotaling JM. Genetics of male infertility. *Urol Clin North Am* 2014; 41:1-17.
- Huang B, Qian K, Li Z, Yue J, Yang W, Zhu G, Zhang H. Neonatal outcomes after early rescue intracytoplasmic sperm injection: an analysis of a 5-year period. *Fertil Steril* 2015; 103:1432-7.e1.
- Inhorn MC, Patrizio P. Infertility around the globe: new thinking on gender, reproductive technologies and global movements in the 21st century. *Hum Reprod Update* 2015; 21:411-26.
- Ito C, Akutsu H, Yao R, Kyono K, Suzuki-Toyota F, Toyama Y, Maekawa M, Noda T, Toshimori K. Oocyte activation ability correlates with head flatness and presence of perinuclear theca substance in human and mouse sperm. *Hum Reprod* 2009; 24:2588-95.
- Jellerette T, He CL, Wu H, Parys JB, Fissore RA. Down-regulation of the inositol 1,4,5-trisphosphate receptor in mouse eggs following fertilization or parthenogenetic activation. *Dev Biol* 2000; 223:238-50.
- Jodar M, Sendler E, Moskovtsev SI, Librach CL, Goodrich R, Swanson S, Hauser R, Diamond MP, Krawetz SA. Absence of sperm RNA elements correlates with idiopathic male infertility. *Sci Transl Med* 2015; 7:295re6.
- Joergensen MW, Agerholm I, Hindkjaer J, Bolund L, Sunde L, Ingerslev HJ, Kirkegaard K. Altered cleavage patterns in human tripronuclear embryos and their association to fertilization method: a time-lapse study. *J Assist Reprod Genet* 2014; 31:435-42.

- Jean C, Haghighirad F, Zhu Y, Chalbi M, Ziyat A, Rubinstein E, Gourier C, Yip P, Wolf JP, Lee JE, Boucheix C, Barraud-Lange V. JUNO, the receptor of sperm IZUMO1, is expressed by the human oocyte and is essential for human fertilisation. *Hum Reprod* 2019; 34:118-126.
- Jia JL, Han YH, Kim HC, Ahn M, Kwon JW, Luo Y, Gunasekaran P, Lee SJ, Lee KS, Kyu Bang J, Kim NH, Namgoong S. Structural basis for recognition of Emi2 by Polo-like kinase 1 and development of peptidomimetics blocking oocyte maturation and fertilization. *Sci Rep* 2015; 5:14626.
- Jones KT, Cruttwell C, Parrington J, Swann K. A mammalian sperm cytosolic phospholipase C activity generates inositol trisphosphate and causes Ca²⁺ release in sea urchin egg homogenates. *FEBS Lett* 1998; 437:297-300.
- Kashir J, Konstantinidis M, Jones C, Heindryckx B, De Sutter P, Parrington J, Wells D, Coward K. Characterization of two heterozygous mutations of the oocyte activation factor phospholipase C zeta (PLC ζ) from an infertile man by use of minisequencing of individual sperm and expression in somatic cells. *Fertil Steril* 2012; 98:423-31.
- Kashir J, Buntwal L, Nomikos M, Calver BL, Stamatiadis P, Ashley P, Vassilakopoulou V, Sanders D, Knaggs P, Livaniou E, Bunkheila A, Swann K, Lai FA. Antigen unmasking enhances visualization efficacy of the oocyte activation factor, phospholipase C zeta, in mammalian sperm. *Mol Hum Reprod* 2017; 23:54-67.
- Kennedy CE, Krieger KB, Sutovsky M, Xu W, Vargovič P, Didion BA, Ellersieck MR, Hennessy ME, Verstegen J, Oko R, Sutovsky P. Protein expression pattern of PAWP in bull spermatozoa is associated with sperm quality and fertility following artificial insemination. *Mol Reprod Dev* 2014; 81:436-49.
- Kim AM, Bernhardt ML, Kong BY, Ahn RW, Vogt S, Woodruff TK, O'Halloran TV. Zinc sparks are triggered by fertilization and facilitate cell cycle resumption in mammalian eggs. *ACS Chem Biol* 2011; 6:716-23.
- Kirkman-Brown J, Pavitt S, Khalaf Y, Lewis S, Hooper R, Bhattacharya S, Coomarasamy A, Sharma V, Brison D, Forbes G, West R, Pacey A, Brian K, Cutting R, Bolton V, Miller D. Sperm selection for assisted reproduction by prior hyaluronan binding: the HABSselect RCT. *Efficacy and Mechanism Evaluation* 2019.
- Kline D, Mehlmann L, Fox C, Terasaki M. The cortical endoplasmic reticulum (ER) of the mouse egg: localization of ER clusters in relation to the generation of repetitive calcium waves. *Dev Biol* 1999; 215:431-42.
- Koscinski I, Elinati E, Fossard C, Redin C, Muller J, Velez de la Calle J, Schmitt F, Ben Khelifa M, Ray PF, Kilani Z, Barratt CL, Viville S. DPY19L2 deletion as a major cause of globozoospermia. *Am J Hum Genet* 2011; 88:344-50.
- Kouchi Z, Shikano T, Nakamura Y, Shirakawa H, Fukami K, Miyazaki S. The role of EF-hand domains and C2 domain in regulation of enzymatic activity of phospholipase Czeta. *J Biol Chem* 2005; 280:21015-21.
- Krauchunas AR, Wolfner MF. Molecular changes during egg activation. *Curr Top Dev Biol* 2013; 102:267-92.
- Kunz G, Beil D, Deininger H, Wildt L, Leyendecker G. The dynamics of rapid sperm transport through the female genital tract: evidence from vaginal sonography of uterine peristalsis and hysterosalpingoscintigraphy. *Hum Reprod* 1996; 11:627-32.
- Kwon WS, Rahman MS, Pang MG. Diagnosis and prognosis of male infertility in mammal: the focusing of tyrosine phosphorylation and phosphotyrosine proteins. *J Proteome Res* 2014; 13:4505-17.
- La Marca A, Sunkara SK. Individualization of controlled ovarian stimulation in IVF using ovarian reserve markers: from theory to practice. *Hum Reprod Update* 2014; 20:124-40.
- Larman MG, Saunders CM, Carroll J, Lai FA, Swann K. Cell cycle-dependent Ca²⁺ oscillations in mouse embryos are regulated by nuclear targeting of PLCzeta. *J Cell Sci* 2004; 117:2513-21.

- Lawrence Y, Whitaker M, Swann K. Sperm-egg fusion is the prelude to the initial Ca²⁺ increase at fertilization in the mouse. *Development* 1997; 124:233-41.
- Lazaros LA, Vartholomatos GA, Hatzi EG, Kaponis AI, Makrydimas GV, Kalantaridou SN, Sofikitis NV, Stefos TI, Zikopoulos KA, Georgiou IA. Assessment of sperm chromatin condensation and ploidy status using flow cytometry correlates to fertilization, embryo quality and pregnancy following in vitro fertilization. *J Assist Reprod Genet* 2011; 28:885-91.
- Lee B, Yoon SY, Malcuit C, Parys JB, Fissore RA. Inositol 1,4,5-trisphosphate receptor 1 degradation in mouse eggs and impact on [Ca²⁺]_i oscillations. *J Cell Physiol*. 2010; 222:238-47.
- Légaré C, Droit A, Fournier F, Bourassa S, Force A, Cloutier F, Tremblay R, Sullivan R. Investigation of male infertility using quantitative comparative proteomics. *J Proteome Res* 2014; 13:5403-14.
- Levine H, Jørgensen N, Martino-Andrade A, Mendiola J, Weksler-Derri D, Mindlis I, Pinotti R, Swan SH. Temporal trends in sperm count: a systematic review and meta-regression analysis. *Hum Reprod Update* 2017; 23:646-659.
- Li J, Huan Y, Xie B, Wang J, Zhao Y, Jiao M, Huang T, Kong Q, Liu Z. Identification and characterization of an oocyte factor required for sperm decondensation in pig. *Reproduction* 2014; 148:367-75.
- Liou J, Fivaz M, Inoue T, Meyer T. Live-cell imaging reveals sequential oligomerization and local plasma membrane targeting of stromal interaction molecule 1 after Ca²⁺ store depletion. *Proc Natl Acad Sci USA* 2007; 104:9301-6.
- Liu L, Yang X. Interplay of maturation-promoting factor and mitogen-activated protein kinase inactivation during metaphase-to-interphase transition of activated bovine oocytes. *Biol Reprod* 1999; 61:1-7.
- Liu L, Blasco M, Trimarchi J, Keefe D. An essential role for functional telomeres in mouse germ cells during fertilization and early development. *Dev Biol*. 2002; 249:74-84.
- Liu X, Liu G, Liu J, Zhu P, Wang J, Wang Y, Wang W, Li N, Wang X, Zhang C, Shen X, Liu F. iTRAQ-based analysis of sperm proteome from normozoospermic men achieving the rescue-ICSI pregnancy after the IVF failure. *Clin Proteomics* 2018; 15:27.
- Luo S, Valencia CA, Zhang J, Lee NC, Slone J, Gui B, Wang X, Li Z, Dell S, Brown J, Chen SM, Chien YH, Hwu WL, Fan PC, Wong LJ, Atwal PS, Huang T. Biparental Inheritance of Mitochondrial DNA in Humans. *Proc Natl Acad Sci USA* 2018; 115:13039-13044.
- Machtinger R, Combelles CM, Missmer SA, Correia KF, Fox JH, Racowsky C. The association between severe obesity and characteristics of failed fertilized oocytes. *Hum Reprod* 2012; 27:3198-207.
- Madgwick S, Jones KT. How eggs arrest at metaphase II: MPF stabilisation plus APC/C inhibition equals Cytostatic Factor. *Cell Div* 2007; 2:4.
- Marangos P, FitzHarris G, Carroll J. Ca²⁺ oscillations at fertilization in mammals are regulated by the formation of pronuclei. *Development* 2003; 130:1461-72.
- Marangos P, Carroll J. The dynamics of cyclin B1 distribution during meiosis I in mouse oocytes. *Reproduction* 2004; 128:153-62.
- Marchetti P, Ballot C, Jouy N, Thomas P, Marchetti C. Influence of mitochondrial membrane potential of spermatozoa on in vitro fertilisation outcome. *Andrologia* 2012; 44:136-41.
- Markoulaki S, Matson S, Ducibella T. Fertilization stimulates long-lasting oscillations of CaMKII activity in mouse eggs. *Dev Biol* 2004; 272:15-25.
- McDowell S, Kroon B, Ford E, Hook Y, Glujovsky D, Yazdani A. Advanced sperm selection techniques for assisted reproduction. *Cochrane Database Syst Rev* 2014; (10):CD010461.
- Mehlmann LM, Carpenter G, Rhee SG, Jaffe LA. SH2 domain-mediated activation of phospholipase Cgamma is not required to initiate Ca²⁺ release at fertilization of mouse eggs. *Dev Biol* 1998; 203:221-32.

- Miao YL, Kikuchi K, Sun QY, Schatten H. Oocyte aging: cellular and molecular changes, developmental potential and reversal possibility. *Hum Reprod Update* 2009; 15:573-85.
- Misell LM, Holochwost D, Boban D, Santi N, Shefi S, Hellerstein MK, Turek PJ. A stable isotope-mass spectrometric method for measuring human spermatogenesis kinetics in vivo. *J Urol* 2006; 175:242-6.
- Moos J, Visconti PE, Moore GD, Schultz RM, Kopf GS. Potential role of mitogen-activated protein kinase in pronuclear envelope assembly and disassembly following fertilization of mouse eggs. *Biol Reprod* 1995; 53:692-9.
- Moos J, Xu Z, Schultz RM, Kopf GS. Regulation of nuclear envelope assembly/disassembly by MAP kinase. *Dev Biol* 1996; 175:358-61.
- Muciaccia B, Sette C, Paronetto MP, Barchi M, Pensini S, D'Agostino A, Gandini L, Geremia R, Stefanini M, Rossi P. Expression of a truncated form of KIT tyrosine kinase in human spermatozoa correlates with sperm DNA integrity. *Hum Reprod* 2010; 25:2188-202.
- Murugesu S, Saso S, Jones BP, Bracewell-Milnes T, Athanasiou T, Mania A, Serhal P, Ben-Nagi J. Does the use of calcium ionophore during artificial oocyte activation demonstrate an effect on pregnancy rate? A meta-analysis. *Fertil Steril* 2017; 108:468-482.e3.
- Nabti I, Marangos P, Bormann J, Kudo NR, Carroll J. Dual-mode regulation of the APC/C by CDK1 and MAPK controls meiosis I progression and fidelity. *J Cell Biol* 2014; 204:891-900.
- Nasr-Esfahani MH, Salehi M, Razavi S, Mardani M, Bahramian H, Steger K, Oreizi F. Effect of protamine-2 deficiency on ICSI outcome. *Reprod Biomed Online* 2004; 9:652-8.
- Nasr-Esfahani MH, Naghshizadian N, Imani H, Razavi S, Mardani M, Kazemi S, Shahvardi H. Can sperm protamine deficiency induce sperm premature chromosomal condensation? *Andrologia* 2006; 38:92-8.
- Nasr-Esfahani MH, Razavi S, Vahdati AA, Fathi F, Tavalae M. Evaluation of sperm selection procedure based on hyaluronic acid binding ability on ICSI outcome. *J Assist Reprod Genet* 2008; 25:197-203.
- Neri QV, Lee B, Rosenwaks Z, Machaca K, Palermo GD. Understanding fertilization through intracytoplasmic sperm injection (ICSI). *Cell Calcium* 2014; 55:24-37.
- Neto FT, Bach PV, Najari BB, Li PS, Goldstein M. Spermatogenesis in humans and its affecting factors. *Semin Cell Dev Biol* 2016; 59:10-26.
- Nikiforaki D, Vanden Meerschaut F, Qian C, De Croo I, Lu Y, Deroo T, Van den Abbeel E, Heindryckx B, De Sutter P. Oocyte cryopreservation and in vitro culture affect calcium signalling during human fertilization. *Hum Reprod* 2014; 29:29-40.
- Nishizuka Y. Membrane phospholipid degradation and protein kinase C for cell signalling. *Neurosci Res* 1992; 15:3-5.
- Nixon VL, Levasseur M, McDougall A, Jones KT. Ca(2+) oscillations promote APC/C-dependent cyclin B1 degradation during metaphase arrest and completion of meiosis in fertilizing mouse eggs. *Curr Biol* 2002; 12:746-50.
- Nixon B, Mitchell LA, Anderson AL, McLaughlin EA, O'bryan MK, Aitken RJ. Proteomic and functional analysis of human sperm detergent resistant membranes. *J Cell Physiol* 2011; 226:2651-65.
- Nomikos M, Yu Y, Elgmati K, Theodoridou M, Campbell K, Vassilakopoulou V, Zikos C, Livaniou E, Amso N, Nounesis G, Swann K, Lai FA. Phospholipase C ζ rescues failed oocyte activation in a prototype of male factor infertility. *Fertil Steril* 2013; 99:76-85.
- Nomikos M, Sanders JR, Theodoridou M, Kashir J, Matthews E, Nounesis G, Lai FA, Swann K. Sperm-specific post-acrosomal WW-domain binding protein (PAWP) does not cause Ca $^{2+}$ release in mouse oocytes. *Mol Hum Reprod* 2014; 20:938-47.
- Nozawa K, Satouh Y, Fujimoto T, Oji A, Ikawa M. Sperm-borne phospholipase C zeta-1 ensures monospermic fertilization in mice. *Sci Rep* 2018; 8:1315.

- Ntostis P, Carter D, Iles D, Huntriss J, Tzetis M, Miller D. Potential sperm contributions to the murine zygote predicted by in silico analysis. *Reproduction* 2017; 154:777-788.
- O'Flynn O'Brien KL, Varghese AC, Agarwal A. The genetic causes of male factor infertility: a review. *Fertil Steril* 2010; 93:1-12.
- Oh JS, Susor A, Conti M. Protein tyrosine kinase Wee1B is essential for metaphase II exit in mouse oocytes. *Science* 2011; 332:462-5.
- Okada Y, Yamaguchi K. Epigenetic modifications and reprogramming in paternal pronucleus: sperm, preimplantation embryo, and beyond. *Cell Mol Life Sci* 2017; 74:1957-1967.
- Oko R, Sutovsky P. Biogenesis of sperm perinuclear theca and its role in sperm functional competence and fertilization. *J Reprod Immunol* 2009; 83:2-7.
- Oliva R, Dixon GH. Vertebrate protamine genes and the histone-to-protamine replacement reaction. *Prog Nucleic Acid Res Mol Biol* 1991; 40:25-94.
- O'Sullivan RJ, Karlseder J. Telomeres: protecting chromosomes against genome instability. *Nature reviews Molecular cell biology* 2010; 11:171-81.
- Ozturk S. Telomerase activity and telomere length in male germ cells. *Biology of reproduction* 2015; 92:53.
- Palermo G, Joris H, Devroey P, Van Steirteghem AC. Pregnancies after intracytoplasmic injection of single spermatozoon into an oocyte. *Lancet*. 1992; 340:17-8.
- Papanikolaou EG, Camus M, Kolibianakis EM, Van Landuyt L, Van Steirteghem A, Devroey P. In vitro fertilization with single blastocyst-stage versus single cleavage-stage embryos. *N Engl J Med* 2006; 354:1139-46.
- Park CY, Hoover PJ, Mullins FM, Bachhawat P, Covington ED, Raunser S, Walz T, Garcia KC, Dolmetsch RE, Lewis RS. STIM1 clusters and activates CRAC channels via direct binding of a cytosolic domain to Orai1. *Cell* 2009; 136:876-90.
- Parmegiani L, Cognigni GE, Ciampaglia W, Pocognoli P, Marchi F, Filicori M. Efficiency of hyaluronic acid (HA) sperm selection. *J Assist Reprod Genet* 2010; 27:13-6.
- Parrington J, Swann K, Shevchenko VI, Sesay AK, Lai FA. Calcium oscillations in mammalian eggs triggered by a soluble sperm protein. *Nature* 1996; 379:364-8.
- Payne C, Rawe V, Ramalho-Santos J, Simerly C, Schatten G. Preferentially localized dynein and perinuclear dynactin associate with nuclear pore complex proteins to mediate genomic union during mammalian fertilization. *J Cell Sci* 2003; 116:4727-38.
- Phillips SV, Yu Y, Rossbach A, Nomikos M, Vassilakopoulou V, Livaniou E, Cumbes B, Lai FA, George CH, Swann K. Divergent effect of mammalian PLC ζ in generating Ca²⁺ oscillations in somatic cells compared with eggs. *Biochem J* 2011; 438:545-53.
- Pixton KL, Deeks ED, Flesch FM, Moseley FL, Björndahl L, Ashton PR, Barratt CL, Brewis IA. Sperm proteome mapping of a patient who experienced failed fertilization at IVF reveals altered expression of at least 20 proteins compared with fertile donors: case report. *Hum Reprod* 2004; 19:1438-47.
- Publicover S, Harper CV, Barratt C. [Ca²⁺]_i signalling in sperm--making the most of what you've got. *Nat Cell Biol* 2007; 9:235-42.
- Pujol A, García D, Obradors A, Rodríguez A, Vassena R. Is there a relation between the time to ICSI and the reproductive outcomes? *Hum Reprod* 2018; 33:797-806.
- Rajagopal S, Fields BL, Burton BK, On C, Reeder AA, Kamatchi GL. Inhibition of protein kinase C (PKC) response of voltage-gated calcium (Cav)_v2.2 channels expressed in *Xenopus* oocytes by Cav β subunits. *Neuroscience* 2014; 280:1-9.

- Rawe VY, Olmedo SB, Nodar FN, Doncel GD, Acosta AA, Vitullo AD. Cytoskeletal organization defects and abortive activation in human oocytes after IVF and ICSI failure. *Mol Hum Reprod* 2000; 6:510-6.
- Rawe VY, Díaz ES, Abdelmassih R, Wójcik C, Morales P, Sutovsky P, Chemes HE. The role of sperm proteasomes during sperm aster formation and early zygote development: implications for fertilization failure in humans. *Hum Reprod* 2008; 23:573-80.
- Ribas-Maynou J, García-Peiró A, Fernandez-Encinas A, Amengual MJ, Prada E, Cortés P, Navarro J, Benet J. Double stranded sperm DNA breaks, measured by Comet assay, are associated with unexplained recurrent miscarriage in couples without a female factor. *PLoS One* 2012; 7:e44679.
- Registro SEF. Informe estadístico de Técnicas de Reproducción Asistida 2016. 2016
- Reichmann J, Nijmeijer B, Hossain MJ, Eguren M, Schneider I, Politi AZ, Roberti MJ, Hufnagel L, Hiiragi T, Ellenberg J. Dual-spindle formation in zygotes keeps parental genomes apart in early mammalian embryos. *Science* 2018; 361:189-193.
- Rienzi L, Ubaldi FM, Iacobelli M, Minasi MG, Romano S, Ferrero S, Sapienza F, Baroni E, Litwicka K, Greco E. Significance of metaphase II human oocyte morphology on ICSI outcome. *Fertil Steril* 2008; 90:1692-700.
- Robinson L, Gallos ID, Conner SJ, Rajkhowa M, Miller D, Lewis S, Kirkman-Brown J, Coomarasamy A. The effect of sperm DNA fragmentation on miscarriage rates: a systematic review and meta-analysis. *Hum Reprod* 2012; 27:2908-17.
- Rocca MS, Speltra E, Menegazzo M, Garolla A, Foresta C, Ferlin A. Sperm telomere length as a parameter of sperm quality in normozoospermic men. *Hum Reprod* 2016; 31:1158-63.
- Rogenhofer N, Dansranjavin T, Schorsch M, Spiess A, Wang H, von Schönfeldt V, Cappallo-Obermann H, Baukloh V, Yang H, Paradowska A, Chen B, Thaler CJ, Weidner W, Schuppe HC, Steger K. The sperm protamine mRNA ratio as a clinical parameter to estimate the fertilizing potential of men taking part in an ART programme. *Hum Reprod* 2013; 28:969-78.
- Rogers NT, Hobson E, Pickering S, Lai FA, Braude P, Swann K. Phospholipase C ζ causes Ca $^{2+}$ oscillations and parthenogenetic activation of human oocytes. *Reproduction* 2004; 128:697-702.
- Rosen MP, Shen S, Dobson AT, Fujimoto VY, McCulloch CE, Cedars MI. Oocyte degeneration after intracytoplasmic sperm injection: a multivariate analysis to assess its importance as a laboratory or clinical marker. *Fertil Steril* 2006; 85:1736-43.
- Rosenbusch BE. Frequency and patterns of premature sperm chromosome condensation in oocytes failing to fertilize after intracytoplasmic sperm injection. *J Assist Reprod Genet* 2000; 17:253-9.
- Roux MM, Townley IK, Raisch M, Reade A, Bradham C, Humphreys G, Gunaratne HJ, Killian CE, Moy G, Su YH, Ettensohn CA, Wilt F, Vacquier VD, Burke RD, Wessel G, Foltz KR. A functional genomic and proteomic perspective of sea urchin calcium signaling and egg activation. *Dev Biol* 2006; 300:416-33.
- Sabetian S, Shamsir MS, Abu Naser M. Functional features and protein network of human sperm-egg interaction. *Syst Biol Reprod Med* 2014; 60:329-37.
- Sakkas D, Ramalingam M, Garrido N, Barratt CL. Sperm selection in natural conception: what can we learn from Mother Nature to improve assisted reproduction outcomes? *Hum Reprod Update* 2015; 21:711-26.
- Sanders JR, Ashley B, Moon A, Woolley TE, Swann K. PLC ζ Induced Ca $^{2+}$ Oscillations in Mouse Eggs Involve a Positive Feedback Cycle of Ca $^{2+}$ -Induced InsP $_3$ Formation From Cytoplasmic PIP $_2$. *Front Cell Dev Biol* 2018; 6:36.
- Sang Q, Li B, Kuang Y, Wang X, Zhang Z, Chen B, Wu L, Lyu Q, Fu Y, Yan Z, Mao X, Xu Y, Mu J, Li Q, Jin L, He L, Wang L. Homozygous Mutations in WEE2 Cause Fertilization Failure and Female Infertility. *Am J Hum Genet* 2018; 102:649-657.

- Sathananthan AH, Ratnam SS, Ng SC, Tarín JJ, Gianaroli L, Trounson A. The sperm centriole: its inheritance, replication and perpetuation in early human embryos. *Hum Reprod* 1996; 11:345-56.
- Sato K, Fukami Y, Stith BJ. Signal transduction pathways leading to Ca²⁺ release in a vertebrate model system: lessons from *Xenopus* eggs. *Semin Cell Dev Biol* 2006; 17:285-92.
- Satouh Y, Nozawa K, Ikawa M. Sperm postacrosomal WW domain-binding protein is not required for mouse egg activation. *Biol Reprod* 2015; 93:94.
- Saunders CM, Larman MG, Parrington J, Cox LJ, Royse J, Blayney LM, Swann K, Lai FA. PLC zeta: a sperm-specific trigger of Ca(2+) oscillations in eggs and embryo development. *Development* 2002; 129:3533-44.
- Schmiady H, Kentenich H. Premature chromosome condensation after in-vitro fertilization. *Hum Reprod* 1989; 4:689-95.
- Sette C, Bevilacqua A, Bianchini A, Mangia F, Geremia R, Rossi P. Parthenogenetic activation of mouse eggs by microinjection of a truncated c-kit tyrosine kinase present in spermatozoa. *Development* 1997; 124:2267-74.
- Sette C, Paronetto MP, Barchi M, Bevilacqua A, Geremia R, Rossi P. Tr-kit-induced resumption of the cell cycle in mouse eggs requires activation of a Src-like kinase. *EMBO J* 2002; 21:5386-95.
- Sfontouris IA, Nastri CO, Lima ML, Tahmasbpourmarzouni E, Raine-Fenning N, Martins WP. Artificial oocyte activation to improve reproductive outcomes in women with previous fertilization failure: a systematic review and meta-analysis of RCTs. *Hum Reprod* 2015; 30:1831-41.
- Shapiro BS, Daneshmand ST, Garner FC, Aguirre M, Ross R. Contrasting patterns in in vitro fertilization pregnancy rates among fresh autologous, fresh oocyte donor, and cryopreserved cycles with the use of day 5 or day 6 blastocysts may reflect differences in embryo-endometrium synchrony. *Fertil Steril* 2008; 89:20-6.
- Shen L, Inoue A, He J, Liu Y, Lu F, Zhang Y. Tet3 and DNA replication mediate demethylation of both the maternal and paternal genomes in mouse zygotes. *Cell Stem Cell*. 2014; 15:459-471.
- Shinar S, Almog B, Levin I, Shwartz T, Amit A, Hasson J. Total fertilization failure in intra-cytoplasmic sperm injection cycles--classification and management. *Gynecol Endocrinol* 2014; 30:593-6.
- Siklenka K, Erkek S, Godmann M, Lambrot R, McGraw S, Lafleur C, Cohen T, Xia J, Suderman M, Hallett M, Trasler J, Peters AH, Kimmins S. Disruption of histone methylation in developing sperm impairs offspring health transgenerationally. *Science* 2015; 350:aab2006.
- Song WH, Yi YJ, Sutovsky M, Meyers S, Sutovsky P. Autophagy and ubiquitin-proteasome system contribute to sperm mitophagy after mammalian fertilization. *Proc Natl Acad Sci USA* 2016; 113:E5261-70.
- Sousa AP, Amaral A, Baptista M, Tavares R, Caballero Campo P, Caballero Peregrín P, Freitas A, Paiva A, Almeida-Santos T, Ramalho-Santos J. Not all sperm are equal: functional mitochondria characterize a subpopulation of human sperm with better fertilization potential. *PLoS One* 2011; 6:e18112.
- Stepoe PC, Edwards RG. Birth after the reimplantation of a human embryo. *Lancet* 1978; 2:366.
- Stricker SA. Comparative biology of calcium signaling during fertilization and egg activation in animals. *Dev Biol* 1999; 211:157-76.
- Sullivan R, Saez F, Girouard J, Frenette G. Role of exosomes in sperm maturation during the transit along the male reproductive tract. *Blood Cells Mol Dis* 2005; 35:1-10.
- Sutovsky P, Navara CS, Schatten G. Fate of the sperm mitochondria, and the incorporation, conversion, and disassembly of the sperm tail structures during bovine fertilization. *Biol Reprod* 1996; 55:1195-205.
- Sutovsky P, Oko R, Hewitson L, Schatten G. The removal of the sperm perinuclear theca and its association with the bovine oocyte surface during fertilization. *Dev Biol* 1997; 188:75-84.

- Sutovsky P, Manandhar G, Wu A, Oko R. Interactions of sperm perinuclear theca with the oocyte: implications for oocyte activation, anti-polyspermy defense, and assisted reproduction. *Microsc Res Tech* 2003; 61:362-78.
- Sutovsky P, Manandhar G, McCauley TC, Caamaño JN, Sutovsky M, Thompson WE, Day BN. Proteasomal interference prevents zona pellucida penetration and fertilization in mammals. *Biol Reprod* 2004; 71:1625-37.
- Swain JE, Pool TB. ART failure: oocyte contributions to unsuccessful fertilization. *Hum Reprod Update* 2008; 14:431-46.
- Swann K. A cytosolic sperm factor stimulates repetitive calcium increases and mimics fertilization in hamster eggs. *Development* 1990; 110:1295-302.
- Swann K, Ozil JP. Dynamics of the calcium signal that triggers mammalian egg activation. *Int Rev Cytol* 1994; 152:183-222.
- Swann K, Yu Y. The dynamics of calcium oscillations that activate mammalian eggs. *Int J Dev Biol* 2008; 52:585-94.
- Tachibana M, Terada Y, Ogonuki N, Ugajin T, Ogura A, Murakami T, Yaegashi N, Okamura K. Functional assessment of centrosomes of spermatozoa and spermatids microinjected into rabbit oocytes. *Mol Reprod Dev* 2009; 76:270-7.
- Tatone C, Delle Monache S, Iorio R, Caserta D, Di Cola M, Colonna R. Possible role for Ca(2+) calmodulin-dependent protein kinase II as an effector of the fertilization Ca(2+) signal in mouse oocyte activation. *Mol Hum Reprod* 2002; 8:750-7.
- Taylor CT, Lawrence YM, Kingsland CR, Biljan MM, Cuthbertson KS. Oscillations in intracellular free calcium induced by spermatozoa in human oocytes at fertilization. *Hum Reprod* 1993; 8:2174-9.
- Taylor CW, Tovey SC, Rossi AM, Lopez Sanjurjo CI, Prole DL, Rahman T. Structural organization of signalling to and from IP3 receptors. *Biochem Soc Trans* 2014; 42:63-70.
- Teixeira DM, Barbosa MA, Ferriani RA, Navarro PA, Raine-Fenning N, Nastri CO, Martins WP. Regular (ICSI) versus ultra-high magnification (IMSI) sperm selection for assisted reproduction. *Cochrane Database Syst Rev* 2013; (7):CD010167.
- Tesarik J, Kopečný V. Development of human male pronucleus: ultrastructure and timing. *Gamete Res* 1989; 24:135-49.
- Tesarik J, Sousa M, Testart J. Human oocyte activation after intracytoplasmic sperm injection. *Hum Reprod* 1994; 9:511-8.
- Tesarik J, Greco E. The probability of abnormal preimplantation development can be predicted by a single static observation on pronuclear stage morphology. *Hum Reprod* 1999; 14:1318-23.
- Tesarik J, Rienzi L, Ubaldi F, Mendoza C, Greco E. Use of a modified intracytoplasmic sperm injection technique to overcome sperm-borne and oocyte-borne oocyte activation failures. *Fertil Steril* 2002; 78:619-24.
- Thilagavathi J, Venkatesh S, Dada R. Telomere length in reproduction. *Andrologia* 2013; 45:289-304.
- Tremoleda JL, Van Haeften T, Stout TA, Colenbrander B, Bevers MM. Cytoskeleton and chromatin reorganization in horse oocytes following intracytoplasmic sperm injection: patterns associated with normal and defective fertilization. *Biol Reprod* 2003; 69:186-94.
- Tsaadon L, Kaplan-Kraicer R, Shalgi R. Myristoylated alanine-rich C kinase substrate, but not Ca²⁺/calmodulin-dependent protein kinase II, is the mediator in cortical granules exocytosis. *Reproduction* 2008; 135:613-24.
- Turner S, Hartshorne GM. Telomere lengths in human pronuclei, oocytes and spermatozoa. *Mol Hum Reprod* 2013; 19:510-8.

- Van Blerkom J. Mitochondrial function in the human oocyte and embryo and their role in developmental competence. *Mitochondrion* 2011; 11:797-813.
- Vanden Meerschaut F, Nikiforaki D, De Gheselle S, Dullaerts V, Van den Abbeel E, Gerris J, Heindryckx B, De Sutter P. Assisted oocyte activation is not beneficial for all patients with a suspected oocyte-related activation deficiency. *Hum Reprod* 2012; 27:1977-84.
- Vanden Meerschaut F, D'Haeseleer E, Gysels H, Thienpont Y, Dewitte G, Heindryckx B, Oostra A, Roeyers H, Van Lierde K, De Sutter P. Neonatal and neurodevelopmental outcome of children aged 3-10 years born following assisted oocyte activation. *Reprod Biomed Online* 2014; 28:54-63.
- Vassena R, Boué S, González-Roca E, Aran B, Auer H, Veiga A, Izpisua Belmonte JC. Waves of early transcriptional activation and pluripotency program initiation during human preimplantation development. *Development* 2011; 138:3699-709.
- Vaughan DA, Sakkas D. Sperm selection methods in the 21st century. *Biol Reprod* 2019.
- Virant-Klun I, Leicht S, Hughes C, Krijgsveld J. Identification of Maturation-Specific Proteins by Single-Cell Proteomics of Human Oocytes. *Mol Cell Proteomics* 2016; 15:2616-27.
- Wang J, Fan HC, Behr B, Quake SR. Genome-wide single-cell analysis of recombination activity and de novo mutation rates in human sperm. *Cell* 2012; 150:402-12.
- Wang C, Machaty Z. Calcium influx in mammalian eggs. *Reproduction* 2013; 145:R97-R105.
- WHO. WHO laboratory manual for the examination and processing of human semen. 5th edition. 2010.
- Williams M, Barratt CL, Hill CJ, Warren MA, Dunphy B, Cooke ID. Recovery of artificially inseminated spermatozoa from the fallopian tubes of a woman undergoing total abdominal hysterectomy. *Hum Reprod* 1992; 7:506-9.
- Wolny YM, Fissore RA, Wu H, Reis MM, Colombero LT, Ergün B, Rosenwaks Z, Palermo GD. Human glucosamine-6-phosphate isomerase, a homologue of hamster oscillin, does not appear to be involved in Ca²⁺ release in mammalian oocytes. *Mol Reprod Dev* 1999; 52:277-87.
- Wu AT, Sutovsky P, Manandhar G, Xu W, Katayama M, Day BN, Park KW, Yi YJ, Xi YW, Prather RS, Oko R. PAWP, a sperm-specific WW domain-binding protein, promotes meiotic resumption and pronuclear development during fertilization. *J Biol Chem* 2007; 282:12164-75.
- Xu YR, Yang WX. Calcium influx and sperm-evoked calcium responses during oocyte maturation and egg activation. *Oncotarget* 2017; 8:89375-89390.
- Yamaguchi T, Ito M, Kuroda K, Takeda S, Tanaka A. The establishment of appropriate methods for egg-activation by human PLCZ1 RNA injection into human oocyte. *Cell Calcium* 2017; 65:22-30.
- Yanagida K, Katayose H, Yazawa H, Kimura Y, Sato A, Yanagimachi H, Yanagimachi R. Successful fertilization and pregnancy following ICSI and electrical oocyte activation. *Hum Reprod* 1999; 14:1307-11.
- Yelumalai S, Yeste M, Jones C, Amdani SN, Kashir J, Mounce G, Da Silva SJ, Barratt CL, McVeigh E, Coward K. Total levels, localization patterns, and proportions of sperm exhibiting phospholipase C zeta are significantly correlated with fertilization rates after intracytoplasmic sperm injection. *Fertil Steril* 2015; 104:561-8.e4.
- Yeste M, Jones C, Amdani SN, Patel S, Coward K. Oocyte activation deficiency: a role for an oocyte contribution? *Hum Reprod Update* 2016; 22:23-47.
- Yoon SY, Jellerette T, Salicioni AM, Lee HC, Yoo MS, Coward K, Parrington J, Grow D, Cibelli JB, Visconti PE, Mager J, Fissore RA. Human sperm devoid of PLC, zeta 1 fail to induce Ca(2+) release and are unable to initiate the first step of embryo development. *J Clin Invest* 2008; 118:3671-81.
- Yoon SY, Eum JH, Lee JE, Lee HC, Kim YS, Han JE, Won HJ, Park SH, Shim SH, Lee WS, Fissore RA, Lee DR, Yoon TK. Recombinant human phospholipase C zeta 1 induces intracellular calcium oscillations and oocyte activation in mouse and human oocytes. *Hum Reprod* 2012; 27:1768-80.

- Zenzes MT, Casper RF. Cytogenetics of human oocytes, zygotes, and embryos after in vitro fertilization. *Hum Genet* 1992; 88:367-75.
- Zhang J, Wang CW, Blaszyck A, Grifo JA, Ozil J, Haberman E, Adler A, Krey LC. Electrical activation and in vitro development of human oocytes that fail to fertilize after intracytoplasmic sperm injection. *Fertil Steril* 1999; 72:509-12.
- Zhao MH, Kwon JW, Liang S, Kim SH, Li YH, Oh JS, Kim NH, Cui XS. Zinc regulates meiotic resumption in porcine oocytes via a protein kinase C-related pathway. *PLoS One*; 9:e102097.

RESUM

Introducció

La infertilitat masculina afecta a un 7% dels homes, pot explicar un 20-30% del total de casos d'infertilitat, i ha incrementat la seva incidència en els últims 40 anys. Diferents alteracions genètiques i, sobretot, defectes en l'espermatogènesi, s'han descrit com a causes d'infertilitat, però l'origen d'aquest problema es desconeix en un 50% dels casos. En part, això es deu a que el diagnòstic de la infertilitat masculina es basa en l'anàlisi de paràmetres bàsics de la mostra de semen (concentració, mobilitat, morfologia), i no hi ha tests que informin adequadament de la funció de l'espermatozoide, ni de la seva capacitat de fecundar i generar un fill/a sa.

Una de les tècniques que més s'utilitza per al tractament de la infertilitat és la injecció intracitoplasmàtica d'espermatozoide (ICSI), tècnica que va sorgir el 1992 i que va suposar una revolució en el camp de la reproducció assistida. La ICSI permet a l'espermatozoide estalviar-se varis passos previs a l'entrada a l'oòcit (com el trànsit pel tracte reproductiu femení, o el reconeixement de l'oòcit i penetració a través de les seves capes externes), i és una tècnica molt eficient ja que presenta unes taxes de fecundació mitjanes al voltant del 70-80%. Tot i així, en un 1-3% dels casos hi ha fallada de fecundació (FF).

La FF pot estar caracteritzada per fecundació anòmala (nombre anormal de pronúclis ($\neq 2$) el dia posterior a la inseminació) o, en la majoria de casos, fallada d'activació oocitària (*oocyte activation failure*, OAF). En aquest segon cas, l'activació de l'oòcit presenta problemes o directament no es produeix, un procés que involucra una senyalització específica de calci, la sortida de l'arrest meiótic, la reacció cortical, la formació de pronúclis i l'entrada a la primera divisió mitòtica. La FF suposa absència d'embrions preimplantacionals que es puguin transferir i per tant nul·les possibilitats d'obtenir un embaràs, té un gran impacte psicològic i econòmic en els pacients, és molt difícil de predir, i no s'han establert protocols específics per la gestió clínica d'aquests casos. Per aquestes raons, hi ha la necessitat d'entendre els mecanismes espermàtics que causen FF i trobar marcadors que permetin el seu diagnòstic i pronòstic.

Diferents factors poden ser causa de FF en ICSI. Algunes alteracions en l'oòcit poden ser l'origen d'aquest problema, com per exemple un estat deficient de maduració citoplasmàtica, incorrecta organització del fus meiótic i/o orgànuls, o mutacions específiques en proteïnes que participen en l'activació (com per exemple la quinasa WEE2). Tot i així, s'ha descrit que el factor masculí és la principal causa d'OAF en ICSI, degut a que l'espermatozoide és l'encarregat de desencadenar l'activació de l'oòcit mitjançant la proteïna PLC ζ . Es tracta d'una proteïna clau perquè es doni una correcta fecundació, i ella sola pot desencadenar oscil·lacions de calci molt similars a les que

succeeixen a l'oòcit en una situació *in vivo*. Diferents alteracions de PLC ζ (en seva localització subcel·lular o en la seva seqüència gènica) s'han descrit com a causes de FF en ICSI. Tot i així, no hi ha estudis que incloguin un elevat nombre de pacients amb FF, per la qual cosa es desconeix quina és la freqüència d'aquestes alteracions, si aquestes estan associades a algun subtipus particular de FF, o si PLC ζ pot ser un marcador útil per a FF en ICSI a la clínica. Aquesta tesi analitza la proteïna PLC ζ i dóna resposta a aquestes preguntes.

Per altra banda, en aquesta tesi s'avaluen dos factors de l'espermatozoide que, segons evidències prèvies, podrien estar involucrats en el procés de fecundació. El primer és PAWP, una proteïna que sembla participar en l'activació de l'oòcit. El segon és la longitud dels telòmers en espermatozoide (*sperm telomere length*, STL), que en cas de presentar alteracions podria originar problemes en la formació de pronuclis tal com s'ha observat en ratolí.

Cal recalcar que, malgrat els diferents factors comentats, el procés de fecundació en humans i les causes de FF es desconeixen en gran mesura. Per exemple, les FF en ICSI podem succeir en pacients sense problemes a PLC ζ i utilitzant oòcits de donant amb fertilitat provada. A més, el rol de l'espermatozoide en la fecundació de l'oòcit va més enllà de desencadenar la senyalització de calci, ja que són necessaris diferents processos posteriors a l'entrada a l'oòcit (decondensació del nucli espermàtic, degradació d'estructures com la beina mitocondrial, alliberament del centrosoma, formació d'una xarxa de microtúbuls anomenada *sperm aster*, i formació del pronucli masculí). Per aquest motiu, és més que probable que altres factors espermàtics estiguin involucrats en la FF en ICSI, els quals s'han intentat identificar en aquesta tesi.

Per fer-ho, en aquesta tesi s'han utilitzat principalment tècniques de proteòmica. Aquest conjunt de tècniques, aplicades a l'espermatozoide humà, han resultat ser molt efectives per caracteritzar i identificar les alteracions presents en diferents grups d'infertilitat masculina (astenozoospermia, nivells elevats de fragmentació en ADN espermàtic, globozoospermia, varicocele, etc.), però mai s'han utilitzat per estudiar mostres amb FF en ICSI.

Per ara, l'ús de l'activació oocitària assistida (AOA) és una de les poques alternatives de tractament en casos de FF mitjançant ICSI. L'AOA, que encara es considera una tècnica experimental, es basa en l'ús de ionòfors de calci per desencadenar l'activació de l'oòcit quan els gàmetes presenten problemes. Tot i així, s'ha demostrat que l'AOA no és beneficiosa per tots els pacients amb FF, i no hi ha un consens sobre en quins casos o situacions és recomanable aplicar aquesta tècnica. Per aquest motiu, en aquesta tesi vam avaluar si un cicle previ amb FF en ICSI és suficient justificació per recomanar AOA a la clínica.

L'objectiu d'aquesta tesi és caracteritzar i identificar les alteracions de l'espermatozoide que causen FF en ICSI. En concret, els objectius principals són: i) caracteritzar les dues proteïnes de l'espermatozoide proposades com a factors necessaris per l'activació de l'oòcit (PLC ζ i PAWP) i avaluar la seva utilitat com a marcadors clínics, ii) identificar nous mecanismes de l'espermatozoide que puguin estar involucrats en les FF en ICSI, mitjançant tècniques de proteòmica.

Aquesta tesi també inclou alguns objectius secundaris relacionats amb el procés de fecundació, com l'anàlisi de la longitud telomèrica en espermatozoide com a marcador de resultats de fecundació i reproductius en ICSI, l'estudi del temps de processat o incubació dels espermatozoides i la seva relació amb les taxes de fecundació i embaràs en ICSI, i una caracterització dels criteris necessaris per recomanar AOA en pacients que han tingut FF en ICSI.

Resultats

En primer lloc, es va analitzar la proteïna PAWP en pacients amb FF en ICSI (n = 8) i donants amb bona fecundació (n = 8). No vam trobar diferències en els nivells proteics de PAWP (avaluats per Western Blot) entre FF i controls (4.0 ± 3.2 vs. 1.6 ± 1.1 ratio PAWP/tubulina, respectivament, $p > 0.05$), ni tampoc van variar els nivells de WBP2, el seu ortòleg. El nombre d'espermatozoides amb marcatge positiu de PAWP (per immunofluorescència) tampoc va ser diferent entre grups ($53.6\% \pm 24.1$ en FF, $65.7\% \pm 12.9$ en controls, $p > 0.05$). A més, vam realitzar el primer estudi de seqüenciació genètica de PAWP en múltiples pacients amb FF. La majoria de les variants genètiques identificades eren compartides entre pacients amb FF i controls, excepte per dues variants *missense* amb afectació clínica desconeguda (les quals estaven presents en dos pacients amb FF però no en els controls): p.Q5E (exó 1, rs17002790) i p.C170F (exó 5, rs17002802).

En segon lloc, es va estudiar PLC ζ en 13 controls amb bones taxes de fecundació i 37 pacients amb FF total o parcial (< 25% taxa de fecundació). Els pacients es van dividir en dos grups: grup OAF, incloent 22 pacients amb FF recurrent (≥ 2 cicles d'ICSI) o fallada d'activació en tots els oòcits no fecundats, i el grup no-OAF, incloent 15 pacients que presenten FF deguda a fecundació anòmala (1PN, 3PN o >3PN). 13 pacients amb FF (35.1%) van presentar com a mínim una mutació en el gen *PLCZ1*, mentre que cap dels controls (0%) va tenir mutació ($p < 0.05$). En total, es van identificar 6 mutacions diferents de *PLCZ1*, 4 d'elles no descrites prèviament en pacients amb FF, incloent 5 variants *missense* (p.I120M, p.R197H, p.L224P, p.H233L i p.S500L) i una mutació *frameshift* (p.V326K*25) que genera una forma proteica truncada. A destacar, la majoria de pacients amb mutació a *PLCZ1* pertanyien al grup OAF (12 de 22, 54.5%), i només 1 dels pacients pertanyia al grup no-OAF (1 de 15, 6.7%). Es van dur a terme anàlisis funcionals mitjançant

l'algoritme MODICT (eina bioinformàtica per a la previsió de l'efecte de mutacions en la funció proteica) i la injecció de cRNA de *PLCZ1* en oòcits humans madurats *in vitro*. Les injeccions amb cRNA de *PLCZ1 wild-type* van poder activar el 74.3% dels oòcits (26/35), el cRNA de diferents mutacions en va activar un percentatge significativament menor, confirmant el seu efecte deleteri: 30% per p.R197H (3/10), 30.8% per p.H233L (4/13) i 0% per p.V326K*25 (0/10) ($p < 0.05$). Vam comprovar que la presència i tipus de mutació no afecta ni els nivells ni la localització subcel·lular de la proteïna PLC ζ . Per últim, 10 pacients amb mutació van realitzar tractament d'ICSI juntament amb AOA (en el/s cicle/s posterior/s a la/les FF); tots ells van recuperar bones taxes de fecundació, i 7 d'ells van aconseguir embaràs i nen nascut.

A continuació, vam avaluar l'STL en 60 donants fèrtils, cada un d'ells utilitzat per a tractament d'ICSI en almenys 6 dones diferents. Això va permetre, per primera vegada, fer un anàlisi aïllant STL del factor femení. Es va extreure ADN genòmic de cada una de les mostres de semen i la STL relativa es va determinar per PCR quantitativa, el valor mitjà de la qual va ser 4.5 ± 1.9 unitats relatives (rang 2.4–14.2). Es van dur a terme anàlisis estadístics univariats i multivariats introduint diverses variables com a factors de confusió (com per exemple l'edat de l'home i la dona, l'origen de l'oòcit (parella o donant), i el nombre d'oòcits inseminats, entre altres), i no es va detectar cap efecte significatiu de l'STL en les taxes de fecundació, embaràs i nen nascut ($p > 0.05$). En una segona part de l'estudi, vam observar que els nivells d'STL de 67 donants eren significativament menors que els de 26 pacients amb FF en ICSI (4.6 ± 1.9 vs. 5.7 ± 2.1 , respectivament).

La segona part de la tesi es va centrar en identificar nous mecanismes potencialment relacionats amb la FF en ICSI. Com a primera aproximació, es va utilitzar la base de dades *PrePPI* per tal de fer una predicció *in silico* d'interaccions proteïna-proteïna (PPI) entre proteïnes específiques d'espermatozoide ($n=416$) i proteïnes de l'oòcit involucrades en la cascada de senyalització durant l'activació oocitària ($n=164$). Aquest anàlisi va predir un total de 151 PPI amb una probabilitat final assignada >0.85 , involucrant 69 proteïnes espermàtiques i 57 proteïnes que participen en l'activació de l'oòcit. Un 23.2% d'aquestes interaccions havien estat prèviament validades a nivell experimental, com la interacció entre ODF2 i PLK1, o entre SPERT i la quinasa Mos. Cal destacar els membres de la família TSSK (quinases específiques d'espermatozoide), els quals estaven involucrats en 38 PPI.

Més endavant, es va realitzar una aproximació més robusta i fiable alhora d'identificar possible alteracions relacionades amb FF en ICSI, aplicant tècniques de proteòmica i un anàlisi bioinformàtic complex. En aquest estudi es van incloure 8 pacients amb bona fecundació per ICSI ($>75\%$) i 4 pacients amb FF recurrent (FF en ≥ 3 cicles d'ICSI consecutius). Les mostres d'ejaculat

d'aquests pacients es van processar per centrifugació amb gradients de densitat (per eliminar les possibles cèl·lules contaminants), es van lisar, i es va procedir al marcatge dels pèptids amb *isobaric tandem mass tags* (TMT) i a la identificació de proteïnes per cromatografia líquida – espectrometria de masses (2D-LC-MS). Es van identificar un total de 232 proteïnes amb valors de quantificació altament fiables (FDR <1%, ≥ 2 PSMs en totes les mostres, i un coeficient de variació <50 % en almenys un 75 % de les mostres), que es van utilitzar per els següents anàlisis. L'anàlisi de grup va identificar 9 proteïnes diferencialment expressades entre tots dos grups (t-test, $p < 0.05$), 4 d'elles amb nivells més baixos en FF (FMR1NB, FAM209B, RAB2B i la proteïna proteasomal PSMA1) i 5 d'elles sobreexpressades en mostres amb FF, totes elles mitocondrials (DLAT, ATP5H, SLC25A3, SLC25A6, i FH). A més, dos anàlisis independents es van dur a terme per tal de fer una caracterització individualitzada de cada pacient amb FF en relació amb els controls: anàlisi d'*outliers* i anàlisi de correlacions estables de proteïnes. Tots dos anàlisis van aportar informació compatible amb l'observat en l'anàlisi de grups (com per exemple la desregulació en els nivells de components del complex enzimàtic PDH i de l'ATP sintasa), i van identificar alteracions en altres factors (com PHB2 o ROPN1) en pacients amb FF concrets.

Per tal de caracteritzar millor els resultats de l'estudi de proteòmica, es van realitzar diferents aproximacions experimentals. L'abundància diferencial es va confirmar per Western Blot per les proteïnes DLAT o component E2 de la piruvat deshidrogenasa (2.44 ± 0.98 ratio proteïna/tubulina en FF, 1.25 ± 0.71 en controls, $p < 0.05$) i per PSMA1 (1.91 ± 0.92 ratio proteïna/tubulina en FF, 3.05 ± 0.84 en controls, $p < 0.05$). Mitjançant l'ús del marcador JC-1 i citometria de flux, vam determinar que el percentatge d'espermatozoides amb activitat mitocondrial en mostres amb FF era menor que en els controls ($71.98 \% \pm 20.2$ i $59.12 \% \pm 12.9$, respectivament). Finalment, mitjançant un anàlisi *in vitro* que mesura la activitat proteolítica per fluorimetria, vam observar que les mostres amb FF en ICSI presentaven menor activitat proteasomal que els controls (0.206 ± 0.08 vs. 0.352 ± 0.18 unitats d'activitat proteasomal, respectivament).

En l'última part de la tesi, es van realitzar dos estudis d'anàlisi de dades clíniques per tal de caracteritzar millor les possibles causes i el tractament de les FF en ICSI. En primer lloc, es va dissenyar un estudi per veure si l'evidència prèvia d'un sol cicle d'ICSI amb FF és suficient motiu per recomanar l'ús d'AOA en un tractament posterior. Per això, es van analitzar retrospectivament les dades de 125 cicles de donació d'òocits i semen de pacient amb FF total o parcial (<20% taxa de fecundació). D'aquests pacients, 115 van realitzar un segon cicle de donació d'òocits canviant de donant (i amb el mateix semen) (grup OD), i en 10 es va utilitzar AOA (grup AOA). El 98.3% (113/115) dels pacients del grup OD van obtenir bona taxa de fecundació. Les taxes de fecundació

en el cicle post-FF van ser similars entre els dos grups (69.0% per OD, 66.3% per AOA), així com també els resultats d'embaràs clínic.

Per últim, vam avaluar si el temps d'incubació de la mostra espermàtica abans de la ICSI pot afectar els resultats de fecundació i reproductius. En aquest estudi retrospectiu es van incorporar dades de 1169 cicles d'ICSI utilitzant semen fresc processat per swim-up, i per primera vegada en un estudi d'aquest tipus, es va incorporar un sistema de radiofreqüència per realitzar un enregistrament del temps de manera exacta i automàtica. Es van analitzar l'efecte de tres intervals temporals (T1: des de l'obtenció de la mostra al swim-up; T2: des del swim-up a l'ICSI; i T: des de l'obtenció de la mostra a l'ICSI (temps total)) en taxa de fecundació, morfologia embrionària, taxes d'embaràs (bioquímic, clínic i en curs) i nascut viu. Després de diferents anàlisis univariats i multivariats ajustant per diferents variables, no es va poder observar cap efecte significatiu d'aquests temps de processat del semen en els resultats d'ICSI ($p > 0.05$ per tots els casos).

Discussió

Actualment, l'avaluació i diagnòstic de la infertilitat masculina es basa en realitzar un seminograma, el qual informa sobre la concentració, mobilitat i morfologia espermàtiques. Tot i que aquestes mesures poden identificar l'origen de la infertilitat en determinats casos, calen noves eines i tests que permetin millorar el diagnòstic, que puguin informar sobre la funció de l'espermatozoide i sobre la seva capacitat de fecundar.

Basant-nos en els nostres resultats, creiem que la seqüenciació del gen *PLCZ1* pot ser útil per al diagnòstic i pronòstic de casos de FF en ICSI. Aquesta eina seria especialment útil en aquells pacients que presenten un problema d'activació de l'oòcit o que han tingut més d'un cicle previ amb FF, la meitat dels quals podrien presentar mutacions a *PLCZ1*. Els nostres resultats no només incrementen el nombre de mutacions en *PLCZ1* identificades fins ara, sinó que, per primera vegada, hem identificat un elevat nombre de pacients amb mutacions en heterozigosi. Això suggereix que la presència d'un sol al·lel mutat pot ser suficient per causar un problema de fallada de fecundació.

Aquests resultats, juntament amb l'anàlisi d'AOA, posen de manifest la necessitat de fer una caracterització i diagnòstic més acurats en els pacients amb FF. La simple presència d'un cicle d'ICSI amb FF no sembla ser evidència suficient per recomanar AOA, i una millor caracterització molecular dels gàmetes pot ajudar a identificar aquells casos en que sí sigui beneficiàl l'ús d'AOA (com és el cas de pacients amb mutacions de *PLCZ1*). De totes maneres, cal no oblidar que el factor femení pot també explicar les FF, especialment en cicles utilitzant els oòcits de la pacient.

Per altra banda, el rol d'altres possible marcadors de FF com PAWP o l'STL no semblen tan prometedors. En el cas de PAWP, en primer lloc, perquè en el nostre estudi no hem trobat diferències rellevants entre mostres amb FF i bona fecundació en ICSI. En segon lloc, tot i que hi ha diferents estudis que indiquen un paper de PAWP o WBP2 en l'activació de l'oòcit, aquest rol no s'ha demostrat de manera robusta en humans. Pel que fa a l'STL, malgrat que hem trobat algunes diferències en els seus nivells en mostres amb FF, creiem que no són clínicament rellevants, sobretot tenint en compte la gran variabilitat en STL entre individus.

És per això que, a continuació, vam realitzar un estudi *in silico* (de predicció de PPI) a nivell exploratori per identificar possibles proteïnes espermàtiques involucrades en l'activació de l'oòcit. Aquest estudi aporta una llista de candidats amb un possible rol, com per exemples les quinases TSSK, les quals no només podrien participar en espermatogènesi sinó també en la fecundació. De totes maneres, en aquest anàlisi no s'han demostrat si les PPI identificades a nivell experimental, i hi ha algunes limitacions que cal mencionar: molts factors que poden participar en l'activació no s'han inclòs en l'anàlisi (per ara, la via de senyalització de l'oòcit no s'ha descrit completament), no s'han considerat possibles mecanismes de regulació diferents a interaccions proteïna-proteïna, i és molt difícil distingir si les interaccions que es prediuen succeeixen en la fecundació de l'oòcit o en esdeveniments anteriors (com l'espermatogènesi).

Per aquest motiu, en el que considerem l'estudi central d'aquesta tesi, es va fer ús de tècniques de proteòmica, noves aproximacions bioinformàtiques i tècniques experimentals per a l'avaluació funcional de mostres amb FF. Aquests anàlisis van permetre identificar possibles marcadors de FF en ICSI (com DLAT o PSMA1 entre d'altres), i van detectar alteracions en les funcionals mitocondrials i proteasomals en l'espermatozoide.

La relació d'aquests mecanismes amb la infertilitat masculina no és nova, però sí que és la primera vegada que s'associen clarament amb FF en ICSI. Els resultats d'estudis previs es poden fer servir per explicar la possible relació amb FF. L'activitat mitocondrial i un correcte metabolisme són essencials per la funció de l'espermatozoide, i les seves anomalies poden causar una capacitat anormal, menor viabilitat, estrès oxidatiu, canvis en senyalització intracel·lular o pH, etc, que a la fi poden afectar la capacitat de fecundació fins i tot després d'ICSI. De fet, en hámster s'ha vist que inhibint la funció de l'enzim PDH (detectat en el nostre estudi: DLAT), els espermatozoides generen FF fins i tot després de ser capaços de penetrar en l'oòcit. Per altra banda, en molts models i malalties, una desregulació en l'activitat mitocondrial pot reduir l'activitat proteasomal. Els proteasomes de l'espermatozoide juguen un paper clau en la fecundació humana, i hi ha indicis que

tenen un paper important per una correcta degradació de la beina mitocondrial, alliberament del centriol i formació de l'*sperm aster* durant la fecundació de l'oòcit.

Cal recordar que, en el context d'un tractament de reproducció assistida, són essencials els protocols de processament i selecció espermàtica, els quals poden tenir efecte en les taxes de fecundació. En general, la cura i processat del oòcits centra tota l'atenció, mentre que els temps d'incubació dels espermatozoides no s'acostuma a considerar important malgrat pot afectar diferent paràmetres moleculars i cel·lulars. En el nostre anàlisi vam analitzar l'efecte d'aquest temps en les taxes de fecundació i resultats reproductius en ICSI, incorporant un gran nombre de pacients (n=1169) i un sistema molt precís d'enregistrament del temps, però no vam poder observar un efecte significatiu.

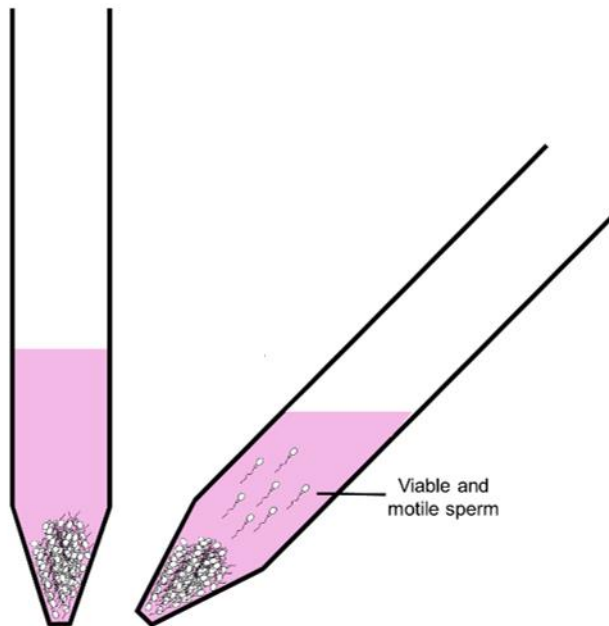
En conjunt, s'ha realitzat una caracterització completa i detallada de la FF post-ICSI causada per alteracions espermàtiques, incloent múltiples tècniques (seqüenciació gènica, proteòmica, estudis funcionals, anàlisi de dades clíniques, etc.) i diferents punts de vista (molecular, cel·lular, clínic, etc.). Aquesta tesi corrobora que les alteracions espermàtiques relacionades amb FF en ICSI són multifactorials, aporta un conjunt de possibles marcadors que poden ser útils a nivell clínic per casos de FF, i creiem que el conjunt de resultats pot ser rellevant per a futurs estudis relacionats amb la fecundació humana.

Conclusions

1. Un elevat percentatge de pacients amb fallada d'activació oocitària i fallada de fecundació recurrent presenten mutacions a la seqüència genètica de PLCZ1. Aquestes mutacions poden alterar la funció proteica i la capacitat de l'espermatozoide per iniciar l'activació de l'oòcit, afectant diferent dominis de la proteïna. En diversos casos, les mutacions en heterozigosi semblen ser suficients per causar un fenotip de fallada de fecundació post-ICSI.
2. Els nivells, localització i variants genètiques de PAWP no semblen estar associats amb les fallades de fecundació en ICSI.
3. La longitud telomèrica en espermatozoide no està associada amb les taxes de fecundació en pacients normozoospermics sense problemes de fecundació.
4. La funció mitocondrial i l'activitat proteasomal són mecanismes cel·lulars necessaris per a una correcta fecundació, i les seves alteracions podrien explicar part de les fallades de fecundació en ICSI.

5. Algunes proteïnes espermàtiques com DLAT o PSMA1 presenten una expressió diferencial en mostres que han tingut fallada de fecundació recurrent en ICSI, i podrien ser utilitzats com a marcadors d'infertilitat a la clínica.
6. L'anàlisi *in silico* de PPI ha predit que factors específics d'espermatozoide (com per exemple les quinases de la família TSSK) podrien tenir un paper en l'activació i senyalització molecular de l'òcit durant la fecundació.
7. El temps d'incubació *in vitro* dels espermatozoides abans de realitzar ICSI no té un efecte significatiu en les taxes de fecundació ni en els resultats reproductius, en cicles en que s'utilitza semen fresc processat per *swim-up*.
8. L'AOA no millora els resultats reproductius en cicles de donació d'òcits quan la única informació disponible és la d'un únic cicle d'ICSI amb fallada de fecundació. Per recomanar aquesta tècnica, s'hauria de realitzar un anàlisi detallat dels defectes en els gàmetes.

ANNEX



ANNEX 1: How long can the sperm wait? Effect of sperm processing time on reproductive outcomes after ICSI

UNDER PREPARATION AS:

Torra-Massana, M; Quintana, A; Barragán, M; García, D; Bellido, R; Rodríguez, A; Vassena, R.
How long can the sperm wait? Effect of sperm processing time on reproductive outcomes after ICSI

Partial contents of this chapter will be included in the following oral presentation:

Quintana, A.; Torra-Massana, M; Barragán, M.; García, D.; Rodríguez, A.; Vassena, R. **Effect of sperm processing time on reproductive outcomes after ICSI**. ESHRE Annual Meeting 2019, Viena, Austria. Accepted abstract for oral presentation.

TITLE: How long can the sperm wait? Effect of sperm processing time on reproductive outcomes after ICSI

RUNNING TITLE: Analysis of sperm incubation time effect on ICSI outcomes

AUTHORS:

Marc Torra-Massana¹, Andreu Quintana¹, Montserrat Barragán¹, Désirée Garcia², Raquel Bellido¹, Amelia Rodríguez¹, Rita Vassena^{1,*}

ADDRESS:

¹ Clínica Eugin, Travessera de les Corts 322, 08029 Barcelona, Spain.

²Fundació Privada EUGIN, Travessera de les Corts 314, 08029 Barcelona, Spain.

***Correspondence:** Clínica EUGIN, Travessera de les Corts 322, 08029 Barcelona, Spain. Email: rvassena@eugin.es

EXTENDED ABSTRACT:

Study question: Do sperm processing times, from obtaining the sample to fertilization, affect reproductive outcomes in ICSI cycles?

Summary answer: Sperm processing times do not seem to affect fertilization rates (FR), pregnancy or live birth rates.

What is known already: Sperm sample processing is necessary in IVF, but processing times differ both between and within facilities. While longer sperm processing times are associated to increased sperm DNA fragmentation, intermediate times seem to be beneficial for capacitation and fertilization after ICSI. So far, there is no established consensus on the optimal sperm incubation time to maximize the reproductive outcomes after ICSI.

Study design, size, duration: Retrospective cohort study including 1,169 ICSI cycles carried out in a single center between January 2012 and December 2017. All cycles were performed with fresh semen from patients and oocytes either from partner or donor, followed by fresh embryo transfer (FET). A radiofrequency-based system was used to record exact sperm processing times; T1: from sample collection to swim-up; T2: from swim-up to ICSI; and T: total time (T1+T2). We analyzed the effect of these time intervals on FR, embryo morphology, biochemical, clinical, and ongoing pregnancy, and live birth (LB) rates.

Participants/materials, setting, methods: Differences in processing times (T1, T2, and T) between positive and negative pregnancy (biochemical, clinical, ongoing) and LB rates were tested by Student's t-test. The likelihood of positive pregnancy and LB was modeled by LOWESS regression and logistic regression, adjusting for man's and woman's age and BMI, semen parameters, number of oocytes, number and morphological score of transferred embryos, and day of ET. The effect of times on FR and embryo morphology were evaluated by generalized linear modelling and ordinal regression, respectively.

Main results and the role of chance: Mean male age was 42.9 (SD 7.5) years, while woman age was 31.5 (SD 7.6) years. Mean sperm concentration and progressive motility were 47.5 (SD 71.0) million/ml and 34.3 (SD 19.8) % a+b, respectively. Mean semen processing times in hours were T1: 0.35 (SD 0.26, range: 0.05-3.42), T2: 3.30 (SD 2.2, range: 0.17-10.9) and T: 3.66 (SD 2.26, range: 0.22-11.2). Biochemical, clinical, ongoing pregnancy and live birth rates overall were 41.9%, 30.5%, 28.0% and 27.4%, respectively. Neither T1, nor T2 or T were significantly different for patients who achieved a pregnancy (biochemical, clinical and ongoing) and LB compared to those who did not ($p > 0.05$). LOWESS regression did not return relevant correlations between T1,

T2 or T and FR or reproductive outcomes. The multivariate analyses did not reveal a significant effect for any of the time intervals on LB rate: T1: OR 0.945 (95%CI: 0.74-1.20), T2: OR 1.134 (95%CI: 0.94-1.36), and T: OR 1.151 (95%CI: 0.93-1.42). Similar results were found for biochemical, clinical and ongoing pregnancy. Multilevel analysis did not show a significant effect of sperm processing times on FR and embryo morphology after ICSI ($p > 0.05$ for T1, T2 and T).

Limitations, reasons for caution: These results should not be extended to ICSI cycles using testicular spermatozoa or samples with severe semen parameters, such as motility $<1\%$ a+b or cryptozoospermia, which were excluded from the study.

Wider implications of the findings: This is the first study evaluating the effect of sperm processing time on ICSI using an exact, radiofrequency-based, operator-independent system on a large cohort. Our results suggest that sperm processing time, especially after swim-up, have undetectable effect on pregnancy and live birth rates after ICSI, within the time interval analyzed.

Study funding/competing interest(s): This work was supported by intramural funding of Clínica EUGIN, and by the Secretary for Universities and Research of the Ministry of Economy and Knowledge of the Government of Catalonia (GENCAT 2015 DI 049 to M. T-M). No competing interest declared.

Trial registration number: NA

KEYWORDS: sperm / time / ICSI / live birth

INTRODUCTION

Semen processing is a necessary step before IUI, IVF, or ICSI in order to select and sometimes concentrate the sample and increase the chances of a successful treatment. In the embryology laboratory, ICSI is usually performed a few hours after receiving the semen sample. This interval can vary among laboratories and, within the same laboratory, among patients.

In general, comparatively little importance is given to sperm processing and selection protocols with respect to the extreme care taken with oocytes, especially in ICSI treatments (Sakkas et al., 2015). Sperm selection is usually limited to isolating a highly motile sperm population either by swim-up or density gradient centrifugation, without much consideration for the time between these procedures and ICSI.

In vitro incubation in capacitating medium can modify sperm motility, vitality, mitochondrial activity and acrosomal status (Robertson et al., 1988; Auger et al., 1989; Sukcharoen & Keith, 1996). While sperm incubation is required to undergo capacitation, extended incubation time prior to ICSI may result in alterations of the sperm nucleus morphology, higher chromatin condensation, higher levels of ROS and DNA fragmentation (Calamera et al., 2001; Peer et al., 2007; Matsuura et al., 2010; Zhang et al., 2011; Rougier et al., 2013). For this reason, molecular and cellular time-dependent changes in sperm could affect early fertilization events and preimplantational development, and also the odds of pregnancy and live birth after ICSI.

Some studies, which recorded sperm handling times manually, did not find a significant effect of sperm incubation times on fertilization rates (FR) after ICSI (Mansour et al., 2008; Ahmed et al., 2018). However, further research is required to establish the effect of sperm processing times on reproductive outcomes up to live birth after ICSI.

The use of a radiofrequency-based witnessing systems in the embryology lab to record exact, operator independent processing times, has allowed to describe the effect of different timings related to the oocyte on reproductive outcomes after ICSI (Bárcena et al., 2016; Pujol et al., 2018). By using this same technology on a large cohort of patients, we aim now to elucidate whether sperm incubation times have an effect on laboratory and reproductive outcomes after ICSI, as well as to determine if there is an optimal sperm processing time in fresh semen samples processed by swim-up.

MATERIALS AND METHODS

Ethical approval

Approval to conduct this research was obtained from the local Ethical Committee for Clinical Research.

Study population

This is a retrospective cohort study including 1,169 men undergoing elective ICSI treatment in a single center between January 2012 and December 2017. In all cycles, fresh semen from the patient was used and fresh embryo transfer (FET) performed at day 2 or 3 post-insemination. Oocytes used were from the female partner (21-46 years old) or from oocyte donors (18-35 years old), either fresh or vitrified.

Ovarian stimulation and laboratory procedures

All women (partners or oocyte donors) underwent controlled ovarian stimulation induced with either recombinant FSH (Gonal[®], Merck-Serono, Spain) or highly purified hMG (Menopur[®], Ferring, Spain). Pituitary inhibition was performed with a GnRH antagonist (Cetrotide[®], Merck Serono Europe Limited, London, UK) administered daily from sixth day of stimulation or GnRH agonists (Decapeptyl[®], Ipsen Pharma, Spain) starting in the second phase of the preceding menstrual cycle. Ovulation was triggered when ≥ 3 follicles of ≥ 18 mm diameter were observed, using either 0.3 mg of Triptorelin (Decapeptyl[®], Ipsen Pharma, France) in oocyte donor or 250 μ g of hCG (Ovitrelle[®], Merck Serono, Italy). Retrieval of cumulus oocyte complexes (COCs) was performed in all cases 36 h later by ultrasound-guided transvaginal follicular aspiration. Mechanical denudation was performed by exposure to 80 IU/ml of hyaluronidase (Hyase-10X[®], Vitrolife, Goteborg, Sweden) followed by gentle pipetting, as previously described (Pujol et al., 2018). MII oocytes were incubated in a specific medium (IVF[®], Vitrolife, Göteborg) until ICSI was performed.

Vitrified oocytes were used in about a quarter of the ICSI cycles included (n = 303; 25.9%). Vitrification was performed using Kuwayama's method 2 hours after oocyte pick up (Kuwayama, 2007), conducted in liquid nitrogen using a Cryotop vitrification open system (KITAZATO BIOPharma Co., Ltd, Fuji, Japan).

ICSI was performed in all cycles included in the study. After ICSI, oocytes were incubated in culture medium (G1[®], Vitrolife, Göteborg) covered with mineral oil (OVOIL[®], Vitrolife, Göteborg) at 37°C in 6% CO₂ and 95% relative humidity.

Fertilization was assessed 16–19 h post ICSI. Embryos were graded based on their morphological score, assessed using the system described by Coroleu and colleagues (Coroleu et al., 2006), which considers the number and symmetry of cells and the percentage of fragmentation. One, two or three embryos were transferred after 2 or 3 days of embryo culture.

Sperm processing

Fresh semen samples were collected on the day of ICSI. Samples were analyzed by an Integrated Semen Analysis System (ISAS[®], PROiSER, Spain) and evaluated according to World Health Organization recommendations (WHO, 2010). Cycles using testicular sperm, and patients with severe oligozoospermia (<1 million sperm / ml) and / or severe asthenozoospermia (<1% progressive motility) were excluded from the study. Sperm selection and capacitation was performed by 5 min centrifugation at 350 g in 5 ml of medium (PureSperm[®] Wash, Nidacon,

Sweden), followed by swim-up at 27°C, 6% CO₂ and 95% relative humidity (IVF[®], Vitrolife, Göteborg).

Timing control

A radiofrequency-based system (Witness[®], RI Ltd, UK) was used to record exact sperm processing times automatically. Three different times were considered: T1, from sample collection to swim-up; T2, swim-up to ICSI; T, total time (T1+T2, from sample collection to ICSI). We analyzed the effect of these time intervals on fertilization rate (FR), embryo morphological score, biochemical, clinical, ongoing pregnancy, and live birth (LB) rates.

Clinical procedures

All patients underwent endometrial preparation for ET by administering 400 mg of progesterone (Utrogestan[®], SEID, Spain, or Progeffik[®], Effik Laboratory, Spain) every 12 h vaginally. Progesterone was started the day of ICSI and ended the day of a negative pregnancy test or four weeks later if positive. The following clinical outcomes were evaluated: biochemical pregnancy (positive β -hCG test performed 14 days after FET); clinical pregnancy (evidence of fetal heart beat at seventh week of gestation); ongoing pregnancy (normally progressing pregnancy at 12 week of gestation) and live birth.

Statistical analysis

Differences in sperm processing times (T1, T2 and T) between positive and negative clinical outcomes were tested by Student's t-test for independent samples. To test whether there is a linear trend between clinical outcomes and time, we categorized times into 10 decile groups (**Supplementary Table I**), each decile containing the same number of cycles, and applied a linear-by-linear test. The probability of positive clinical outcome (pregnancy and live birth), the FR, and the mean embryo morphological score across the three times were further evaluated by means of Locally Weighted Scatterplot Smoothing (LOWESS) regression.

The likelihood for a positive clinical outcome was also modelled by logistic regression, for each of the sperm processing times, adjusting by female and male age and BMI, semen volume, sperm concentration and sperm motility (% a+b), oocyte origin (fresh or vitrified), number of inseminated oocytes, number of transferred embryos, transfer day and mean quality score of the transferred embryos. The effect of time on the FR was modelled by a Generalized Linear Modelling (GLM) adjusting by male age and BMI, sperm volume, concentration, and motility (% a+b), and oocyte origin (fresh or vitrified). The effect of time on the mean morphological score of the embryo cohort was assessed by ordinal regression adjusting for female and male age and BMI, number of

inseminated oocytes, number of obtained 2PN, sperm volume, concentration, and motility (% a+b), and oocyte status (fresh vs. vitrified). In all cases, female age was considered as the age of the woman providing the oocytes (partner or donor).

Statistical package IBM SPSS 18.0 (New York, USA); Software R version 2.15.1 (The R Foundation for Statistical Computing); and Stata software v13.0 (Stata Corp., College Station, Texas) were used to conduct all the statistical analyses. Statistical significance was set at $p < 0.05$.

RESULTS

Baseline and cycle characteristics

The men included in the study ($n = 1,169$) were 42.9 ± 7.5 years old on average and had a BMI of 25.7 ± 3.6 kg/m². The mean sperm concentration and progressive motility were 47.5 ± 71 million/ml and 34.3 ± 19.8 % a+b, respectively (**Table I**). The mean age of the women providing the oocytes was 31.5 (SD 7.6) years old. Partner oocytes were used in 47.4% of cycles, while donor oocytes were used in 52.6% of cycles (**Table I**).

All ICSI cycles involved a fresh embryo transfer at day 2 (45.9%) or 3 (54.1%) post-ICSI, of 1 (16.7%), 2 (74.5%), or 3 embryos (8.8%) (**Table I**). The FR after ICSI was 70.2 ± 21.8 , and the mean morphological score of the cohort of embryos was 7.16 ± 1.1 on a 1–10 scale (**Table I**).

Table I. Demographic and cycle characteristics of all patients included in the study (n = 1,169), fertilization rate, reproductive outcomes (biochemical, clinical and ongoing pregnancy, and live birth) and mean sperm processing times (T1, sample collection - swim up; T2, swim up - ICSI; T, sample collection - ICSI).

Demographic variables	
Male age; mean (SD) [range]	42.9 (7.5) [24-77]
Male BMI; mean (SD) [range]	25.7 (3.6) [18.6-48.3]
Female partner age; mean (SD) [range]	39.7 (4.9) [21-50]
Female partner BMI; mean (SD) [range]	23.9 (4.2) [18.1-41]
Oocyte donor age; mean (SD) [range]	25.9 (4.4) [19-36]
Oocyte donor BMI; mean (SD) [range]	23.4 (3.6) [18-40]
Age of woman providing oocytes; mean (SD) [range]	31.5 (7.6) [18-46]
Information of gametes	
Semen volume (ml); mean (SD) [range]	3.18 (1.9) [0.1-11.2]
Sperm concentration (million/ml); mean (SD) [range]	47.5 (71) [1-935]
Sperm progressive motility (%a+b); mean (SD) [range]	34.3 (19.8) [1.1-96.9]
Oocyte origin	
Oocyte donor; n (%)	615 (52.6)
Female partner; n (%)	554 (47.4)
Oocyte status	
Fresh; n (%)	866 (74.1)
Vitrified; n (%)	303 (25.9)
Sperm processing times	
T1, sample collection – swim up (h); mean (SD) [range]	0.35 (0.26) [0.05-3.42]
T2, swim up - ICSI (h); mean (SD) [range]	3.31 (2.23) [0.17-10.9]
T, sample collection – ICSI (h); mean (SD) [range]	3.66 (2.26) [0.23-11.18]
ICSI cycle characteristics	
MII oocytes inseminated; mean (SD) [range]	6.4 (2.7) [1-19]
Mean morphology score of transferred embryos; n (%)	
0-2	-
3-4	13 (1.1)
5-6	428 (36.6)
7-8	604 (51.7)
9-10	109 (9.3)
Missing	15 (1.3)
Transfer day; n (%)	
+2	536 (45.9)
+3	633 (54.1)
Number of transferred embryos; n (%)	
1	195 (16.7)
2	871 (74.5)
3	103 (8.8)
Laboratory outcomes	
2PN obtained; mean (SD) [range]	4.4 (2.2) [1-17]
Fertilization rate (%); mean (SD) [range]	70.2 (21.8) [13-100]
Embryo morphological score; mean (SD) [range]	7.16 (1.1) [4-10]
Reproductive outcomes	
Biochemical pregnancy; n (%)	490 (41.9)
Clinical pregnancy; n (%)	356 (30.5)
Ongoing pregnancy; n (%)	327 (28)
Livebirth; n (%)	320 (27.4)

Sperm processing times and analysis of its effect on laboratory outcomes

The mean sperm processing times in hours were 0.35 (~ 0 h 21 min) (SD 0.26, range: 0.05-3.42) for sample collection – swim-up (T1), 3.31 (~ 3 h 19 min) (SD 2.23, range: 0.17-10.9) for swim-up – ICSI (T2), and 3.66 (~ 3 h 40 min) (SD 2.26, range: 0.23-11.18) for sample collection – ICSI (T), times which showed a high variability between patients (**Figure 1**).

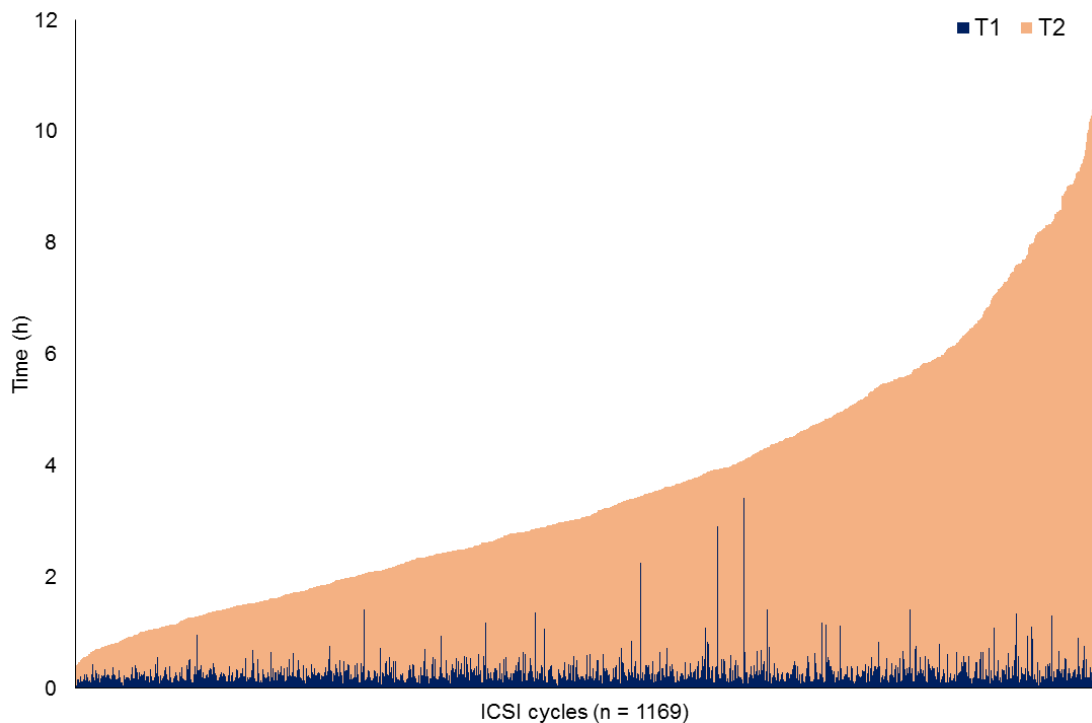


Figure 1. Distribution of sperm processing times (T1 and T2) in the ICSI cycles included in the study (n = 1169). T1, sample collection – swim-up; T2, swim-up - ICSI; T, sample collection - ICSI.

Overall, T1 and T2 times did not show significant effect on FR (**Table II**). We could observe a negative tendency of sample collection – swim-up time (T1) on FR ($B = -0.090$, 95% CI -0.188 , 0.009 ; $p = 0.074$), that can be visualized in the LOWESS regression (Supplementary Figure 1). However, neither the LOWESS regression nor the multivariate analysis indicated a significant effect of T1 and T2 on the mean morphological score of the embryo cohort (**Table II**, **Supplementary Figure 1**). The models generated to analyze the effect of total time (T) identified some variables affecting clinical outcomes (such as oocyte origin (fresh vs. vitrified) and number of MII oocytes) but did not return any significant effect on FR and mean embryo morphology after ICSI (**Supplementary Table II**).

Table II. Multilevel regression analysis of the association between T1 (sample collection - swim up) and T2 (swim up - ICSI) sperm processing times and fertilization rate and mean embryo morphological score after ICSI. The effect of T1 and T2 on both laboratory outcomes is adjusted by semen parameters (volume, concentration, motility), woman characteristics (age, BMI) and oocyte status (fresh vs. vitrified).

		Coefficient	95% CI		p
			Lower	Upper	
Fertilization rate	T1 (log-h)	-0.0895	-0.188	0.009	0.074
	T2 (log-h)	-0.0012	-0.081	0.079	0.976
	Woman age (y)	0.0025	-0.005	0.010	0.529
	Woman BMI (kg/m ²)	-0.0021	-0.027	0.022	0.869
	Semen volume (ml)	0.0181	-0.013	0.050	0.261
	Sperm concentration (million/ml)	0.0001	-0.001	0.001	0.82
	Sperm motility (% a+b)	0.0045	0.001	0.008	0.01
	Oocyte status (fresh vs. vitrified)	0.1909	0.064	0.318	0.003
Embryo morphological score	T1 (log-h)	0.052	-0.132	0.237	0.577
	T2 (log-h)	-0.097	-0.236	0.041	0.167
	MII obtained	-0.079	-0.142	-0.016	0.015
	2PN obtained	0.003	-0.073	0.078	0.943
	Woman age (y)	0.001	-0.014	0.015	0.928
	Woman BMI (kg/m ²)	-0.012	-0.053	0.030	0.587
	Sperm volume (ml)	-0.020	-0.077	0.038	0.502
	Sperm concentration (million/ml)	0.001	-0.001	0.002	0.419
	Sperm motility (% a+b)	0.001	-0.005	0.007	0.697
	Oocyte status (fresh vs. vitrified)	-0.603	-0.850	-0.357	<0.001

Analysis of reproductive outcomes by sperm processing time deciles

As indicated in **Table I**, the ICSI reproductive outcomes after fresh ET were 41.9%, 30.5%, 28% and 27.4% for biochemical, clinical, ongoing pregnancy rates, and live birth rate, respectively. None of the assayed sperm processing times (T1, T2, T) were different for ICSI cycles with positive or a negative biochemical, clinical or ongoing pregnancy, or with or without a live birth (**Table III**).

Table III. Analysis of sperm processing times (T1, sample collection – swim up; T2, swim up – ICSI; T, sample collection – ICSI; expressed as mean (SD)) by occurrence of pregnancy (biochemical, clinical, ongoing) and live birth. *Student-t test for independent samples.

	Biochemical pregnancy			Clinical pregnancy			Ongoing pregnancy			Livebirth		
	No	Yes	P*	No	Yes	P*	No	Yes	P*	No	Yes	P*
T1	0.35 (0.28)	0.34 (0.24)	0.40	0.35 (0.27)	0.34 (0.25)	0.60	0.35 (0.27)	0.34 (0.25)	0.62	0.35 (0.27)	0.34 (0.25)	0.52
T2	3.34 (2.26)	3.27 (2.2)	0.72	3.3 (2.25)	3.35 (2.19)	0.77	3.29 (2.27)	3.37 (2.13)	0.73	3.29 (2.27)	3.39 (2.12)	0.57
T	3.7 (2.28)	3.61 (2.22)	0.60	3.65 (2.27)	3.69 (2.22)	0.76	3.64 (2.29)	3.72 (2.16)	0.47	3.63 (2.29)	3.74 (2.15)	0.50

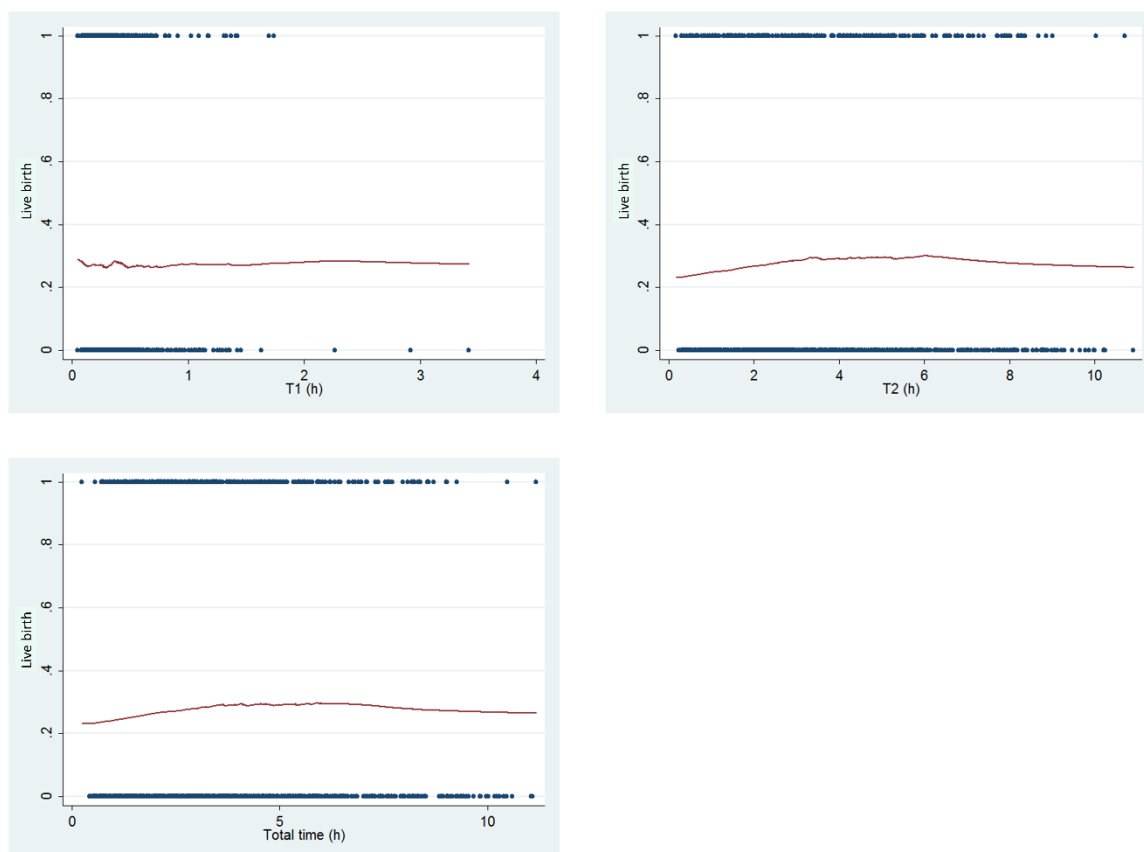


Figure 2. Live birth rate across the different sperm processing times (T1, sample collection – swim-up; T2, swim-up - ICSI; T, sample collection – ICSI) by means of Locally Weighted Scatterplot Smoothing (LOWESS) regression.

In order to assess if there are specific time intervals which maximize pregnancy and live birth rates after ICSI, we performed statistical analysis categorizing the time by deciles. However, this analysis did not provide any significant trend towards lower or higher pregnancy and live birth rates with each 1-h increase in T1, T2 or T (**Table IV**).

Table IV. Observed probability of pregnancy and live birth by each sperm processing time period including the same number of ICSI cycles per decile (n = 117). * Linear-by-linear test.

			Decile	p *									
Biochemical pregnancy	T1	n	53	47	40	63	52	45	46	47	45	52	0.185
		%	45.3%	40.2%	34.2%	53.8%	44.4%	38.8%	39.3%	40.2%	38.5%	44.4%	
	T2	n	52	45	52	48	48	57	41	50	52	45	0.644
		%	44.4%	38.5%	44.4%	41.0%	41.0%	49.1%	35.0%	42.7%	44.4%	38.5%	
	T	n	53	46	48	53	45	53	42	52	55	43	0.607
		%	45.3%	39.3%	41.0%	45.3%	38.5%	45.7%	35.9%	44.4%	47.0%	36.8%	
Clinical pregnancy	T1	n	39	32	27	49	37	32	38	33	31	38	0.148
		%	33.3%	27.4%	23.1%	41.9%	31.6%	27.6%	32.5%	28.2%	26.5%	32.5%	
	T2	n	35	29	37	34	34	45	30	40	38	34	0.507
		%	29.9%	24.8%	31.6%	29.1%	29.1%	38.8%	25.6%	34.2%	32.5%	29.1%	
	T	n	36	31	32	38	34	39	32	42	39	33	0.817
		%	30.8%	26.5%	27.4%	32.5%	29.1%	33.6%	27.4%	35.9%	33.3%	28.2%	
Ongoing pregnancy	T1	n	38	30	22	44	33	30	37	26	30	37	0.071
		%	32.5%	25.6%	18.8%	37.6%	28.2%	25.9%	31.6%	22.2%	25.6%	31.6%	
	T2	n	29	23	37	32	30	42	30	39	35	30	0.206
		%	24.8%	19.7%	31.6%	27.4%	25.6%	36.2%	25.6%	33.3%	29.9%	25.6%	
	T	n	29	26	32	36	30	37	31	42	34	30	0.5
		%	24.8%	22.2%	27.4%	30.8%	25.6%	31.9%	26.5%	35.9%	29.1%	25.6%	
Live birth	T1	n	38	30	21	41	33	30	36	25	30	36	0.114
		%	32.5%	25.6%	17.9%	35.0%	28.2%	25.9%	30.8%	21.4%	25.6%	30.8%	
	T2	n	27	22	36	32	29	42	30	39	33	30	0.141
		%	23.1%	18.8%	30.8%	27.4%	24.8%	36.2%	25.6%	33.3%	28.2%	25.6%	
	T	n	27	25	31	36	29	37	31	42	32	30	0.349
		%	23.1%	21.4%	26.5%	30.8%	24.8%	31.9%	26.5%	35.9%	27.4%	25.6%	

Analysis of pregnancy and live birth rates by LOWESS and logistic regressions

By LOWESS regression analysis, no relevant correlations were observed between the sperm processing times (T1, T2, and T) and biochemical and clinical pregnancy rates (**Supplementary Figure 2**). Interestingly, this analysis indicated a slight trend towards higher probability of ongoing pregnancy and live birth within the first 4 hours of T (sample collection – ICSI) (**Figure 2**).

To verify whether the time from sample collection to ICSI, and the two intermediate times, have an effect on reproductive outcomes after ICSI, we performed a logistic regression analysis, adjusting by male and female age, number of inseminated oocytes, embryo morphological score,

number of transferred embryos, or day of embryonic development at transfer, among others (**Table V**). Nevertheless, we could not observe any significant effect of T1, T2 and T on pregnancy rates (biochemical, clinical and ongoing) and live birth rates (**Table V, Supplementary Table III**).

Table V. Logistic multilevel regression analysis of the association between sperm intermediate processing times (T1, sample collection - swim up; T2, swim up - ICSI) and reproductive outcomes after ICSI. The effect of T1 and T2 on live birth rate is adjusted by male and female age and BMI, sperm parameters (volume, concentration, and motility), number of inseminated oocytes and its status (fresh or vitrified), number of embryos transfer, day of ET and average embryo morphological score.

		B	OR	OR 95% CI		P
				Lower	Upper	
Biochemical pregnancy	T1 (log-h)	-0.067	0.936	0.752	1.164	0.551
	T2 (log-h)	-0.083	0.921	0.780	1.086	0.327
	Male age (y)	-0.042	0.959	0.939	0.979	<0.001
	Female age (y)	-0.020	0.980	0.963	0.997	0.025
	Male BMI (kg/m ²)	-0.030	0.970	0.940	1.002	0.064
	Female BMI (kg/m ²)	-0.019	0.981	0.932	1.032	0.463
	Semen volume (ml)	-0.015	0.985	0.921	1.055	0.673
	Sperm concentration (million/ml)	-0.001	0.999	0.997	1.001	0.425
	Sperm motility (% a+b)	-0.004	0.996	0.989	1.003	0.221
	Oocyte status (fresh vs. vitrified)	0.014	1.014	0.736	1.398	0.930
	Number of inseminated oocytes	0.083	1.086	1.011	1.167	0.024
	Transfer day (3 vs. 2)	0.922	2.514	1.648	3.833	<0.001
	Number of transferred embryos (2 vs. 1)	0.725	2.065	1.120	3.806	0.020
	Number of transferred embryos (3 vs. 1)	0.356	1.428	1.059	1.927	0.020
Average embryo morphological score	0.300	1.349	1.201	1.516	<0.001	
Clinical pregnancy	T1 (log-h)	-0.051	0.950	0.753	1.198	0.665
	T2 (log-h)	0.019	1.019	0.854	1.215	0.836
	Male age (y)	-0.045	0.956	0.934	0.977	<0.001
	Female age (y)	-0.019	0.982	0.964	1.000	0.051
	Male BMI (kg/m ²)	-0.023	0.977	0.945	1.011	0.189
	Female BMI (kg/m ²)	-0.011	0.989	0.938	1.043	0.683
	Semen volume (ml)	0.019	1.019	0.949	1.095	0.600
	Sperm concentration (million/ml)	0.000	1.000	0.998	1.002	0.975
	Sperm motility (% a+b)	-0.004	0.996	0.989	1.004	0.309
	Oocyte status (fresh vs. vitrified)	0.129	1.138	0.813	1.591	0.451
	Number of inseminated oocytes	0.080	1.083	1.006	1.167	0.034

	Transfer day (3 vs. 2)	1.128	3.089	1.842	5.182	<0.001
	Number of transferred embryos (2 vs. 1)	1.083	2.953	1.455	5.993	0.003
	Number of transferred embryos (3 vs. 1)	0.298	1.348	0.982	1.850	0.065
	Average embryo morphological score	0.283	1.327	1.173	1.502	<0.001
Ongoing pregnancy	T1 (log-h)	-0.055	0.947	0.746	1.201	0.652
	T2 (log-h)	0.095	1.100	0.916	1.321	0.307
	Male age (y)	-0.053	0.948	0.927	0.970	<0.001
	Female age (y)	-0.022	0.978	0.960	0.997	0.025
	Male BMI (kg/m ²)	-0.031	0.969	0.936	1.004	0.082
	Female BMI (kg/m ²)	-0.022	0.978	0.926	1.034	0.437
	Semen volume (ml)	0.022	1.022	0.950	1.099	0.561
	Sperm concentration (million/ml)	0.000	1.000	0.998	1.002	0.963
	Sperm motility (% a+b)	-0.004	0.996	0.988	1.003	0.280
	Oocyte status (fresh vs. vitrified)	0.204	1.227	0.871	1.727	0.242
	Number of inseminated oocytes	0.065	1.067	0.989	1.150	0.093
	Transfer day (3 vs. 2)	1.144	3.139	1.829	5.386	<0.001
	Number of transferred embryos (2 vs. 1)	0.840	2.317	1.075	4.992	0.032
	Number of transferred embryos (3 vs. 1)	0.281	1.324	0.957	1.833	0.090
	Average embryo morphological score	0.255	1.290	1.136	1.464	<0.001
Live birth	T1 (log-h)	-0.056	0.945	0.744	1.202	0.647
	T2 (log-h)	0.126	1.134	0.942	1.364	0.183
	Male age (y)	-0.054	0.948	0.926	0.970	<0.001
	Female age (y)	-0.025	0.975	0.957	0.994	0.011
	Male BMI (kg/m ²)	-0.036	0.964	0.930	0.999	0.046
	Female BMI (kg/m ²)	-0.021	0.979	0.926	1.035	0.458
	Semen volume (ml)	0.031	1.032	0.959	1.110	0.400
	Sperm concentration (million/ml)	0.000	1.000	0.998	1.002	0.980
	Sperm motility (% a+b)	-0.004	0.996	0.988	1.003	0.246
	Oocyte status (fresh vs. vitrified)	0.266	1.305	0.924	1.843	0.130
	Number of inseminated oocytes	0.055	1.057	0.980	1.140	0.153

	Transfer day (3 vs. 2)	1.111	3.038	1.769	5.217	<0.001
	Number of transferred embryos (2 vs. 1)	0.839	2.315	1.074	4.990	0.032
	Number of transferred embryos (3 vs. 1)	0.302	1.353	0.975	1.878	0.070
	Average embryo morphological score	0.235	1.265	1.114	1.437	<0.001

DISCUSSION

This is the first study evaluating the effect of sperm processing times on ICSI using an operator independent, radiofrequency-based system, on a large cohort of patients. With this technology, time recording is exact and operator-independent. As indicated by our results, a considerable variability in the time of processing of the gametes may exist between different patients and ICSI cycles within a fertility clinic, especially for T2 (time from swim-up to ICSI). In our study, the total time (from sample collection to ICSI) was around 3 – 4 h in most cycles but, under rare circumstances, this interval was as short as few minutes (~ 14 min) or as long as 10-11 hours. We believe our results are helpful to understand if these differences might be relevant or not.

Mansour and colleagues found that different incubation times of sperm processed by swim-up before ICSI did not result in differences in fertilization rate (70%, 74% and 67% FR for 1, 3 and 5 h incubation, respectively) (Mansour et al., 2008). These results are confirmed and extended by our results: 69.7%, 73.9% and 68.6% FR for 0.5-1.5 h, 2.5-3.5 h and 4.5-5.5 h incubation (T), respectively. We also observed a trend associating longer T1 with lower FR. These observations suggest that a total sperm incubation time of around 3 h including a quick sperm wash (which may be beneficial to minimize the effect of extracellular ROS on sperm integrity) should be the optimal to maximize FR in ICSI. However, after performing multilevel analysis adjusting for different variables (including age and sperm parameters, among others), we did not find any significant effect of the three times considered (T1, T2 and T) on fertilization rates. This indicates that time-dependent molecular and cellular changes occurring in sperm are very subtle and have little or negligible effect on fertilizing ability through ICSI.

Longer time of sperm incubation has been associated to higher levels of DNA fragmentation, which in turn has been reported to reduce the quality of the preimplantation embryo (Morris et al., 2002; Ni et al., 2014). By adjusted ordinal regression analysis, we found no significant effect of T1, T2 and T on the mean morphological score of the embryo cohort. Our protocol was designed specifically to minimize iatrogenic DNA damage to the sperm, something which could diminish the potential for time-dependent damage in sperm, and explain the absence of significant changes

to laboratory outcomes: samples were incubated at 27°C (not at 37°C), and we used pellet swim-up, reported to induce less DNA fragmentation than direct swim-up or density gradient centrifugation (Volpes et al., 2016).

Our study includes a high number of cases, allowing categorization of the time in deciles for the analysis of reproductive outcomes after ICSI. Small differences were observed between deciles and along time by LOWESS regression, but we did not find any specific time interval which resulted in significantly higher pregnancy and live birth rates after ICSI. The absence of significant effect of T1, T2, and T on these reproductive outcomes was confirmed by logistic regression, adjusting by variables like woman and man age, day of ET and the morphology of transferred embryos, all of them well-described to affect pregnancy and live birth rates (Rhenman et al., 2015; McPherson et al., 2018).

We recognize some limitations to our study. The results that we report cannot be extrapolated to ICSI cycles for severe male factor, other techniques for sperm selection (such as density gradient centrifugation), use of cryopreserved semen, or cycles involving the transfer of cryopreserved embryos, as all these were excluded from our analysis. In addition, given its retrospective nature, we cannot exclude the influence of uncontrolled for variables on our results.

In conclusion, we found that sperm processing times do not have a detectable clinical effect on pregnancy and live birth rates after ICSI. We believe these results to be relevant from a clinical perspective, as well as for the adequate planning of the embryology laboratory workflow.

AUTHORS ROLES

M.T-M. and A.Q.: study design, data collection and analysis and article preparation. M.B. and D.G.: study design, data analysis and article preparation. R.B.: data collection and analysis. A.R.: expert knowledge and article approval. R.V.: study design, implementation and supervision, expert knowledge and article preparation.

ACKNOWLEDGEMENTS

The authors wish to thank Francesc Figueras for statistical support and Sarai Brazal for database support.

FUNDING

This work was supported by intramural funding of Clínica EUGIN, and by the Secretary for Universities and Research of the Ministry of Economy and Knowledge of the Government of Catalonia (GENCAT 2015 DI 049 to M. T-M).

CONFLICT OF INTEREST

The authors declare that they have no conflict of interest.

REFERENCES

- Ahmed I, Abdelateef S, Laqqan M, Amor H, Abdel-Lah MA, Hammadeh ME. Influence of extended incubation time on Human sperm chromatin condensation, sperm DNA strand breaks and their effect on fertilisation rate. *Andrologia* 2018.
- Auger J, Ronot X, Dadoune JP. Human sperm mitochondrial function related to motility: a flow and image cytometric assessment. *J Androl* 1989; 10(6):439-48.
- Bárcena P, Rodríguez M, Obradors A, Vernaev V, Vassena R. Should we worry about the clock? Relationship between time to ICSI and reproductive outcomes in cycles with fresh and vitrified oocytes. *Hum Reprod* 2016; 31(6):1182-91.
- Calamera JC, Fernandez PJ, Buffone MG, Acosta AA, Doncel GF. Effects of long-term in vitro incubation of human spermatozoa: functional parameters and catalase effect. *Andrologia* 2001; 33(2):79-86.
- Mansour RT, Serour MG, Abbas AM, Kamal A, Tawab NA, Aboulghar MA, Serour GI. The impact of spermatozoa preincubation time and spontaneous acrosome reaction in intracytoplasmic sperm injection: a controlled randomized study. *Fertil Steril* 2008; 90(3):584-91.
- Matsuura R, Takeuchi T, Yoshida A. Preparation and incubation conditions affect the DNA integrity of ejaculated human spermatozoa. *Asian J Androl* 2010; 12(5):753-9.
- McPherson NO, Zander-Fox D, Vincent AD, Lane M. Combined advanced parental age has an additive negative effect on live birth rates-data from 4057 first IVF/ICSI cycles. *J Assist Reprod Genet* 2018; 35(2):279-287.
- Morris ID, Ilott S, Dixon L, Brison DR. The spectrum of DNA damage in human sperm assessed by single cell gel electrophoresis (Comet assay) and its relationship to fertilization and embryo development. *Hum Reprod* 2002; 17(4):990-8.
- Ni W, Xiao S, Qiu X, Jin J, Pan C, Li Y, Fei Q, Yang X, Zhang L, Huang X. Effect of sperm DNA fragmentation on clinical outcome of frozen-thawed embryo transfer and on blastocyst formation. *PLoS One* 2014; 9(4):e94956.
- Peer S, Eltes F, Berkovitz A, Yehuda R, Itsykson P, Bartoov B. Is fine morphology of the human sperm nuclei affected by in vitro incubation at 37 degrees C? *Fertil Steril* 2007; 88(6):1589-94.
- Pujol A, García D, Obradors A, Rodríguez A, Vassena R. Is there a relation between the time to ICSI and the reproductive outcomes? *Hum Reprod* 2018; 33(5):797-806.

Rhenman A, Berglund L, Brodin T, Olovsson M, Milton K, Hadziosmanovic N, Holte J. Which set of embryo variables is most predictive for live birth? A prospective study in 6252 single embryo transfers to construct an embryo score for the ranking and selection of embryos. *Hum Reprod* 2015; 30(1):28-36.

Robertson L, Wolf DP, Tash JS. Temporal changes in motility parameters related to acrosomal status: identification and characterization of populations of hyperactivated human sperm. *Biol Reprod* 1988; 39(4):797-805.

Rougier N, Uriondo H, Papier S, Checa MA, Sueldo C, Alvarez Sedó C. Changes in DNA fragmentation during sperm preparation for intracytoplasmic sperm injection over time. *Fertil Steril* 2013; 100(1):69-74.

Sakkas D, Ramalingam M, Garrido N, Barratt CL. Sperm selection in natural conception: what can we learn from Mother Nature to improve assisted reproduction outcomes? *Hum Reprod Update* 2015; 21(6):711-26.

Schmidt-Sarosi C, Centola GM, Abeyawardene S, Sarosi P. Viable pregnancies can occur after 24-hour incubation of ejaculated sperm before intracytoplasmic sperm injection. *Fertil Steril* 2009; 91(4 Suppl):1408-10.

Sukcharoen N, Keith J. Evaluation of the percentage of sperm motility at 24 h and sperm survival ratio for prediction of in vitro fertilization. *Andrologia* 1996; 28(4):203-10.

Volpes A, Sammartano F, Rizzari S, Gullo S, Marino A, Allegra A. The pellet swim-up is the best technique for sperm preparation during in vitro fertilization procedures. *J Assist Reprod Genet* 2016; 33(6):765-70.

Zhang XD, Chen MY, Gao Y, Han W, Liu DY, Huang GN. The effects of different sperm preparation methods and incubation time on the sperm DNA fragmentation. *Hum Fertil* 2011; 14(3):187-91.

SUPPLEMENTARY INFORMATION

Supplementary Table I. Range of deciles for the different sperm processing times (T1, samples collection - swim up; T2, swim up – ICSI; T, samples collection – ICSI). The minimum and the maximum values of time in hours are indicated for each decile. Each decile contains the same number of cycles (n = 117).

	T1 (sample collection – swim up)	T2 (swim up – ICSI)	T (sample collection – ICSI)
1st	0.05-0.14	0.17-0.88	0.23-1.17
2nd	0.14-0.18	0.89-1.33	1.18-1.64
3rd	0.18-0.21	1.34-1.8	1.65-2.12
4th	0.21-0.25	1.81-2.24	2.13-2.62
5th	0.25-0.28	2.24-2.78	2.63-3.09
6th	0.28-0.32	2.78-3.39	3.09-3.74
7th	0.32-0.38	3.4-4.18	3.75-4.52
8th	0.38-0.45	4.19-5.15	4.52-5.53
9th	0.45-0.58	5.15-6.64	5.54-7.08
10th	0.59-3.42	6.64-10.91	7.1-11.18

Supplementary Table II. Multilevel regression analysis of the association between T total sperm processing time (T, sample collection - ICSI) and fertilization rate and mean embryo morphological score after ICSI. The effect of T on both laboratory outcomes is adjusted by semen parameters (volume, concentration, motility), woman characteristics (age, BMI) and oocyte status (fresh vs. vitrified).

		Coefficient	95% CI		p
			Lower	Upper	
Fertilization rate	T (log-h)	-0,0201	-0,1129	0,0727	0,671
	Woman age (y)	0,0018	-0,0060	0,0096	0,649
	Woman BMI (kg/m ²)	0,0015	-0,0263	0,0232	0,905
	Semen volume (ml)	0,0176	-0,0140	0,0492	0,274
	Sperm concentration (million/ml)	0,0001	-0,0010	0,0012	0,841
	Sperm motility (% a+b)	0,0045	0,0010	0,0079	0,011
	Oocyte status (fresh vs. vitrified)	0,1904	0,0635	0,3173	0,003
Embryo morphological score	T (log-h)	-0.108	-0.267	0.050	0.179
	MII obtained	-0.078	-0.141	-0.014	0.016
	2PN obtained	0.001	-0.074	0.076	0.981
	Woman age (y)	0.001	-0.013	0.016	0.863
	Woman BMI (kg/m ²)	-0.012	-0.054	0.030	0.579
	Semen volumen (ml)	-0.020	-0.077	0.037	0.497
	Sperm concentration (million/ml)	0.001	-0.001	0.002	0.415
	Sperm motility (% a+b)	0.001	-0.005	0.007	0.684
	Oocyte origin (fresh vs. vitrified)	-0.602	-0.848	-0.355	<0.001

Supplementary Table III. Logistic multilevel regression analysis of the association between total sperm processing time (T, sample collection - ICSI) and reproductive outcomes after ICSI. The effect of T on pregnancy (biochemical, clinical and ongoing) and live birth rates is adjusted by male and female age and BMI, sperm parameters (volume, concentration, motility), number of inseminated oocytes and its status (fresh or vitrified), number of embryos transfer, day of ET and average embryo morphological score.

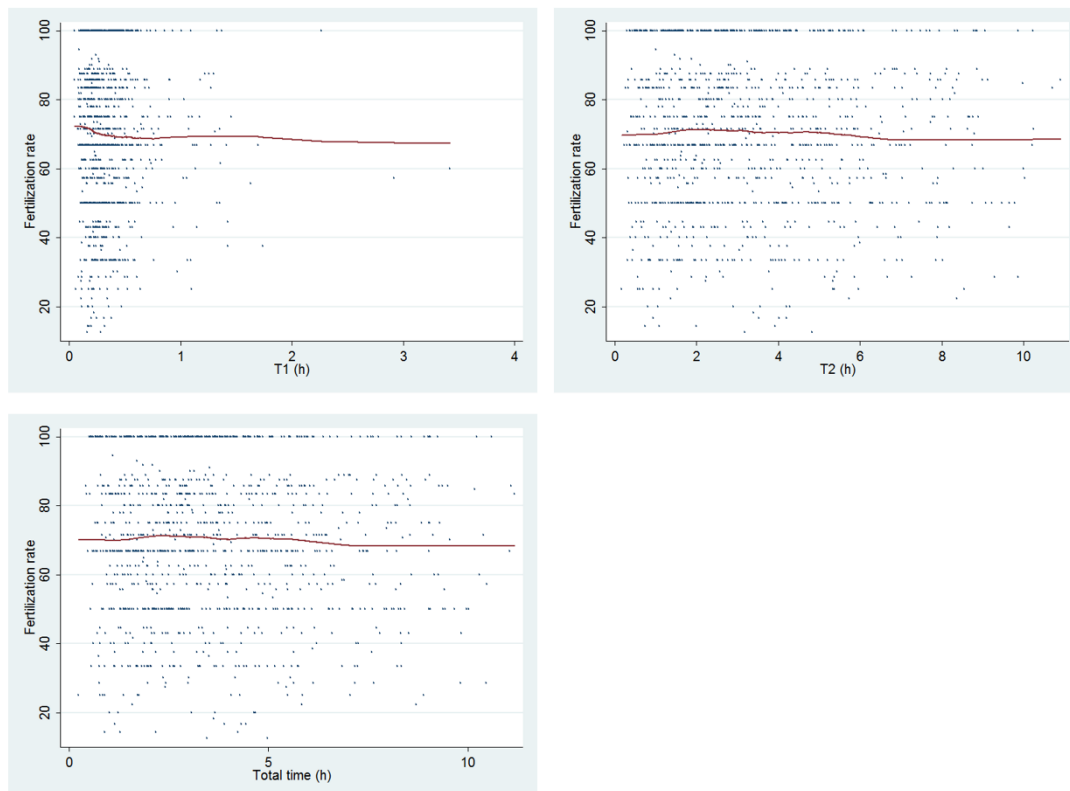
		B	OR	OR 95% CI		p
				Lower	Upper	
Biochemical pregnancy	T (log-h)	-0.100	0.905	0.749	1.093	0.300
	Male age (y)	-0.042	0.959	0.939	0.979	<0.001
	Female age (y)	-0.020	0.980	0.963	0.997	0.021
	Male BMI (kg/m ²)	-0.030	0.970	0.939	1.002	0.063
	Female BMI (kg/m ²)	-0.019	0.981	0.932	1.032	0.464
	Semen volume (ml)	-0.015	0.985	0.921	1.055	0.671
	Sperm concentration (million/ml)	-0.001	0.999	0.997	1.001	0.420

	Sperm motility (% a+b)	-0.004	0.996	0.989	1.003	0.216
	Oocyte status (fresh vs. vitrified)	0.014	1.014	0.736	1.398	0.931
	Number of inseminated oocytes	0.084	1.088	1.012	1.168	0.022
	Transfer day (3 vs. 2)	0.920	2.508	1.645	3.823	<0.001
	Number of transferred embryos (2 vs. 1)	0.723	2.061	1.118	3.797	0.020
	Number of transferred embryos (3 vs. 1)	0.354	1.424	1.056	1.921	0.021
	Average embryo morphological score	0.300	1.349	1.201	1.516	<0.001
Clinical pregnancy	T (log-h)	0.021	1.021	0.835	1.249	0.839
	Male age (y)	-0.045	0.956	0.935	0.978	<0.001
	Female age (y)	-0.019	0.981	0.963	1.000	0.045
	Male BMI (kg/m ²)	-0.023	0.977	0.945	1.011	0.186
	Female BMI (kg/m ²)	-0.011	0.989	0.938	1.043	0.683
	Semen volume (ml)	0.019	1.019	0.949	1.095	0.597
	Sperm concentration (million/ml)	0.000	1.000	0.998	1.002	0.965
	Sperm motility (% a+b)	-0.004	0.996	0.989	1.003	0.306
	Oocyte status (fresh vs. vitrified)	0.131	1.140	0.815	1.594	0.446
	Number of inseminated oocytes	0.081	1.085	1.008	1.168	0.031
	Transfer day (3 vs. 2)	1.125	3.079	1.836	5.163	<0.001
	Number of transferred embryos (2 vs. 1)	1.080	2.943	1.451	5.972	0.003
	Number of transferred embryos (3 vs. 1)	0.297	1.345	0.980	1.847	0.066
Average embryo morphological score	0.283	1.327	1.173	1.502	<0.001	
Ongoing pregnancy	T (log-h)	0.106	1.111	0.902	1.369	0.321
	Male age (y)	-0.053	0.948	0.927	0.970	<0.001
	Female age (y)	-0.022	0.978	0.959	0.997	0.021
	Male BMI (kg/m ²)	-0.032	0.969	0.935	1.004	0.080
	Female BMI (kg/m ²)	-0.022	0.978	0.926	1.034	0.439
	Semen volume (ml)	0.022	1.022	0.950	1.100	0.556
	Sperm concentration (million/ml)	<0.001	1.000	0.998	1.002	0.951

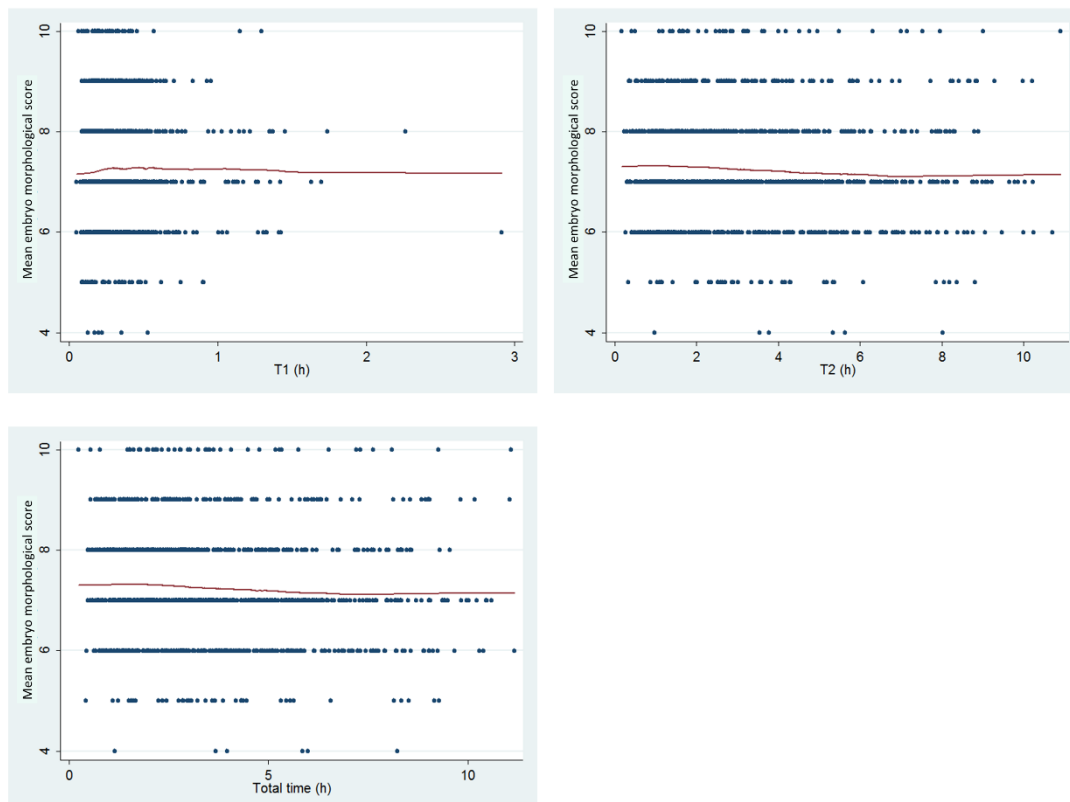
	Sperm motility (% a+b)	-0.004	0.996	0.988	1.003	0.275
	Oocyte status (fresh vs. vitrified)	0.206	1.229	0.873	1.731	0.237
	Number of inseminated oocytes	0.066	1.068	0.991	1.152	0.085
	Transfer day (3 vs. 2)	1.139	3.124	1.822	5.358	<0.001
	Number of transferred embryos (2 vs. 1)	0.836	2.307	1.071	4.969	0.033
	Number of transferred embryos (3 vs. 1)	0.279	1.322	0.955	1.830	0.092
	Average embryo morphological score	0.255	1.290	1.137	1.464	<0.001
Live birth	T (log-h)	0.141	1.151	0.932	1.421	0.191
	Male age (y)	-0.054	0.948	0.926	0.970	<0.001
	Female age (y)	-0.026	0.975	0.956	0.994	0.009
	Male BMI (kg/m ²)	-0.037	0.964	0.930	0.999	0.045
	Female BMI (kg/m ²)	-0.021	0.979	0.926	1.035	0.461
	Semen volume (ml)	0.032	1.032	0.959	1.111	0.395
	Sperm concentration (million/ml)	<0.001	1.000	0.998	1.002	0.965
	Sperm motility (% a+b)	-0.005	0.996	0.988	1.003	0.242
	Oocyte status (fresh vs. vitrified)	0.269	1.308	0.926	1.848	0.127
	Number of inseminated oocytes	0.057	1.058	0.981	1.141	0.141
	Transfer day (3 vs. 2)	1.106	3.023	1.761	5.189	<0.001
	Number of transferred embryos (2 vs. 1)	0.835	2.304	1.069	4.964	0.033
	Number of transferred embryos (3 vs. 1)	0.301	1.351	0.974	1.874	0.072
	Average embryo morphological score	0.235	1.265	1.114	1.437	<0.001

Supplementary Figure 1. Fertilization rate (A) and mean morphological score of the embryo cohort (B) across the different sperm processing times (T1, T2 and T) in hours by means of Locally Weighted Scatterplot Smoothing (LOWESS) regression.

A



B



Supplementary Figure 2. Biochemical (A), clinical (B) and ongoing (C) pregnancy rates across the different sperm processing times (T1, T2 and T) by means of Locally Weighted Scatterplot Smoothing (LOWESS) regression.

